THE UNIVERSITY
of EDINBURGH

The development of Biologics for use in translational medicine

SAURABH JAIN

Thesis submitted for the degree of Doctor of Philosophy

The University of Edinburgh

2015

DECLARATION

I declare that I have composed this thesis and that I performed all work described herein, otherwise any contributions from other members of group have been clearly mentioned. I confirm that this work has not been submitted for any other degree or professional qualification.

Saurabh Jain

ABSTRACT

In this research, we developed a wide range of biological tools against two distinct targets from future diagnostic or therapeutic points of view. Firstly, we demonstrate that sporadic canine B cell lymphoma mimics the features of human equivalents which in turn will be advantageous for development of canine as well as human therapeutics. With a comparative oncological approach, here we developed a monoclonal antibody (NCD1.2) against canine CD20 which also binds to its human counterpart. Using flow cytometry and tissue microarray, we show that NCD1.2 binds specifically to canine B cell lymphomas ($CD20^{+}$) and not T-cell lymphoma ($CD20^{-}$). We also cloned scFv scaffold by linking variable heavy and light chains from NCD1.2 hybridoma by a serine-glycine linker to see if it was active as a biological tool for future therapeutics. Intriguingly, we obtained two different kappa light chains from a single hybridoma cell (scFv3 and scFv7) after antibody phage display. These scFvs were cloned into mammalian vectors for expression in CHO cells and ADEPT - CpG2 vector for yeast expression to see if the activity of these scFvs was retained. Our data suggests that recombinant anti-CD20 scFv might be a useful tool for bioconjugate directed immunotherapies in comparative medicine.

Secondly, in addition to mAbs we also developed peptide aptamers which are seldom described but have become attractive agents that typically target a specific biomolecule of interest. Parkinson's disease (PD) is characterized by formation of lewy bodies (inclusion bodies) in the substantia nigra and the major content of lewy bodies is α-synuclein. To begin with we made recombinant α-synuclein and biophysically characterize this protein under different conditions on a native gel. We also performed Circular dichroism to look at its structure and demonstrate that α helicity could be achieved in presence of SDS. The aim of this project was to develop peptide aptamers, mAbs to α-synuclein, map the binding sites onto the peptides derived from the protein and also on recombinant protein. Further we demonstrated the development of biological tools and their potential ability against α-synuclein in α-synuclein expressing cell lines from future PD therapeutic perspective. Monoclonal antibodies were developed and mAb (3.1) was found to be immunopositive for α-synuclein in parts of kidney and brain. Moreover to estimate

the oligomeric state of α-synuclein, we developed assays such as co-transfection of two different constructs i.e. cherry and GFP tagged α-synuclein and Proximity ligation assay to show its self - interaction. Peptide phage display screening (NEB Ph.D. 12 mer library) on recombinant WT α-synuclein was performed to identify aptamers and ultimately novel binding proteins. The peptides were selected based on iteration number and out of the selected panel of peptides; SHACWWDECTGS was found to effectively bind α-synuclein using ELISA. Scanning of peptide GDGNSVLKPGNW (highest iteration number) led to identification of interacting proteins with α-synuclein. Thus in conclusion, we show the validation of different antibody scaffolds and peptide aptamers which could be useful tools from future therapeutics point of view against two well characterized antigens in B cell lymphoma and Parkinson's disease, respectively.

Table of contents

Chapter 2: Materials and Methods

Chapter 3: Development of monoclonal antibodies and Bioconjugate against canine CD20 receptor (a receptor, scFv model)

Chapter 4: Developing monoclonal antibodies and assays to biophysically characterized α-synuclein

Chapter 5: Peptide phage display screening against α-synuclein

Figures and tables

Figures

Tables

Abbreviations

A	Adenine
A	Alanine
AADC	Aromatic amino acid decarboxylase
AD	Alzheimer's disease
ADC	Antibody drug conjugates
ADCC	Antibody dependent cellular cytotoxicity
ADCP	Antibody dependent cellular phagocytosis
ADEPT	Antibody directed enzyme prodrug therapy
AML	Acute myelogenous leukemia
Amp	Ampicillin
APC	Antigen presenting cells
ATP	Adenosine tri phosphate
BLAST	Basic local alignment search tool
bp	Base pairs
BSA	Bovine serum albumin
bsDb	Bispecific diabodies
B-SLL	B-cell small lymphocytic
C	Cysteine
C1, c2, c3 and c5 proteins	Complement proteins
$CaCl_2$	Calcium chloride
CD	Cluster of differentiation
CD	Circular Dichroism
CDC	Complement dependent cytotoxicity
CDR	Complementary determining region
CEA	Carcinoembryonic antigen
cfu	colony forming units
CH	Constant heavy chain
CHO	Chinese hamster ovary

CH_3COOK	Potassium acetate
CLL	Chronic lymphocytic leukaemia
cmAb	Chimpanzee antibody
CpG2	Carboxypeptidase 2
CPL	Circular polarized light
DAPI	4', 6-diamino-2-phenylindole
DLBCL	Diffuse Large B-cell lymphoma
DMSO	Dimethyl sulfoxide
DNA	Deoxy ribonucleic acid
dNTP	Deoxynucleotide tri phosphate
DOX	Doxycycline
DTT	Dithiothreitol
ECL	Enhanced chemiluminescence
EDTA	Ethylenediaminetetraacetic acid
EGFR	Epidermal growth factor receptor
ELISA	Enzyme linked Immunosorbent Assay
Fab	Fragment antigen binding region
FACS	Fluorescence activated cell sorting
FBS	Foetal bovine serum
Fc	Fragment crystallizable region of antibody
FcγR	Fc gamma receptors
FDA	Food and drug administration
FITC	Fluorescein isothiocynate
FL	Follicular Lymphoma
FLIM	Fluorescence lifetime imaging microscopy
FRET	Fluorescence resonance energy transfer
G	grams
G	Glycine
GFP	Green fluorescent protein
$(G_4S)_4$	Glycine serine linker
H	Histidine
H_2SO_4	sulphuric acid

HADH	Hydroxyl-coenyme A dehydrogenase
HAMA	Human anti- murine antibody
HAT	Hypoxanthine aminopterin thymidine
HCAbs	Heavy chain antibodies
HCL	Hydrochloric acid
HER	Human epidermal growth factor
HGPRT	Hypoxanthine-Guanine Phosphoribosyl Transferase
HPLC	High performance liquid chromatography
HRP	Horse radish peroxidase
HPMA	N-(2-hydroxypropyl) methacrylamide
I	Isoleucine
Ig	Immunoglobulin
IGFR	Insulin growth factor receptor
IGF1	Insulin like growth factor
IF	Immunofluorescence
IFITM1	Interferon induced transmembrane protein-1
IHC	Immunohistochemistry
IMAC	Immobilized metal affinity chromatography
IPTG	Isopropyl β-D-1 thiogalactopyranoside
K	Lysine
kb	kilo bases
KCl	potassium chloride
L	Leucine
L	litre
lacZ	gene coding for β-galactosidase
LB	Lysogeny broth
LB	lewy bodies
M	molar
M	Methionine
mAb	monoclonal antibody
MAC	membrane attack complex
mg	milligram

$MgCl_2$	Magnesium chloride
$MgSO_4$	Magnesium sulphate
mRNA	messenger RNA
MRW	Mean residual weight
MZL	Marginal Zone Lymphoma
N	Asparagine
NAC	non-amyloid component
NaCl	Sodium chloride
$NaHCO_3$	Sodium bicarbonate
NaOH	Sodium hydroxide
NCD1.2	monoclonal antibody against canine CD20
ng	nanogram
NGS	Next generation sequencing
ND	Neurological disorder
NHL	Non-Hodgkin's lymphoma
NK	Natural killer cells
NMR	Nuclear magnetic resonance
OD	Optical density
PARK7	Parkinson protein 7
PBS	Phosphate buffered saline
PBS-T	Phosphate buffered saline with Tween-20
PCR	Polymerase chain reaction
PD	Parkinson's disease
PDGFR	platelet-derived growth factor receptor
PEG	Polyethylene glycol
PFA	paraformaldehyde
Ph.D. 12 library	Phage display 12 mer library
PINK1	PTEN induced putative kinase-1
PLA	Proximity ligation assay
PTCL	Lymphoma and Peripheral T-cell Lymphoma

PTK	protein tyrosine kinases
RbCl	Rubidium chloride
RNA	Ribose nucleic acid
Rpm	revolutions per minute
RT	Reverse transcriptase
SANH	Succinimidyl 6-hydrazinonicotinate acetone hydrazone
SDS	Sodium dodecyl sulphate
scFv	single chain fragment variable antibody
SNARE	Soluble N-ethylmaleimide sensitive factor attachment protein receptor
SNCA	non A4 component of amyloid precursor (α-synuclein)
TaFv	Tandem scFv
TBS	Tris buffered saline
VEGFR	Vascular endothelial growth factor receptor
VL	Variable light chain
VH	Variable heavy chain
VHH	single variable domain antibody
TEMED	Tetramethylethylenediamine
TMA	Tissue microarray
TMB	3,3',5,5'- tetramethylbenzadine
TRAF6	TNF receptor associated factor
WT	wild type
YNB	Yeast nitrogen base
µg	microgram
µM	micromolar
µL	microliter

Acknowledgements

This thesis would not have been possible without the help of my supervisor Professor Ted Hupp who continuously helped and supported me throughout my PhD. This has been one of the smoothest journeys in my life with continuous support from the members of Hupp and Ball laboratory. Especially I would like to thank Dr. Erin Worrall who advised and helped me during the early phase of my PhD. I am very grateful to all members of Hupp and Ball laboratory along with members of Borek Vojtesek's laboratory who helped in some ways and encouraged me throughout the years.

Thanks to Dr Euan Murray for sharing his tremendous knowledge in almost all the fields, to proof read whole of my PhD thesis and helping me to plan experiments. Thanks to my fiancé Manali Hirani for being with me, taking the pain of travelling to London for lectures on every Wednesday and making my journey a lot smoother than I expected. It was a beautiful 3 years journey in a spectacular city of Edinburgh after my MSc in Nottingham, UK. I cannot miss out my family who have always my support throughout and I do apologize for not coming back to India after my PhD as I will move to Sheffield for my Post doc.

Not to forget the amount of friends I made during my PhD and how they have contributed in making this journey better than ever. Maria, Bindhu, Liz, Kalai, Jianguo, Jenny and Terry have become such good friends that I will be seeing most of my friends in my wedding next year. I will miss working under Professor Ted Hupp and Kathryn Ball and also my friends including my flatmates (Kunal, Piyush and Antonio). Lastly I will miss Edinburgh and its best working environment!

CHAPTER 1: Introduction

1.1. Biologics

1.1.1. Biologics and small molecules

Biologics include a wide variety of biologically derived tools that specifically target different types of cells including cancer cells and stimulate an immune response. The biologics differ from conventional drugs in the way that the former products are made in cells or living organisms, whereas conventional drugs are made in laboratory using several chemical reactions. The first biologic product ever to gain clinical significance and FDA approval was Humulin, a recombinant human insulin developed by Genentech [8]. Traditional therapeutic biologics include blood products, human and animal cells; however modern biologics that have been developed using biotechnology include products such as monoclonal antibodies, cytokines and growth factors.

Biologics are expected to account for 75% of the total revenues generated from the top 10 selling drugs by the end of 2014, with 5 out of 10 predicted to be monoclonal antibodies and it is also believed that one third of newly developed therapeutic tools are a form of biologics [9]. They are often used in combination with different therapies and biologics are further subdivided into three types: (i) alternative proteins which are identical to body's signalling proteins, that in turn can activate the immune system to fight various diseases, (ii) monoclonal antibodies including antibody fragments designed against a target of interest in a specific type of disease and (iii) tools that have an ability to cause changes in the cellular processes and in turn induce anti-tumor effects. Chemically, biologics form a secondary structure (secondary, tertiary or quaternary) which is in contrast to the small molecules [10]. Biologics are largely administered parenterally i.e. intravenously as oral delivery is limited by the barriers such as pH dependent degradation, solubility, low epithelial permeability and instability [5]. The characteristic differences between drugs (small molecules) and biologics are shown below in table 1.1.

Property	Small molecules	Biologics
Manufacture	made by chemical synthesis	biotechnologically produced by host cell lines
Size	Small (<500Da)	Large (>1000Da)
Structure	Defined structure	Heterogeneous structure
Physiochemical properties	Well defined	complex properties
Entry into blood	enter systemic circulation through blood capillaries	larger molecules reach blood via lymphatic system
Route of administration	Oral administration	Parenterally administered

Table 1.1: Difference between small molecules and biologics: *Based on several properties such as manufacture, size, structure, physiochemical properties, entry into blood and route of administration, both small molecules and biologics have been compared [5]*

From a biologics point of view, approval of Adalimumab (manufactured by AbbVie and Zydus Cadila) for the treatment of rheumatoid arthritis provides an insight into monoclonal antibodies as the fastest growing and most promising category of biologics. Adalimumab (also called Humira) binds to TNFα which normally binds to TNFα receptors and best evaluated for use in treatment of inflammatory joint disease. An issue that is always associated with biologics is the high cost of production as on average it costs $1.2 billion to bring a new biologic agent into the market [11]. This cost includes basic laboratory research, pre-clinical testing, clinical trials and production. For producing an effective pre-clinical model study for any biological tool, it is important to choose a relevant animal that is pharmacologically responsive to therapies. Other important factors for biologics to succeed in the clinic include its ability to bind to the target in animal model as well as in its human counterpart. Here we focus on the application of monoclonal antibodies and peptide aptamers as important biological tools to different targets in order to develop therapeutic tools.

1.1.2. Immunotherapy

Immunotherapy is a biologic treatment which is classified into active and passive types based on its mode of action. Introduction of immunotherapy has resulted in providing long term immunity to various diseases that operate by boosting the body's natural defence mechanisms. Active immunotherapy has been useful in fighting and inducing immunity against self-limiting infections which requires the interaction of antigen presenting cells (APCs) and T cells. Immunotherapy has potential applications such as induction of long term immune response and has been implicated in treatment of various diseases such as anaphylaxis, asthma, cancer, etc. In comparison to conventional immunotherapy, modern immunotherapy is safer as it is capable of producing T cell responses with minimized risk of developing anaphylaxis [12]. Effective vaccines (type of active immunotherapy) have been developed against infectious agents such as typhoid, cholera, rabies, hepatitis B, mumps, tetanus and diphtheria toxins [13]. Types of vaccines developed include peptide, dendritic cells, whole tumor cell and viral vector vaccines. In fact preclinical studies indicate that combination of therapies might assist in enhancing initiating immune response causing destruction at the desired site. A major disadvantage with active immunotherapy is that it is much less effective against some diseases including cancer that have developed ways to escape immune response by different means. The best available example from effective active immunotherapy is cytotoxic T lymphocyte antigen-4 against which negative immunoregulatory mechanisms become potent in order to avoid destructive mechanisms that could further lead to disease [14].

Another type of immunotherapy is passive immunotherapy which involves all possible biological tools that target a specific antigen within a disease, for example monoclonal antibodies, drug conjugates, etc. Monoclonal antibodies by far have been the most attractive and effective tool with several modifications designed to increase their affinity, tissue penetrability and effective response following therapy. Antibodies have been used in conjugation with toxins, for example anti-CD25 (LMB-2) or anti-CD22 specific antibody has successfully induced remissions in hairy cell leukemia patients [15]. Another approach to passive immunotherapy

includes radioimmunoconjugates that delivers radioactivity to the tumor site to achieve high efficacy. Combined therapies such as monoclonal antibodies combined with cancer cell vaccine have managed to increase the uptake of cells and enhanced expression of co-stimulatory on dendritic cells triggering greater specific immune response compared with an agent alone [16].

1.2. Target selection for antibody therapy

Selection of target is one of the major criteria to be considered towards development of monoclonal antibodies and two different approaches have been assigned to target selection. The first approach is based on the targets that have already been validated using biological tools or known to be clinically relevant based on available literature. The second approach is mainly focussed on targets newly identified via proteomic studies using tissue biopsies, fluid samples, etc. It is very important to identify the relative expression pattern of a chosen target in normal and affected cells, treatment should be planned in such a manner that it does not affect normal cells. Once a suitable target has been identified, immunotherapy becomes an ideal tool for specifically targeting the antigen without affecting normal cells. Passive immunization has gained its clinical relevance with more than 30 monoclonal antibodies approved against various diseases following success with in-vivo studies and minimal side effects. First generation antibodies such as Rituximab, trastuzumab and Cetuximab are directed against well validated targets i.e. CD20, HER2 and EGFR respectively [17].

Following the success of first generation monoclonal antibodies, antibodies were either modified or targeted to a different epitope onto the same target eliciting a different mechanism of action. These modified antibodies are described as second or third generation antibodies. Second generation antibodies include modifications in the variable domains, increasing the affinity of the antibody and also various antibody fragments targeting antigen [18]. The examples of second generation class of antibodies is ofatumamab which is more human in nature and was developed following Rituximab as well as Adalimumab [17]. The third generation of antibodies is more focused on triggering other mechanisms of action and these are engineered to improve half-life and Fc mediated activity [18]. An example of a third generation

antibody is obinutuzumab targeting CD20 is found to be less immunogenic as compared to rituximab and is engineered to increase cytotoxic effects [19]. This immunogenicity is attributed to its different mechanism of action and also due to the fact that it is glyco-engineered to trigger increased cytotoxicity[20].

1.3. Monoclonal antibody (Full length IgG)

An antibody is a specialized immune glycoprotein secreted by B cells which is produced in response to the introduction of an antigen within the body and possesses the ability to neutralize the antigen. Such glycoproteins are divided into two: polyclonal and monoclonal antibodies, where polyclonal antibodies indicate the production of a pool of antibodies against different epitopes and possess a risk of antibodies cross reacting with other biomolecules containing similar epitopes. To circumvent this issue, concept of monoclonal antibodies has resulted in an antibody binding to a specific epitope of the target antigen. With the invention in 1970s by Kohler and Milstein, monoclonal antibodies have taken a strong hold in the area of clinical research where it is defined as magic bullet against tumour antigens as well as several other diseases [21].

The standard protocol developed by Kohler and Milstein (figure 1.1) initiated with immunization of a suitable animal with target of interest. Once a suitable antibody titre is obtained, the immunized animal is sacrificed and splenocytes are recovered. The splenocytes were then fused with myeloma cells using polyethylene glycol (PEG), the fused hybridoma cells are selected in a medium that supports hybridoma survival. The cells are cultured in hypoxanthine aminopterin thymidine (HAT) medium where aminopterin plays a major role in blocking de novo synthesis or purines and pyrimidines required for DNA synthesis. This is when the cells use salvage pathway and the enzymes involved in this selection pathway are Thymidine kinase and Hypoxanthine-Guanine Phosphoribosyl Transferase (HGPRT). The myelomas lack HGPRT, thus unfused myeloma cells cannot proliferate in the medium and ultimately die, however the unfused splenocytes do possess HGPRT but only have a limited lifetime and thus die within two weeks. The hybridoma cells then grow indefinitely in the selection medium. Many hybridoma cells are obtained following this fusion protocol and each might have a different specificity towards the

immunized target. To identify the specifically binding candidate, hybridoma cell supernatants are tested via limiting dilution onto target of interest using Enzyme linked Immunosorbent Assay (ELISA). Following screening, a well containing a single positive cell is selected and cloned for stable expression of hybridoma so that it does not lose its potential ability to produce monoclonal antibody.

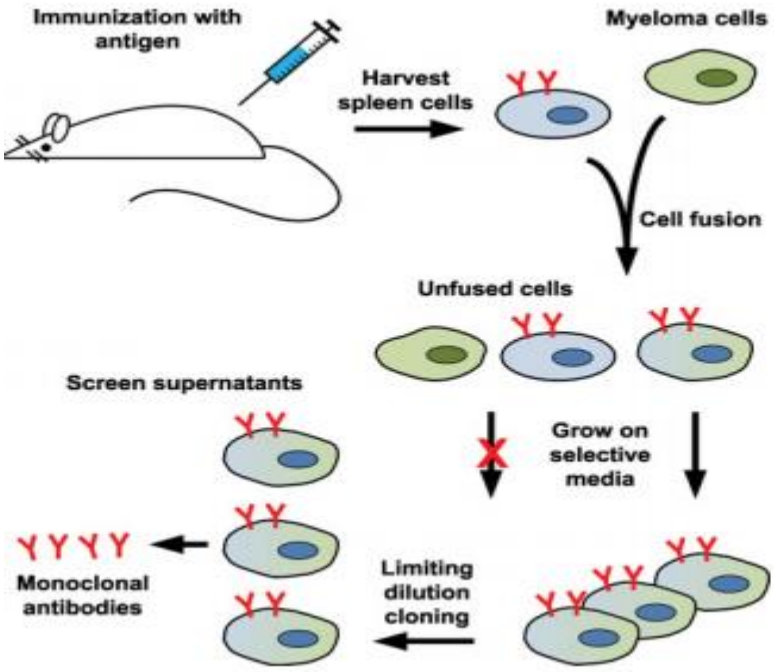

Figure 1.1: Production of monoclonal antibody: *Mice immunized with antigen of interest, following cycles of immunizations mice sacrificed and spleen/ B cells isolated. These B cells producing antibodies are fused with myeloma cells to obtain hybridoma population. Individual hybridomas are tested onto ELISA plate coated with antigen by limiting dilution [6].*

The advent of hybridoma technology has enabled researchers to produce large quantities of monoclonal antibody by immortalizing the antibody producing B lymphocytes from the spleen of immunized mice. In 1986, the first ever monoclonal antibody (OKT3) targeting CD3 was approved by US Food and Drug administration (FDA) for use in treating patients with acute transplant rejection and is used as a drug in humans [22]. Since then, the field of antibody therapeutics has flourished and has gained immense clinical significance against different types of diseases. In the past 25 years according to the antibody society more than 30 monoclonal antibodies have been approved and many have been under pre-clinical and clinical trials (table 1.2).

A key criterion to be considered for development of antibody therapeutics is to identify a suitable target in the disease. The antibody can induce anti-tumor effects via a range of mechanisms such as mediating alteration in antigen, activating immune modulatory functions such as involvement of T cells and Fc receptors or lastly by drug conjugate targeting at the tumor site [23-25]. Recent advances in antibody engineering as well as molecular biology have resulted in the development of various manipulative forms of antibodies such as humanized, chimeric and fully human antibodies with an aim to overcome the issues such as human anti-mouse antibody response raised by mouse monoclonal antibodies [25]. Table 1.2 shows monoclonal antibodies approved till date and also antibodies in final stage of clinical trials.

Generic name	**Trade name**	**Antibody format**	**Antigen**	**Target disease**	**Sponser**
Muromomab	Orthoclone	Murine IgG2a	CD3	Allograft rejection in allogenic renal transplantation	Ortho Biotech Inc
Abciximab	Reopro	Chimeric Fab	GPIIb/IIIa receptor	Prevention of cardiac ishemic complications	Centocor
Rituximab	Rituxan	Chimeric IgG	CD20	Non-Hodgkin's lymphoms, chronic lymphoms leukemia and rheumatid arthritis	Genentech and Biogen Idec
Daclizumab	Zenapax	humanized IgG1κ	IL-2Rα	Prophylaxis of acute organ rejection in renal transplants	Hoffman-La Roche
Basiliximab	Simulect	chimeric IgG1κ	IL-2Rα	Prophylaxis of acute organ rejection in renal transplants	Novartis
Palivizumab	Synagis	humanized IgG1κ	RSV F protein	Respiratory syncytial virus infection	Medimmune
Infliximab	Remicade	chimeric IgG1κ	TNFα	crohn's disease and rheumatoid arthritis	Centocor
Trastuzumab	Herceptin	humanized IgG1κ	Her2	Breast cancer	Genentech
Gemtuzumab Ozogamicin	Mylotarg	chalicheamicin-humanized IgG4κ	CD33	Acute myeloid leukemia	Wyeth/Pfizer
Alemtuzumab	Campath	humanized IgG1κ	CD52	B cell chronic lymphocytic leukemia	Ilex/Genzyme
Ibritumomab	Zevalin	Y^{90}- murine IgG1κ	CD20	B cell lymphoma non-Hodgkin's lymphoma	Biogen Idec/ Spectrum
Adalimumab	Humira	human IgG1κ	TNFα	Rheumatoid arthritis and Crohn's diseases	Abbott
Omalizumab	Xolair	humanized	IgE	Moderate to severe	Genentech

		IgG1κ		persistant asthma	
Tositumomab	Bexxar	I^{131}- murine IgG2aλ	CD20	Non-Hodgkin's lymphoma	Corixa
Efalizumab	Raptiva	humanized IgG1κ	CD11a	Moderate to severe plaque psoriasis	Genentech
Cetuximab	Erbitux	chimeric IgG1κ	EGFR	Head and neck cancer, colorectal cancer	Inclone/ BMS/ Merch
Bevacizumab	Avastin	humanized IgG1κ	VEGF-A	various solid tumors	Genentech
Natalizumab	Tysabri	humanized IgG4κ	α4-integrin	multiple sclerosis and Crohn's disease	Biogen Idec/Elan
Ranibizumab	Lucentis	humanized Fab	VEGF-A	Age related macular degeneration	Genentech
Panizumumab	Vectibix	human IgG2κ	EGFR	Metastatic colorectal carcinoma	Amgen
Eculizumab	Soliris	humanized IgG2/4κ	C5	Paroxysmal nocturnal hemoglobinuria	Alexion
Certolizumab	Cimzia	Peglated humanized Fab	TNFα	Crohns disease and rheumatoid arthritis	UCB, Inc
Golimumab	Simponi	human IgG1κ	TNFα	Rheumatoid arthritis, psoriatic arthritis and ankylosing spondlylitis	Centocor Ortho Biotech
Canakinumab	Ilaris	human IgG1κ	IL-1β	Cryopyrin-associated periodic syndromes	Novartis
Ustekinumab	Stelara	human IgG1κ	IL-12/IL-23	Plaque psoriasis	Centocor Ortho Biotech
Ofatumumab	Arzerra	human IgG1κ	CD20	Chronic lymphocytic leukemia	Glaxo Grp ltd
Tocilizumab	Actemra	humanized IgG1κ	IL-6R	Rheumatoid arthritis	Roche/Chu gai
Denosumab	Prolia	human IgG2κ	RANK ligand	Postmenopausal women with risk of psteoporosis	Amgen
Catumaxomab	Removab	murine/rat hybrid IgG	EpCAM and CD3	Intraperitoneal treatment of malignant ascites in patients with EpCAN-positive carcinomas	TRION Pharma
Edrecolomab	Panorex	murine IgG2a	EpCAM	Colon cancer	Wellcome/ Centocor
I^{131}- TNT	Cotara	I^{131}-chimeric IgG1	DNA	Lung cancer	MediPharm Biotech
Nimotuzumab	Theracim	humanized IgG1	EGFR	Nasopharyngeal carcinomas and head and neck tumors	CIM/CIM AB/YM Bioscience
Belimumab	Benlysta	human IgG1	BLyS	Systemic lupus erythematosus	GSK
Ipilimumab	Yervoy	human IgG1	CTLA-4	Metastatic melanoma	Bristol-Myers Squibb Australia Pty Ltd

Brentuximab vedotin	Adcretis	chimeric IgG1	CD30	Hodgkin lymphoma	Takeda Pharma A/S, Denmark
Pertuzumab	Perjeta	humanized IgG1	HER2	Breast cancer	Genentech
Raxibacumab	(Pending)	human IgG1	B anthrasis PA	Anthrax infection	Human Genome Sciences Inc.
Trastuzumab emtansine	Kadcyla	humanized IgG1 immunoconjugate	HER2	Breast cancer	Hoffman La-Roche
Vedolizumab	Entyvio	humanized IgG1	αβ7 integrin	Ulcerative colitis, Crohn's disease	Millenniu m. Pharmaceu ticals Inc.

Table 1.2: Approved monoclonal antibodies: *Different types of monoclonal antibodies (including conjugates) approved against various targets. The table shows mAb targets, Ab formats, type of disease and manufacturing company [4].*

1.3.1. Structure of antibodies

Monoclonal antibodies are large molecules and each molecule is comprised of two larger subunits known as heavy chains (50 kDa) and two smaller subunits i.e. light chains (23 kDa). The antibodies are classified into 5 different subtypes on the basis of their heavy chain constant regions IgM, IgG, IgA, IgE and IgD. IgG, IgD and IgE possess a common Y-shaped structure, with IgM being pentameric in nature. IgG is a monomeric immunoglobulin and has a molecular weight of 150 kDa and is the most widely studied immunoglobulin because of its higher occurrence in the human body. It is the most versatile immunoglobulin and forms the major part (75%) of the whole Ig content of serum in the body. Moreover, it is the only class that crosses the placenta and is further subdivided into 4 different classes: IgG1, IgG2, IgG3 and IgG4. The heavy and light chains are annealed together by a disulphide bonds and on the basis of similarity of amino acid sequence each chain is further classified into variable and constant domains. Another fragment of antibody not known to bind antigen is called the Fc (fragment crystallizable) portion of antibody. Within the Fab region (region excluding Fc), the regions with greatest variability are described as hypervariable regions or complementary determining regions (CDRs) and further

classified into CDR1, CDR2 and CDR3 from the amino terminus of the antibody molecule. Intervening regions between three different CDRs contain amino acids that have less variability among them and are described as framework residues. The light chain of IgG is composed of two domains VL and CL, whereas heavy chain is composed of VL and CH1, CH2 and CH3. Also the light chains are of two different types, namely kappa (κ) and lambda (λ) light chain, but only a single type of light chain is thought to occur within any single antibody molecule. According to experiments carried out by Porter it was demonstrated that the antigen binding site is embedded in the Fab portion of the antibody whereas Fc portion binds to various cell receptors. Fc region of antibody binds to receptors such as Fc receptors and immune cells and mediates effector functions to the antibody [26].

The Fc portion which is composed of hinge region and constant domains (CH2 and CH3) communicates with immune system for induction of effector functions such as antibody dependent cellular cytotoxicity (ADCC), antibody dependent cellular phagocytosis (ADCP) and complement dependent cytotoxicity (CDC). Among the four known IgG isotype, IgG4 possesses a unique property of monovalency and bispecificity which is due to the presence of CPSCP instead of CPPCP sequences (IgG1) in the hinge region [27]. This leads to interchain as well as intrachain disulphide bonds within each heavy chain which can further cause dissociation of heavy chain form each other. The structure of the whole antibody molecule along with its antigen binding sites is shown in figure 1.2.

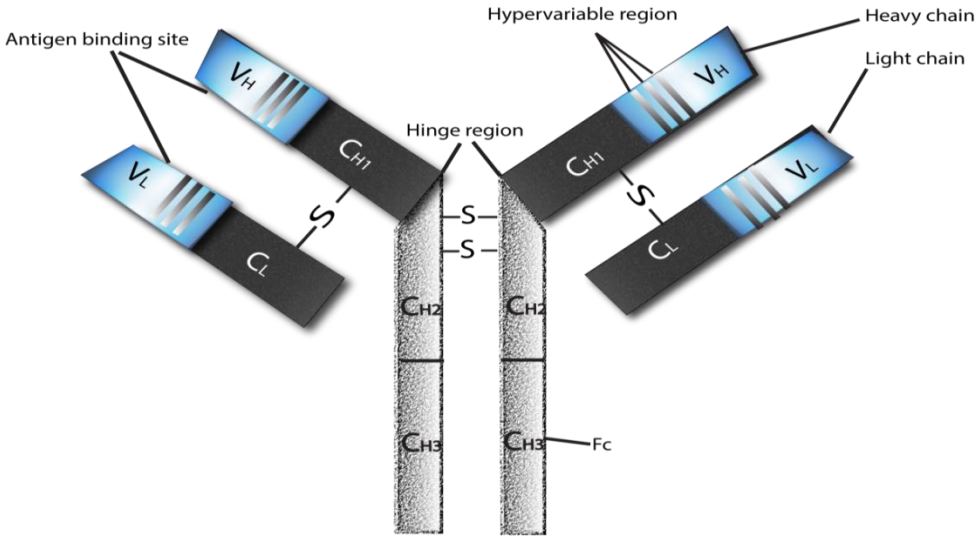

Figure 1.2: Structure of an antibody molecule: *Heavy and light chains both containing constant as well as variable domains connected by disulphide bonds. The antigen binding site resides in the variable domains of both chains. Variable domains contain complementary determining regions (CDRs) and framework regions that highly assist in antigen binding. Heavy chain constant domain is divided into three parts i.e. CH1, CH2 and CH3 where both CH2 and CH3 form Fc portion of the antibody responsible for its effector functions.*

1.3.2. Selection criteria for monoclonal antibodies

Based on the origin of the monoclonal antibody, it can be classified into 4 different categories: (i) murine antibodies, (ii) chimeric antibodies, (iii) humanized antibodies and (iv) human antibodies. Infact, the most difficult step in developing a monoclonal antibody is the target selection and biochemical pathways that might be associated with it. To start with, one has to preferentially choose a target that is expressed only on the tumor cell; however this is not possible in all the cases. Thus for developing antibody therapeutics, targets should be present in a limited number of cell types and highly expressed on tumor cells. One such example is mAb trastuzumab targeting HER-2 which is present in a limited number of cell types and overexpressed in at least 30% of breast cancers [28, 29].

Mouse monoclonal antibodies were first among the antibody tools obtained from immunized mice and to show any activity in inducing anti-tumor effects. As the name suggests murine antibodies are totally murine in nature which contributes to their immunogenicity. However there are a few limitations to mouse monoclonal antibodies, (i) high immunogenicity of these foreign proteins in humans leading to development of human anti- murine antibody (HAMA) response which restricts repetitive dosing of antibody [30-32]. This immunogenicity is the result of human immune system recognising murine antibodies as foreign materials and thus in turn developing antibodies against such proteins, (ii) relatively shorter circulating half-life compared to human antibodies [33]. To circumvent these limitations, various attempts were made with the help of genetic engineering to overcome immunogenicity either by developing chimeric, humanized or human antibodies.

1.4. Recombinant antibodies

1.4.1. Developmental trends in antibody

To overcome very well defined issues associated with mouse monoclonal antibodies, recombinant antibodies have been developed. Recombinant antibodies have been classified into two different types: Type 1 comprises of full length antibodies with changes in variable domains i.e. chimeric and humanized antibodies, whereas type 2 includes all antibody fragments that have been engineered from the mAb. Recombinant DNA technology has been applied to construct chimeric antibodies that comprise the variable region of the mouse antibody annealed to the constant region of the human antibody thus retaining the binding efficiency of the original monoclonal antibody and reducing introduction of foreign material within the body [34]. Moreover, improved ADCC and other types of anti-tumor effects have been reported with chimeric antibodies [34]. Since the whole variable region is still of mouse origin, there is still considerable risk of immunogenicity in some patients, known as human anti-chimeric antibody (HACA) responses.

Soon after the introduction of chimeric antibodies, the concept of 'reshaping antibodies', now called humanized antibodies evolved with an aim of improved anti-tumor effects and less immunogenicity. The development of a humanized antibody involves substitution of mouse CDRs that contain the antigen binding site and Fc portion by human germline amino acids [35]. Thus around 90-95% sequences are of human origin and 5-10% of sequences are murine in nature [36]. One main issue with chimerization or humanization is the binding affinity of the final antibody could be reduced if the certain murine sequences that play a role in antigen binding are not transferred to the final modified antibody molecule. To overcome such issues raised by murine, humanized or chimeric antibody, several attempts have been made to develop fully human antibodies which would in principle have minimal immunogenicity in humans. Currently available techniques to develop human antibodies include phage display of libraries, transgenic mice, human-human hybridoma, B cell immortalization, Hybrid hybridoma and cloning which are explained briefly below:

Phage display is a very well-known candidate for developing human antibodies that involves displaying of human antibody onto engineered bacteriophage [37]. Each phage displays a different antibody on its surface and such phage displaying antibodies are then selected for binding to antigen. The benefit of phage display is the diversity of the antibodies obtained from the huge size of the libraries. This in turn can lead to a number of antibodies from the same library targeting different epitopes on the same protein. A major advantage that phage displaying antibodies hold over other available candidates is the ease of obtaining antibodies and also it avoids the need for immunization of animals. There have been two types of vectors involved in order to favour display of antibodies onto phage i.e. phage vector and phagemid vector. Phagemid vectors advantages over phage vectors such as better transformation efficiency and can also be modified for direct secretion into the periplasmic space without subcloning [38]. Similarly, displaying antibody fragments onto yeast provides an advantage of post-translational modifications to the antibodies which does not occur in prokaryotes, however these modifications might differ when antibodies are administered in humans [39]. However the antibodies obtained initially might elicit low affinity towards the target; some optimizations such as affinity maturation might be needed in order to increase the affinity of the antibody. Adalimumab was the first monoclonal antibody derived from phage display that was approved by FDA for treatment of rheumatoid arthritis [40]. The use of transgenic mice is another way of developing human antibodies by genetically engineering the mice with humanized humoral immune system and the remaining components remain murine in nature. Thus, the antibodies can be obtained by standard hybridoma technology and such obtained proteins are highly human in nature.

1.4.2. Antibody fragments

In the recent past, 'Engineered antibodies' have made a significant impact on the biotechnological market with their ability to genetically manipulate antibody fragments [41]. The trouble with full length antibodies is sometimes their longer serum half-life which can lead to inappropriate activation of Fc receptor expressing cells, ultimately causing undesirable cytokine release and toxic effects [42]. Moreover even if the binding efficiency of the IgG is significantly higher in vitro, its

binding ability in-vivo always remains a question to be answered. It has been demonstrated that the half-life of such fragments can be increased from a few hours to weeks through PEGylation i.e. conjugation to PEG (polyethylene glycol) [43]. The selection of antibody fragments (scFv or Fab) is carried out by phage display, however with growing antibody engineering techniques scFv and Fabs have been reformatted into a recombinant IgG which is often required for functional assays. For improving the antibody fragments pharmacokinetics, two studies using scFv diabody and Fab have indicated glycosylation to be highly effective in increasing the half-life by at least two fold along with increased tumor uptake [44, 45]. These antibody fragments have also been modified by either linking Fc to only variable domains of heavy and light chains or by dimerizing scFv or Fab. Various formats of antibodies show different expression and solubility levels depending upon their folding nature, different formats of antibody have been shown below in figure 1.3.

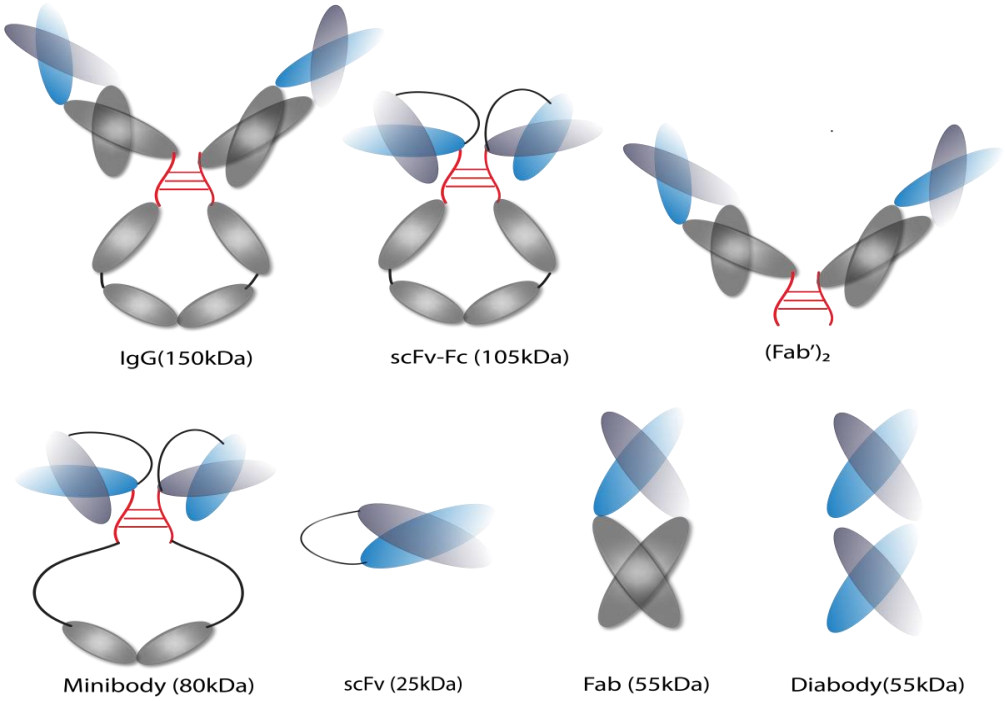

Figure 1.3: Antibody formats: *Top panel shows full length IgG molecule, scFv (annealed heavy and light chain variable domains) linked to Fc region and lastly Fab region containing variable and constant domains from heavy and light chains with no Fc portion of antibody. Lower panel shows minibody containing only variable domains attached to CH3 domain of Fc portion, scFv containing only variable heavy and light chain domains connected by a flexible linker, Fab containing both variable and constant domains of heavy and light chain with no Fc region and diabodies formed by linkage of two scFvs.*

Importantly, IgG form of antibody can be expressed in *E.coli* but is inefficient in binding to the target due to minimized glycosylation and therefore it becomes necessary to clone the V regions from the antibody into expression constructs containing remaining parts of IgG [46]. The first attempt in expressing recombinant antibodies did not succeed due to improper folding and aggregation of polypeptides in the bacterial cytoplasm [41, 47]. The breakthrough for competent *E.coli* expression of antibody fragments was brought about by introducing phagemid vectors which offers soluble antibody secretion directly into the cytoplasm by means of oxidising environment [48, 49]. The oxidising environment facilitates correct folding of disulphide bonds in cytoplasm by exchanging cysteine residues and importantly can vary depending upon antibody class [50]. Following the success of scFv expression, phage display technology has been widely used to express other fragments such as Fab [51], di-sulphide stabilized fragments [52] and diabodies [53] onto phage. In comparison to the parental antibody, antibody fragments are much shorter in length and retain the antigen binding sites of the antibody. These antibody fragments have several advantages over full length mAb such as better penetration, more rapid blood clearance and lower immunogenicity. Different types of antibody fragments are described below.

Fragment antigen binding (Fab)

Fragment antigen binding (Fab) is a monovalent antibody fragment with a molecular weight of 50 kDa containing only a single antigen binding site. It is composed of a single variable domain and one constant domain of each of heavy and light chain. Papain cleavage is used to create two Fab fragments and a Fc fragment, whereas enzyme pepsin cleaves below the hinge region and yields $F(ab)_2$ and partial Fc region fragments. These agents are the oldest and most successful among antibody fragment therapeutics and account for 49% of all antibody fragments to have entered clinical trials [54]. Jostock *et al* reported the first fully recombinant IgG constructed from Fab construct developed using phage display against Tie-1, a receptor tyrosine kinase involved in angiogenesis [55]. They nearly account for 50% of all identified antibody

fragments that enter clinical trials and are more stable for storage as compared to full length IgG [56].

Single chain fragment variable (scFv)

Single chain fragment variable (scFv) antibody is made up of a variable domain of heavy chain (V_H) connected by a flexible peptide linker to the variable domain of light chain (V_L) which is about 35 nm in length and both orientations of scFv i.e. VH-L-VL and VL-L-VH have been made. It is important that the peptide linker does not interrupt the proper folding of the scFv when expressed in bacteria. The most extensively used linker to anneal the variable heavy and light chains is composed of Glycine and serine residues which provides flexibility and enhances solubilisation [57]. One of the most popular methods for annealing is PCR which was first described by Horton *et al* [58]. The annealed product can be ligated into a phage or phagemid vector, followed by transformation in order to construct the antibody library [59]. Antibody engineering has enabled researchers to develop scFv linked to another scFv resulting in diabodies which might increase the serum half-life and also its binding affinity. Also with sophisticated molecular biology and rational modelling techniques available now, several modified formats such as complementary scFv and bispecific tandem scFv have been constructed [60]. Interestingly, shortening of the length of the linker by three residues could promote formation of trimers or tetramers depending on the length of linker and also the orientation of the variable heavy and light chain domains [61-63]. Use of scFv as a potential tool for cancer therapy has gained significant clinical importance in the recent past by facilitating different effector functions [64].

1.5. Phage display

1.5.1. Concept and types of phage display

The concept of linkage of foreign DNA fragments with gene III coat protein of a non-lytic filamentous phage was first revealed by Smith in 1985 [65]. Five years

later, McCafferty et al [66] demonstrated for the first time that scFv could be displayed on the surface of the virion as a functional protein retaining its antigen binding capacity. pCOMB3xSS is the most common phagemid vector used for antibody expression [67], all the structure proteins needed for phage packaging are provided by M13KO7 that acts as a helper phage. Several formats of antibody fragments have been displayed onto phage such as scFv, Fabs and diabody fragments [66, 68, 69]. A Phage displaying antibody library can be easily constructed with huge library size as shown in figure 1.4. Depending upon the origin of the antibody, three types of antibody libraries have been described i.e. immune libraries, naïve libraries and synthetic libraries.

(i) Immune libraries: Variable domain repertoires can be created from B cells obtained from mice immunized with the target of interest. As compared to a library made from hybridoma cells, library made from spleen might give better diversity but also contain non-specific antibodies. The construction of such libraries has been carried out in various species such as chicken [70, 71], humans [72, 73], mouse [68, 74, 75], rabbit and camels [76]. The biggest advantage of immune libraries is the variable genes that encode antibodies are biased towards a specific target. However this can also be considered as a potential drawback as for each target, a new phage library has to be constructed each time from B cells following immunization of mice which can take upto three months.

(ii) Naïve libraries (libraries from non-immunized donors): Such unbiased libraries provide an advantage as they contain antibodies to a range of targets including self, non-immunogenic, toxic antigens and are constructed from B cells of unimmunized human donors. The affinity of an antibody towards a specific target varies proportionally with size of the library [77]. The reliable source of variable domains amplification is either IgM mRNA or total mRNA, as building libraries from IgG mRNA do not perform well due to unrelated immune response [78].

(iii) Synthetic libraries: In this case, antibody is built artificially by in-vitro assembly (PCR) of variable gene segments and D/J segments with highly optimized human frameworks [79]. Most structural and sequence diversity is found in CDR3 region of the heavy chain, with the other five CDRs possessing limited

variation [80]. High affinity antibodies can be generated against most antigens by introducing diversity in particular positions within four of all six CDRs. Independent of the origin of the antibody, optimizations might be needed to increase the affinity of the antibody which can be achieved by affinity maturation. This essentially involves introduction of diversity in the V regions which might be achieved by error prone PCR [81], chain shuffling [69], DNA shuffling [82] and oligonucleotide directed mutagenesis [83].

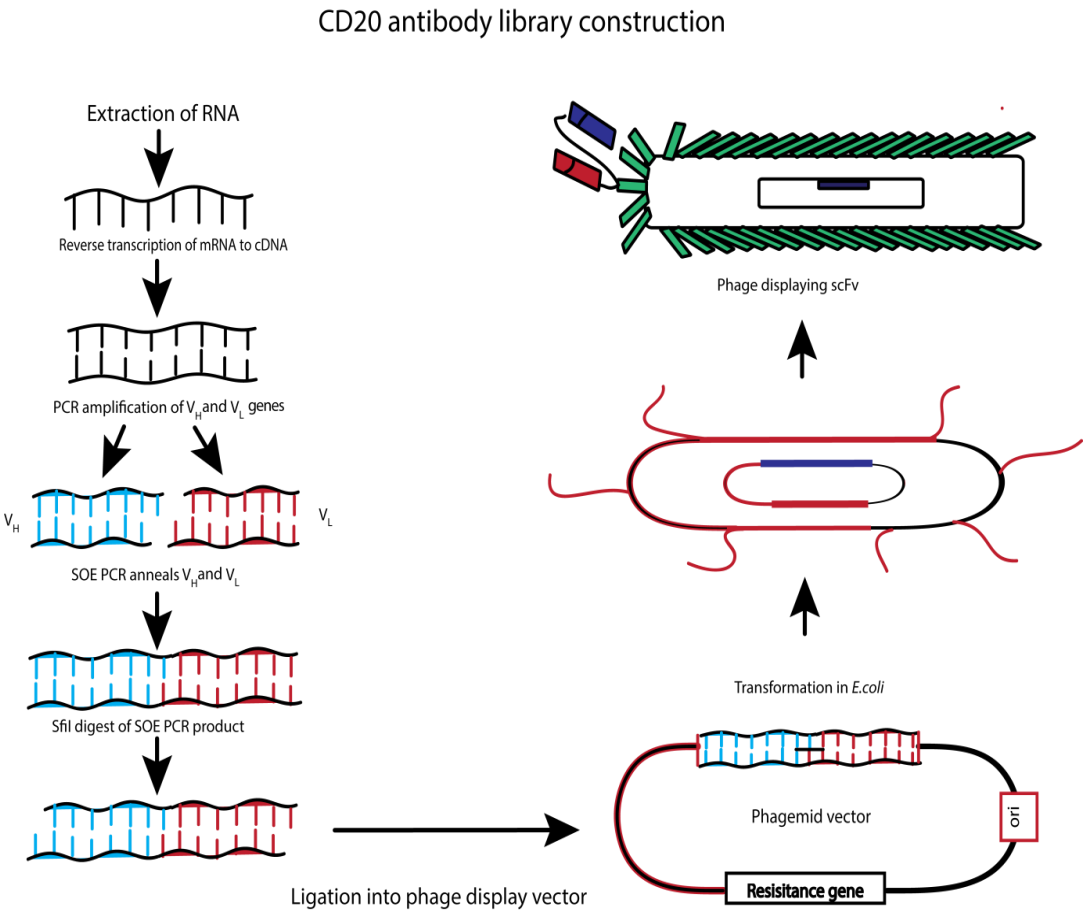

Figure 1.4: Construction of antibody library: *Following hybridoma technology mRNA was isolated from antibody producing cells; prepared cDNA from RNA was used to amplify variable domains of heavy and light chains via PCR. These variable regions were annealed using a glycine serine linker by second round of PCR, subsequently purified products digested along with vector DNA and finally ligated into phagemid vector to represent phage displaying scFv*

The activity of the scFv has been modified by fusing scFv with radioisotopes for cancer imaging [84-86], enzymes in Antibody directed enzyme prodrug therapy (ADEPT) [87], toxins for targeted tumor cell targeting [88] and biosensors for real time detection of target molecules. scFv antibody fragments are known to diffuse 6 times faster than IgG due to their small size [89]. These tools have been developed against hapten [90], receptors [91], tumor antigens [92, 93], carbohydrates [94] and proteins [95] with high potential for diagnostic or therapeutic applications.

1.5.2. Different species for phage display

Chimpanzee: Chimpanzees have been employed as another species for production of monoclonal antibodies to human targets. The variable regions have been cloned from immunized chimpanzees and a panel of antibodies has been identified in a study carried out against antigen DENV- 4 [96]. One of the positive clones from the panel was cloned with human sequences to construct humanized IgG1for expression in CHO cells [96]. Chimpanzees are highly genetically similar to humans [97], for this reason it is very likely that the effector functions imparted by Fc portion of chimpanzee antibody (cmAbs) could be highly functional in case of humans. However on few occasions it has been shown that cmAb might not bind to its human counterpart or other related species [98].

Mouse: Antibody fragments have been constructed from hybridoma as well as splenic cells obtained from immunized mice on various occasions. Following the advent of hybridoma technology, mouse models have become an ideal candidate for production of antibody fragments from different sources such as spleen and hybridoma cells. In fact from a combinatorial immunotherapy point of view, mice immunized with phage displaying scFv instead of soluble scFv could result in the production of anti-idiotypic antibodies which could provide insights into immune response [64].

Camelids: Although significant efforts have led to construction of scFv and Fabs in various species, it was not until 1993 when Hamers- Casterman discovered an unique type of antibody in species called Camlids [99]. In sera of camelids, classical antibody isotype as well as heavy chain antibodies (HCAbs) have been identified and

each of them contributes to the immune response of these animals. Studies with camelid antibodies have indicated the occurrence of three different isotypes: IgG1, IgG2 and IgG3, out of which IgG1resembles a conventional monoclonal antibody whereas IgG2 and IgG3 do not associate with the light chains [99]. The antigen binding site resides in a single domain defined as VHH or nanobody and is the smallest effective molecule with respect to the binding efficiency. The main difference between VH and VHH is based on amino acid length, CDR1 and CDR3 are much longer in the case of VHH as compared to VH [100]. Also VH contains more hydrophobic amino acids, whereas VHH contain more hydrophilic bonds providing an evidence for absence of VL association [101]. Studies have indicated the possibility of retrieving useful binders using a naive camelid library [100].

Rabbits: Since some epitopes are not immunogenic in mice, another species might provide an advantage of being immunogenic and eliciting an immune response. Polyclonal rabbit antibodies have already been implicated in diagnostic applications and since then rabbits have been an interesting choice for production of antibodies. Rabbit mAbs have been utilized for decades now and have become an outstanding source for production of antibodies with high binding affinity and specificity [102]. Rabbit antibody fragments (scFv or Fab) have been displayed on phage usually via PCR similar to antibody fragments expressed in other species. Antibody fragments from this species have shown therapeutic potential in chronic lymphocytic leukemia cells [103]. From the immunized rabbits, antibody fragments were displayed onto phage and Rader et al for the first time reported humanization of such fragments [104]. Interestingly unlike human and mice, rabbits possess two different types of kappa light chains (K1 and K2) in which the dominating light chain is K1 [105].

Sharks: In cartilaginous fishes such as sharks, a new member of immunoglobulin has been reported from a nurse shark species *Ginglymostoma cirratum* [106]. This member similar to camelid antibodies does not possess any light chain and contains one variable as well as five constant domains in serum. Moreover these single domain (IgNAR) antibody fragments from immunized sharks have been well characterized via phage display [107]. It has been demonstrated by Dooley et al that

IgNAR antibody isolated against HEL are highly stable, highly specific and binds to HEL in nanomolar range [107].

Chicken: The variable domains of the chicken antibodies are similar to those in humans, however the constant heavy region has an extra domain i.e. CH4.The production and extraction of antibodies from egg yolk (IgY) exhibits high stability to pH as well as temperature changes [108]. For construction of chicken antibody library, only single 5' primer is required in contrast to mammalian variable gene amplification primers [109]. These study models could be preferred over mice models in future as they are known to exhibit more vigorous immune response. Jennifer *et al* constructed three different types (scFv, diabody and Fab) libraries from bone marrow against BSA [110]. Chicken antibody might offer several advantages such as large quantity of antibody production and has led to decreased background in immunological assays due to phylogenetic differences between avian and mammalian species.

Canine: Following the discovery and similarity of canine genome with humans, it was realized that use of dogs as a companion model could be an important step from veterinary care point of view. Recently canine specific antibody against CD52 (Aratana therapeutics) has been approved for treatment of T cell lymphoma in dogs. Antibody fragment libraries from such species have been constructed either from immunized dog or from spleen of domestic dogs. With the need for more useful animal models in human disease drug development, canine models offer a close linkage to its human counterpart. For the first time Andrea et al described the designing of degenerative primers for amplification of variable heavy and light chains to construct scFv [111].

1.5.3. Expression of antibody fragments

As mentioned above, like other antibody fragments scFv is cloned using PCR assembly and finally ligated into the most frequently used phagemid vector pCOMB3XSS followed by electroporation to present the antibody library with each phage representing a scFv. The size of the antibody library is calculated based on the titres and can vary depending upon factors such as efficiency of transformation,

concentration of DNA, etc The specific clones are obtained and selected using a selection procedure carried out on an immunotube described as 'biopanning'. The selection procedure is carried out against the target used for immunization in case of immunized libraries, however in case of naïve libraries it is carried out against target of interests. There are two kinds of bonds in disulphide bonds in an antibody molecule i.e. inter domain bonds which are not present in the scFv and intra domain bonds which are present in immunoglobulin fold and also in scFv. These intra domain bonds are very crucial in maintaining the stability of the antibody [112]. For expression of scFv, prokaryotic expression (*E.coli*) has proved to be the most cost effective and indeed best for solubilizing into periplasmic space as compared to yeast [113], plants [91] and insect cells [114] expression. There have been different strategies used for expression of scFv in *E.coli* with or without signal peptide, in absence of signal peptide the polypeptides are well expressed in bacterial cytoplasm along with formation of insoluble aggregates called inclusion bodies [48, 115]. To circumvent this inclusion body issue, expression using signal peptide directs secretion of scFv into periplasmic space. Also, lac Z is the most common promoter used to control expression and expression is induced by isopropyl β-D-1 thiogalactopyranoside (IPTG).

1.6. Bispecific antibodies

Bispecific antibodies represent another second generation antibody tool which is engineered to bind to two antigens and are capable of inducing immune response. Production of bispecific antibodies was engineered by either chemically cross linking or fusion of hybridoma cell lines containing different antigen binding sites. Currently available platforms employed for development of bispecific antibodies have been described below:

1.6.1. Trifunctional hybrid antibodies

Trifunctional hybrid antibodies (Triomab) is a mixture of portions of two antibodies that has one site binding to the tumor whereas the other site binding to the CD3 expressed on T cell which assists in T cell mediated response. The examples of antibodies developed using this technology are catumaxomab (anti-EpCAM – anti-

CD3), ertumaxomab (anti-HER2–anti-CD3) and FBTA05 (anti-CD20-anti-CD3) [116]. Another recent evolved technology is using scFv to develop either tandem scFv (TaFv) or bispecific diabodies (bsDb).

1.6.2. Small bispecific constructs

Tandem scFv (TaFv) can be constructed by covalently bonding of two different scFv with a flexible peptide linker in a tandem orientation. Bispecific T cell engagers (BiTE) is a type of TaFv that causes cell lysis via formation of synapses between target and effector cells resulting in release of cytotoxic effector molecules [117]. One BiTE that has advanced in the clinical studies is Blinatumomab derived from murine scFvs targeting human CD19 and CD3. Multiple trials are ongoing to determine treatment schedule, clinical efficacy and side effects in NHL and leukemia patients. Other TaFv constructs have been developed targeting different antigens following humanization to avoid HAMA responses and are being evaluated in clinical trials [118].

Bispecific diabodies (bsDb) are formed by non –covalent association of two scFvs, comprising of variable heavy and light chains from a different parental antibody connected by a linker. Both attached chains are oriented in opposite directions but the stability of the antibody might still be a limiting factor as there is a possible chance of disintegration, dimerization and aggregate formation [116]. Based on the length of linker bsDb can be multimerized and increasing the disulphide bonds between the chains might increase stability of the antibody.

Moreover, Fc domain of antibody molecule enhances the serum half – life and hence it is important to consider that the above mentioned antibody fragments may result in quick clearance without showing significant effects. To extend half-life most common techniques that have been employed include PEGylation and N-glycosylation [119]. Such bispecific small antibody tools as compared to IgG (150 kDa) have better tissue penetrance ability and tend to have prolonged target retention with homogenous distribution within tumors [42]. Bispecific antibodies thus provide

a ray of hope with advanced antibody engineering to target antigens and engage effector functions.

1.7. Antibody drug conjugates

The whole idea of drug conjugation is selectively ablating cancer cells by covalently linking monoclonal antibody binding specifically to an antigen with a highly potent cytotoxic agent. The aim behind developing such antibody drug conjugates (ADC) constructs is the enhancement of the mAb activity which can be achieved by selective delivery of highly potent cytotoxic drugs to tumor cells [120]. Several issues were addressed with first generation drug conjugates such as selection of antigen, type of toxin as well as format of the antibody used. Refinement in antibody fragments generation, well studied cytotoxic agents in combination with deeper understanding of targets have led to the emergence of second generation ADCs. The first tumoricidal agents to be linked to monoclonal antibodies were plant derived protein toxins i.e. gelonin, ricin and pokeweed antiviral protein, and bacterial toxins such as Diphtheria toxin [121-123]. The second generation conjugates involved linkage of antibody fragments which are much smaller in size and DNA sequence coding the toxin to facilitate effective tumor targeting.

Another strategy involved covalent linkage of antibody with radionuclide with a goal to deliver sufficiently high dose of radiation to eradicate the tumor while not affecting the normal tissue. The most critical factor in this design is the dose of radionuclide delivered as radiation can easily damage cells that lie in close proximity to tumor cells [124]. Such tools have been developed for treatment for Non-Hodgkin's lymphoma with an FDA approval for two such candidates: ^{131}I-tositumomab (Bexxar) and ^{90}Y- Ibritumomab tiuxetin (Zevalin) [125]. Following these two inventions and significant progress in conjugation studies, in 2000 gemtuzumab ozogamicin became the first ADC to be FDA approved for treatment of acute myelogenous leukemia (AML). However this drug was withdrawn from the market in 2010 as it failed to meet the efficacy targets that were required for approval by FDA. Another two Ab drug conjugate have been approved by FDA, namely trastuzumab emtansine (2013) [126] and brentuximab vedotin (2011) [127] for breast cancer and Hodgkin's lymphoma respectively.

For developing effective ADCs, it is important to determine the water solubility and prolonged stability of the compounds in aqueous formulations and in plasma [124]. Even behaviour of linker is an important factor in developing conjugates as they must be stable in circulation as their cleavage causes release of drug to the target tissue and should ideally increase the solubility [128, 129].

1.7.1. Antibody directed enzyme prodrug therapy (ADEPT)

Antibody directed enzyme conjugated prodrug therapy (ADEPT) is a relatively novel therapeutic approach that uses an enzymatic approach to convert a non-toxic prodrug into an active cytotoxic drug. ADEPT involves a two-step mechanism in order to carry out effective tumor targeting [130]. The first step involves administration of antibody conjugated with enzyme to the tumor site and allowed to accumulate at the tumor site along with clearance from blood and normal tissues. In the second step, a non-toxic prodrug is administered which is converted into a cytotoxic drug by the enzyme that is present in the antibody conjugate [131]. It is very important to characterize the antibody very well by measuring its binding potential to the target before linking it to any enzyme and it was realized that using antibody fragments would be beneficial because of their penetrability advantage over IgGs. On previous occasions, ADEPT has mainly used enzymes of non-human origin to activate the prodrug at the tumor site as the bacterial enzymes have activities orthogonal to the human proteome [132]. The conjugation of antibody to enzyme always raised a question whether enzyme would mask the binding site of antibody and similarly if antibody would mask enzymatic site needed for prodrug activation.

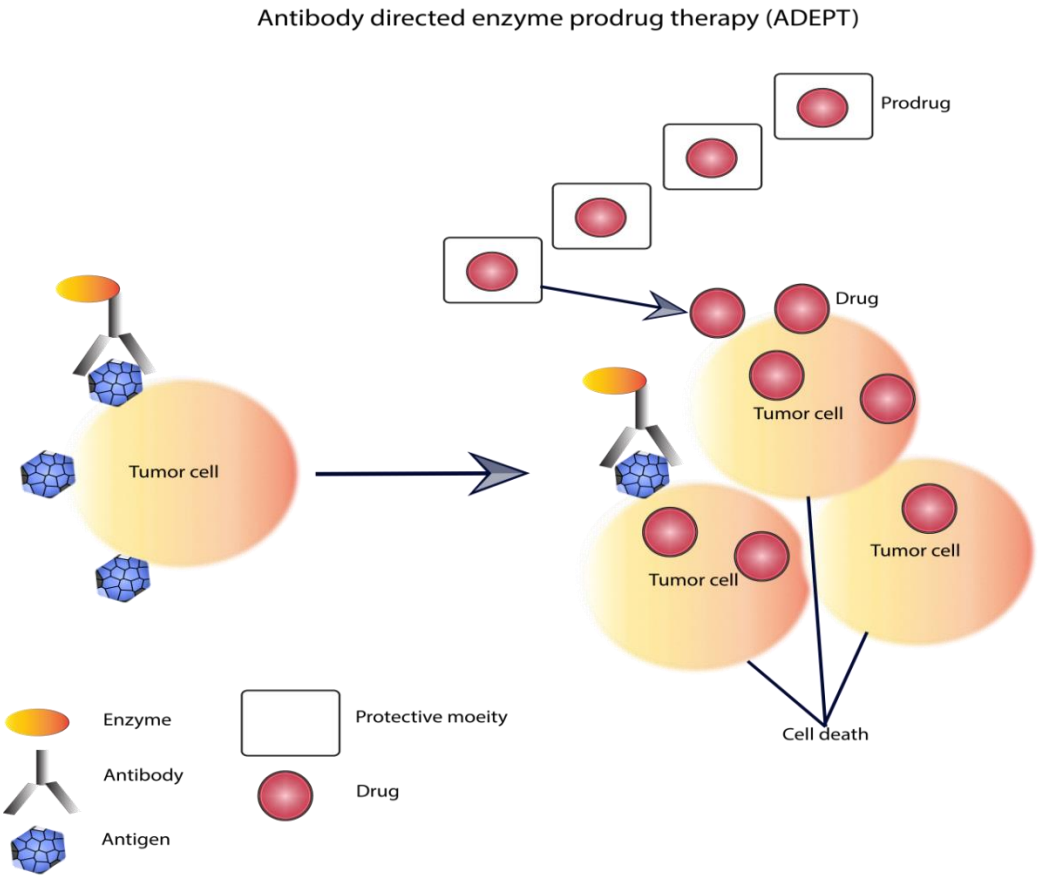

Figure 1.5: Antibody directed enzyme prodrug therapy: *Antibody conjugated to an enzyme is first delivered to a tumor site, following accumulation at the tumor site and clearance from blood prodrug is administered in the body. The prodrug then becomes cytotoxic at the tumor site where antibody enzyme conjugate resides. Finally this cytotoxic drug then induces cell death.*

The first compound that was approved as prodrug was acetanilide, which was brought into the medical practice by Cahn and Hepp in 1867 as an antipyretic agent [133]. The term prodrug was introduced in 1958 by Adien Albert, described as biologically inert derivative of drug molecules that undergo enzymatic conversion into a pharmacologically active parent drug [134]. In ADEPT, leak back is an issue to be addressed as the delivered drug could leak back into the blood and other susceptible tissues due to longer half-life [135]. However, one study has shown to decrease or diminish the enzyme from the blood by delivering an antibody to the enzyme antibody conjugate in CEA positive colon cancer Xenograft model [136].

1.8. Mechanism of action of antibodies

Antibodies operate through various mechanisms in directing cytotoxic effects at the tumor site [137]. Monoclonal antibodies in combination with immune cells target tumor cells via mechanisms such as antibody dependent cellular cytotoxicity (ADCC), complement directed cytotoxicity (CDC) or using prodrug application as in the case of ADEPT system. Amongst the effector functions reported i.e. ADCC, ADCP and CDC; the first two mediate their effect via interaction of antibody with Fc gamma receptors, whereas CDC is mediated through a series of blood proteins that constitute complement cascade proteins. FcγR receptors are classified into three different types: FcγRI (CD64), FcRγII (CD32) and FcRγIII (CD16), class II and III are subdivided into type A and B. several mechanisms of action by which antibodies can induce anti-tumor effects are shown in figure 1.6.

1.8.1. Antibody dependent cellular cytotoxicity (ADCC)

Antibody dependent cellular cytotoxicity is said to occur when antibodies bind to antigen and employ Fc portion of the antibody which interacts with Fc receptors on the immune effector cells such as neutrophils, macrophages and natural killer cells [138]. The importance of Fc receptors in inducing ADCC was studied by Clynes and Ravetch by examining the effect of clinically effective monoclonal antibodies against human tumor xenografts in FcγRIII knockout mice. It was noted that anti-tumor activity was diminished in case of FcγRIII knockout mice and retained or enhanced when inhibitory Fcγ - receptor isoform was deleted [139]. Full length IgG1 provides effector functions, however if the presence of effector functions is detrimental then switching to IgG4 might be more desirable. ADCC largely depends on activation state of NK cells [140] as well as affinity of IgG for FcγR [141].

1.8.2. Complement dependent cytotoxicity (CDC)

Another common mechanism by which antibodies induce anti-tumor effects is phagocytosis via a series of proteins defined as complement cascade proteins. Complement dependent cytotoxicity is mediated by binding of complement cascade protein c1q to Fc portion of the IgG bound to the target site. C1 also cleaves C2 into

C2a and C2b which in turn forms C3 convertase that enzymatically cleaves C3 into C3a and C3b. Like C3b, C5b is also accumulated on the cell surface and subsequent complement protein formation C6 to C9 leads to the formation of membrane attack complex (MAC). This MAC leads to the formation of pores within the target cell leading to its lysis and is thus defined as complement mediated cytotoxicity. There have been several mechanisms controlling the activation of complement proteins and their ultimate effect [142]. Although IgM is the most effective isotype in activating complement cascade cycle, it does not hold clinical importance in most cases as it cannot escape from vascular structures and is also hard to purify [4].

1.8.3. Phagocytosis

Phagocytosis can be initiated by a variety of mechanisms but the common mechanism studied is Fc receptor mediated phagocytosis. The therapeutic antibody depends highly on macrophages and associated FcγR for their efficient activity on target cells [143, 144]. This typically depends on opsonized target cells and effector cells cultured together for few hours, however effector cell lines for deeper understanding of phagocytosis is not available. Flow cytometry is the most common method used as it is a rapid, accurate and a reliable quantitative method available when two cell populations are present.

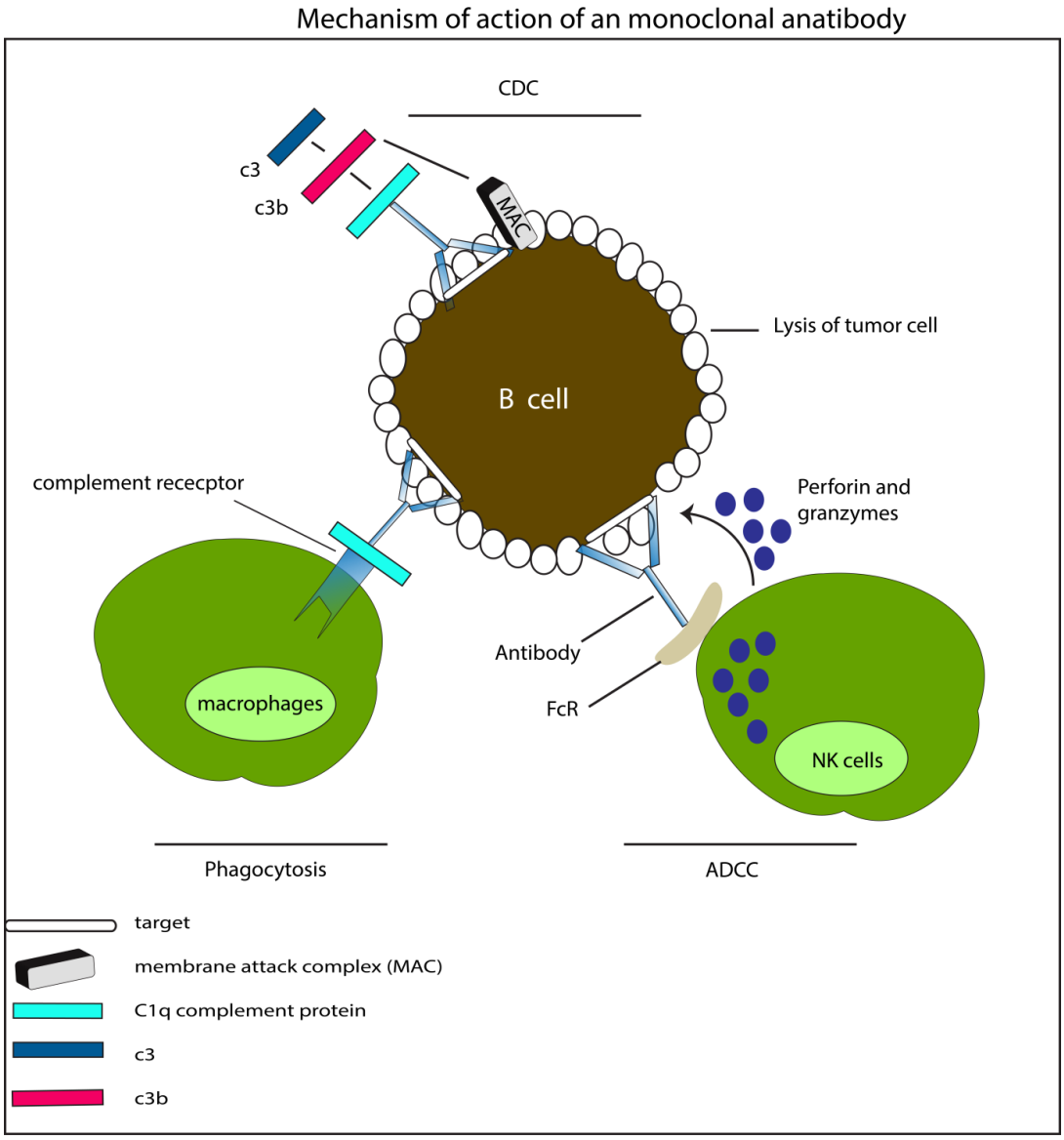

Figure 1.6: Three different mechanisms of action of monoclonal antibodies: *Complement dependent cytotoxicity (CDC) mode of action using a series of complement proteins via formation of membrane attack complex***.** *Antibody dependent cellular cytotoxicity (ADCC) activated via enrolment of FcγR region on antigen presenting cells (APCs) with release of perforins and granzymes causing lysis of tumor cells. Lastly phagocytosis targeting affected cells after antibody binding via engagement of immune cells*

1.9. Other biologics

1.9.1. Tyrosine kinase inhibitors

Protein tyrosine kinases are an important member of signalling pathway proteins that are involved in protein-protein interactions. They are mainly divided into two types: transmembrane receptor kinases that are characterized by membranous locations and non- receptor kinases that are located in the cytoplasm. Examples of protein tyrosine kinases (PTKs) include members of epidermal growth factor receptor (EGFR), vascular endothelial growth factor (VEGFR), platelet-derived growth factor receptor PDGFR and insulin growth factor receptor (IGFR) [145]. A number of tyrosine kinase inhibitors have been developed for treatment of cancer and have depicted the importance of tyrosine kinases as prime targets for treatment therapy. TKIs have an ability to bind to the ATP binding site inhibiting the protein catalytic activity which has been done in reversible as well as irreversible ways. Potential inhibitors of EGFR and HER2 have been the most successful clinical evaluated candidate in lung, head and neck, ovarian, colorectal and breast cancer [146]. More than 14 tyrosine kinase inhibitors have been approved for different types of cancers and can be administered orally with inexpensive production cost. The overall clinical outcome using such small tools has resulted in side effects and non-specific targeting on a few occasions with very short half – life [147].

1.9.2. Peptides

1.9.2.1. Peptides as useful tools

In recent years, another type of biologics i.e. peptide aptamers are emerging as a tool for targeting different markers in several diseases. Peptide aptamers are approximately 10-25 amino acids in length conformationally constrained derived from combinatorial libraries and are known to inhibit the activity of target with high affinity [148, 149]. Peptides are short amino acid sequences that can be produced biosynthetically, either chemically such as peptide synthesis or recombinant microbial production. In comparison to monoclonal antibodies, aptamers are relatively much small (10 - 20 kDa) with reduced immunogenicity [150]. These small molecules when conformationally constrained hold several advantages over

disordered peptides such as exposure of buried hydrophobic amino acids under aqueous conditions within the cells, often exhibit higher binding affinities as compared to unstructured peptides. Such peptide aptamers act by binding to the cell surface proteins and inhibit one or more signal transduction pathway [151].

1.9.2.2. Current status of peptide aptamers

Various roles of peptide aptamers as a therapeutic agent have been demonstrated such as binding to the DNA binding domain of Stat3, inducing apoptosis in tumor cells and phage display derived peptide binding neuroblastoma tumor cells [152, 153]. Peptides have two major advantages over large molecules (monoclonal antibodies and larger protein molecules) such as good delivery to the tumor site due to small size and they do not induce dose limiting toxicity to liver and bone marrow [154]. More than 60 approved peptide drugs are available in the market generating total revenue $13 billion with the number of peptide drugs entering the market has been increasing [151]. Peptides have been used in different ways such as peptides directly, vaccines, hormones and peptides linked to cytotoxic drugs with higher specificity towards the target.

Natural peptides can be designed using crystallography to study the receptor ligand binding and the specific interface that is known to be critical in protein interaction. This could also be a very useful tool when a certain specific mutation in a gene is known to cause a disease. An example of such useful tools is peptide binding to TRAF6 derived from sequence of its natural binders [151]. An advantage of natural peptides is because its sequence is already known; screening using a library is not needed as such peptides can be straight away manipulated to visualize the binding efficiency into the target protein.

Peptide aptamers could be really useful if the structure of protein or its interface with interacting proteins is unknown as peptides can be selected from synthetic peptide libraries of randomized peptide sequences. The high complexity of peptide libraries (i.e. presence of millions of peptide sequences) provides a high probability of identifying peptides binding to different domains within the protein. Moreover diverse peptide libraries can have peptides that can bind to domains that might play a

role in decreasing the effects of protein involved in aberrant mechanisms or can also bind specifically to the domain involved in dimerization or oligomerization. The most common way of selection of peptide aptamers from the diverse libraries is via *in vitro* phage display technique and many peptides have been identified using such approach against extracellular targets, for example IGF-1, EGF, MCP1, etc [155, 156].

Significant progress has been made with peptides as therapeutic option for various diseases and chemical modifications of peptides have been performed to increase the binding efficacy. Since the peptides are really small in length, it is necessary to determine the binding efficacy following change in precise amino acid as amino acid at different positions might increase or decrease binding affinity. From therapeutics point of view, peptides have been used as hormones, radionuclide carrier, peptide vaccines and as cytotoxic drugs carrier. Due to great advancement in synthesis of peptides, it will be soon possible to make peptides as a cost effective small molecule tool.

1.10. The future of biologics

With the tremendous amount of success in treatment approaches to many diseases, biologics is one field where pharmaceutical industry has been investing heavily. With over 30 monoclonal antibodies approved by FDA, these biologics have indeed become the main focus for many researchers as an important tool to fight against various diseases. Due to advancement in molecular biology techniques, hybrid structures that combine biologics with well-defined entities have taken such tools to a different level to treat diseases. As mentioned in section 1.1 monoclonal antibodies form the backbone of biologics therapy for several diseases, however the cost of production is a major issue associated with such tools.. The third generation antibodies (especially antibody fragments) have still not managed to achieve high efficacy when compared to second generation antibodies. However with the success of full length conventional antibodies in recent years, it will be very intriguing to see how antibodies including fragments, Fc modified antibodies, peptide aptamers and drug conjugates will have an impact on the market. With ease of availability of peptide libraries as well as production of antibody libraries, it is an important step

forward to increase the affinity of tools by subjecting them to various modifications such as Fc engineering, mutagenesis, etc [157].

1.11. AIM

The aim of our research was to develop different types of biologics against two well characterized distinct targets. Firstly, we intended to develop full length monoclonal antibody (mAb) as well as single chain fragment variable antibody (scFv) against canine CD20 receptor in B cell lymphoma. Moreover we also planned to make different conjugates with scFv to increase the binding affinity of the antibody. Secondly, we developed biologics such as mAb and peptide aptamers to a protein called α-synuclein that is aberrantly expressed in Parkinson's disease (PD). Also here we aimed to develop new assays that will be useful in future to study a protein's native state. The individual aims of the project are described in more detail in respective chapters.

CHAPTER 2: Materials and Methods

2.1 General microbiological techniques

All the microbiological techniques were carried out using sterile glass, plastic apparatus and under strict aseptic conditions. Different techniques used in the lab have been described below:

2.1.1 Preparation of competent cells for heat shock transformation method

E.coli bacteria from a glycerol stocks were inoculated into 3 mls of Lysogeny Broth (LB) medium (1% (w/v) tryptone, 0.5 % (w/v) yeast extract, 1% (w/v) NaCl; sterilized by autoclaving) and incubated overnight in an incubator shaking at 37^0C, 220 rprm. 500 µl of overnight culture was added to 100 ml fresh LB and further incubated until an OD_{600nm} of 0.4 was reached. All the steps from here on were carried out at 4^0C in the cold room. The culture was then cooled down on ice and centrifuged at 2,200 g for 15 minutes at 4^0C. The pellet was gently resuspended in 32 mL of ice-cold buffer I (table 2.1) and incubated for 10 mins on ice. The cells were again centrifuged as before and the cell pellet was resuspended in 4 mL of ice cold buffer II (table 2.1), incubated on ice for 10 mins and quickly aliquoted into pre-chilled sterile microcentrifuge tubes. The aliquots were snap frozen in liquid nitrogen and stored at -80^0C. The transformation efficiency of the prepared cells was checked via transformation of a competent cell aliquot with plasmid DNA.

Buffer I:	Buffer II:
100 mM RbCl	10 mM MOPS
40 mM $MgCl_2.6H_2O$	10 mM RbCl
60 mM CH_3COOK	75 mM $CaCl_2$. H_2O
100 mM $CaCl_2.2H_2O$	15% (v/v) Glycerol
15% Glycerol	Adjust the pH to 6.5 with NaOH and sterilize by filtration (0.22 µM)
Adjust the pH to 5.8 with CH_3COOH and sterilize by filtration (0.22 µm)	

Table 2.1: Composition of buffers: *Composition of buffer1 and 2 for creating competent cells for heat shock transformation method*

2.1.2 Transformation of bacterial competent cells

Between 50 to 200 ng of plasmid DNA or 5 µl of ligation product was added to a 50 µl cell aliquot of *E.coli* DH5α cells for plasmid propagation and BL21/DE3 for plasmid transcription and translation. The cell aliquots containing DNA were incubated on ice for 30 mins, placed in a water bath at 42^0C for 45 sec and back on ice for 2 mins. Under sterile conditions, 500 µl of fresh LB medium was added to the cell aliquot and incubated shaking at 37^0C for 60 mins. LB agar 10 cm dishes were prepared (LB containing 1.5% (w/v) agar) with 100 µg/ml Ampicillin (#A9618, Sigma) or 25 µg/ml Kanamycin (#11815032, Invitrogen), depending on the appropriate antibiotic resistance encoded by plasmid. All the unused plates were stored at 4^0C upside down, sealed in parafilm and pre-warmed in 37^0C incubator before use. In a sterilized area, 50-200 µl of the culture was plated out onto the pre warmed LB plate using the glass spreader. Plates were incubated overnight upside down in 37^0C incubator.

2.1.3 Purification of plasmid DNA

Under sterile conditions, a single colony was picked from the transformed plate using a sterile tip. The colony was dropped into a 5 ml LB medium (100 µg/ml Ampicillin or 25 µg/ml) in a 15 ml falcon tube (for small scale purification). The tube was incubated overnight at 37^0C, 220 rpm and the following day the tube was centrifuged at 4000 rpm for 10 mins at 4^0C. Following centrifugation, the tip and supernatant was discarded carefully. QIAprep Spin Miniprep Kit (#27106, Qiagen) instructions were followed to extract and purify plasmid DNA which was then further eluted in 30-50 µl of elusion buffer. The concentration of the DNA was measured on a Nanodrop and stored at -20^0C.

For a larger scale purification of plasmid DNA, colony was dropped in a similar way but the volume of LB containing appropriate antibiotic was increased to 150-200 mL and grown overnight at 37^0C. HiSpeed Plasmid Kit (#12663, Qiagen) was used for extraction and purification of plasmid DNA, and finally DNA was eluted in 1 ml of elusion buffer and stored at -20^0C.

2.1.4 Bacterial glycerol stocks

From the overnight culture of a picked colony, 750 µl was aliquoted in a sterile microcentrifuge tube and 250 µl of sterile 70% (v/v) glycerol was added to the tube and mixed gently. The glycerol stocks were immediately snap frozen and stored at -80^{0}C. For setting up starter cultures, a sterile tip was used to take a stab from the glycerol stock and streaked onto the LB agar plate containing appropriate antibiotic in a sterile manner. The plate was then incubated overnight at 37^{0}C and a colony was picked up and grown to make a starter culture.

2.1.5 Expression and purification of recombinant protein (α-synuclein)

Expression:

E.coli BL21 (DE3) cells were transformed with 2 µl DNA coding for α-synuclein in pT7-7 vector (from C. Robert) via heat shock transformation technique. Single colony was grown overnight at 37^{0}C in 5 ml LB (100 µg/ml Amp.) and this overnight culture was used to inoculate 3-4 litres of LB media (100 µg/ml Amp). This inoculated culture was grown at 37^{0}C until an OD_{600nm} of 0.4 was reached ($\sim$ 2 hours). Once an OD_{600nm} of 0.4 was reached, the cells were induced using 1 mM IPTG with an incubation period of 5 hours at 30^{0}C. 1 ml of sample was taken from the culture before induction and another 1 ml after 5 hours of induction to check for protein expression on the SDS gel. The cells were then pelleted down by centrifuging at 5,000 g for 15 minutes at 4^{0}C, the pellets were snap frozen and stored at -80^{0}C until used.

Purification:

1. The cell pellets were resuspended in **lysis buffer**:

   20 mM Tris-HCL, pH 7.5 (measure at RT, Δ pH=0.028/^{0}C);

   1 mM EDTA; Protease inhibitor mixture (Roche, cat# 11873580001);

1 tablet/25 ml lysis buffer;

1 mM DTT

Make upto 100 ml with water

2. Each of 1 litre pellets was resuspended in 30ml lysis buffer and lysozyme (50 mg) was added to the lysate. The resuspended mixture was incubated on ice for 30 minutes for lysis to occur and was subjected to freeze thaw protocol to enhance lysis.
3. Subsequently, the cells were sonicated 3 x 15 seconds with an interval of 10 seconds. The lysate was centrifuged at 16,000 g for 15 minutes at 4^0C and the supernatant was transferred to a new tube.
4. This obtained lysate was centrifuged at 18,000 g for 30 minutes to remove any possible debris. This clarified lysate supernatant was collected and the pH was adjusted to 3.5 to precipitate any E.coli contaminating proteins.
5. The mixture was stirred for 30 mins at RT, followed by centrifugation at full speed for 1 hour at 4^0C.
6. Meanwhile, 500 ml of buffer A and buffer B were prepared and incubated on ice.

   Buffer A (low salt): Tris- HCL pH 7.5 + 25 mM NaCl

   Buffer B (high salt): Tris- HCL pH 7.5 + 1 M NaCl

   The pH of each of the buffer was measured once the solutions were cooled to 4^0C. Purification was performed using a 5 ml His trap column which was washed by low salt buffer (Buffer A) with a flow rate of 1 ml/min.
7. The supernatant was collected and pH was adjusted to 7.5. This supernatant was filtered and stored on ice.
8. Following washes of column with buffer A, the tubing was placed in a flask containing the filtered lysate at a flow rate of 1 ml/min.
9. The filtered lysate was collected and snap frozen in order to analyse onto the gel.

10. Once the lysate was passed through the column, high salt buffer was passed through the column using gradient apparatus to elute the protein.

    Gradient tube preparation: 60 test tubes were placed in the round gradient tubing apparatus and each containing 1.5 ml eppendorf labelled from 1 to 60 in order to elute the protein. Buffer A was poured in the inner round flask whereas the outer chamber was filled with buffer B. the knob was then placed upside down in such a way that buffer B can enter buffer A chamber. The flow rate was set up at 1 ml/min.
11. Once the fractionation was finished, all the fractions were snap frozen and stored at -80^{0}C.

To determine the efficiency of purification, 10 µl of each of the fraction from the purification step was taken and mixed with 2 X sample buffer to be analysed onto 12% SDS gel.

2.2. Immunofluorescence

For Immunofluorescence, the cells were seeded at the same density onto the required number of chambers. The following day transfection was performed in a similar way as mentioned above and subsequently chambers containing cells were washed thrice with PBS. The cells were then fixed onto the chambers via 4% (v/v) Paraformaldehyde in PBS and incubated for 15 minutes at RT. The cells were then permeabilised with 500 µl of 1% (v/v) Triton X 100 in PBS and incubated for 10 minutes at RT. Following incubation, the chambers were washed thrice with PBS, blocked with 500 µl of 3% (w/v) BSA in PBS and incubated at RT for 30 minutes. The blocking agent was discarded and primary antibody diluted 1:1000 in antibody diluent was added to the chambers. This antibody incubation was carried out for 1 hour at RT or overnight in humidity chamber at 4^{0}C. Then the chambers were washed thrice with PBS and secondary antibody (Rabbit anti-mouse 488 nm) diluted 1:1000 in antibody diluent was added to the chambers with an incubation period of 1 hour in humidity chamber at RT. The chambers were again washed thrice with PBS and were prepared for mounting. For mounting, 3 µl of DAPI fluorescent stain was made up in 10 drops of mounting medium (DAKO) and placed onto the slides before placing the chambers on it. The chambers were then placed with cells facing the

slides and stored in the dark until dried. Once the slides containing the chambers had dried, slides were ready for imaging.

2.3. Molecular biology techniques

All primers were designed and ordered from Sigma Genosys, whereas all enzymes and buffers were ordered from New England Biolabs unless stated otherwise.

The plasmids used and their sources were:

pGEX6p1 (28-9546-48, GE Healthcare)

pcDNA 3.1+ (V790-20, Invitrogen)

pEGFP (N and C terminal vector) (Addgene)

pMCherry (N and C terminal vector) (Addgene)

pCOMB3Xss (Erin Worrall)

DNA quantification

The concentration of DNA was measured using Nanodrop spectrophotometer (absorbance at 260 nm).

2.3.1 mRNA extraction and reverse transcription

mRNA was extracted from harvested SHSY5Y cells using RNeasy Mini kit (#74104, Qiagen) handbook. The concentration of RNA was also quantified using Nanodrop. One µg of mRNA was reverse transcribed using the Omniscript reverse transcription kit (#205110, Qiagen). Following manufacturer's protocol the concentration of cDNA was measured as mentioned above.

2.3.2 Polymerase chain reaction

A suitable template as cDNA or plasmid DNA is used to amplify the desired gene by PCR. The primers were designed in such a way that forward primer contains a restriction site which cuts at the 5'end of the gene and a reverse primer which has a

site attached at the 3' end of the primer. A list of primers with their restriction sites have been mentioned in each chapter separately.

While designing the primers, it was ensured that the gene was in frame with the N-terminal of the vector sequence. Few base pairs were added to the 5'end of the primers before the restriction sites in order to allow efficient binding of the restriction sites to the primer and allow significant digestion of the insert. Also, primer length was manipulated to get a suitable melting temperature and presence of GC at the primer extremities was favoured. PCR reactions were carried out on ice in nuclease free tubes with 2 X high Fidelity Phusion Master mix (#M2075 NEB), 100ng of plasmid DNA, 0.5 µM of each primer, nuclease free H_2O made up to 50 µl.

Thermal cycling conditions were:

95^0C for 2 min

95^0C for 20 sec
58^0C for 40 sec } repeated 30 times
72^0C for 3 min

72^0C for 5 min

4^0C forever

5-10 µl of PCR reaction was run on a 1.5% (w/v) agarose gel to check if the desired band for the amplification of the gene was obtained. Multiple PCR reactions were run on 1.5% (w/v) agarose gel until maximum separation of the desired and non-specific bands was achieved. The desired band was cut using a sterile scalpel and this excised gel was purified by using Gel extraction kit (#28704, Qiagen) manufacturer's protocol. The DNA was eluted in 30-50 µl of elusion buffer (Buffer EB) and the concentration of the DNA was determined using Nanodrop (OD_{600nm}).

2.3.3 Restriction digestion of the purified PCR product and destination Vector DNA

For these above purified PCR products, double digestion was performed using two different enzymes and compatible buffers recommended by supplier. The destination vector along with the insert was digested using these two enzymes and incubated for 1-2 hours depending upon the amount of the vector and insert. To ensure efficient digestion has taken place, controls were set up such as single digestion using enzyme 1 and enzyme 2 individually as well as no enzymes.

2.4. Cell lines

2.4.1 Maintenance of cell lines

Cell lines were maintained in the appropriate medium supplemented with 10% (v/v) foetal bovine serum (FBS; Autogen Bioclear). Cells were incubated at 37^0C in a humidified 5% CO_2 incubator or 10% CO_2 for specific cell lines (table 2.2).

Cell line	Cell line type	Culture medium	Origin
A375	Adherent human amelanotic malignant melanoma	DMEM (Gibco, Invitrogen)	Prof. Paul Smith
HCT116 $p53^+/p53^-$	Adherent human colon carcinoma	Mc Coy's 5A (Gibco, Invitrogen)	Dr. Bert Voelstein
H1299	Adherent lung carcinoma	RPMI 1640 (Gibco, Invitrogen)	Americacn Type culture Collection, LGC Standards, UK
SHSY5Y	Neuroblastoma cell line	RPMI 1640 (Gibco, Invitrogen)	SK-N-SH (ECACC)

Table 2.2: Cell lines: *Various cell lines used within the experiments along with their origin, supplemented growth medium.*

Cells were maintained in 10 cm tissue culture dishes and were sub-cultured 2-3 times a week once the confluency rate reached ~90%. The appropriate media needed for the cell line was warmed upto 37^0C in the water bath along with trypsin. Medium was removed and cells were washed with 7-8 ml of sterile PBS. The PBS was poured off and cells were trypsinised using 2 ml of trypsin –EDTA 0.5% (#25300, Gibco, Invitrogen) with an incubation period of 5 minutes at 37^0C. Following 5 minutes of trypsinisation, 8 ml of pre-warmed fresh media was added and 2 ml was transferred to a new 10 cm dish containing 8 ml of fresh relevant media. The dishes were then incubated at 37^0C overnight.

2.4.2. Transfection of mammalian cells

Cells were seeded in such a way that they reached a confluency of 50-70% in order to transfect. Cell lines used in transfection: SHSY5Y (Dox repressible), SHSY5Y (low α-synuclein), HCT116+ and H1299 cells. Transfection was carried out under laminar air flow in tissue culture room. For transfection, sterile eppendorfs as well as filter sterile tips were used after spraying with 70% ethanol. For preparing transfection reaction mix, 100 µl of respective serum free media (based on the cell line) was taken in a sterile eppendorf. To this media, appropriate amount of DNA was added (0.5, 1 and 5 µg) along with 5 µl of transfection reagent. The reactions were then incubated for 15 minutes. Subsequently, the transfection reactions were added to the cells that were seeded before 12-14 hours previously. The plates were incubated for 18- 24 hours in a 37^0C with 5% CO_2.

2.4.3 Harvesting of cells

The cells were washed once within the 10cm plate with PBS and 1ml of PBS was added in order to harvest the cells. The cells were harvested by using a plastic scraper and harvested cells were then transferred into a fresh sterile eppendorf. The cells were centrifuged at 5,000 rpm for 5 minutes and the pellet was snap frozen and stored in -80^0C.

2.4.4. Lysis of cells

Lysis buffer (10%Triton)

- Triton 10%
- KCl -1 M
- B- glycero phosphate (10 mM)
- Potease Inhibitor tablet
- EDTA (100 mM)
- EGTA (100 mM)
- Na_2VO_3 (100 mM)

The cells were incubated on ice for 30 minutes for lysis and centrifuged at 10000 rpm and the supernatant were transferred to a sterile eppendorf. The protein concentration within the lysate was determined by Bradford assay (Bio-Rad) after reading the plate at wavelength of 595 nm. The samples were then prepared using 2X sample buffer containing 1 M DTT and normalized with water. The prepared samples were heated at 85^0C for 5 minutes and loaded onto an appropriate percentage SDS gel.

2.5. SDS gel preparation and Immunoblotting:

2.5.1. 2X Sample buffer preparation:

2 ml Tris (1 M, pH 6.8)

4.6 ml glycerol (50%)

1.6 ml SDS (10%)

0.4 ml bromophenol blue (0.5%)

0.4 ml β- mercaptoethanol

The samples after normalizing were made up to a certain amount with 2X sample buffer. Based on the size of protein, the lysate/ protein were run on an appropriate percentage of SDS polyacrylamide gel. The samples were loaded onto the gel along

with a pre-stained ladder and the gel was run in 1X running buffer at 150 V for 1 hour at RT. Solutions needed for Tris glycine SDS - polyacrylamide gel electrophoresis- three different size of combs: 0.75 mm, 1.0 mm and 1.5 mm (10, 15 wells), the appropriate percentage of SDS gel was made based on the molecular weight of the protein. The ratio of all the ingredients has been mentioned below (table 2.3):

Solution Components	**Component volumes (ml) per gel mold volume of**							
	5ml	**10ml**	**15ml**	**20ml**	**25ml**	**30ml**	**40ml**	**50ml**
6%								
H2O	2.6	5.3	7.9	10.6	13.2	15.9	21.2	26.5
30% Acrylamide	1.0	2.0	3.0	4.0	5.0	6.0	8.0	10.0
1.5M Tris (pH8.8)	1.3	2.5	3.8	5.0	6.3	7.5	10.0	12.5
10% SDS	0.05	0.1	0.15	0.2	0.25	0.3	0.4	0.5
10% ammonium persulfate	0.05	0.1	0.15	0.2	0.25	0.3	0.4	0.5
TEMED	0.004	0.008	0.012	0.016	0.02	0.024	0.032	0.04
8%								
H2O	2.3	4.6	6.9	9.3	11.5	13.9	18.5	23.2
30% Acrylamide	1.3	2.7	4.0	5.3	6.7	8.0	10.7	13.3
1.5M Tris (pH8.8)	1.3	2.5	3.8	5.0	6.3	7.5	10.0	12.5
10% SDS	0.05	0.1	0.15	0.2	0.25	0.3	0.4	0.5
10% ammonium persulfate	0.05	0.1	0.15	0.2	0.25	0.3	0.4	0.5
TEMED TEMED	0.003	0.006	0.009	0.012	0.015	0.018	0.024	0.03
10%								
H2O	1.9	4.0	5.9	7.9	9.9	11.9	15.9	19.8
30% Acrylamide	1.7	3.3	5.0	6.7	8.3	10.0	13.3	16.7
1.5M Tris (pH8.8)	1.3	2.5	3.8	5.0	6.3	7.5	10.0	12.5
10% SDS	0.05	0.1	0.15	0.2	0.25	0.3	0.4	0.5
10% ammonium persulfate	0.05	0.1	0.15	0.2	0.25	0.3	0.4	0.5
TEMED	0.002	0.004	0.006	0.008	0.01	0.012	0.016	0.02

12%								
H2O	1.6	3.3	4.9	6.6	8.2	9.9	13.2	16.5
30% Acrylamide	2.0	4.0	6.0	8.0	10.0	12.0	16.0	20.0
1.5M Tris (pH8.8)	1.3	2.5	3.8	5.0	6.3	7.5	10.0	12.5
10% SDS	0.05	0.1	0.15	0.2	0.25	0.3	0.4	0.5
10% ammonium persulfate	0.05	0.1	0.15	0.2	0.25	0.3	0.4	0.5
TEMED	0.002	0.004	0.006	0.008	0.01	0.012	0.016	0.02
15%								
H2O	1.1	2.3	3.4	4.6	5.7	6.9	9.2	11.5
30% Acrylamide	2.5	5.0	7.5	10.0	12.5	15.0	20.0	25.0
1.5M Tris (pH8.8)	1.3	2.5	3.8	5.0	6.3	7.5	10.0	12.5
10% SDS	0.05	0.1	0.15	0.2	0.25	0.3	0.4	0.5
10% ammonium persulfate	0.05	0.1	0.15	0.2	0.25	0.3	0.4	0.5
TEMED	0.002	0.004	0.006	0.008	0.01	0.012	0.016	0.02

Solution Components	**Component volumes (ml) per gel mold volume of**							
	5ml	**10ml**	**15ml**	**20ml**	**25ml**	**30ml**	**40ml**	**50ml**
H2O	0.68	1.4	2.1	2.7	3.4	4.1	5.5	6.8
30% Acrylamide	0.17	0.33	0.5	0.67	0.83	1.0	1.3	1.7
1.0M Tris (pH6.8)	0.13	0.25	0.38	0.5	0.63	0.75	1.0	1.25
10% SDS	0.01	0.02	0.03	0.04	0.05	0.06	0.08	0.1
10% ammonium persulfate	0.01	0.02	0.03	0.04	0.05	0.06	0.08	0.1
TEMED	0.001	0.002	0.003	0.004	0.005	0.006	0.008	0.01

Table 2.3: SDS gel ingredients: *different percentage of gel based on thickness to run higher and lower molecular weight proteins. Both resolving as well as stacking gels have been mentioned in the table with respective volume of each component*

2.5.2 Coomassie staining

Following SDS-PAGE, visualization of proteins was performed by Coomassie staining. The gels were immersed in 20-25 ml of Coomassie stain and kept shaking for 1hour at RT followed by destaining until distinct bands become visible. The gel was then dried using a gel dryer. The staining solution comprised of 50% (v/v) methanol, 10% (v/v) glacial acetic acid and 0.2% (w/v) Coomassie brilliant blue R-250. The destaining solution was made up using 7.5% (v/v) methanol, 10% (v/v) glacial acetic acid.

2.5.3 Western blot

Once the gel was run, it was transferred onto nitrocellulose membrane in such a way: Black side of cassette – sponge - blotting paper – gel - membrane – blotting paper – sponge. 10 X transfer buffer was diluted down to 1 X with an addition of 200 ml of methanol to enhance transfer of small proteins. The western blot was performed at 100 V for 1 hour with an ice block. Subsequently, the membrane was ink stained and blocked with 5% (w/v) skimmed milk in PBS-T (0.1%) for 1 hour. Following on, primary antibody was diluted in 5% milk (in PBS-T) and added to the blocked membrane and incubated for 1 hour at RT or overnight at 4^0C. The blot was then washed thrice with PBS - T (0.1% (v/v)) and HRP conjugated appropriate secondary antibody was diluted in blocking buffer and added to the blot and again incubated for hour. The blots were then washed thrice again with PBS-T 0.1% (v/v) and the results were analysed by overlaying the blots with ECL (1+2) for 2 minutes.

ECL I	ECL II
100 mM Tris HCL pH 8.5	100 mM Tris HCL pH 8.5
2.5 mM Luminol	0.02% (v/v) H_2O_2
0.4 mM p- Coumaric acid	-
Make up with H_2O upto 100 ml	Make up with H_2O upto 100 ml

2.6. ELISA

2.6.1. Streptavidin coated overnight plate for measuring antibody binding to the biotinylated peptides (epitope mapping)

96 well ELISA plate (Nunc) was coated with streptavidin (200 ng/well) and incubated overnight at 4^0C. The following day the plate was washed thrice with PBS - Tween 20 (0.1% v/v) and the overlapping peptides were diluted down to 100 ng/well in 3% (w/v) BSA. The peptides were added in four different dilutions to each respective well and incubated at RT for 1 hour. Subsequently, the plate was washed thrice with 0.1% (v/v) PBS-T and was blocked for 1 hour at RT with 3% (w/v) BSA in PBS. Meanwhile several dilutions for antibody were prepared in 3% (w/v) BSA and following blocking these antibody dilutions were added to each respective well of the plate and incubated for 1 hour at room temperature. Following this, the wells were washed once again 3 X PBS-T and HRP conjugated anti-rabbit anti-mouse/ swine anti-rabbit was added at a dilution of 1:1000 prepared in 3% (w/v) BSA with an incubation period of 1 hour. During the incubation period, the TMB (3, 3', 5, 5'- tetramethylbenzadine) substrate was prepared.

100 µl of TMB substrate was added to each well and the plate was incubated with shaking gently at RT for 15 minutes. The reaction in the wells was stopped once colour change was observed from colourless to blue. Following incubation, 50 µl stopping solution was added to each well (blue to yellow) and the plate was read at an absorbance of 450 nm. In all the experiments we made use of negative controls and blank.

2.6.2. Binding of antibody to WT protein

96 well plate (Nunc) was coated with protein of interest diluted at 200 ng/ well in $NaHCO_3$ buffer and incubated overnight at 4^0C. Following day the plate was washed thrice using 3 X PBS-T and blocked with 3% (w/v) BSA in PBS for 1 hour. During

this blocking stage antibody dilutions in 3% BSA (w/v) were prepared and this step was preceded by addition of primary antibody to each well for an incubation period of 1 hour. The plates were then washed thrice with 0.1% (v/v) PBS-T and HRP conjugated secondary antibody (Rabbit anti-mouse/ swine anti- rabbit @ 1:1000) was added to all the wells and incubated for another hour. After the incubation was done, the wells were again washed 3 x PBST and developed using TMB as a substrate. Once the blue colour was developed within the wells, the reaction was stopped using dilute H_2SO_4.

2.6.3. TMB substrate

Citrate/acetate buffer: 1 ml 0.1M sodium acetate + 40 µl 0.1 M citric acid

Diluted H_2O_2: 15 µl 30% H_2O_2 + 10 µl H_2O

TMB: 100 µl diluted TMB

Make upto 10 ml with H_2O

Stopping solution: Dilute H_2SO_4- 5 ml H_2SO_4 + 195 ml H_2O

50 µl of substrate was added to each ELISA well and incubated for 15-30 minutes. This is followed by addition of stopping solution each well just before reading the plate at 450 nm.

2.7. Monoclonal antibody isolation against canine CD20

2.7.1. Immunization of BALB/c mice with canine CD20 peptide (NCDPANPSEKNSLSIQYCGS)

BALB/c mice aged 6-8 weeks was initially immunized with a final concentration of 100 µg/ml CD20, mixed in a 1:1 ratio with Freund's complete adjuvant. A volume of 200µl was injected into the peritoneal cavity of the BALB/c mice for immunization. Subsequent injections were performed with 25 µg/ ml CD20 peptide mixed in a ratio 1:1 with Freund's incomplete adjuvant. A tail bleed was taken from the mice 7 days after injection and the antibody titre against CD20 was determined. Once a high titre was reached, the mice was given a final boost into the peritoneal cavity and then sacrificed 7 days later.

PEP32: SGSGNCDPANPSEKNSLSIQYCGS

PEP33: SGSGDPANPSEKNSLSIQYCGSIR

PEP34: SGSGNCDPANPSEKNSLSIQ

PEP35: SGSGNCDPANPSEKNSL

PEP36: SGSGNCDPANPSEK

PEP37: SGSGNCDPANP

PEP38: SGSGPSEKNSLSIQYCGSIR

2.7.2. Octet binding antibody-peptide binding assay.

The binding assay was carried out using streptavidin-coated biosensors on an Octet RED biolayer interferometry system (FortéBio Inc.) that measures binding to the sensor tip as a wavelength shift (in nm) in real time. All the steps of the assay process were performed at 30 °C with the plate shaking speed set at 1000 rpm. 96-well microtitre plates (Greiner Bio) were made up using 200 µl volumes. Analytes were diluted with PBS (pH 7.4) containing 0.02 % Tween 20, 0.005 % sodium azide

and 100 µg/mL bovine serum albumin (Kinetics Buffer – Forte Bio). Biotinylated CD20 peptide was loaded onto to 8 sensors from a 2 µg/mL solution containing 2 mM dithiothreitol (Sigma-Aldrich) until a wavelength shift of 0.5 nm had been achieved. The association data were collected for 10 minutes from solutions of monoclonal CD20 antibody where the concentration was varied between 32 nM and 0.5 nM by half serial dilution. The dissociation step was carried out over a 40 minute time period in Kinetics Buffer. The assay data were processed using Data Analysis (version 6.3 – Forte Bio) to obtain kinetic values. Briefly, a buffer blank was used as a reference cell subtraction and the data series was evaluated using a global fit algorithm for 1:1 binding interaction.

Fluorescent polarization assay was performed using anti-canine monoclonal antibody onto FITC tagged human CD20 peptide, with the human-mouse chimeric monoclonal antibody Rituximab as the control antibody. Purified monoclonal antibody NCD1.2 and Rituximab diluted in PBS were titrated against 30 nM fluorescein-labelled peptide corresponding to human CD20 (NCEPANPSEKNSPSTQYCYS) in assay buffer (PBS, 0.05% Tween-20). To subtract the nonspecific binding, we used purified mouse immunoglobulins with the same concentration as analysed antibodies. All reactions were carried out in a total volume of 60 µl per well of a 96-well black Nunc Plate (Sigma-Aldrich). The plate was incubated for 1 hr at room temperature with shaking. Fluorescence polarization was measured at 21 °C using FilterMax™ F5 Multimode Microplate Reader (Molecular Devices) with excitation and emission wavelengths of 485 nm and 535 nm, respectively.

2.7.3. Transfection of GFP-CD20 into H1299 cells

Primers introducing BamHI and XhoI sites at the ends of reported sequence (Genbank accession number NP_068769.2) of human CD20 were designed for its amplification. Forward primer introduced the Kozak consensus sequence in front of the initiation codon. The PCR product was digested and cloned into the mammalian expression vector pCDNA 3.1 (Clontech) digested using the same enzymes. Specificity of primers was confirmed by BLAST programme. GFP- CD20 expression

was driven by EF1 promoter, a strong promoter in mammalian cells, also the plasmid contained Ampicillin (Sigma Aldrich) resistance gene as a selectable marker. Once the gene was cloned, the specificity and efficiency of cloning was determined via re-digestion and DNA sequencing. H1299 cells were grown as monolayers in RPMI 1640 supplemented with 10% fetal bovine serum (FBS). 0.25, 0.5 and 1 µg of DNA (GFP - CD20) was transfected in H1299 cells, along with GFP as a negative control using Attractene in order to measure the binding efficiency of the mouse anti-canine monoclonal antibody to its human CD20 counterpart. The activity was determined via Western blot as well as Immunofluorescence. Chemical fractionation into compartments was carried out using a fraction kit (Calbiochem) that separates into cytosolic, membrane/organelle, nuclear and insoluble proteomes. Cell lysis and membrane fractionation were performed in collaboration with Lisa Pang (David Argyle's lab) to analyse the expression of CD20.

2.7.4. Fluorescence activated cell sorting (FACS)

Flow cytometry (FCM) expression of CD20 was evaluated on fine needle aspirate biopsies in RPMI 1640 medium (Invitrogen) obtained from dogs with different lymphoma subtypes with help of Stefano Comazzi (Department of Veterinary Science, Via Celoria, Milano, Italy). On each sample immunophenotyping was performed according to the previously published protocols in order to define immunophenotype and to identify the lymphoma subtype. Evaluation of expression of membranous CD20 was performed using the following procedure: To avoid any non-specific binding, cells (adjusted at 5x 105 cells per tube) were incubated in RPMI 1640 medium containing 5% fetal bovine serum (FBS) and 0.2% sodium azide, followed by resuspension in PBS. One µl of mouse anti- canine CD20 Ab was added and incubated for 20 mins at 4 ^{0}C. After two washes in RPMI/ FCS/ sodium azide, 2 µl of goat anti-mouse Ig (FITC, Becton Dickinson) was added and incubated in the dark for 20 mins at 4 ^{0}C. To evaluate non-specific binding of secondary antibody, one of the vials was used with lack of primary antibody. Isotype control was not used due to the lack of isotype matched available antibody. Following the incubation, cells were washed and cells were acquired using FacScalibur equipment (Becton Dickinson). The acquisition parameters were kept constant for the duration

of the study and the machine was routinely calibrated using calibration beads (CaliBRITE, Becton Dickinson, San Jose, CA, USA) to ensure comparable readings between different days. A minimum of 10,000 events were gated to exclude dead cells, and analysis was performed with Cell Quest software (Becton Dickinson, San Jose, CA, USA). Thus, the efficiency of anti-canine CD20 antibody was determined on different types of B and T cell lymphomas that are meant to be positive and negative for CD20, respectively using FACS.

2.7.5. Immunohistochemistry

Biopsies were obtained from dogs with different types of B and T cell lymphomas, including Diffuse Large B-cell lymphoma (DLBCL), Marginal Zone Lymphoma (MZL), Follicular Lymphoma (FL), B-cell small lymphocytic (B-SLL), and Lymphoma and Peripheral T-cell Lymphoma (PTCL). All lymphoma samples were taken as part of normal diagnostic procedures from dogs with newly diagnosed, previously untreated lymphoma. For tissue microarray (TMA), hematoxylin and eosin-stained sections from each paraffin-embedded, formalin fixed block were used to define diagnostic areas and cores were obtained from each case and inserted in a grid pattern into a recipient paraffin block using a tissue arrayer. Sections were then cut and stained with antibodies to CD20 as well as CD79. Following deparaffinization, heat induced antigen retrieval techniques were used for each antibody. Sections were analysed for presence of positive immunolabelling to the mouse anti-canine CD20 antibody.

2.7.6. Characterization of anti-CD20 mAb on Raji cells by Immunofluorescence

Immunofluorescence was performed on CD20 expressing human Raji cells using mouse anti-CD20 mAb. This experiment was performed in order to measure the activity of anti-CD20 mAb onto human CD20 expressing cells. A488 was used as a detection fluorescent tag attached to the secondary antibody. Rituximab coupled to A488 and secondary antibody coupled to A488 were used as positive and negative control respectively.

2.8. Construction of mouse scFv antibody library

2.8.1. Extraction and isolation of total RNA from immunized mice

Prior to the extraction procedure, some preparatory steps are followed. Oakridge tubes are cleaned with Virkon® to remove any contamination. They are then washed with RNAse free water (Sigma), sprayed with RnaseZap® (Sigma) and left overnight to make sure no contaminating Rnases are present. The homogenizer is thoroughly washed with 'Rnase free' water, autoclaved and then baked in a 60 ^{0}C oven overnight. A laminar flow hood is de-contaminated by cleaning with 70% ethanol prepared in Rnase free water and also all the materials used for the extraction procedure are decontaminated. The mice was sacrificed by cervical dislocation, spleen was removed and placed in Rnase free tube. The spleen was then homogenized in 10 ml Trizol reagent using a sterile homogenizer and the tubes were centrifuged in an Eppendorf 5810r centrifuge at 1575 g for 10 minutes at 4 ^{0}C. The supernatant was removed into 50 ml Oakridge tubes containing 2 ml of chloroform. This was mixed well by shaking and incubated at RT for 15 minutes. This incubated sample was then centrifuged at 17500 g for 20 minutes at 4 ^{0}C. Following centrifugation, three layers become visible. The upper aqueous layer is carefully removed ensuring that none of the organic layer is transferred from the interphase. This aqueous layer is added to a large Oakridge tube with 5 ml of isopropanol for precipitation. This is mixed and left at RT for 10 minutes. It is then centrifuged at 17500 g for 20 minutes at 4^{0}C. The supernatant is carefully removed and discarded ensuring that the pellet is not disrupted. The RNA pellet is washed by adding 10 ml of 75% ethanol. This is centrifuged again at 17500 g for 10 minutes at 4^{o}C and the supernatant is again discarded. The pellet is air dried in laminar flow cabinet and gently resuspended in 250 µl of molecular grade water (Sigma). The RNA is then subsequently quantified on Nanodrop and cDNA synthesis is performed.

2.8.2. Reverse transcription of total RNA to cDNA

Omniscript Reverse transcription kit (Qiagen) was used in order to make cDNA from RNA

Component	Volume/ reaction	Final concentration
Master mix 10X Buffer RT	2 µl	1 x
dNTP mix (5 mM each dNTP)	2 µl	0.5 mM each dNTP
Oligo –dT primer (10 µM)	2 µl	1 µM
RNAse inhibitor (10 units/ µl)	1 µl	10 units (per 20 µl)
Omniscript Reverse transcription	1 µl	4 units (per 20 µl)
RNAse free water	variable	
Template RNA Template RNA, added at step 5	variable	Upto 2 µg (per 20 µl reaction)
Total volume	20 µl	

Table 2.4: Reverse transcription: *Qiagen protocol for reverse transcription (RNA to cDNA)*

2.8.3. PCR primers for the construction of a murine scFv library (pCOMB3xSS vector)

A set of total 17 forward primers (5') and 3 reverse primers (3') was used for the amplification of variable kappa light chain, two primers for amplification of lambda light chain (3', 5'). For amplification of heavy chain a total of 19 forward primers (5') were used with 3 reverse primers (3'). The sequence of all the primers used has been mentioned below:

V_K 5' Sense primers

MSCVK-1

5' GGG CCC AGG CGG CCG AGC TCG AYA TCC AGC TGA CTC AGC C 3'

MSCVK-2

5' GGG CCC AGG CGG CCG AGC TCG AYA TTG TTC TCW CCC AGT C 3'

MSCVK-3

5' GGG CCC AGG CGG CCG AGC TCG AYA TTG TGM TMA CTC AGT C 3'

MSCVK-4

5' GGG CCC AGG CGG CCG AGC TCG AYA TTG TGY TRA CAC AGT C 3'

MSCVK-5

5' GGG CCC AGG CGG CCG AGC TCG AYA TTG TRA TGA CMC AGT C 3'

MSCVK-6

5' GGG CCC AGG CGG CCG AGC TCG AYA TTM AGA TRA MCC AGT C 3'

MSCVK-7

5' GGG CCC AGG CGG CCG AGC TCG AYA TTC AGA TGA YDC AGT C 3'

MSCVK-8

5' GGG CCC AGG CGG CCG AGC TCG AYA TYC AGA TGA CAC AGA C 3'

MSCVK-9

5' GGG CCC AGG CGG CCG AGC TCG AYA TTG TTC TCA WCC AGT C 3'

MSCVK-10

5' GGGCCC AGG CGG CCG AGC TCG AYA TTG WGC TSA CCC AAT C 3'

MSCVK-11

5’ GGG CCC AGG CGG CCG AGC TCG AYA TTS TRA TGA CCC ART C 3’

MSCVK-12

5’ GGG CCC AGG CGG CCG AGC TCG AYR TTK TGA TGA CCC ARA C 3’

MSCVK-13

5’ GGG CCC AGG CGG CCG AGC TCG AYA TTG TGA TGA CBC AGK C 3’

MSCVK-14

5’ GGG CCC AGG CGG CCG AGC TCG AYA TTG TGA TAA CYC AGG A 3’

MSCVK-15

5’ GGG CCC AGG CGG CCG AGC TCG AYA TTG TGA TGA CCC AGW T 3’

MSCVK-16

5’ GGG CCC AGG CGG CCG AGC TCG AYA TTG TGA TGA CAC AAC C 3’

MSCVK-17

5’ GGG CCC AGG CGG CCG AGC TCG AYA TTT TGC TGA CTC AGT C 3’

VK 3’ Reverse primer

MSCJK12-BL

5’ GGA AGA TCT AGA GGA ACC CCC ACC ACC GCC CGA GCC ACC GCC ACC AGA GGA TIT KAT TTC CAG YTT GGT CCC 3’

MSCJK4-BL

5’ GGA AGA TCT AGA GGA ACC ACC CCC ACC ACC GCC CGA GCC ACC GCC ACC AGA GGA TTT TAT TTC CAA CTT TGT CCC 3’

MSCVJK5-BL

5’ GGA AGA TCT AGA GGA ACC ACC CCC ACC ACC GCC CGA GCC ACC GCC ACC AGA GGA TTT CAG CTC CAG CTT GGT CCC 3’

V_λ 5' sense primer

MSCVL-1

5' GGG CCC AGG CGG CCG AGC TCG ATG CTG TTG TGA CTC AGG AAT C 3'

V_λ 3' reverse primer

MSCJL-BL

5' GGA AGA TCT AGA GGA ACC ACC CCC ACC ACC GCC CGA GCC ACC GCC ACC AGA GGA GCC TAG GAC AGT CAG TTT GG 3'

V_H 5' Sense primers

MSCVH1

5' GGT GGT TCC TCT AGA TCT TCC CTC GAG GTR MAG CTT CAG GAG TC 3'

MSCVH2

5' GGT GGT TCC TCT AGA TCT TCC CTC GAG GTB CAG CTB CAG CAG TC 3'

MSCVH3

5' GGT GGT TCC TCT AGA TCT TCC CTC GAG GTG CAG CTG AAG SAS TC 3'

MSCVH4

5' GGT GGT TCC TCT AGA TCT TCC CTC GAG GTC CAR CTG CAA CAR TC 3'

MSCVH5

5' GGT GGT TCC TCT AGA TCT TCC CTC GAG GTY CAG CTB CAG CAR TC 3'

MSCVH6

5’ GGT GGT TCC TCT AGA TCT TCC CTC GAG GTY CAR CTG CAG CAG TC 3’

MSCVH7

5’ GGT GGT TCC TCT AGA TCT TCC CTC GAG GTC CAC GTG AAG CAG TC 3’

MSCVH8

5’ GGT GGT TCC TCT AGA TCT TCC CTC GAG GTG AAS STG GTG GAA TC 3’

MSCVH9

5’ GGT GGT TCC TCT AGA TCT TCC CTC GAG GTG AWG YTG GTG GAG TC 3’

MSCVH10

5’ GGT GGT TCC TCT AGA TCT TCC CTC GAG GTG CAG SKG GTG GAG TC 3’

MSCVH11

5’ GGT GGT TCC TCT AGA TCT TCC CTC GAG GTG CAM CTG GTG GAG TC 3’

MSCVH12

5’ GGT GGT TCC TCT AGA TCT TCC CTC GAG GTG AAG CTG ATG GAR TC 3’

MSCVH13

5’ GGT GGT TCC TCT AGA TCT TCC CTC GAG GTG CAR CTT GTT GAG TC 3’

MSCVH14

5’ GGT GGT TCC TCT AGA TCT TCC CTC GAG GTR AAG CTT CTC GAG TC 3’

MSCVH15

5’ GGT GGT TCC TCT AGA TCT TCC CTC GAG GTG AAR STT GAG GAG TC 3’

MSCVH16

5’ GGT GGT TCC TCT AGA TCT TCC CTC GAG GTT ACT CTR AAA GWG TST G 3’

MSCVH17

5’ GGT GGT TCC TCT AGA TCT TCC CTC GAG GTC CAA CTV CAG CAR CC 3’

MSCVH18

5’ GGT GGT TCC TCT AGA TCT TCC CTC GAG GTG AAC TTG GAA GTG TC 3’

MSCVH19

5’ GGT GGT TCC TCT AGA TCT TCC CTC GAG GTG AAG GTC ATC GAG TC 3’

V_H 3’ Reverse primers

MSCGlab-B

5’ CCT GGC CGG CCT GGC CAC TAG TGAA CAG ATG GGG STG TYG TTT TGG C 3’

MSCG3-B

5’ CCT GGC CGG CCT GGC CAC TAG TGA CAG ATG GGG CTG TTG TTG T 3’

MSCM-B

5’ CCT GGC CGG CCT GGC CAC TAG TGA CAT TTG GGA AGG ACT GAC TCT C 3’

2.8.4. Overlap Extension primers

For splicing heavy and light chains i.e. making scFv, another round of PCR was performed using 100 ng of each purified variable heavy and light chain. The primers used in this PCR contain the site for digestion with SfiI as well as linker sequence to anneal the two chains. The sequence of each of the primer has been mentioned below:

RSC-F (sense)

5’ GAG GAG GAG GAG GAG GAG GCG GGG CCC AGG CGG CCG AGC TC 3’

RSC-B (reverse)

5’ GAG GAG GAG GAG GAG GAG CCT GGC CGG CCT GGC CAC TAG TG 3’

Amplification of antibody variable domain genes using pCOMB series primers

The standard PCR reaction components and conditions were as follows:

Component	**Concentration in 50 µl reaction**
cDNA	0.5 µg
2x Phusion master mix (Phusion polymerase, dNTPs and Phusion buffer)	25 µl
Forward primer	60 pM
Reverse primer	60 pM

This mixture is made up to 50 µl with Mg H_2O.

PCR amplification of the variable domains from murine cDNA was performed in a Biometra $T_{Gradient}$ PCR machine and under the following conditions:

Step 1:	94^{o}C for 5 minutes	
Step 2:	30 cycles of;	94^{o}C for 15 seconds
		56^{o}C for 30 seconds
		72^{o}C for 90 seconds
Step 3:		72^{o}C for 10 minutes

After the amplification of the variable regions, five microliters of each PCR product was analysed on a 2% (w/v) agarose gel. The reaction was scaled up (10 X) in order to obtain more of PCR product and then PCR products were pooled together and ethanol precipitated to extract DNA using 3 M sodium acetate. The PCR products were purified on a 1.5% (w/v) agarose gel, DNA was quantified using Nanodrop at an absorbance of 260nm.

2.8.5. Splicing of purified PCR products by overlap extension PCR

In SOE - PCR, appropriate purified variable heavy and light chains (V_H and V_L) are mixed in equal ratios in order to generate the overlap product. Both the purified variable fragments are joined together via a glycine serine linker $(G_4 S)_4$, producing a fragment of approximately 750 bp. A total of 10 µg of total product was made via PCR and gel extraction in order to proceed to the next step.

SOE PCR components for amplification of mixed variable heavy and light chains;

Component	Concentration in 50 µl reaction
Phusion Mastermix (2X)	25 µl

V_H	100 ng
V_L	100 ng
Forward primer	60 pM
Reverse primer	60 pM

The mixture was made up to 50 µl with Mg H_2O.

The PCR amplification was again performed in a Biometra $T_{Gradient}$ PCR machine under following conditions:

Step 1	94°C for 5 minutes
Step 2	
20 cycles of;	94°C for 15 seconds
	56 °C for 15 seconds
	72 °C for 2 minutes
Step 3	72 °C for 10 minutes

2.8.6. Restriction digest of the purified overlap PCR product and vector DNA

Restriction digest of the purified overlap PCR product:

- Component concentration per reaction 1 X
- Purified overlap PCR product 10 ng
- *SfiI* (36 U per µg of DNA) 360 U
- NEB Buffer 2 (10 X) 1 X
- BSA (100 X) 1 X
- Molecular grade was added to a final volume of 500 µl.

Restriction digest of the purified vector DNA:

- Component Concentration per reaction 1 X
- Vector DNA (pCOMB3xSS) 20 µg
- SfiI (6 U per µg of DNA) 120 U
- NEB Buffer 2 (10 X) 1 X
- BSA (100 X) 1 X
- Molecular grade water was added to a total volume of 200 µl.

The digestion reactions were incubated for 5 hours at 50^0C. PCR products were pooled together and ethanol precipitated. The digested PCR fragment and pCOMB3xSS vector along with stuffer fragment were purified on a 1% (w/v) agarose gel and 0.6% (w/v) agarose gel, respectively. DNA was quantified by measuring the absorbance at 260 nm on Nanodrop.

2.8.7. Ligation of the digested overlap PCR product with vector DNA

The gel purified SfiI restricted scFv insert fragment was cloned into digested pCOMB3xSS facilitated by T_4 DNA ligase.

- Component Concentration per reaction 20 X
- pCOMB3xSS (digested and purified) 1.4 µg
- Overlap PCR product (digested and purified) 700 ng
- T4 DNA ligase buffer 1 X
- T4 DNA ligase 10 µl
- Molecular grade water was added to a total volume of 400 µl.

Ligation reaction was incubated at 16^0C overnight. The ligation reaction was then purified the following day by mini purification kit (Invitrogen) and DNA pellet was resuspended in 10 µl of molecular grade water and transformed into *E.coli* TG1 electrocompetent cells by electroporation.

2.8.8. Transformation of *E.coli* TG1 cells with pCOMB3xSS vector containing variable heavy and light chains and measurement of transformation efficiencies

The eluted 10 µl purified ligation reaction (5 x 2 µl) was transformed into TG1 cells. 30 µl of cells were added to each reaction in electrocuvettes and stored on ice for 1 minute. This was followed by electroporation at 2.5 kV, immediately flushed with 250 µl of SOC media. These electroporated samples were then incubated for 1 hour at 37^0C. Following incubation, serial dilutions from 10^{-1} to 10^{-8} (library titre) were prepared for both i.e. vector containing insert as well as vector DNA only. Also rest of the transformed culture was plated out on a large assay plate containing LB (100 µg/ml Ampicillin) with 2% glucose. 100 µl of each dilution was poured onto the respective LB plates containing 100 µg/ml carbenicillin and all the plates were incubated overnight at 37^0C.

The total transformants were the number of colonies from the titered plates, multiplied by total culture volume (1.3 ml) and divided by plating volume (0.1 ml). The whole library was scrapped off using LB media containing 2% glucose and glycerol. Also, OD of the library was measured and the optimum amount of library to be used for biopanning experiment was calculated. Library stocks were flash frozen in liquid nitrogen and stored at -80^0C.

2.9. Biopanning (following Barbas protocol)

All biopanning experiments were carried out in a clean area to avoid any contamination in the prep lab. Liquid waste including blocking solutions were decanted into glassware containing either Virkon or bleach. The liquid waste will be handled in method outlined in the SOP for handling aflatoxin and phycotoxin material.

Personal protective equipment has to worn when working with toxic materials, and also during decontamination, disposal and spillage procedures. Gloves to be worn at all times and all the waste materials should be discarded into a waste container.

Glassware, centrifuge chambers, etc to be used were soaked in Virkon overnight, rinsed and following day rinsed with tap water. Centrifuge chambers were then autoclaved. The parameters set in different rounds of panning are mentioned in table 2.5.

Immunogen: canine CD20 peptide (NCDPANPSEKNSPSTQYCSI)

Parameters	PAN1	PAN2	PAN3	PAN4
culture volume (ml)	1000	100	100	100
CD20 peptide (µg)	100	50	25	10
Washes	3x PBS-T 3x PBS	5x PBS-T 5x PBS	10x PBS-T 10x PBS	13x PBS-T 13x PBS

Table 2.5: Parameters for different rounds of panning: *Culture volume, peptide concentration and number of washes in each of the four rounds of biopanning.*

The transformed library was transferred to 1000 ml LB containing 100 µg/ml ampicillin and the cells were grown at 37^0C to an OD_{600nm} of 0.6. One ml of 1×10^{11} pfu/ ml helper phage was added and culture was incubated stationary at 37^0C for 30 minutes. The culture was then propagated at 200 rpm and 37^0C for 2 hours. Subsequently kanamycin (50 µg/ml) (Invitrogen) was added and the cultures were incubated overnight at 200 rpm at 30^0C. Also, overnight cultures (5 ml) of *E.coli* TG1 cells were prepared for sub-culturing following day to prepare phage titres. 500 µl of streptavidin was coated onto the immunotube; the tube was covered in parafilm and stored upright at 4^0C overnight.

Requirements:

- LB media
- 100 mg/ml Ampicillin
- 4 autoclaved 250 ml centrifuge chambers

- PEG/ NaCl
- GSA Rotor (4^0C)
- 3% BSA in PBS

2.9.1. Panning round I:

Several dilutions (1:1000, 1:2000, 1:4000 and 1:8000) of the overnight TG1 cells were sub-cultured in 20 ml LB and grown to an OD_{600nm} of 0.6 (Use fresh electrocompetent cells for each overnight i.e. aliquot cells to prevent phage contamination).

Phage preparation

- The overnight phage library was placed in 4 x 250 ml centrifuge bottles (250 ml per centrifuge bottle). Centrifuge at 9000rpm in a GSA rotor (brake off) for 20 minutes.
- The phage supernatant was transferred to fresh 250 ml centrifuge bottles containing 8 g of PEG (4% w/v) and 6 g of NaCl (3% w/v). These centrifuge bottles were placed in a shaker at 200 rpm for 20 minutes until PEG and NaCl were fully dissolved. This precipitated mixture was placed on ice for 30 minutes.
- Centrifuge at 9000 rpm in a black rotor (brake off) for 15 mins at 4^0C. Discard supernatant and dry inverted on tissue for 10 minutes.
- Resuspend the pellet thoroughly using 2 ml 3% (w/v) BSA and transfer to a microcentrifuge tube. Centrifuge again at full speed for 5 minutes at 4^0C. Transfer the supernatant (input phage) into a fresh microcentrifuge and store at 4^0C.

2.9.2. Panning –Round 2, 3 and 4

Several dilutions (1:1000, 1:2000, 1:4000 and 1:8000) of the overnight TG1 cells were sub-cultured in 20 ml LB and grown to an OD_{600nm} of 0.6 (Use fresh

electrocompetent cells for each O/N i.e. aliquot cells to prevent phage contamination).

Phage preparation

- The overnight phage library was placed in 2 x 50 ml centrifuge bottles (50 ml per chamber). Centrifuge at 9000 rpm in a GSA rotor (brake off) for 20 minutes.
- The phage supernatant was transferred to fresh 50ml chambers containing 2 g of PEG (4% w/v) and 1.5 g of NaCl (3% w/v). These chambers were placed in a shaker at 200 rpm for 20minutes until PEG and NaCl were fully dissolved. This precipitated mixture was placed on ice for 30 minutes.
- Spin at 9000 rpm in a black rotor (brake off) for 15 mins at 4^0C. Discard supernatant and dry inverted on tissue for 10 minutes.
- Resuspend the pellet thoroughly using 2 ml 3% (w/v) BSA and transfer to a microcentrifuge tube. Spin again at full speed for 5 minutes at 4^0C. Transfer the supernatant (input phage) into a fresh microcentrifuge and store at 4^0C.

Protocol:

- An immunotube was coated overnight with streptavidin
- Following day, the tube was washed 3 x PBS-T and CD20 peptide was added to the immunotube and incubated shaking for 1 hour at RT.
- The immunotube was then blocked with 3% (w/v) BSA for 1 hour at RT.
- The immunotube was washed once with PBS-T – fill up the immunotube and tap off the excess.
- 1ml of input phage (precipitated phage) was added onto the immunotube and incubated for 2 hours at RT rotating.
- The phage was then discarded into bleach waste bucket. The immunotube was then washed with required amount of times depending on the round of panning and washing was discarded into bleach bucket.

- For elusion of binding phages, 1 ml of 10 mg/ml trypsin (in PBS) was added and placed on a rotator for 15 minutes. This was pipetted up and down to obtain all the binding phage.
- This eluted phage (800 µl) was then infected into *E.coli* TG1 cells (5 mls) that have been grown to an OD_{600nm} of 0.6 and incubated static at 37^0C for 15 minutes.
- This TG1 infected phage culture was added to 6 mls of pre warmed LB medium in a 50 ml falcon tube. This 12 ml culture was incubated at 37^0C for 1 hour with shaking at 220 rpm.
- After 1 hour, 800 µl of commercial M13KO7 helper phage (NEB N0315S) was added. This was transferred to a new glass conical flask (250 ml) that contains 88 ml of pre-warmed media containing 100 µl ampicillin and kept shaking for 2 hours at 37^0C.
- Following 2 hours incubation, 200 µl of kanamycin (50 µg/ml) was added and incubated overnight shaking at 220 rpm at 30^0C.

- **Output titres** (eluted phage): A series of dilutions (10^{-1} to 10^{-8}) was prepared using 2 µl of eluted phage in 223 µl *E.coli* TG1 cells (OD_{600nm} ~0.6). The eppendorfs were then incubated static at 37^0C for 30 minutes and 100 µl of dilutions (10^{-5} to 10^{-8}) were plated out after incubation onto LB (Amp) plates.
- **Input titres** (phage before adding to the immunotube for selection) and similarly for preparing input titres, a series of titration (10^{-1} to 10^{-12}) was prepared in 223 µl E.coli TG1 cells in sterile eppendorfs.
- Following overnight incubation at 30^0C, the culture was centrifuged at 3,200 g in an Eppendorf 5810r centrifuge for 15 minutes at 4^0C. The supernatant was PEG precipitated as mentioned in the above section.
- As mentioned in above section, overnight fresh TG1 cultures were set up and immunotube coated overnight with streptavidin for next rounds and similar mentioned protocol was followed.

2.9.3. Polyclonal phage pool ELISA and colony pick PCR

A Nunc Maxisorb^{TM} plate was coated with 100 µl of 1 µg/ml streptavidin and incubated overnight at 4^0C. Following day, the plate was washed with 3 x PBS-T (0.1% (w/v)) and 100 µl of biotinylated CD20 peptide (1 µg/ml) was added and the plate was incubated for 1 hour at RT. The excess conjugate was discarded and the plate was subsequently blocked with 200 µl of 3% (w/v) BSA in PBS for 1 hour. The blocked plate was washed again 3 x PBS-T (0.1% (w/v)) and the stored phage pool from all the rounds was added to different wells of the plate and incubated for 1 hour at RT.

The excess phage was discarded in the bleach bucket, plate was washed again 3 x PBS-T (0.1% (w/v)) and 100 µl of HRP conjugated anti-M13 secondary antibody (1:1000) in PBS containing 3% (w/v) BSA. The plate was incubated for 1 hour, washed 3 x PBS-T (0.1% (w/v)) and 100µl of TMB substrate (Sigma) was added to each well. After incubating the plate for 30 mins, the reaction was stopped using dilute H_2SO_4 (10% (v/v)) and the absorbance was read at 450 nm on a Tecan Safire2^{TM} plate reader.

Also, 10 single colonies were randomly picked from the 3rd and 4th round of panning to ensure the vector was harbouring the scFv fragment. A sterile tip was used to pick up a colony and placed in the below mentioned reaction mixture. The PCR reaction was run in a Biometra $T_{GRADIENT}$ PCR machine, the amplified scFv fragment from the colonies were analysed on gel electrophoresis on a 1% (w/v) agarose gel.

Component	**Concentration in 50 µl reaction**
Phusion Master mix	2 X
cDNA	colony
Forward primer	60 pM
Reverse primer	60 pM

The reaction was made upto 50 µl with dH_2O.

Below mentioned conditions were used in order to run PCR reaction on $T_{GRADIENT}$ PCR machine:

Step 1:		94^{o}C for 5 minutes
Step 2:	30 cycles of;	94^{o}C for 15 seconds
		56^{o}C for 30 seconds
		72^{o}C for 90 seconds
Step 3:		72^{o}C for 10 minutes

2.9.4. Monoclonal ELISA for detection of CD20 specific scFv

Individual colonies (192) from round 3, 4 were picked up and grown in single wells containing 100 µl of LB (100 µg/ml amp). These were labelled as stock plates and were grown overnight shaking at 220 rpm at 37^{0}C. Following day, the stock plates were then sub cultured (30 µl) into 2 ml 96 well plate (Greiner Bio One) containing 500 µl of LB (100 µg/ml amp) containing 1 x 505 (0.5% (v/v) glycerol, 0.05% (v/v) glucose final concentration), 1 mM $MgSO_4$ 100 µg/ml ampicillin. The plate was incubated with shaking at 220 rpm at 37^{0}C for 3 hours until an OD_{600nm} of 0.6 is reached and 70% (v/v) was added to the overnight stock plates to a final concentration of 15% (v/v) and the transferred to a -80^{0}C freezer for long term storage. Expression was induced by addition of 1 mM IPTG and finally incubated at 30^{0}C overnight with shaking at 220 rpm. Also, alongside two Nunc Maxisorb^{TM} plates were coated with streptavidin (200 ng/ well) and left overnight at 37^{0}C. Following day, the plate was washed 3 x PBS-T (0.1% (v/v)) and 1 µg/ml of CD20 peptide was added to all the wells with an incubation period of 1 hour. The plates were then washed 3x PBS-T (0.1% (v/v)) and blocked with 3% (w/v) BSA in PBS. Meanwhile, the overnight plates containing expressed clones were removed from the

incubator and subjected to freeze thaw protocol for the production of scFv enriched lysate. The plates were first placed at -80^{0}C until fully frozen and then thawed at 37^{0}C (freeze-thaw protocol repeated 3 times). The plates were then centrifuged at 3,220 g for 15 minutes in an Eppendorf 5810r centrifuge, to obtain the scFv enriched lysate. The lysate supernatant (100 µl) was added to the corresponding well in the respective ELISA plate, mixed gently and incubated for 1 hour at RT. The plates were then washed 3 x PBS-T (0.1% (v/v)) and 100 µl of HRP labelled protein A antibody at a dilution of 1:1000 in 3% (w/v) BSA. The plates were incubated for 1 hour and washed again three times. TMB was again added as a substrate onto all the wells of the ELISA plate, the reaction was stopped again after 30 minutes incubation period by using 10% (v/v) H_2SO_4 and the absorbance was read at 450nm on a Tecan Safire2^{TM} plate reader.

2.9.5. Antibody expression and purification

10 ml LB media containing 1% (w/v) glucose and 100 µg/ml ampicillin was inoculated with 100 µl of transformed scFv stocks and grown overnight at 37^0 C, while shaking at 220 rpm. The overnight cultures were then used to seed 500 ml LB media containing 1 x 505 supplement and 100 µg/ml ampicillin and grown until an OD_{600nm} of 0.6 was reached. The cultures were then induced by the addition of 1mM IPTG and incubated overnight at 30^0 C, while shaking at 220 rpm. The following day the cultures were centrifuged at 3,220 g for 30 minutes at 4^{0}C and the supernatant was discarded. The cell pellet was resuspended in 10 ml lysis buffer (50 mM $Na_2H_2PO_4$, 300 mM NaCl, 10 mM imidazole, pH 8). This was sonicated on ice three times for 45 seconds (5 seconds interval) at amplitude of 40, using a microtip Vibra Cell^{TM} sonicator. The cell debris was then removed by centrifuging at 15,000 g for 10 minutes at 4^{0}C in an Eppendorf 5810r centrifuge.

The lysate supernatant was filtered through a 0.2 µm filter to remove any residual cell debris, prior to subsequent purification. 2 ml of Ni-NTA slurry (Qiagen) was added to a 20 ml column and equilibrated with lysis buffer (50 mM $Na_2H_2PO_4$, 300 mM NaCl, 10 mM imidazole, pH 8). The filtered lysate was added to the

equilibrated column and the flowthrough was collected. The column was then washed with 20 ml of 50 mM $Na_2H_2PO_4$, 300 mM NaCl, pH 8. 20 mls of 50 mM $Na_2H_2PO_4$, 300 mM NaCl, 10 mM imidazole, pH 8 was added to the column to remove any loosely bound proteins. Elusion of bound scFv was performed by adding 5 ml of 50 mM $Na_2H_2PO_4$, 300 mM NaCl, 250 mM imidazole, pH 8 to the column. Antibody containing fractions were buffer exchanged against filtered PBS using a 5 kDa cut off Vivaspin^{TM} column (AGB, VS0611). The buffer exchanged scFv was quantified using Nanodrop and the resultant antibody solution was stored at 20^0C until required.

2.10. Phage bound scFv

10 random colonies were picked up from round 3, 4 and grown in 15 ml LB (100 µg/ml amp) and grown to an OD_{600nm} of 0.6 in a 50 ml falcon tube in a 37^0C incubator, shaking at 220 rpm. The helper phage was then added to the individual tube and incubated static for 30 minutes, followed by shaking at shaking at 220 rpm at 37^0C. This was followed by addition of kanamycin (50 µg/ml) and incubated overnight at 30^0C. Also, a Nunc Maxisorb^{TM} plate was incubated overnight with streptavidin (200 ng/well).

The following day, the falcon tubes were centrifuged and PEG precipitated in a similar manner as mentioned above. The phage pellet was then resuspended in 200 µl of PBS and was added to the respective ELISA well. ELISA was performed in several titrations and similarly to the above mentioned protocol (Section 2.6).

2.10.1. Cloning of scFv3 and 7 into mammalian and bacterial expression system

a. Mammalian and Bacterial expression of scFv-3 and scFv-7

scFv-3 and scFv-7 were cloned into bacterial and mammalian expression vectors, pTRCHisB and pCDNA3.1 (Clontech), respectively. The mammalian expression was carried out by transfection of CHO-k1 cells with the indicated scFv expression vector (Jianguo Shi, Ted Hupp lab) using Attractene Reagent. A day before transfection, CHO cells were split in 3 wells of a 6-well plate at density of 1 x 104, 5 x 104, and 1

x 105, respectively. Next day, for each well cells, 0.2 µg of construct was mixed with 60 µl medium (without serum) first, then 1.5 µl of Attractene Reagent (Qiagen) was added in the above solution mixed. The solutions were incubated at RT for 15 min to allow the complex formation, and then the transfection complexes were added drop-wise onto the cells in 2 ml of fresh media. The cells from each well were split into 100 mm tissue culture dishes the following day in 10 ml selective medium to allow individual colonies formation. Finally, the individual colonies were transferred into 24-well plate (one colony per well, 96 colonies were picked up for each antibody). After 4 rounds selection by ELISA, the best colonies (higher yield and low cell density) were cultured at a large scale in selective media [DMEM supplemented with 10 % low IgG FBS (Life Technologies Ltd, USA), 1% Penicillin/Streptomycin , 2% L-glutamine, 250 µg/ml Mycophenolic acid (Sigma Aldrich, UK), 12.5 µg/ml Xanthine (Sigma Aldrich, UK), 200 ng/ml Geneticin (Invitrogen Ltd, UK). The bacterial expression of was carried out in BL21 after induction of expression using IPTG. The resuspended pellets were thawed in ice and resuspended in 10 ml lysis buffer (50 mM NaH_2PO_4, 300 mM NaCl, 10 mM imidazole, pH 8.0). Lysozyme was directly added at a final concentration of 1 mg/ml and the solution was stirred on ice for 30 minutes. Cells were sonicated on ice for 7 x 12 seconds with a 15 seconds interval between each cycle and the crude lysate was centrifuged for 30 minutes at 10,000 g at 4˚C to remove cellular debris. The supernatant was transferred to a clean tube for subsequent purification.

b. Purification of His-tagged scFv and scFv-CPG2 bio conjugates via metal affinity chromatography

The E. coli lysate was added to the NTA magnetic agarose beads (QIAGEN) in a 6ml column and equilibrated with 15 ml equilibration column buffer (50 mM NaH_2PO_4, 300 mM NaCl, 10 mM imidazole, pH 8.0) and incubated overnight rotating at 4˚C. The following day, the column was allowed to empty by gravity flow and the flow-through was collected in a 15 ml Falcon tube. The column was then washed with 100 ml washing buffer (50 mM NaH_2PO_4, 300 mM NaCl, 20 mM imidazole, pH 8.0) to remove any non-specifically bound proteins. After washing, 4 ml elution buffer (50 mM NaH_2PO_4, 300 mM NaCl, 250 mM imidazole, pH 8.0)

was added to the column and incubated at 4˚C for 1 hour. Following this incubation step, the sample was collected at room temperature. The efficiency of the purification process was evaluated using SDS-PAGE and Western Blot. The eluted antibody was buffer exchanged into PBS via the dialysis technique (technique used for removal of small, unwanted compounds by selective diffusion through a semi permeable membrane). The concentration of the resultant antibody was determined using a Nanodrop 1000 spectrophotometer and then the solution was stored at -20˚C. For Cloning of scFv 3, 7 into CPG2, a bacterial expression system contained a derivative of CPG2 that has previously been used as a bioconjugate to scFv targeting CEA41 and was provided by Mologics (Bedford, UK). The fusion protein was highly insoluble using the scFv lysis buffer (above) but soluble protein could be recovered in lysis buffer containing 100 mM Tris (pH 8.0), 500 mm NaCl, 10% Glycerol, 1 mM PMSF, 1 mg/ml lysozyme, 1 mm DTT, 2 mm MgCl2, and benzonase. Protein was eluted in imidazole buffer from the nickel affinity column in stabilization buffer containing 50 mM Tris pH 8, 500 mM NaCl, 10% glycerol, 1 M betain, 0,5% Triton x-100, and 250 mM imidazole).

2.10.2. Cloning of scFv 3 into *Pichia* for antibody expression

The cloning and expression of scFv into *Pichia* was carried out with help of post - doctoral scientists in the Hupp laboratory (Jianguo Shi and Euan Murray).

Materials required:

- Buffered Glycerol complex Medium (BMGY)
- Buffered Methanol complex Medium (BMMY)
- 1% yeast extract
- 2% peptone
- 100 mM potassium phosphate, pH 6.0
- 1.34 % YNB
- 4×10^{-5} % biotin
- 1% glycerol or 0.5% methanol

Dissolve 10 g of yeast extract, 20 g peptone in 700 ml water and autoclave for 20 minutes on liquid cycle. Let it cool down to room temperature and add following ingredients:

- 100 ml 1 M potassium phosphate buffer, pH 6.0
- 100 ml 10 X YNB
- 2 ml 500X B, 100 ml 10X GY

For BMMY, add methanol (10X M) instead of glycerol.

The growth temperature for yeast is in the range of 28-30^{0}C for cultures, plates and slant. The storage life of BMMY/BMGY buffer is atleast 2 months at 4^{0}C. After cloning of scFv into yeast expression vector, 25 ml BMGY medium was inoculated using a single colony and grown at 28-30^{0}C in a shaking incubator until an OD_{600nm} of 2-6 is reached (approximately 24 hours). Cells were harvested by centrifuging at 1500-3000 g for 5 minutes at room temperature and pellet was resuspended in BMMY medium to induce expression. This flask was then covered with 2 layers of sterile tissues and incubated again in a shaking incubator. Methanol (100%) was added to a final concentration of 0.5% to maintain induction. 1ml of induction sample was taken out daily at different time points, centrifuged and pellets were stored to be run on a SDS gel to analyse the expression level. The expression and purification of yeast CpG2 scFv construct is explained in detail in section 3.2.13.

2.11. Expression and purification of recombinant α-synuclein

The protocol followed for expression and purification of α-synuclein is already mentioned in section 2.1.5.

2.12. Native gel

α-synuclein was run on a native gel after purification to determine its precise molecular weight. The native gel preparation is very similar to SDS gel preparation, except no SDS, DTT and avoids heating the samples. The running buffer (10x) and loading buffer (4x) were prepared in the following way:

10X running buffer: 30.28 g Tris

144.13 g Glycine

Check pH ~ 8.3

4X loading buffer: 50% glycerol

0.6 M Tris pH 6.8

<=0.4%w/v bromophenol blue

Working sample buffer (1 ml): 400 µl 4X stock + 600 µl H_2O

The running buffer (10 X and 1 X) were both stored in a 4^0 C cold room overnight. The gel prepared was 10%, 10 wells and stored in running buffer overnight in cold room. The samples were normalized and diluted in 4 X sample buffer and not heated. The amount of protein ran on the gel is usually double the amount we run on SDS gel. The following day the gel was pre-run at 4^0 C for 1 hour and the running buffer was then discarded. Subsequently, fresh 1 X running buffer was added to the gel apparatus, samples were loaded onto the gel along with an unstained ladder and the gel was run at 50 V for 2 hours until loading dye reaches the end of stacking gel. Once it passes that, the gel was run at 100 V for 4 hours in the cold room. Following this step, gels were used for Coomassie staining or Immunoblotting in same ways as SDS gels. The purified protein was incubated at three different temperatures and loaded onto 12% native gel. The gel was run at 4^0C and RT to investigate the nature of the protein at different conditions. Following optimization of gel running conditions, different amounts of SDS was titrated onto the same amount of purified α-synuclein. We also performed a time course (0 to 6 hours) of 0.1% (w/v) SDS addition to α-synuclein was carried out at RT. Also activity of several detergents such as Triton 100%, Tween - 20 was determined after an overnight incubation with purified α-synuclein.

2.13. Circular Dichroism

Circular Dichroism spectroscopy measures the differential absorbance of left and right handed circularly polarized light when it passes through a sample containing any chiral molecules. The CD signals arise when absorption of radiation occurs and thus the spectral bands correspond to structural pattern of the molecule. CD has been used for studying structural changes by predicting the conformation of protein.

Circular Dichroism = $\Delta A = A(\lambda)_{LCPL} - A(\lambda)_{RCPL}$,

where λ is the wavelength, LCPL: left circular polarized light and RCPL: right circular polarized light

CD is performed by placing diluted sample in a small cuvette in JASCO CD spectropolarimeter. As described in 4.2.3., CD was performed on three different types of sample preparation of α-synuclein. Sample preparation was carefully carried out for α-synuclein with and without SDS in the cuvette with respective dilution. The selected total visible wavelength range was between 185 to 285nm for visualisation of signal to noise ratio. Several algorithms are available online for performing deconvulation but each requires considerable technical effort to execute the program from source file. The main issue with different database is the method of input and the file format from the CD machine which might not be compatible with each database. DICHROWEB is a very user friendly interface which accepts various file formats and can easily interpret CD data using reference data and available algorithms. DICHROWEB supports five different algorithms for analysing CD data: SELCON 3, CONTIN, CDSSTR, VARSLC and K2d. The obtained data was interpreted using DICHROWEB software and the secondary structure was determined

2.14. Development of antibodies and epitope mapping against α-synuclein

Monoclonal antibodies were developed against α-synuclein in a similar manner to the one described in section 2.7.1. The epitope of all mAbs was demonstrated by epitope mapping (ELISA) onto a panel of peptides as shown in section 4.2.5.

Subsequently, we tested the potential ability of all positive IgGs onto α-synuclein in α-synuclein expressing neuroblastoma cell line. Also described in section 4.2.8 is immunoblotting after different types of lysis described below probed with anti-α-synuclein antibody (BD Biosciences). We performed lysis of SHSY5Y cells in 4 different ways (+/- paraformaldehyde):

(i) 10% Triton buffer (described in section 2.4.4.)

(ii) RIPA buffer : 50mM Tris – HCL, pH 7.5, 1% (v/v) NP-40, 0.5% Na-deoxycholate, 0.1% SDS, 150 mM NaCl, 2mM EDTA and 50 mM NaF

(iii) Hypotonic buffer : 20 mM Hepes 7.4, 2 mM EGTA and 2 mM $MgCl_2$

(iv) 8 M Urea buffer : 8M Urea, 300 mM NaCl, 0.5% NP40, 50 mM Na_2HPO_4, 50 mM Tris pH 8, 1 mM PMSF, 1 ng/ml Aprotinin. Make up total volume with Millipore H_2O.

Paraformaldehyde in PBS was used at 0.4% on the immunoblot for 30 minutes following immunoblot transfer before blocking.

2.15. Immunofluorescence and Immunohistochemistry

Immunofluorescence was performed on SHSY5Y cells in 25 mm coverslips with antibody 3.1 at a dilution of 1:500 and commercial antibody as positive control at a dilution of 1:1000. The protocol followed for IF was similar to the one described in section 2.2. Moreover, we performed immunohistochemistry on brain and kidney tissue samples (Henle's loop, brain gray matter, skin and mast cells, etc) in collaboration with Rudolf Nenutil, Brno, Czech Republic. The protocol followed for IHC was similar to the protocol described in section 2.7.5

2.16. Assay development

2.16.1. α-synuclein constructs in pEGFP-(C) as well as pMCherry – (C)

RNA was extracted from SHSY5Y cells, followed by reverse transcription in order to make cDNA. This cDNA was used for the amplification of α-synuclein with

BamHI and XhoI sites flanking the DNA sequence of the gene. The sequence of the designed primers is mentioned below:

Forward (XhoI): 5’ GC CTC GAG ATG GAT GTA TTC ATG A 3’

Reverse (BamHI): 5’ GC GGA TCC GGC TTC AGG TTC GTA G 3’

The purified DNA obtained after PCR amplification as well as vector DNA was double digested with BamHI and XhoI. These products were once again gel extracted and ligated into each other with a ratio of 5:1 (Insert: Vector). The ligation product was then transformed into DH5α cells, a single colony was grown overnight from the plate and miniprep purified. This DNA was sequenced, maxiprep purified and concentration of DNA was determined using Nanodrop.

2.16.2. Co-localization of α-synuclein and interacting proteins in SHSY5Y and HCT116 (WT) cells

GFP and Cherry tagged α-synuclein constructs were co-transfected in SHSY5Y as well as HCT cells. Different amount of DNA was transfected into cells using attractene to see a significant expression in these cells lines. For initial experiments, 0.25; 0.5 and 1 µg of GFP, cherry tagged α-synuclein was transfected in 6 well plates and an optimum level of DNA was determined that showed a significant amount which was analysed by Immunoblotting.

2.16.3. Proximity ligation assay (PLA)

As means of developing new assay to demonstrate co-localization of α-synuclein, we performed PLA onto SHSY5Y cells. SHSY5Y cells were grown on a 19 mm cover slip for 18-24 hours before proceeding with PLA. Following day coverslips were made ready for PLA to be carried in 2 days.

PLA using Duolink

DAY 1

- Wash cover slips 3x Sterile Ice cold PBS
- Fix in 4% PFA for 15 minutes at RT
- Wash cover slips 3x Sterile Ice cold PBS
- Permeabilise with 0.25% Triton X-100 in PBS for 10 minutes

- Wash cover slips 3x Sterile Ice cold PBS
- Block coverslips using 3% BSA in PBS for 30 minutes
- Remove blocking buffer and add primary (diluted 1:250 in 3% BSA in PBS), incubate overnight at 4^{o} C/ 2hours at RT in humidified chamber

Minimum sufficient amount of each prepared solution should atleast be 40 µl and all solutions were prepared fresh.

DAY 2

- Make PLA probe mixture and incubate 20 minutes
    a. Ab diluent 32 µl
    b. PLA plus 4 µl
    c. PLA minus 4 µl
- Wash cover slips 3x Sterile PBS for 5 minutes each
- Add 40 µl of PLA probe mix to each cover slip
- Incubate on parafilm in foiled small box for 1 hour at 37^{o}C
- Wash cover slips 3x with Wash buffer A for 5 minutes each
- 40 µl Ligation mix added to each cover slip
    d. 5x Ligation Stock 8 µl
    e. High purity water 31 µl
    f. Ligase 1 µl (add to solution immediately before adding to slide)
- Incubate on parafilm in box covered in foil for 30 minutes at 37^{o}C
- Wash cover slips 3x with Wash buffer A for 5 minutes each
- 40 µl of polymerase amplification mix added
    g. 5x Amplification stock 8 µl
    h. High purity water 31.5 µl
    i. Polymerase 0.5 µl (add to solution immediately before adding to slide)
- Incubate on parafilm in box covered in foil for 2 hours at 37^{o}C
- Wash cover slips 2 x with 1x Wash buffer A for 5 minutes each, wash cover slips 3x with 1x Wash buffer B for 5 minutes each
- Add phalloidin diluted 1:10 in 1x Wash buffer B for 30 minutes, wash 2x with 0.01x Wash buffer B for 5 minutes
- Dilute DAPI 1:2500 in 0.01x Wash buffer B and incubate in dark for 5 minutes, wash 2x with 0.01x Wash buffer B for 5 minutes
- Mount onto slides using Dako fluorescent mounting medium (20 µl per coverslip)

2.17. Peptide phage display

Peptide phage display was carried out using Peptide phage display library (12 amino acids) from New England Biolabs. Biopanning was used as the selection process which is carried out by incubating the phage displaying library onto the plate coated overnight with α-synuclein (target), washing away unbound phage and eluting the specific binding phage displaying peptides. This dodecapeptide premade library consists of more than 10^9 clones. In both 7 mer and 12 mer library, the first residue of the peptide pIII fusion is first randomized position. Displayed peptides are expressed at the N terminus of the coding region of phage and are linked by a short linker sequence Gly - Gly - Gly - Ser.

To avoid any sort of phage contamination, all plastic, sterile tips and glassware apparatus were sterilised or autoclaved. As severe contamination can lead to contamination in subsequent panning rounds, so all steps were carried out under aseptic conditions and solutions were re-autoclaved for each round.

2.17.1. Panning procedure

Panning procedure on α-synuclein was performed in two ways based on long and short washes. An ELISA 96 well plate was coated overnight with 1 µg/ml of WT α-synuclein in 100 µl of coating buffer ($NaHCO_3$ pH 6.8) and incubated overnight at 4^0C. The following day the coating solution was poured off and the wells were washed 3 times using TBST (TBS 1X (50 mM Tris pH 7.5, 150 mM NaCl) - 0.1% (v/v) Tween-20), the wells were then blocked using blocking buffer (3% (w/v) BSA in TBST) and kept on a rotator for 1 hour at room temperature. The phage library (10^{11} phages) was then diluted in TBST, added to the plate and incubated for 1 hour rocking at room temperature. The wells coated with target of interest were then washed quickly 10 times using TBST for quick washes whereas the wells for slow washes were incubated with TBST for an interval of 5 minutes for each wash to

remove the unbound phages. The specific bound phage particles were eluted with 100 µl of 0.2 M Glycine pH 2.2, 1 mg/ml of BSA, incubating gently rocking for 10 minutes and neutralized with15 µl of 1M Tris pH 9.1. Eluted phage were stored at 4^0Cup to 1 week until further used.

Eluted phages were then amplified by infection of ER2378 cells and the phage particles were PEG precipitated. This was repeated two more times and approximately 10^{11} pfu of the first or second amplified eluate were used as input phage.

2.17.2. Phage amplification

The *E.coli* strain E2378 was streaked out onto the agar plate containing tetracycline (20 µg/ml) and incubated overnight at 37^0C. 20 ml of LB (20 µg/ml) was inoculated with a colony picked up from above mentioned streaked plate and incubated shaking at 200 rpm at 37^0C until OD_{600nm} of ~0.05 was reached. Once such an O.D. was reached, cells in their early log phase were infected with 70% of the phage eluate and further grown for 4.5 hours. These cultures were then centrifuged at 12000 g for 10 minutes at 4^0C. The supernatant was then transferred to a fresh tube and recentrifuged. The upper portion (80%) of the supernatant was transferred to a new tube and $1/6^{th}$ volume of 20% (w/v) PEG - 2.5 M NaCl was added and mixed. The phage was precipitated by incubating overnight at 4^0C, following overnight incubation the precipitated phages were pelleted at 12000 g for 15 mins at 4^0C. The supernatant was discarded; recentrifuged briefly and the remaining liquid was removed. The pellet was resuspended in TBS 1X in a microcentrifuge tube and was centrifuged at 16,100g for 5 mins at 4^0C. The phage supernatant was transferred to a new tube and re-precipitated by incubating at 4^0C using $1/6^{th}$ volume of PEG NaCl. Once again phages were pelleted by centrifuging at 16,000 g for 10 mins at 4^0C, supernatant was discarded and the tube was re-centrifuged briefly to remove any residual liquid. This final amplified pellet was then resuspended in 200 µl of TBS 1X. Amplified phages were stored at 4^0C for up to 3 weeks after incubation at 65^0C for 15 mins in order to kill any remaining residual bacteria.

2.17.3. Phage - titering

10 mls of LB-tetracycline was inoculated with a colony of E2378 and incubated in a bacterial shaking incubator at 37^0C until an OD of 0.5. 3 ml of melted LB agar was aliquoted in a 15 ml falcon tubes and maintained at 45^0C in a water bath. LB plates containing IPTG (0.05 µg/ml) and Xgal (5 bromo 3 chloro 3 indolyl-β-D-galactoside (0.04 µg/ml)) were freshly prepared and kept at 37^0C until inoculation step.

A serial dilution was performed for both amplified and unamplified phage from all three rounds. The amplified phages were diluted in 200 µl LB from 10^5 to 10^9 whereas the unamplified phage eluates were diluted from 10 to 10^4. Once the cells reached an OD of 0.5, 200 µl was aliquoted into 1 ml eppendorf for each dilution. For infection, each tube was infected with 10 µl phage eluate, vortexed and incubated at room temperature for 5 mins. These infected cells were the added to 3 ml of melted LB agar containing IPTG - Xgal. The melted agar was carefully poured into the plates and evenly distributed throughout the plate. After the plates were fully set, the plates were incubated overnight at 37^0C. The following day, blue plaques were counted from the plates in order to determine the phage titre of each sample.

2.18. Next generation deep sequencing

2.18.1. PCR for phage DNA amplification

Eluted phage pools were used for amplification of phage DNA. Specific primers were designed for Illumina HiSeq2000 multiplexed paired end read PE100 sequencing and are shown below (table 2.6). Forward primers were ordered PAGE purified whereas reverse primers were ordered HPLC purified from Sigma Genosys. These primers were then resuspended using DNAse/ RNAse free water.

Each sequencing reaction is read in either direction for each individual DNA and starts after Illumina adaptor sequences, being the sample key. The insert sequence length is 36 bp for 12mer library which is followed by 3 glycine spacer and preceded

by TCT which is not present in the wild type phage. Thus, the size of the phage containing insert has a size of 182 bp whereas the wild type phage on its own has a size of 167 bp.

PCR reactions were prepared on ice in nuclease free tubes with 1X Herculase II Fusion DNA polymerase buffer (supplied with polymerase) , 0.5 M Betaine solution for PCR, 13.2 mM Trehalose, 500 µM dNTP, 500 nM of each forward and reverse primer. To this, 5 µl of phage sample was added along with 1 µl of Herculase II Fusion polymerase and nuclease free water up to 50 µl.

PCR thermal cycling conditions:

95^0C for 1 min

95^0C for 15 sec
55^0C for 20 sec
70^0C for for 1 min
} repeated 30 times

70^0C for 3.5mins

4^0C forever

Primer	Sequence (5'-3')
Forward 1	GTGACTGGAGTTCAGACGTGTGCTCTTCCGATCT ACTCGCAATTCCTTTAGTGGTACC
Forward 2	GTGACTGGAGTTCAGACGTGTGCTCTTCCGATCT ACGCGCAATTCCTTTAGTGGTACC
Forward 3	GTGACTGGAGTTCAGACGTGTGCTCTTCCGATCT ACCCGCAATTCCTTTAGTGGTACC
Forward 4	GTGACTGGAGTTCAGACGTGTGCTCTTCCGATCTT AACGCAATTCCTTTAGTGGTACC
Forward 5	GTGACTGGAGTTCAGACGTGTGCTCTTCCGATCTT ATCGCAATTCCTTTAGTGGTACC
Forward 6	GTGACTGGAGTTCAGACGTGTGCTCTTCCGATCTT

	AGCGCAATTCCTTTAGTGGTACC
Forward 7	GTGACTGGAGTTCAGACGTGTGCTCTTCCGATCTT ACCGCAATTCCTTTAGTGGTACC
Forward 8	GTGACTGGAGTTCAGACGTGTGCTCTTCCGATCTT TACGCAATTCCTTTAGTGGTACC
Forward 9	GTGACTGGAGTTCAGACGTGTGCTCTTCCGATCTT TTCGCAATTCCTTTAGTGGTACC
Forward 10	GTGACTGGAGTTCAGACGTGTGCTCTTCCGATCTT TGCGCAATTCCTTTAGTGGTACC
Forward 11	GTGACTGGAGTTCAGACGTGTGCTCTTCCGATCTT TCCGCAATTCCTTTAGTGGTACC
Forward 12	GTGACTGGAGTTCAGACGTGTGCTCTTCCGATCTT GACGCAATTCCTTTAGTGGTACC
Reverse primer	ACACGACGCTCTTCCGATCTCTGTATGGGATTTTGCTAA AC

Table 2.6: Set of primer sequences: *Sequence of forward and reverse primers designed for amplification of α-synuclein binding peptides*

2.18.2. DNA purification and quantification

The entire PCR reaction was loaded onto a 2% (w/v) agarose gel. The amplicon of the correct size was gel extracted on 2% (w/v) agarose gel and 182bp band was cut (avoiding WT phage band 167 bp) and placed in a tube. Following excision of the bands, DNA was purified using gel extraction kit (#28704 Qiagen) using manufacturer's instructions including recommended steps. Finally DNA was eluted in 40µl of nuclease free water. DNA concentration was accurately quantified on ultrasensitive fluorescent nucleic acid stain for double stranded DNA in solution using Quant-iT Picogreen dsDNA kit (#P7589, Life Technologies) following manufacturer's instructions. Equal amount of each DNA based on the concentration were pooled together in order to obtain 5 µg of total DNA for deep sequencing.

2.18.3. Deep sequencing of phage pool

Amplicon pool was sent to Otogenetics, USA for sequencing. Data in fastq format was extracted and changed into excel format in collaboration with Stuart Aitken (University of Edinburgh) and Adam Krejci (RECAMO, Brno). Two million sequences were obtained from the next generation deep sequencing and these obtained 12 amino acid peptides were arranged in descending order on the basis of number of repeats obtained. The selection of the unique peptides was performed by considering the incidence of highly occurring peptide sequences against α-synuclein in comparison to other proteins, negative control and parental library. The selected peptides designed with an N-terminal biotin tag and were ordered from Mimotopes, Victoria, Australia.

2.18.4. Peptide protein binding efficiency

100 ng of α-synuclein was coated onto each well of the ELISA plate (Nunc) overnight as well as for 1 hour in order to measure the binding efficiency of all the ordered peptides. The plates were then washed thrice with 0.1% (v/v) PBS-T and all the peptides obtained from phage screening were added at a concentration of 1 µg/ml to each well (50 µl in 3% BSA) in the presence and absence of 1 mM DTT. The peptides were incubated for 1 hour, washed thrice with 0.1% PBS-T and blocked using 3% (w/v) BSA. Subsequently anti-α-synuclein antibody (BD biosciences) was added at a dilution of 1:1000 in 3% BSA to all the wells and incubated for 1 hour at RT. The wells of the plates were again washed thrice with 0.1% PBS-T and HRP conjugated rabbit anti-mouse was added at a dilution of 1:1000 in 3% BSA. The plates were washed again thrice with 0.1% PBS-T and the TMB substrate was added to all the wells of the plates and further read at 450 nm.

2.18.5. MEME analysis and co-transfection

Alongside, all the higher occurring peptides were subjected to MEME analysis for identification of motifs. The interacting proteins which were identified from blast analysis of these motifs were cloned into pEGFP-C vector. These interacting proteins

after cloning were then co-transfected and transfected on its own to see its effect on SHSY5Y and HCT116^{+} cells. Once again the transfection was carried out in different ratios i.e. 0.1, 0.5 and 5 µg DNA made up in 100 µl serum free media into both cell lines that were seeded with same density. Also a titration of cells was carried out in order to see if the effect of any of these genes was cell density dependent using GFP itself as a control and non-transfected as the negative control. DNA was transfected as well as co-transfected with different proteins in several amounts until a certain amount of DNA showed its significant effect onto HCT116^{+} and SHSY5Y cells. Subsequently, cells were harvested following day, lysed in 10% Triton lysis buffer and incubated for 30 minutes in order to lyse the cells. The concentration of the protein was measured via Bradford assay and 30-50 µg of protein was run on a gel and was probed for α-synuclein using commercial anti-α-synuclein antibody (BD Biosciences). GFP-HADH transfection was carried out in 6 well dishes into SHSY5Y and HCT116^{+} cells with different amount of HADH DNA, GFP only as a control and non-transfected cells as negative control. Transfection efficiency of HADH gene was compared using different transfection reagents: attractene, lipofectamine and effectene.

2.18.6. Peptide pull down assay

To determine the binding ability of peptides identified through peptide phage display screening we performed peptide pull down assay described below against α-synuclein expressing cells (figure 2.1).

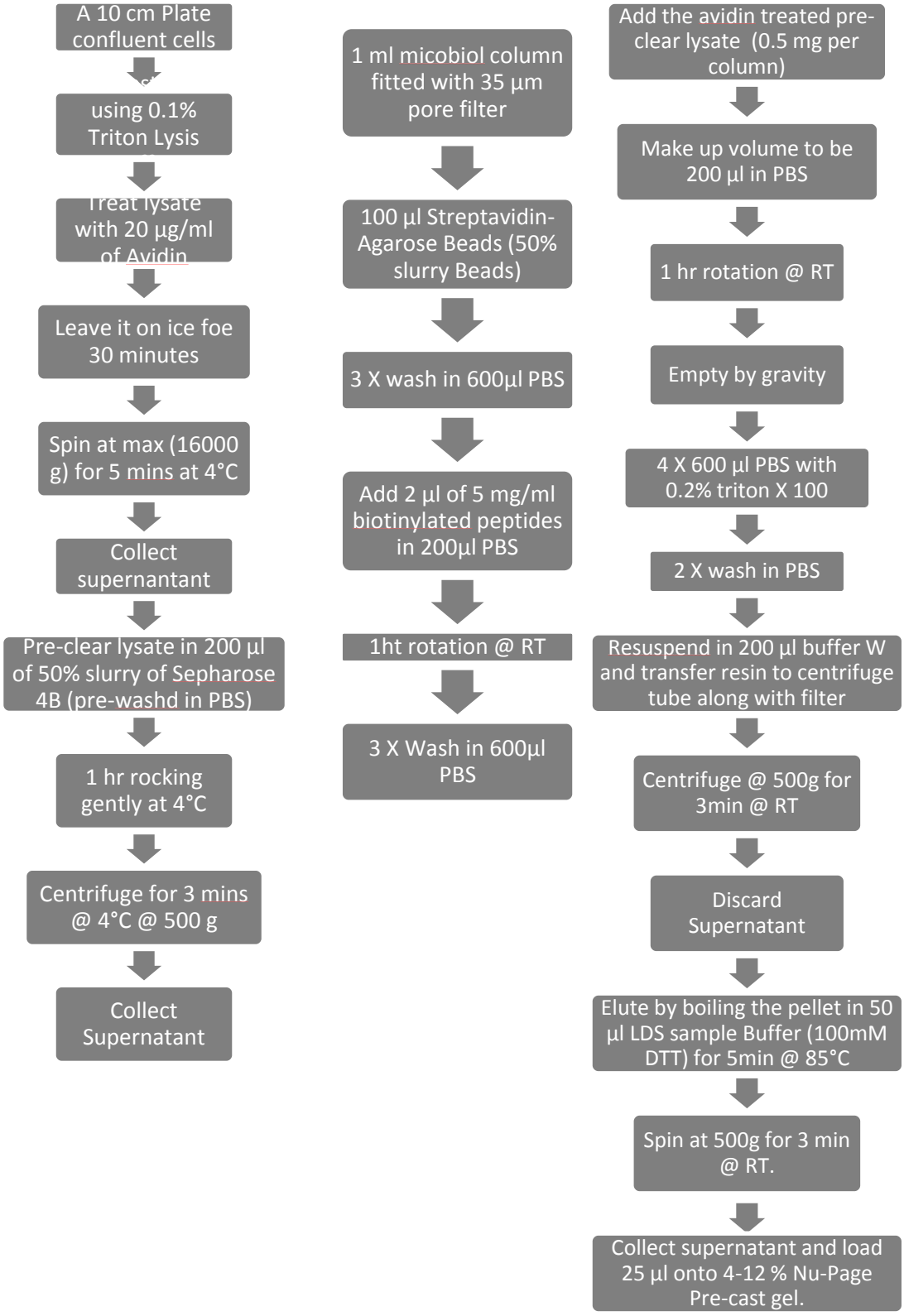

Figure 2.1: Peptide pull down assay: *Using the cell lysate to pull out α-synuclein by adding the cell lysate to beads pre-incubated with peptides found through peptide phage display screening.*

CHAPTER 3: Development of monoclonal antibodies and Bioconjugate to canine CD20 receptor (a receptor, scFv model)

3.1. Introduction

3.1.1. Cancer

Cancer remains one of the world's leading causes of death in humans and the total economic impact of premature death and disability from cancer represents 1.5% of the world's GDP, not including the direct cost of treatment of patient suffering [158]. In the early 1990s when the molecular basis of cancer was poorly understood, scientists focussed on assessing the morphology of cancer cells. Now, research has expanded to study the changes occurring at a subcellular level in cancer cells and their environment and to explore the molecular pathways controlling the development and progression of cancer [159]. Biologically cancer is defined as abnormal growth of cells which overcome any checkpoints and finally lead to sequential accumulation of defects in DNA which was identified in European people when no treatment was available [160, 161]. The outstanding challenge in cancer research is the implementation of inter-disciplinary translation of rapidly growing knowledge of tumour biology into new anti-cancer treatment modalities as preclinical models have not predicted high success rate in the recent past in the clinic [162]. Following continuous research in the field of oncology over the past 100 years, more than 200 types of cancer have been identified. Several phenomena responsible to cause cancer have been described such as mutations, oncogenes and tumor suppressor genes which are described below.

3.1.2. Concept of mutations, oncogenes and tumour suppressor gene

Mutations are the abnormal changes in the DNA which are defined by changes in arrangement of a single or more base pairs of the gene. A mutation in the form of single pair substitution can result in major effects and it is further classified into hereditary and acquired mutations depending upon the origin of the mutation. Most of the oncogenes are mutations of normal genes and are defined as proto-oncogenes. Oncogenes are defined as those genes that become active when they are not supposed to be active and cause unnecessary changes in the cells making it cancerous on occasions. Oncogenes can be mutated in such a way that they could render the gene constitutively active in certain condition which would otherwise be non-active as a wild type gene [160]. Tumor suppressor genes are genes that are known to play a role in maintaining cell cycle, establish DNA repair mechanisms and cause programmed cell death when needed called apoptosis. Tumor suppressor genes become problematic when mutations in some genes that are known to play role in several mechanisms reduce their activity and become inactive when needed. Both oncogenes and tumor suppressor gene mutations operate at a similar physiological level by driving the cancerous effects by increase in tumor cell number via stimulation of such abnormal cells and/or inhibition of cell death or cell arrest [160]. Along with these above mentioned mechanisms, cancer cells can also have profound alterations in the DNA methylation suggesting epigenetic alterations may play important roles in cancer development and regulation [163]. Transcriptional reprogramming has emerged as another mechanism indicating changes in gene expression initiated by various transcription factors and has been studied extensively in endoplasmic reticulum [164].

3.1.3. Comparative oncology

Comparative oncology is a fairly new discipline that plays a major role in integrating as well as translating naturally occurring cancers in animals into studies of human cancer biology and developing therapies [165]. Comparative medicine has been the framework from which inter species models can generate knowledge that in turn can be translated to impact on health and welfare. This involves the establishment of collaborative ventures in clinical care, surveillance and control of cross-species

disease, education and research into disease pathogenesis, diagnosis, therapy and vaccination [166]. Naturally occurring cancers in companion animals (pets) have led to significant investigations in studying cancer biology and drug development. The most frequently used animal model in past has been mice which possesses advantages such as short gestation period, small size and inexpensive as compared to other mammals. A well-known limitation in mouse models is that human tumours occur spontaneously whereas in most of the mice the tumours have to be induced. Such limitations suggest that there is a need of another animal model which presents similar gene interactions and similar if not same clinical outcome following treatment. The development of models using companion animals may overcome some of these limitations.

The worldwide veterinary oncology field can offer compelling sporadic models of carcinogenesis in companion models (cats and dogs) that mimic certain aspects of cancer development such as metastasis and immune host cell interactions [167, 168]. Pet owners are highly motivated to seek novel treatment options for curing cancer if the existing options do not meet their goals. Study of tumour biology and cancer therapy is not a novel concept, in fact in last 20-30 years a significant amount of research has been carried out in order to study the biology, several therapies in osteosarcoma, lymphoma, melanoma and other cancers [169-171].

3.1.4. Mouse vs dogs as a relevant study model for humans

One of the reasons for the failure of some novel drugs to get FDA approval is pre-clinical testing of the drug in the conventional pre-clinical models [172]. Investigations of cancer in dogs is not novel due to well-known anatomical as well as physiological history that dogs share with humans and several studies have been reported since early 1960s [173-176]. The published genome sequence analysis of humans and canine indicate that there is a high degree of similarity between them [177, 178]. The current treatment options available for naturally occurring canine tumours are chemotherapy, anti-angiogenic therapy and other approaches that have already been approved for human cancers. The dose intensity of chemotherapy and anti-angiogenic agents is generally lower in dogs which ultimately results in lower success rate [179]. This calls for urgent need for development of canine therapeutics

with growing interest of pet owners. Domesticated dogs (*Canis lupus*) are an excellent animal model for studying human diseases for reasons such as phenotypic diversity and naturally occurring diseases of all land mammals [180]. In recent years, the inclusion of dog from different breeds in clinical trials provides a great cross sectional value that is usually higher than that obtained in the studies of inbred laboratory animals, reason being the genetic similarity that dogs share with humans [181]. Around 400 inherited diseases which are similar in development to humans have been characterized in dogs such as cancer, heart diseases and neurological disorder [182, 183]. Another advantage that dogs hold over mice is the similarity of tumour histology to humans and responds similarly to conventional therapies. The time needed for clinical trials is significantly shorter and the disease free interval time in dogs treated for cancer is 18 months compared to humans where the time interval is more than 7 years in order to assess the disease outcome [179].

Furthermore, tumours are difficult to be reproduced in immuno competent laboratory animals, thereby limiting some clinical trials which are not the case in dogs due to genetic similarity and immune response they share with humans. Cancer is the leading cause of death among dogs and naturally occurring cancer have been well described in several breeds of dogs [184, 185]. It has been shown on previous occasions that certain breeds of dogs are more susceptible to genetic diseases and cancers [186] and this indicates that the development of such breeds on occasions might cause unintentional inclusion of deleterious alleles. The lack of standard treatment regimens in veterinary cancer patients has compelled researchers to carry out clinical trials as well as research for novel therapeutic and diagnostic strategies [170]. The major benefit that dogs hold over any other laboratory animal models is that the comparative oncologists can study the novel treatment strategies in canine cancer model within a short time scale.

3.1.5. Lymphoma

Lymphoma is a malignant cancer which involves the lymphatic system and starts in cells called lymphocytes (B and T cells) which are one of the most important constituent of the immune system. Lymphoma is a very well defined cancer type and its tumour classification serves the purpose of providing the insights into histology,

pathology and basic research to study the current available treatment options [187]. This has allowed for the development of new tools and their significant effects on the treatment of different types of lymphoma. There are mainly two types of lymphoma, Hodgkin lymphoma which is named after Dr. Thomas Hodgkin and when seen under microscope it is characterized by the presence of Reed-Sternberg cells. Reed-Sternberg cells are giant cells found in biopsies which are either multinucleated or have a bi-lobed nucleus. The most common and other type of lymphoma is non-Hodgkin lymphoma which has now more than 61 subtypes, out of which the most common ones are DLBCL (Diffuse large B cell lymphoma), Follicular lymphoma and Marginal Zone lymphoma. Non-Hodgkin lymphoma is the sixth most common cancer in UK, accounting for 4% of all new cases of cancer. Lymphoma is quite common in dogs accounting for one third of all canine cancers and occurs spontaneously as in case of humans [171]. Canine lymphoma demonstrates histopathological and biological features that are similar if not same to that of humans [188] accounts for 10-20% of all cancers in dogs. Lymphohematopoietic disorders are common in dogs, with non-Hodgkin's lymphoma (NHL) making upto 83% of all canine hematopoietic malignancies [188]. Several types of spontaneous canine cancers have been proposed as possible models for human cancers, reason being the molecular and biological similarity both species share. The treatment options for non-Hodgkin's human and canine lymphoma predominantly included chemotherapy and radiotherapy.

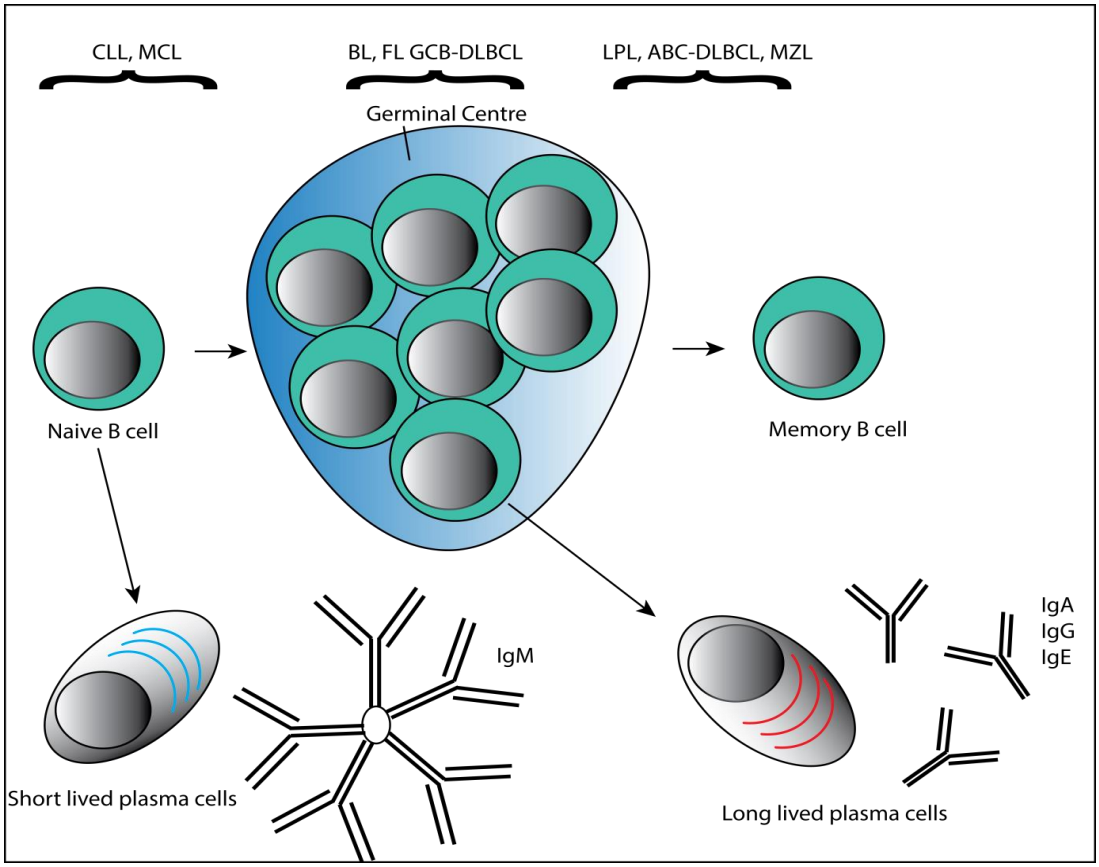

Figure 3.1: B cell lymphoma during B cell development: *Early stages of B cell development are associated with chronic lymphocytic leukemia and mantle cell lymphoma. During maturation stage in germinal centre, cancers such as Burkitt lymphoma, Follicular lymphoma and germinal centre diffuse large B cell lymphoma. Lastly during maturation stage into memory B cells cancers prevalent are lymphoplasmacytic lymphoma, activated B cell diffuse large B cell lymphoma and Marginal Zone lymphoma*

B cells play a role in mediated immune response by producing antibodies to fight against diseases. Bone marrow hematopoietic cells give rise to B cells and go through a series of developmental changes resulting in the formation of cell types such as plasma cells [189]. Spleen and lymph node germinal centres are two major sites for activated B cell affinity maturation. These germinal centres are formed mainly as a result of antigen recognition by B cells, activated helper T cells and antigen presenting dendritic cells [190, 191]. As shown in figure 3.1, development of B cell lymphomas takes place at different stages of B cells i.e. from naïve B cell to plasma cells. The immunoglobulin idiotype present on the lymphoma B cells is

totally distinct from their non-malignant counterparts, however regulatory approval has not yet been obtained for active immunotherapy for lymphoma despite the benefit and clinical efficacy [192]. Various B- cell differentiation antigens have been discovered as markers in B cell lymphoma including CD5, CD22, CD79, CD23 and CD25. The expression pattern of CD25, CD22, CD23 and CD5 has been described before in B cell lymphoma [193]. Out of the known B cell differentiation antigens, CD20 is highly expressed (around 75%) in different types of B cell lymphoma and significantly lower in T cell originated lymphoma [194]. In addition to this, immunophenotyping has played a major role in identifying lymphoma of B cell origin and further characterizing the antigenic markers.

3.1.6. CD20 structure and its role in B cell lymphoma

After understanding the significance of canine cancer as a fairly novel study model for immunotherapeutics, we focussed on proto oncogenic target i.e. CD20 receptor. As most of B cell lymphomas express CD20 and the most frequently used approved drug against these different types is Rituximab, the need for more effective CD20 specific antibody still remains [195]. The identification of this target was done by Lee Nadler has allowed extensive research for developing therapeutic tools against this target. Another interesting aspect that makes CD20 a suitable target is its membranous expression and does not exist as free protein in the blood. However, there have been reports suggesting that CD20 along with CD19, CD24 and CD37 can be present on subpopulations of exosomes [196]. Exosomes are nanosized membrane vesicles which are released upon fusion of multivesicular bodies with the plasma membrane [197]. The extent of exosomes secretion varies depending upon the cell type and the observation that tumor cells release exosomes containing several tumor antigens can be of significant importance. More than 90% of B cell lymphoma are known to express this B cell receptor but the intensity of the expression of CD20 varies depending upon the type of lymphoma [194]. CD20 is a 33 kDa tetraspanning transmembrane phosphoprotein which is expressed in pre B cells but the precise function of CD20 is still unknown [198]. It has been proposed that CD20 plays a major role in the regulation of B cells required for cell cycle progression [199] and

has also been shown to regulate calcium channel transport [200]. It is not phosphorylated in resting B cells but is heavily phosphorylated following mitogen stimulation of B cells and is found to be a dominant phosphoprotein [201]. On previous occasions it has been shown that CD20 can be phosphorylated by several kinases at unique residues which could change the functional status of CD20 under physiological conditions [201]. The structure of CD20 is shown in figure 3.2 and it has been shown on various occasions that chemical cross linking can cause CD20 to exist as a monomer, dimer and tetramer.

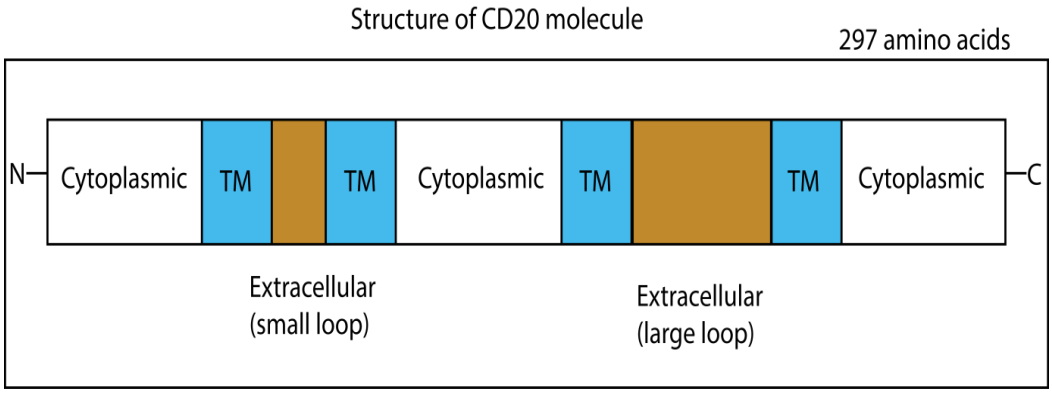

Figure 3.2: Structure of CD20: *CD20 is a 297 amino acids protein with membrane spanned four times containing smaller and larger loops of*

In fact CD20 was the first molecule to be successful as an immunotherapeutic target. Rituximab is a chimeric monoclonal antibody which consist of murine variable regions (C2E8 mAb) and human constant regions which has been approved against non-Hodgkin's lymphoma in humans [202, 203]. Also recent data shows that in combination with chemotherapeutic agents, Rituximab might be more efficient in cases of DLBCL [204]. Although antibodies such as Rituximab have been approved against human CD20, it does not cross react to its canine orthologue due a single amino acid change in the extracellular loop [201]. Rituximab targets CD20 receptor in B cell related malignancies and has provided a compelling proof of concept that a recombinant monoclonal antibody can be used as a biologic based drug treatment [205, 206]. The mechanism of action used by Rituximab is based on Fab domain binding to the CD20 antigen on B cells and Fc domain of the antibody recruiting immune effector functions in order to mediate lysis of the B cell [207]. There is growing evidence that Rituximab can affect other disease indications such as

rheumatoid arthritis [208], immune related indications [209-211], and in transplantation [212]. It is thought that Rituximab acts by eliminating B cells either by complement mediated lysis of cells, ADCC or causing cell death i.e. apoptosis.

Given the widespread potential ability of Rituximab to bind to CD20 expressing cells, there are Rituximab "biosimilars" such as Ibritumomab and Tositumomab [213, 214]. These second generation antibodies have better affinity to CD20 but still do not bind to canine CD20, thus the need for antibody specifically binding to canine CD20 still remains. The fact that some patients are refractory or relapsed and also few might develop resistance to Rituximab; this indicates that the need for improving anti-CD20 modalities still remains [215]. Moreover, although Rituximab can induce significant anti-tumor effects but there are severe side effects associated with it and patients that become resistant to Rituximab have shown inefficacy of this antibody. Rituximab mediates direct killing of the CD20 positive cells via various mechanisms such as CDC and ADCC, the common side effects associated with Rituximab are fever, bone lesions, etc [216]. The use of live vaccines during Rituximab therapy can result in increased risk of developing an acute infection [217], another well-known adverse effect is the result of B-cell depletion after therapy which in turn can compromise the immune system [218]. With this B-cell depletion, the concentration of immunoglobulins have significantly fallen down making hard for body to develop any type of immune response [219]. One innovate approach for developing such immunotherapeutic approach towards this target could be use of canine diffuse large B cell lymphoma that have a similar fingerprint to the human counterpart [198].

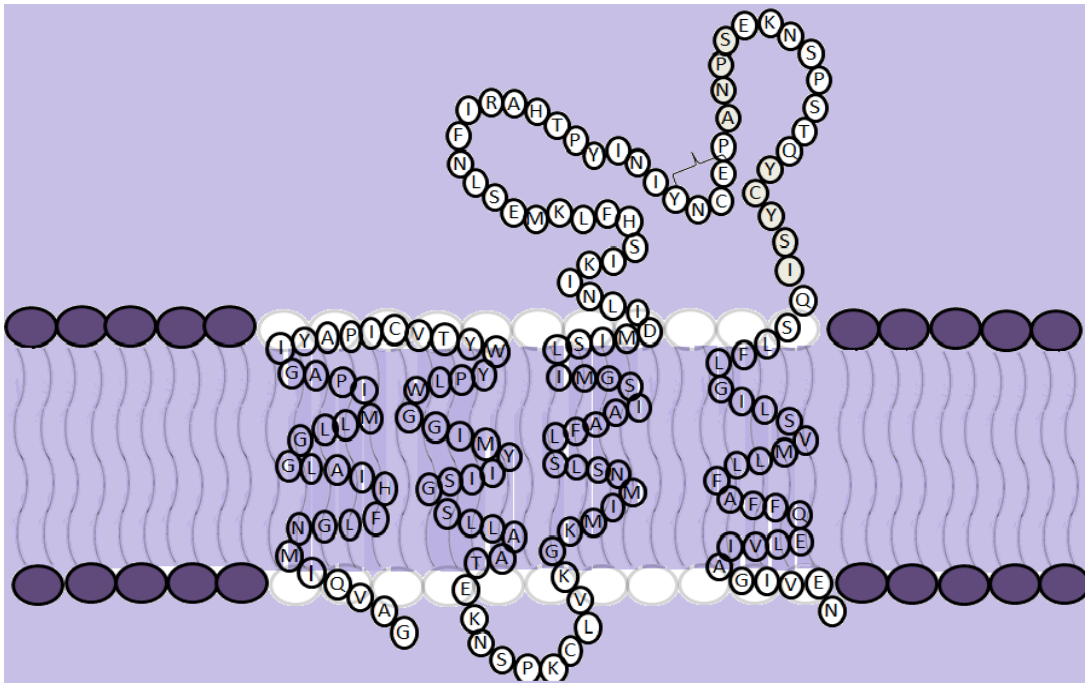

Figure 3.3.: Detailed structure of human CD20: *Tetraspanning transmembrane protein with smaller and larger extracellular loop containing the region where Rituximab binds.*

This first FDA approved monoclonal antibody Rituximab binds to larger extracellular loop of the human CD20. Presence of amino acids alanine (170) and proline (172) have found to be critical for antibodies to bind to CD20 positive cells [220]. Extensive research has been done by few research groups on Rituximab to determine precisely its discontinuous epitope (170) YCYSI (173) and (182) ANPS (185) [221]. As shown in figure 3.3, Rituximab binds to the discontinuous epitope on larger loop of the extracellular domain of CD20. This non-glycosylated phosphoprotein spans the membrane four times and only 44 amino acid residues of all 297 amino acids lie in the extracellular region of CD20. The homology of the human and canine CD20 can be seen in figure 3.4. The efficiency of rituximab binding could be limiting on occasions when the lymphoma patients develop resistance. There could be a range of reasons for such resistance development i.e. overexpression of complement regulatory proteins that impair CDC [222], blocking ADCC via deposition of C3b complement component [223], over-expression of anti-apoptotic proteins [224] or down regulation of CD20 which could be due to internalization by rituximab loss of CD20 protein [225].

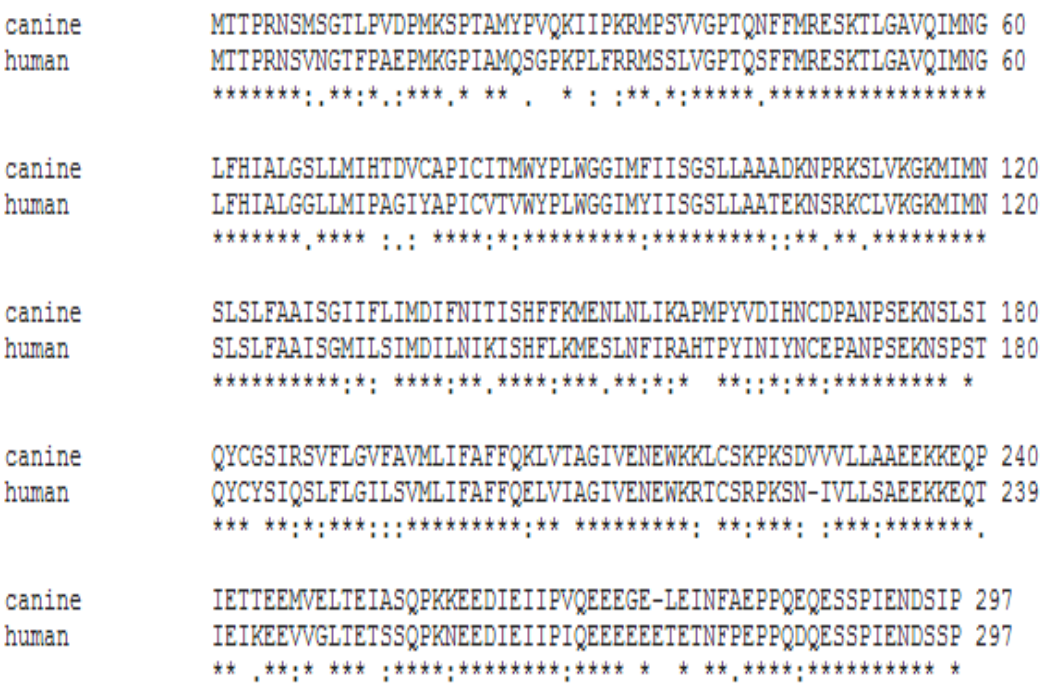

Figure 3.4: Clustalw analysis of CD20: *Amino acid sequence homology comparison between human and canine CD20 by Clustalw analysis.*

3.1.7 Monoclonal antibodies against CD20

Over the years, several anti-CD20 monoclonal antibodies have been under clinical investigations. These antibodies are either human or humanized unlike Rituximab which is a chimeric mAb as the aim of these mAb remains to increase the binding efficacy to the target and cause CDC or apoptosis of lymphoma cells. Table 3.1 shows different monoclonal antibodies approved by FDA for the treatment of B cell lymphoma.

Antibody	Characteristics	Activity compared with Rituximab	Phase of development
Ofatumumab	Type I, full human	Increased CDC and slower off rate	FDA approval for CLL and phase III trials in NHL
Veltumzumab	Type I, humanized	Slower off rate	Phase I/II of subcutaneous administration in NHL and CLL
Ocrelizumab	Type I, humanized	Increased ADCC and lower CDC	Phase II in NHL
PRO131921	Type I, humanized with modified Fc	Increased ADCC	Phase I/II in NHL
AME-133v	Type I, humanized with modified Fc	Increased ADCC	Phase I/II in NHL
GA101	Type II, humanized with glycol-engineered Fc	Increased ADCC and apoptosis	Phase I/II in NHL and DLBCL

Table 3.1: mAbs against CD20: *Approved different forms of monoclonal antibodies against human CD20 in several types of lymphoma with different mechanism of action.*

Ofatumumab, one of leading anti-CD20 fully mAb candidate that binds a unique epitope in the small extracellular loop of CD20 and has exceptional ability to recruit C1q and lyse through complement activation [226]. Interestingly results from studies with rituximab resistant FL have shown disappointing overall response rate (ORR), suggesting ofatumamab monotherapy is ineffective; however it might be effective when used in combination with chemotherapy [227]. Another Study from Meerten et al showed Ofatumumab to be highly effective when used along with CHOP chemotherapy in previously untreated FL patients [228].

Humanized antibodies

Ocrelizumab

Ocrelizumab is a second generation humanized antibody derived from murine 2H7 anti- CD20 antibody which binds to an overlapping epitope of the large extracellular loop of CD20 antigen compared with Rituximab. As far as efficacy of Ocrelizumab in comparison to Rituximab is concerned, Ocrelizumab induces two to five fold higher ADCC and two to five fold decreased CDC [228]. In a study carried out by Morschhausser et al, it was shown that in patients with relapsed/refractory FL following Rituximab treatment, ORR was reportedly 38% with few adverse effects, likely due to decreased complement activation. Due to the fact that death rates considerably increased, the drug was suspended in 2010; however studies (phase III trials) are still ongoing for use inmultiple sclerosis [192]. PRO131921 is again a humanized modified version of Ocrelizumab which has been developed in order to improve the binding efficacy to FCγRIIIa. This has entered phase II trials for the treatment of relapsed or refractory CLL and indolent NHL[229].

Veltuzumab

Veltuzumab is a humanized IgG1 generated by using the same framework regions as epratuzumab (humanized anti-CD22) [228]. Veltuzumab has a better activity as compared to Rituximab, the reason being a single amino acid change in CDR3 of the heavy chain and is shown to have better off rate as well as improved activity in vivo [229]. This humanized antibody has ORR of 44% which is comparable to that of Rituximab in patients with relapsed, refractory FL[230]. It is currently being evaluated in phase II clinical trial studies for NHL and CLL.

PRO131921, AME133v and GA-101

These antibodies are third generation anti-CD20 mAbs developed by modification of fc portion of the antibody in order to increase the affinity of the antibody and enhance its cytotoxic effects. Both antibodies have been under different phases of clinical trials and until now have proved superior to Rituximab [231]. GA-101 is a type II third generation antibody that has glycol-engineered Fc fragment to enhance

its affinity and thereby ADCC. This induced direct immune cell-mediated killing and in pre-clinical models has shown to be more effective than Rituximab with some promising results in clinical trials [232].

Antibody fragments such as scFv and Fab have been under trials and have shown clinical efficacy in the trials so far. Infact one study has developed humanized scFv from Rituximab to retain the binding affinity onto CD20 and has succeeded in supressing proliferation of CD20 expressing Raji cells [233]. In another study by Chu et al, Fab fragments were linked to N-(2-hydroxypropyl) methacrylamide (HPMA) and such conjugates have effectively resulted in causing apoptosis of affected B cells [234].

3.1.8. AIM

The objective of this study was to develop different antibody scaffold against canine CD20 and its human counterpart. With significant amount of clinical validation of CD20, we thought of developing antibodies and determine its binding efficiency in several B cell lymphomas which are known to express CD20. Another aim following antibody development was to develop a technology to make stable scFv tools and modify such tools by cloning into CpG2 to favour ADEPT to see if the affinity of the antibody was increased.

3.2. RESULTS:

3.2.1. Production of mouse anti-canine CD20 from murine hybridomas

Balb/c mice were immunized with a peptide derived from canine CD20 NCDPANPSEKNSLIQYCGS; Figure 3.5 (A) that comprise the minimal epitope bound by Rituximab. Hybridomas obtained following fusion were tested for activity against canine CD20 immunized peptide as well as canine CD20 protein. The hybridomas producing IgG monoclonal (NCD1.2) that recognised recombinant bacterially expressed canine CD20 protein (amino acids 140-190 comprising the extracellular domain) was sub-cloned twice by limiting dilution to obtain pure hybridoma population.

The NCD1.2 (anti-canine CD20 mouse mAb) was purified with high salt using protein A column and the concentration of the antibody was found to be 1.38 mg/ml. As it can be seen in figure 3.5B, anti-canine CD20 mAb binds to cross linked oligomeric form of CD20 (no DTT) and also binds to the DTT reduced monomeric form. For determining its binding efficiency in canine B cells, we used 3132 lymphoma cells (canine B cell lymphoma cell line provided by Lisa Pang, Roslin) lysed in different lysis buffer to determine optimal extraction buffer and the extracted lysate was separated by SDS-PAGE followed by western blot to detect endogenous CD20 protein. These cells were also subjected to chemical fractionation (Fr1-Fr4, as indicated) to isolate different cellular compartments to determine the dominant localization of CD20 protein in 3132 cells. The monoclonal antibody was able to recognize endogenous canine CD20 protein in canine CD20 expressing 3132 lymphoma cells (Figure 3.5 C and D) and also shows that the CD20 protein is mainly localized within the cytoplasm. Interestingly, CD20 expression was seen in cytoplasm and not on the membrane which could be the case of vigorous lysis of CD20 expressing cells. Thus in future mild lysis of these cells could in turn show the expression to be membranous rather than cytoplasmic.

Furthermore, a human CD20 construct coupled with GFP was developed by Erin Worrall (Hupp lab) for testing the binding ability of anti -canine CD20 mAb onto

human counterpart. The human GFP-CD20 construct following cloning was sequenced and transfected in H1299 cells. The antibody was used at a dilution of 1:1000. As seen in figure 3.5 E and F, NCD1.2 binds to human CD20 showing it cross-binding to the human orthologue. The blot was also probed with anti-GFP antibody in order to ensure that the binding of NCD1.2 was precisely to 62 kDa GFP tagged human CD20. This promising cross-reactivity between canine and human counterpart would permit cross-species therapeutic model for development of $CD20^{+}$ diseases in future. Because of such cross reactivity between the species, we decided to measure the binding efficiency as well as investigating the binding ability of the antibody in-vivo.

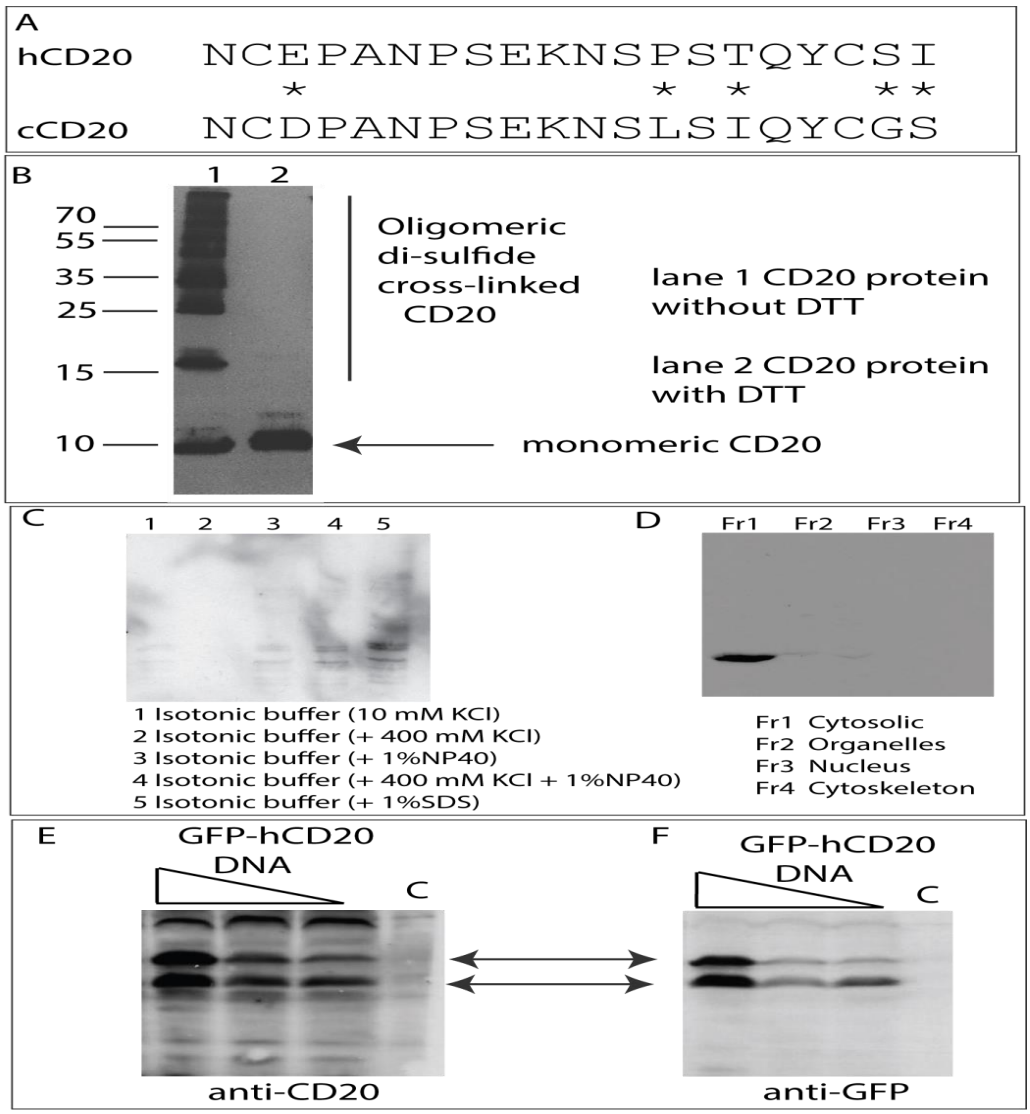

Figure 3.5.: Isolation of a mouse CD20-specific monoclonal antibody that can recognize human and canine CD20 protein: *(A). Amino acid sequence of human and canine CD20 region surrounding the Rituximab epitope. The asterisks highlight divergence between human (hCD20) and canine (cCD20) proteins.* ***(****B). Immunoblotting of recombinant canine CD20 protein. Bacterially expressed his tagged canine CD20 protein (amino acids 140-190) was purified by nickel chromatography and after electrophoresis without and with DTT, immunoblotted with mAb NCD1.2. The laddering observed without DTT presumably reflects intermolecular disulphide bonds through the two cysteine residues. (C and D). (C). Immunoblotting of authentic endogenous canine CD20 protein. 3132 canine lymphoma cells were lysed with different lysis buffers (as indicated) to determine optimal extraction buffer to immunoblot endogenous CD20 protein. (D). 3132 canine lymphoma cells were subjected to chemical fraction (Fr1-Fr4, as indicated) to isolate compartments to determine the dominant localization of CD20 protein in 3132 cells. (E and F). Immunoblotting of human CD20 protein. Transfection of human GFP-CD20 into H1299 cells demonstrated that NCD1.2 can bind to human CD20 (Left panel) with and anti-GFP monoclonal antibody as a control for protein expression and relative molecular mass (right panel).*

3.2.2. Designing peptides spanning the extracellular region of CD20

After looking at the binding ability of the antibody to canine CD20 protein and its human counterpart, we thought of looking at the precise binding site of antibody. For this reason we designed a panel of peptides for the region spanning the whole large loop of the extracellular domain of canine CD20 with a N terminal biotin tag. Figure 3.6a shows sequence analysis of designed overlapping peptides, whereas figure 3.6b shows the comparison of human and canine CD20 in the large loop of the extracellular region and encircled is the binding site of NCD1.2 i.e. DPANP of canine CD20. Figure 3.6b also shows three dimensional figure of CD20 along with difference in canine and human CD20 in their extracellular loop sequence.

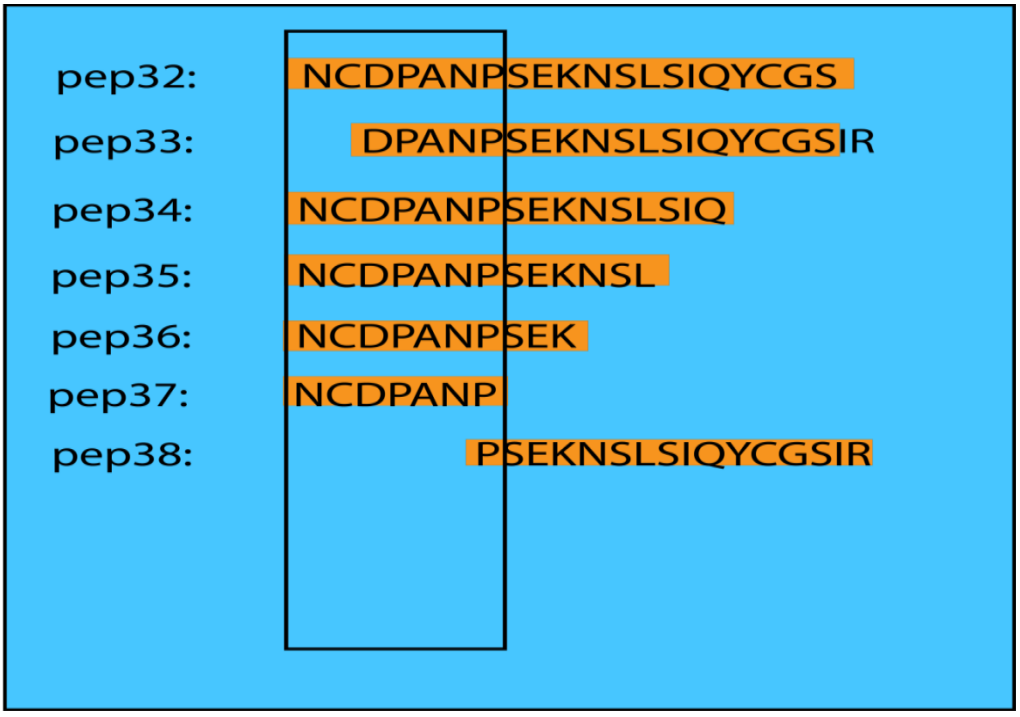

(A)

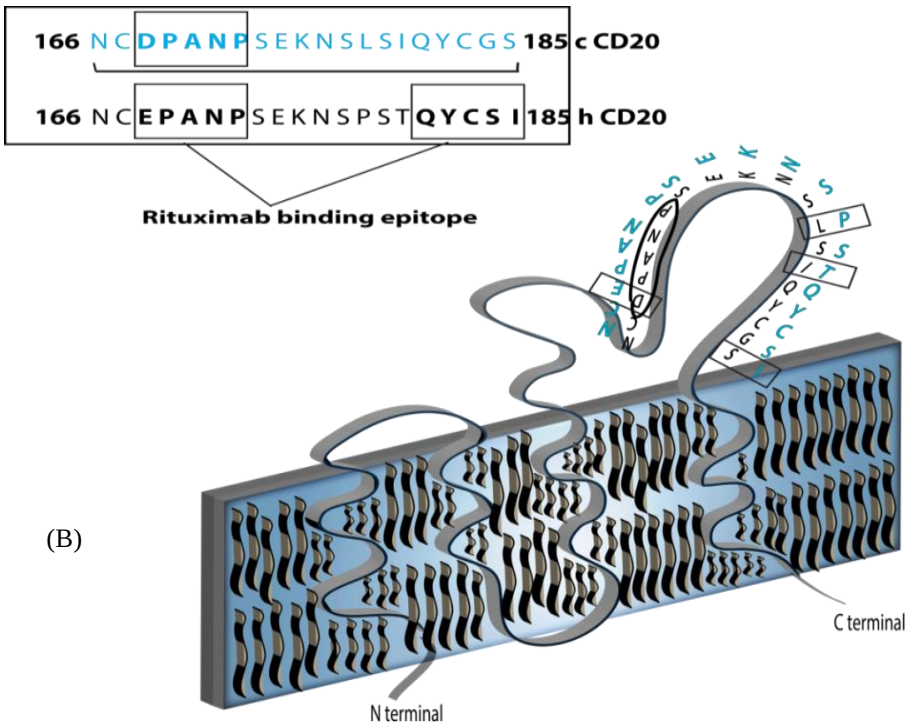

(B)

Figure 3.6: CD20 derived peptides and 3D structure of CD20: *(a) Sequence analysis of the overlapping peptides deigned from the extracellular domain of canine CD20. Peptide immunization sequence (pep 32): NCDPANPSEKNSLSIQYCGS forming the loop of the extracellular domain of canine CD20, only peptide 38 is devoid of NCDPAN region of CD20 loop. (b) Canine peptide used for immunization compared with human CD20 loop sequence. Three dimensional structure of CD20 protein showing difference between human CD20 and its canine counterpart in the longer loop of extracellular region.*

3.2.3. Epitope mapping of the anti- CD20 mAb

Once the antibody was shown to bind canine CD20 and its human orthologue, NCD1.2 was subjected to epitope mapping to a set of overlapping biotinylated peptides spanning the extracellular region of canine CD20 via ELISA. The ELISA was performed onto the below mentioned biotinylated peptides in several titrations (3, 6, 15, 30, 60 125, 250 and 500 ng) and NCD1.2 was used at a dilution of 1:1000. A colour change was observed after adding TMB onto all the wells and absorbance was measured at 450 nm as it can be seen in figure 3.7, NCD1.2 binds to the peptides from number 32-37 (all contain DPANP), whereas it only binds very weakly to

peptide 38 (figure 3.7). Thus, on the basis of this, the precise epitope of the antibody was found to be **DPANP**.

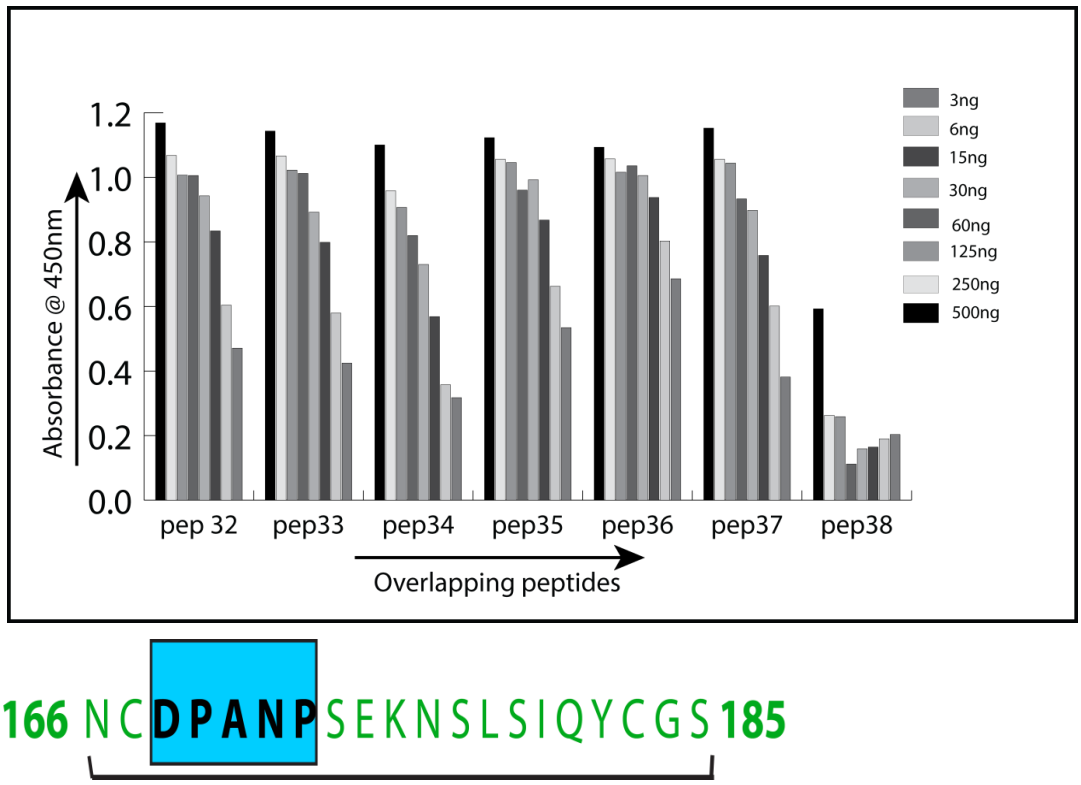

Figure 3.7.: Epitope mapping of NCD1.2: *Epitope mapping of the NCD1.2 mAb onto ELISA Nunc maxisorp plate which was coated overnight with streptavidin. CD20 peptides covering the extracellular loop were added at a series of dilutions per well (3,6, 12, 30, 60, 125, 250 and 500ng) followed by blocking using 3% BSA. NCD1.2 was added at a concentration of 1:1000 followed by HRP conjugated rabbit anti-mouse as the secondary antibody. The absorbance was read at 450nm after adding TMB and stopping the reaction using dilute H_2SO_4. Shown below is the precise epitope of canine CD20 to which NCD1.2 binds.*

3.2.4. Immunofluorescence

To visualize the binding pattern of anti-CD20 mAb onto human CD20 expressing cells, we performed immunostaining of mAb onto human Raji cells at a final dilution of 1:1000 (figure 3.8 c). As seen in figure 3.8, no spots were observed in the control experiment where only secondary antibody was used (figure 3.8a), spots were observed in the positive control staining (figure 3.8b) where 488 conjugated Rituximab was used. Following the control experiments, immunostaining using anti-

CD20 monoclonal antibody did not show any conclusive results. This non-conclusive staining pattern could be because some antibodies do not work by IF because of the epitope being masked or protein expressed in a different manner.

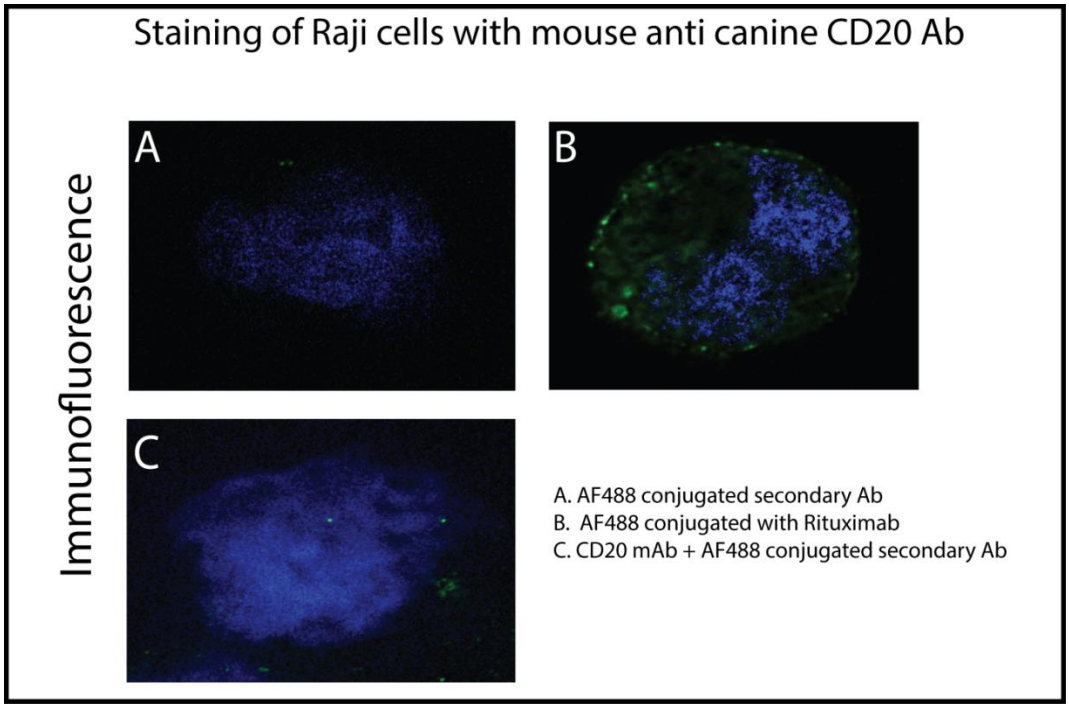

Figure 3.8.: Immunostaining of NCD1.2 onto human CD20 expressing cells: *Immunofluorescence staining of NCD1.2 onto CD20 expressing human Raji cells. (a) AF488 conjugated rabbit anti-mouse as negative control (b) AF488 tagged Rituximab used as a positive control , and (c) staining with NCD1.2.*

3.2.5. Octet binding assay

We also evaluated the relative binding affinity of the monoclonal antibody NCD1.2 to determine whether it might have use as a potential diagnostic or therapeutic in future (Peter Muller, Brno, Czech Republic). The Octet red system was used for measuring the relative on and off rates of the antibody to the biotinylated CD20 peptide on the solid phase. The relative K_d was defined to be 340pM, this was also carried out in presence and absence of DTT in the reaction, which might disrupt potential intra-intermolecular di-sulphide bonds in the epitope. But as it can be seen in the figure 3.9, no significant effect was seen on the binding reaction as the K_d was determined to be 310 pM (figure 3.9). However we cannot rule out the possibility

that the complex structure and oxidation of full length CD20 protein might affect the epitope affinity in live cells.

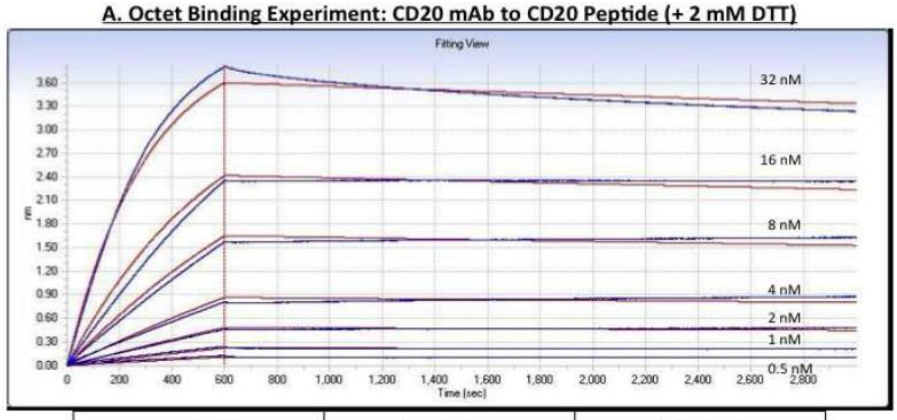

KD (nM)	kon (1/Ms)	kdis (1/s)
0.31	103600 ± 432	$3.19 \times 10^{-5} \pm 3.24 \times 10^{-7}$

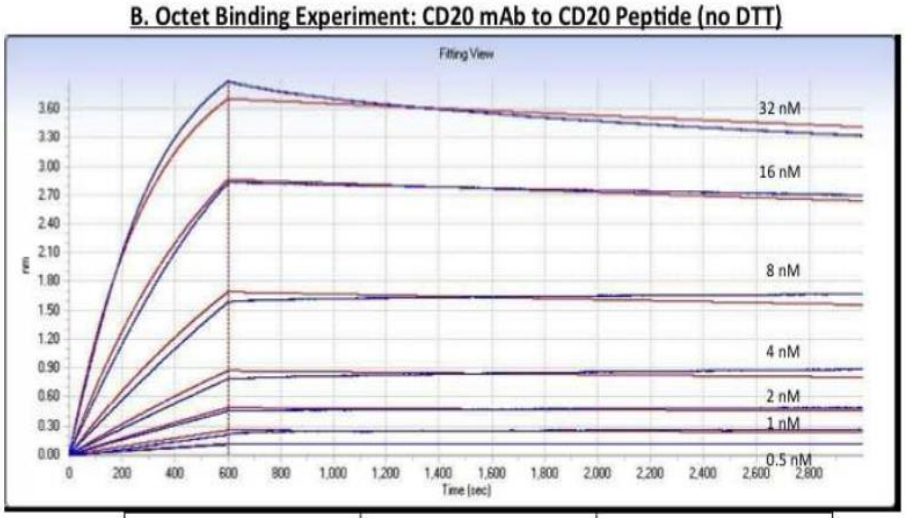

KD (nM)	kon (1/Ms)	kdis (1/s)
0.34	101200 ± 382	$3.41 \times 10^{-5} \pm 2.84 \times 10^{-7}$

Figure 3.9.: Definition of the relative affinity of the NCD1.2 mAb towards the epitope peptide: *(A and B). NCD1.2 was titrated into reactions containing canine CD20 peptide on the solid phase in the absence or presence of DTT to evaluate potential oxidation effects on epitope binding. An Octet RED biolayer interferometry system that measures binding to the sensor tip as a wavelength shift (in nm) in real time. The assay data were processed using Data Analysis (version 6.3 – Forte Bio) to obtain kinetic values as in the materials and methods and tabulated as Kd, Kon and Kdis.*

3.2.6. Fluorescence polarization assay

For further characterization of NCD1.2, we developed a fluorescent (FITC) tagged version of human CD20 peptide to carry out fluorescent polarization assay to determine the relative affinity of the NCD1.2 monoclonal antibody in comparison to Rituximab (Figure 3.10). Purified monoclonal antibody NCD1.2 and Rituximab diluted in PBS were titrated against 30 nM fluorescein-labeled peptide corresponding to human CD20 (NCEPANPSEKNSPSTQYCYS) in assay buffer (PBS, 0.05% Tween-20). Thus these above mentioned experiments confirm that the NCD1.2 Mab binds to both canine CD20 and its human counterpart. Rituximab was used as a control, however, there was no detectable binding in this assay relative to NCD1.2, presumably as Rituximab binds to a complex epitope on human CD20 [8]. These data also suggest that mAb NCD1.2 has a different epitope than Rituximab since NCD1.2: (i) binds to canine and human CD20 peptide (unlike Rituximab) and (ii) NCD1.2 binds to a linear epitope in human and canine peptide CD20 sequence (unlike Rituximab).

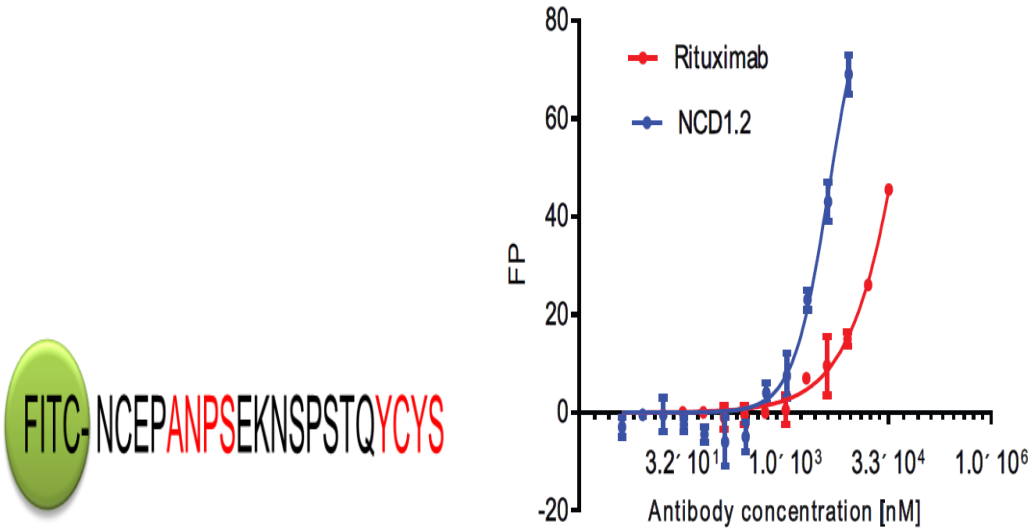

Figure 3.10.: Fluorescence polarization assay: *NCD1.2 and Rituximab were titrated into reactions containing fixed amounts of fluorescent human CD20 peptide (FITC; 30 nm peptide) and relative binding affinities were compared to each other in order to determine how the epitopes for the two monoclonal antibodies might differ. The data are plotted as changes in polarization as a function of increasing antibody concentration*.

3.2.7. Reactivity of NCD1.2 to canine CD20 protein from clinical samples

3.2.7.1. Fluorescence activated cell sorting (FACS)

After determining the kD and relative affinity of the NCD1.2 onto the CD20 immunized peptide, NCD1.2 was then tested onto CD20 expressing canine lymphoma cells as well as on tissue biopsies. The anti-CD20 antibody was evaluated using lymph nodal fine needle aspirates and blood samples preserved in RPMI 1640 medium from dogs with different lymphoma subtypes using flow cytometry. On each sample immunophenotyping was performed according to the previously published procedures, in order to define cell origin and to identify the lymphoma subtype. The highlighted cell population subset was selected and further processed.

These data reveal that NCD1.2 Mab can detect $CD20^+$ cells ($CD21^+$) canine cells in peripheral blood (Figure 3.11A) which correlates with the study carried out by Jubala et al, 2005 where they show the presence of CD20 in peripheral blood as well as canine B cells [198]. As seen in figure 3.11 B the NCD1.2 does not bind to a subset of peripheral T cells and is negative for $CD20^-$ ($CD21^-$), the reason being no or very less expression of CD20 in T cell lymphoma. In another type of B cell lymphoma i.e. medium sized B cell lymphoma (Figure 3.11 C), NCD1.2 stains positive for $CD20^+$ ($CD21^+$). In figure 3.11 D, NCD 1.2 stains positive in another and the most common type of B cell lymphoma in dogs i.e. Diffuse Large B-cell Lymphoma (DLBCL). These results gave an indication that NCD1.2 mAb is highly specific to B cell population as no staining was noticed in T cell lymphoma.

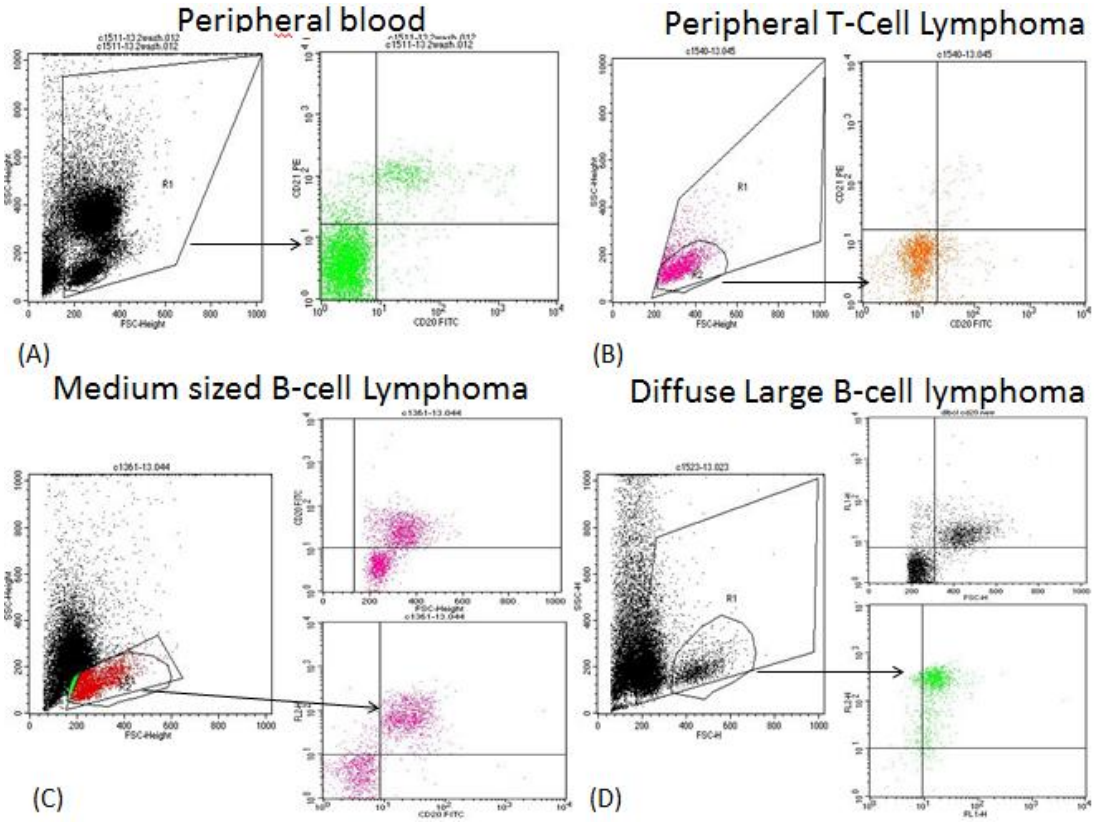

Figure 3.11.: Expression of canine CD20 in clinical cell populations: *The highlighted cell sample populations were isolated and processed as indicated in the materials and methods. Expression of CD20 (and CD21) in the population of cells were analyzed by FACS and include (A) peripheral blood; (B) peripheral T-cell lymphoma ; (C) Medium sized B-cell lymphoma; and (D) Diffuse Large B-cell lymphoma.*

3.2.7.2. Immunohistochemistry

Following such encouraging results obtained from FACS data, we also examined the expression of CD20 using NCD1.2 on formalin fixed samples obtained from tissue biopsies of different types of canine cancer. IHC studies were carried out in collaboration with our Italian collaborators (Stefano). The staining using NCD1.2 revealed diffuse membrane staining in Diffuse Large B cell lymphomas (Figure 3.12A) which was similar to the rabbit polyclonal antibody used for clinical diagnosis (Figure 3.12B). Expression of CD20 was also observed as expected in a range of other lymphoma histotypes of B-cell origin, including Marginal Zone lymphoma (Figure 3.12C), Follicular lymphoma and small lymphocytic lymphoma. The expected negative expression of CD20 protein in peripheral T cell lymphoma was consistent with our FACS data (Figure 3.12D). Collectively, this validation of

the full length monoclonal antibody NCD1.2 including its binding to human and canine CD20 protein and its expression in the correct clinical tissue (B cells), prompted us to clone the antibody variable regions from NCD1.2 to (i) determine whether it would be active as a recombinant antibody, (ii) sequence the scFv to make antibody sequence publically available to allow validation by other research laboratories.

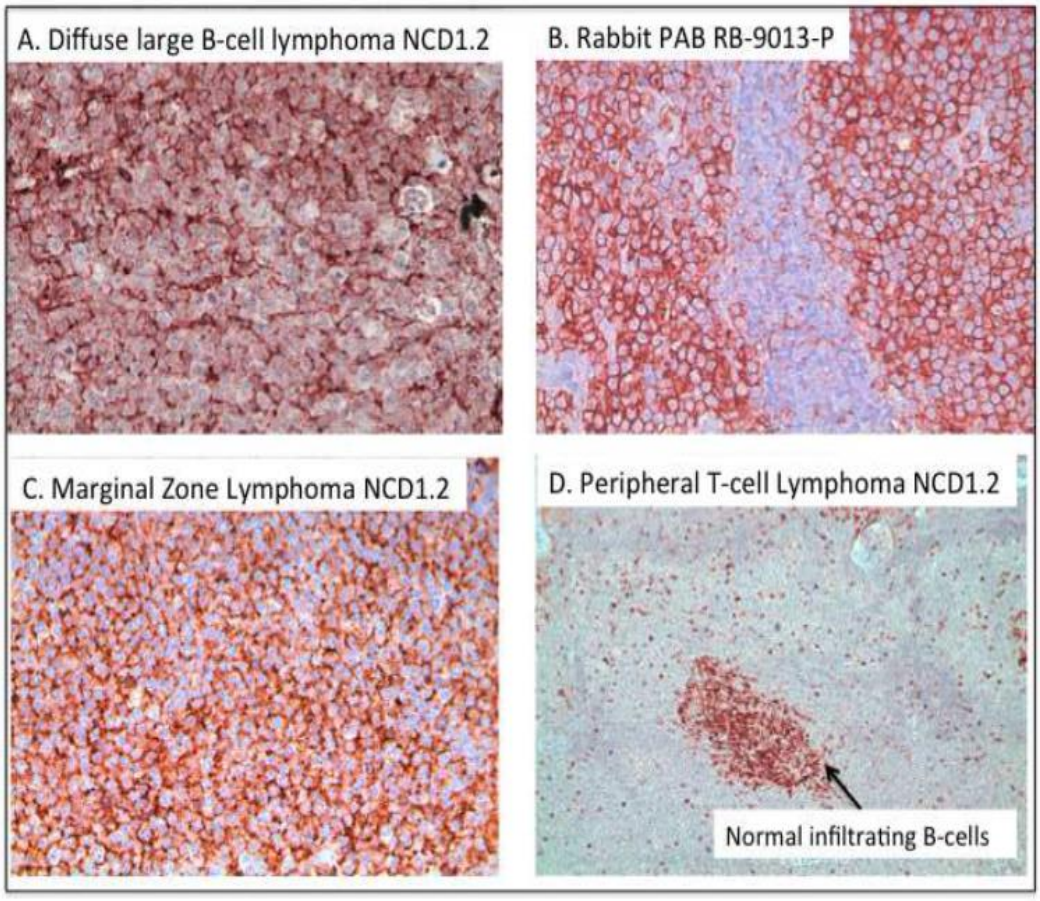

Figure 3.12.: Expression of canine CD20 protein in formalin fixed paraffin embedded cancer tissue: *The indicated tissues were processed using immunohistochemistry as indicated in the materials and methods; and include representative images: (A) NCD1.2 in diffuse large B cell lymphoma (20x); (B) polyclonal anti-cd20 rabbit antibody in DLBCL (20x); (C) NCD1.2 in marginal zone lymphoma (20x); and (D) NCD1.2 in peripheral T-cell lymphoma (10x) with infiltrating normal B-cells that are CD20+ highlighted by the arrow. The staining in brown highlights the position of the NCD1.2 reactive protein with nuclei stained in blue.*

3.2.8. Developing a scFv antibody phage library from hybridoma cell NCD1.2

3.2.8.1. Isolation of RNA from the obtained murine spleen containing B cells

RNA was isolated from mouse spleen using RNA extraction kit as well as traditional Trizol method i.e. phenol: chloroform method. The extracted RNA was quantified using Nanodrop and was further resolved on 1% (w/v) agarose gel to determine the quality of RNA. As shown in the figure 3.13a, good quality of RNA was successfully isolated using Trizol method. Reverse transcription i.e. cDNA was prepared from RNA using the Omniscript Qiagen kit. This cDNA was used as a DNA template for first round of PCR in order to amplify variable heavy and light chain (λ and κ) regions. Also it was noticed that the quality of RNA differed depending upon the source of extraction i.e. spleen or hybridoma cells.

3.2.8.2. First round of PCR (Amplification of variable domain of heavy and light chains)

Variable heavy and light chains (λ, κ) were amplified by Polymerase chain reaction using mouse scFv specific primers. Several optimizations were carried such as increase in annealing temperature, using different types of Taq polymerase, etc. While carrying out PCR to amplify variable heavy and light chain domains using Taq polymerase, no amplification was seen with any of the primers. For further optimization we used additives such as DMSO to favour amplification via PCR. However, no difference was noticed even with additives as well as different types of polymerases in PCR mixture. Finally, using Phusion mater mix (NEB) turned out to be a breakthrough for PCR amplification with additive playing a significant role in diminishing non-specific bands. Also while testing the annealing temperature as well as number of PCR cycles ideally needed for amplification process it was noticed that 56^0C as annealing temperature and 25 PCR cycle were well suited for amplification process. Around 250 PCR reactions were performed for each of the heavy and light chain order to have enough of these products to generate the overlap product (scFv).

Also it is important to mention here that primers used in building first antibody library were purified by desalting method and favoured mutations via PCR amplification. For this reason we used HPLC purified primers and notice that overall mutations decrease when antibody clones were sequenced. The use of HPLC purified mouse scFv primers individually amplified the heavy and light chains but not similar ones when compared to non HPLC purified primers. For amplification of heavy chain, PCR reactions were carried out with each of 19 forward primers and a set of 3 reverse primers. However for amplification of light chain, 17 forward primers and a set of 3 primers were used for amplification of variable kappa light chain (V_κ). Multiple PCR reactions and the reactions were pooled together separately for heavy and light chains. These reactions were then gel extracted and analysed on 1.5% gel and a total of 5 µg of each purified product was made. For amplification of lambda light chain (V_λ), a forward and a reverse primer was used for amplification followed by gel extraction. Figure 3.13 shows the amplification of variable light chain (figure 3.13c) and heavy chain (3.13d).

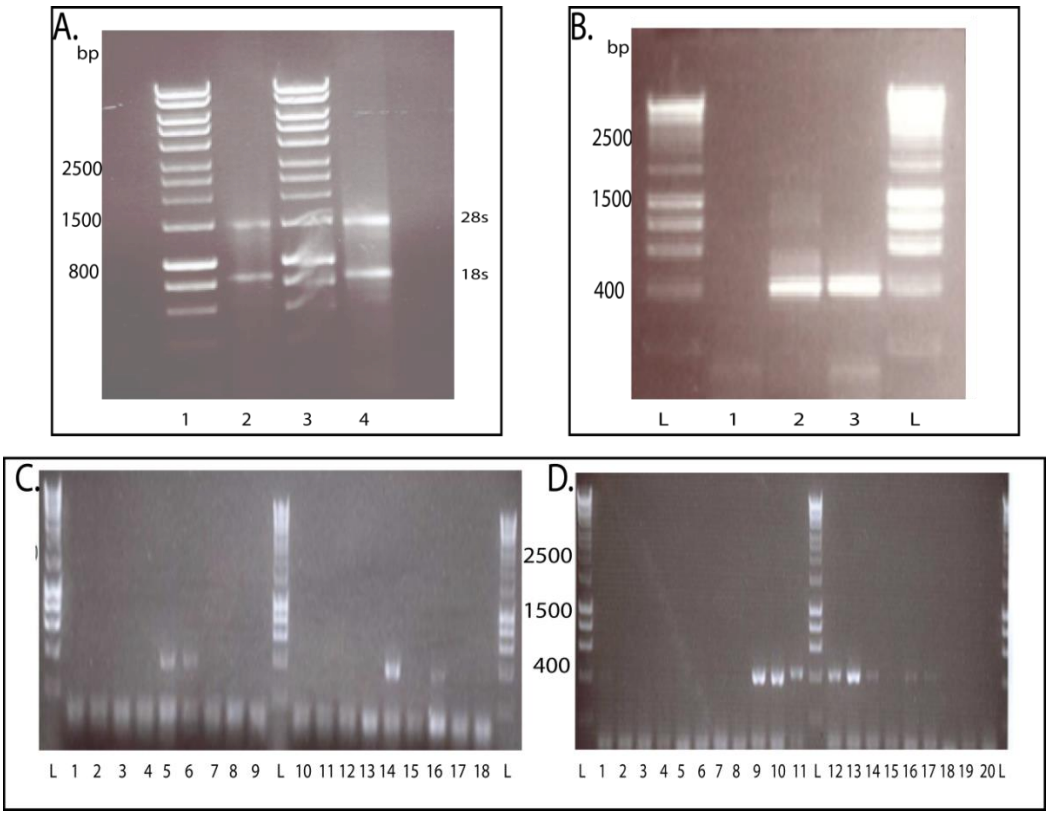

Figure 3.13.: Amplification of variable heavy and light chains: *(a) Isolation of RNA resolved on 1% agarose gel; Lane 1, 3- Hyper Ladder; Lane 2, 4: 2 and 5 µl of isolated RNA using new Trizol. Both subunits i.e. 18s and 28s can be seen after RNA isolation from the spleen of the mouse. (B) Expression of light chains (PCR product) from the prepared cDNA resolved at 1.5% Agarose gel. (a) Lane L: DNA Ladder; Lane 2: negative control; Lane 3: Vκ; Lane 4: Vλ.(C) Amplification of variable light chain through PCR with Phusion protein using 19 different sense primers (5') and 3 reverse primers (3').Lane : DNA Ladder; Lane 2-9: PCR using 5'primers MSCVK1-MSCVK8, respectively; Lane11: DNA Ladder; Lane10-18: PCR using 5' primers MSCVK9-MSCVK17 respectively; (D) Amplification of heavy chain using 19 PCR reactions, resolved on 1.5% gel. Lane L: Ladder, Lane*

These pooled PCR products were gel extracted using the gel extraction kit (Qiagen) and 1 µl of each of the purified variable regions was run on a 1.5 % (w/v) to measure the concentration of each DNA (Figure 3.14a). The concentration was measured via Nanodrop as well as compared to corresponding band on the hyper ladder (Figure 3.14).

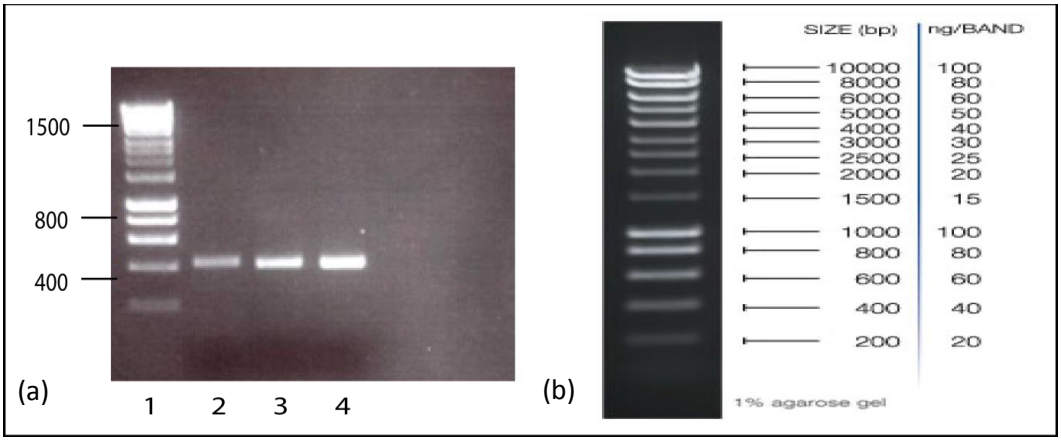

Figure 3.14.: Purified variable heavy and light chains: *(a) Lane 1: Ladder, Lane 2: purified heavy chain; Lane 3: purified V_λ and Lane 4: purified V_κ. (b) Bioline 100 bp Hyper ladder with each band corresponding to a certain concentration of DNA (20-100 ng).*

3.2.8.3. Second round of PCR (overlap extension PCR)

After quantifying the amount of DNA, purified variable heavy and light chains were spliced together using second round of PCR. For generation of 800 bp overlap product, various ratios of V_κ and V_λ template were examined via PCR. To start with, 100 ng of each of the variable heavy and light (λ or κ) were used to anneal together

but it was seen that there was no 800 bp band obtained. On performing PCR amplification using different concentrations of each variable chain, it was found out that 10 ng of each of the variable chain was most efficient for annealing. However this along with this overlap product, there was a non-specific amplification around 1000 bp. To get rid of this non-specific band, a number of additives have been proven to enhance PCR amplification and minimizing other bands. Several optimization reactions such as a touch down PCR with 2% (v/v) DMSO as an additive was found to be efficient to amplify 800 bp product and also minimize any other non-specific bands (figure 3.15a). Further, different types of polymerases were also examined via PCR with an objective to investigate if the amplification could be maximized by the use of different polymerases.

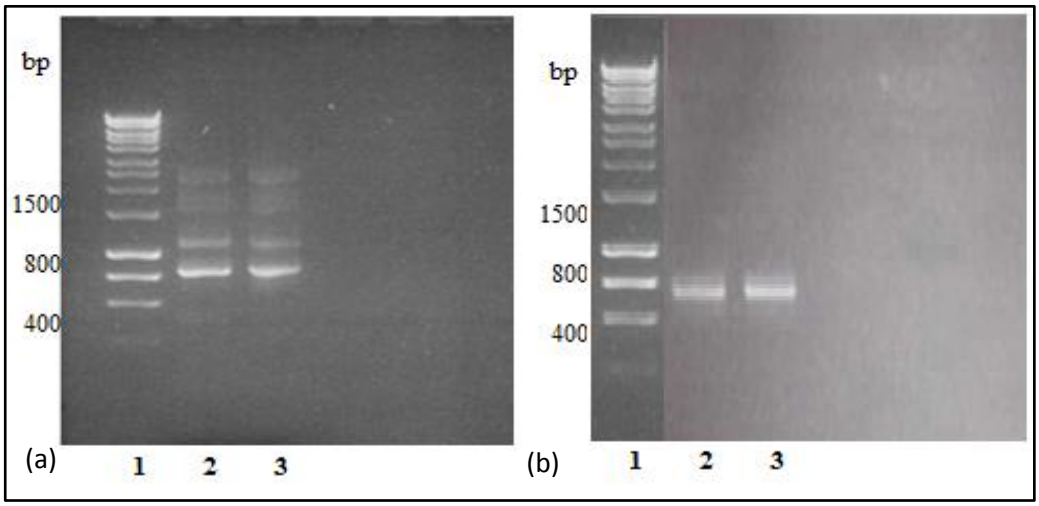

Figure 3.15.: Second round of PCR (Touch down PCR): *(a) Lane 1: Ladder, lane II, III: 5µl PCR using 2%DMSO as an additive and no additive, respectively. (b) Purified PCR product Lane I, II: 1 and 2µl of purified PCR overlap product, respectively.*

A total of 120 reactions touchdown PCR reactions were performed in order to have enough of purified overlap PCR product i.e. around 10 µg for proceeding to next step. These PCR reactions were pooled together; gel extracted on 1.5% (w/v) agarose gel and purified using gel extraction kit. The extracted DNA was pooled together and once again 1µl of DNA was analysed on the gel to estimate the concentration of the DNA (Figure 3.15b).

3.2.8.4. Restriction digest, Ligation of purified PCR product and vector DNA (pCOMB3xSS)

Restriction digest reactions using SfiI enzyme were set up for the purified insert (scFv) as well as vector DNA to favour ligation. The reactions were incubated at 50°C for 5 hours. The purified PCR product was resolved on 1% (w/v) gel, whereas the reaction containing vector DNA (pCOMB3xSS) was resolved on 0.6% (w/v) agarose gel. These products were then gel extracted and the concentration was determined using Nanodrop as well as hyper ladder. Each of the digested products was run on a 1% (w/v) agarose gel (shown in figure 3.16). These purified digested products were ligated together. Ligation reaction was carried out for vector DNA containing scFv as well as vector DNA only to check for ligation efficiency and percentage insert.

As mentioned in the methods section the reactions were made up and then incubated at 16^0C overnight. Following overnight ligations, purification of the ligated samples was carried out using mini PCR purification kit (Invitrogen) and eluted in 10 µl elusion buffer. The eluted mixture was divided into 5 tubes (2 µl/tube) and transformed into TG1 cells using electroporation technique. To each 2 µl DNA aliquot, 250 µl of SOC medium was added quickly to all electroporation columns and incubated for 1 hour at 37^0 C. Following this, the electroporated mixture from all columns was mixed, a series of dilutions was prepared using 100 µl of the mixture in LB (10^{-1} – 10^{-8}) and plated out onto LB ampicillin plates. Rest of the electroporated mixture was plated out on a large assay plate. Subsequently all the plates were incubated overnight at 37°C.

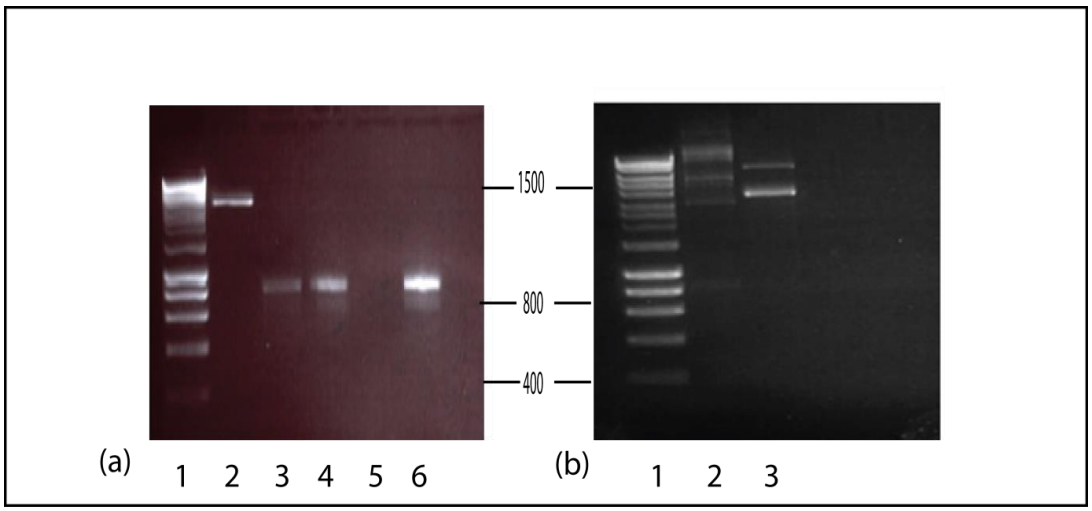

Figure 3.16.: Restriction digestion and ligation of scFv, pCOMB3xSS: (*a) Restriction digestion; Lane I: Ladder, Lane II: purified pCOMB3xSS, Lane III, IV and VI: 1, and 5 µl of purified SfiI digested insert, respectively. (b) Lane I: Ladder, Lane II: Ligated scFv into pCOMB3xSS and lane III: Ligated vector DNA*

3.2.8.5 Library size

The mixture plated onto the large assay plate contains the library and this library was scraped using LB medium, 50% Glucose and 30% glycerol. This library was snap frozen and stored at -80^0 C until further used. The size of the library was calculated on the basis of number of colonies obtained onto the smaller 10 cm plates. A total of 4 antibody libraries were made from mouse spleen and hybridoma cells using differently purified sets of degenerative primers. The size of the libraries obtained were 1.4 x 10^9, 4.0 x 10^8 and 2.6 x 10^8 cfu /ml which were two orders of magnitude higher as compared to vector DNA only. Here magnitude of vector DNA indicates the count obtained from colonies containing self - ligated vector DNA only.

10 colonies were grown from vector containing insert plates as well as vector only plates in 5 ml LB medium (100 µg/ml Amp). Following this, miniprep (Qiagen) was performed for all of these colonies and the concentration of the obtained DNA was measured through Nanodrop. Subsequently, restriction digestion 15µl reaction of these clones using SfiI was performed in order to ensure that vector DNA contains insert. 24 out of 30 clones showed the presence of insert i.e. 80% and were further sequenced (for example figure 3.17).

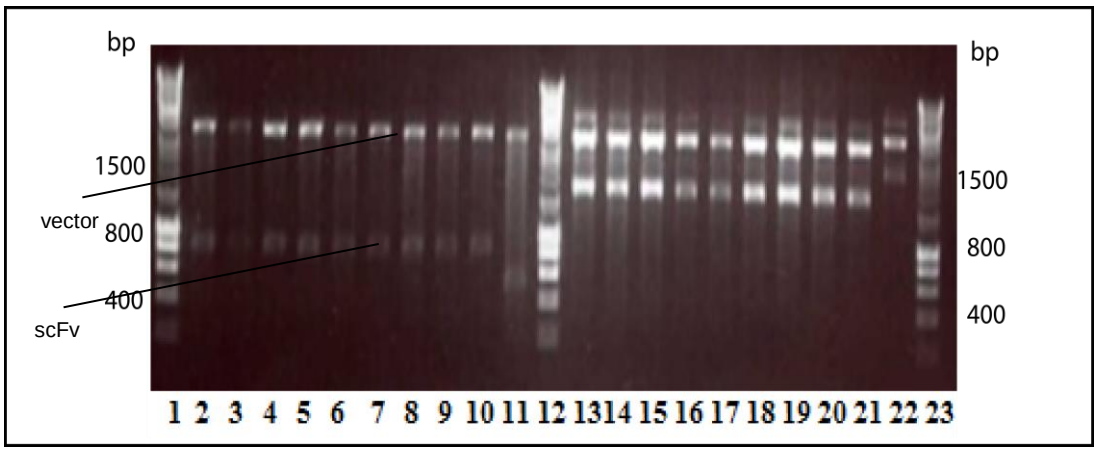

Figure 3.17: Restriction digestion of picked colonies: *Lane I: Ladder, Lane II-XI: Restriction digestion of miniprep purified DNA extracted from serially diluted vector containing insert plates, Lane 12: Ladder; Lane 13- 22: Restriction digestion of miniprep purified DNA extracted from serially diluted vector only plates, Lane 23: Ladder.*

The sequencing data of these purified DNA clones from 1st library (non-HPLC purified primers) showed that 7 out of 10 scFvs were out of frame. However, when HPLC purified primers were used the clones containing insert increased to 50% in frame. The complementary determining regions (CDRs) and the framework regions (FRs) were identified from the antibody sequences. As explained above in section 3.2.8.3, the heavy and light chains are linked together by a long serine glycine linker with a His tag at the end. In order to overcome the frame shift mutation which might have come via PCR or at any other stage, 3 more antibody libraries were developed using either HPLC purified primers or using spleen or using hybridoma cells. Based on the sequencing data obtained from all of these libraries, the one that was made from hybridoma cells was found to be the best one and was taken forward. The scFv was cloned in such a way that the OmpA sequence (sequence present in pCOMB3xSS just before SfiI restriction site) is followed by light chain. This light chain is linked to the heavy chain via a linker which has been shown below in figure 3.18:

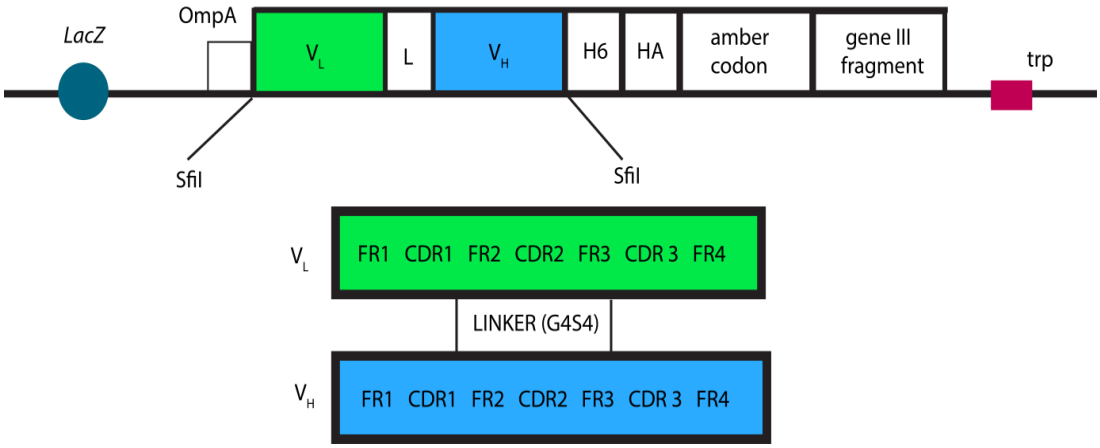

Figure 3.18: scFv in pCOMB3xSS: *Variable heavy and light chain connected by a peptide linker (L) with SfiI digestion sites at the 5' and 3' of light and heavy chain respectively. Each chain of scFv is comprised of 3 CDRs and 4 framework regions.*

3.2.9 Biopanning

Using 1µl of antibody library, OD_{600nm} was measured and the amount of library needed to produce 100 copies was calculated. Subsequently the antibody library was grown overnight at 30^0C, PEG precipitated and the clearly visible phage pellet was resuspended in PBS. A total of 4 rounds were carried out and the amount of washes were increased every round. Also, the concentration of the protein used in each round was decreased to half in order to get highly specific binding clones to the target CD20 peptide. The antibody library was subjected to the process of biopanning in an immunotube coated with CD20 peptide in order to select for CD20 binding antibody clones. Also during all rounds of biopanning, several titrations of the phage pools was carried out (as in theory, the amount of phage should decrease every round and the specific phage should be eluted). The dilutions of the phage was performed in 225 µl *E.coli* TG1 cells and dilutions in a range of 10^{-6} to 10^{-8} were prepared, incubated at 37^0 C for 30 minutes and plated out on LB + ampicillin plates. 96 colonies from round 3 and 4 were grown in 100 µl of media containing 100 µg/ml ampicillin and sub-cultured in 200 µl media (Amp) containing growth supplements in 1 ml deep well plate. These were grown until an OD of 0.6 was reached and 1 mM IPTG was added to each well and incubated overnight at 30^0 C. The following day,

lysis (freeze thaw protocol) was performed three times and the plate was centrifuged at 4000 g for 15 minutes. This supernatant contained secreted antibody without any phage and used as primary antibody.

100 µl of this lysate was added to the respective well of the CD20 peptide coated plate and incubated for one hour at RT. Subsequently, HRP conjugated protein A (1:1000) was added to all the wells of the plate and the plate was then read at 450 nm after adding TMB. As shown below out of 96 clones, 6 of the clones showed significant binding as compared to other clones. The lysates were added fresh while performing this ELISA (figure 3.19); however when ELISA was performed the following day using the same lysate as the primary antibody the activity of all of the positive clones were close to zero. From the glycerol stocks of these antibody clones expression was carried out on a large scale to see if any activity was retained after lysis, but the results from ELISA again show that the secreted antibody was inactive. Thus, on the basis of results obtained from secreted antibody expression, it was concluded that scFv are highly unstable as the activity of the antibody was not even retained for 24 hours. This instability of recombinant antibody has been reported previously [235]. For selecting more stable and CD20 binding specific clones, troubleshooting in various ways was carried out such as increasing the number of rounds of panning, 5% milk as blocking buffer instead of 3% BSA used in earlier case and increasing the number of washes as well as using different reagents for elusion of specific binding phages.

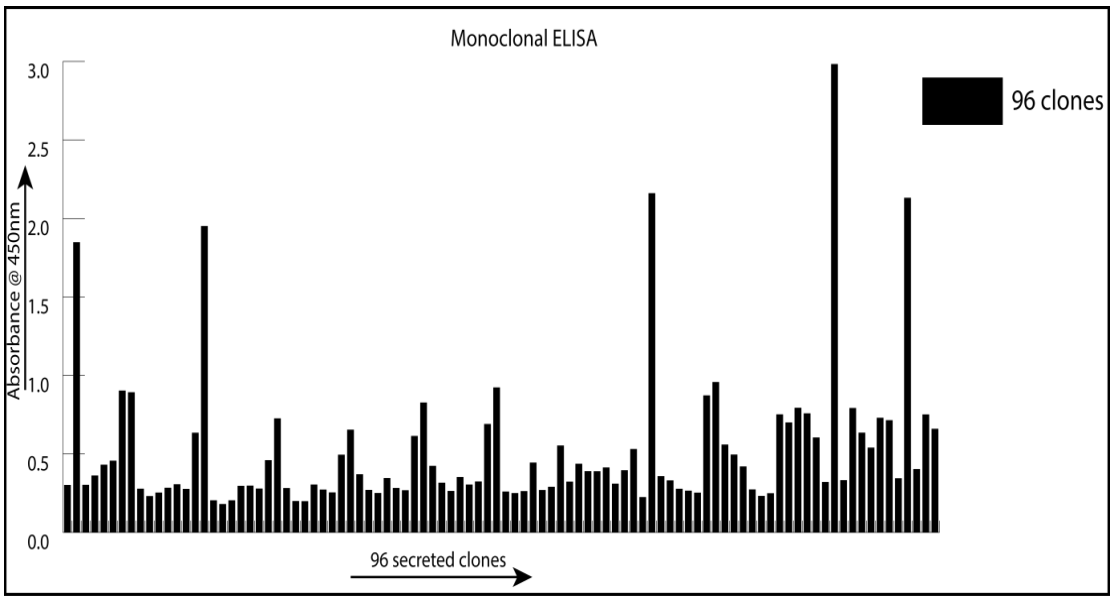

Figure 3.19: Biopanning: *Analysis of 96 colonies by monoclonal ELISA: 96 colonies were grown overnight at 37^{0}C, following day sub cultured and grown in 200 µl LB media (100 µg/ml amp) for 2-3 hours until an OD of 0.6 was reached in a 1ml deep well plate. The expression was then induced by addition of 1 mM IPTG overnight at 30^{0}C, shaking 220 rpm. The plate was then subjected to freeze thaw protocol thrice and centrifuged to obtain scFv enriched lysate. This was added as primary antibody onto wells coated with CD20 peptide overnight. The binding activity was resolved using TMB and the plate was read at 450 nm.*

In order to overcome this stability issue of the recombinant antibody, expression was optimized using different elution methods for binding phages and 8 colonies from output round 3 and 4 were grown in 10 ml LB media (100 µg/ml Amp) until an OD of 0.6 was reached. Once an OD of 0.6 was reached, 10 µl helper phage was added, incubated static for 30 minutes followed by shaking at 220 rpm for 2 hours. Following this, kanamycin (50 µg/ml) was added to the cultures and incubated overnight at 30^{0}C. Next day the falcon tubes were centrifuged at 4000rpm for 10 minutes and supernatant PEG precipitated, final pellet was resuspended in 200 µl of PBS and added to ELISA wells that were coated overnight with CD20. As seen below in figure 3.20, 2 colonies out of 8 showed significant activity via ELISA when carried out in titrations and probed using M13 antibody. The activity of these clones was tested again after 5 days and both clones retained activity the same as day zero. The stability of antibody was thus achieved when scFv was expressed on phage surface rather than secreted scFv antibody with no phage. As it can be seen scFv 3

binds to CD20 peptide better than scFv 7 and following this both phage linked scFv (3 and 7) were tested and compared for activity onto peptide 32 (NCDPANPSEKSLSIQYCGSIR) and 38 (PSEKNSLSIQYCGSIR). Interestingly these results showed scFv 3 and 7 bound better to peptide 38 as compared to 32, which was in contrast to the full length monoclonal antibody epitope which bound strongly to peptide 32 and weakly to peptide 38. Previously it has been shown by few research groups that recombinant antibody might not bind as better as the full length mAb, which might be due to the way epitope is exposed or could be the confirmation of the antibody or target protein.

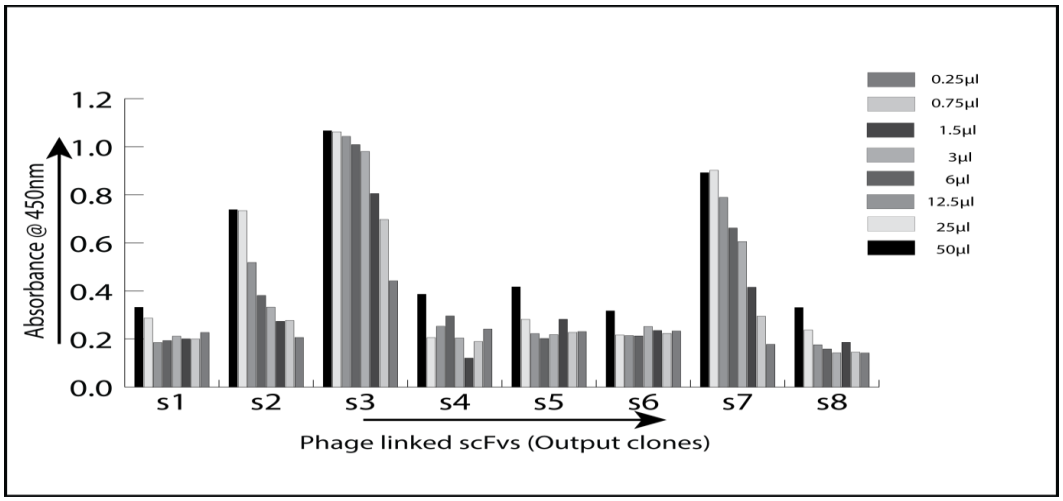

Figure 3.20: Phage expressing scFv ELISA: *Phage producing plaques from rounds 3 and 4 were grown overnight, the scFv-phage in the supernatant was PEG precipitated, and assayed in an ELISA using biotinylated CD20 peptide 32. Active scFv-phage was detected using an M13-phage antibody and binding activity was resolved using TMB and measured as optical density (450 nm). Eight representative scFv-gIII fusion phage are highlighted where two bioactive recombinant (3 and 7) were isolated.*

3.2.10. Bacterial and mammalian expression of scFv

Once this optimization was successful to obtain positive phage linked scFv clones, we hypothesized that both of these scFv antibodies targeting CD20 could be used by our community as a recombinant bioconjugate in the development of immunotherapeutic models in canine cancer. As mentioned in methods section both scFv 3 and 7 were cloned into bacterial as well as mammalian expression vectors to determine if they could be manipulated and used in principle for future therapeutic or diagnostic applications. The scFv3 and scFv7 were active when fused to gIII M13 coat protein figure 3.21. When the scFv was cloned into a mammalian expression

vector that directs its secretion from CHO cells, then both scFv3 and scFv7 supernatants were shown to produce active recombinant antibody using either CD20 protein (Figure 3.21 i) or CD20 peptide 32 (Figure 3.21 ii).

This indicates that the CHO system can be used in principle to direct the production of large amounts of recombinant protein for diagnostics, or therapeutics, in the future. Both scFv 3, 7 were expressed and the supernatants were used for performing ELISA onto plates coated with CD20 protein as well as CD20 peptide 32. The results shown in figure 3.21 demonstrate that both scFv were expressed and bound to CD20 protein and peptide, also scFv 3 bound better as compared to scFv 7. CHO system has been the ideal choice for antibody expression in mammalian cells because of the antibody yield obtained.

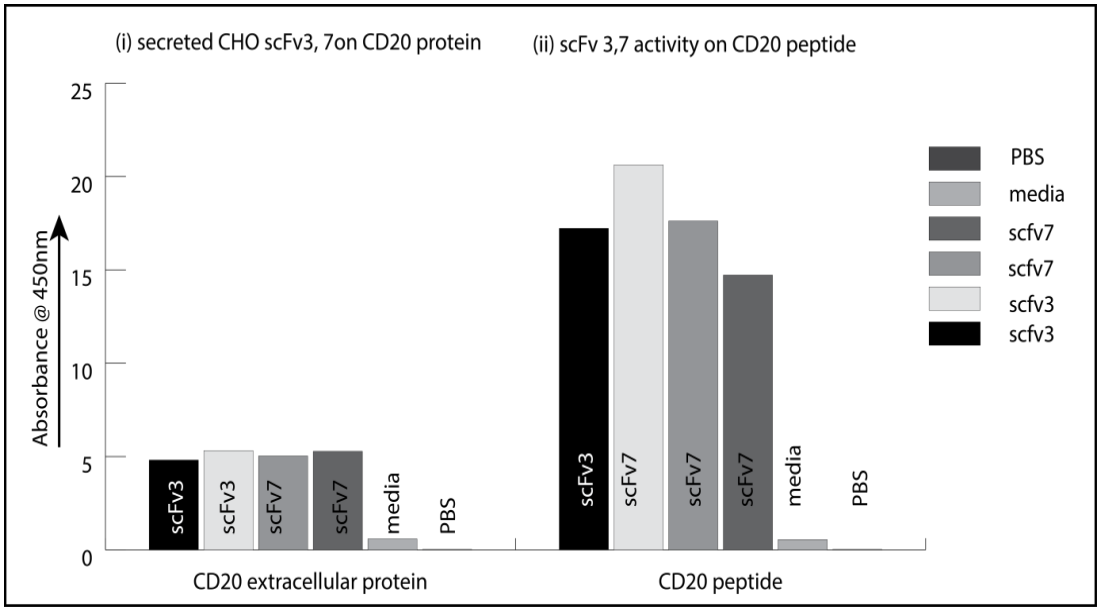

Figure 3.21: Mammalian expression of scFv: *The indicated scFv (3 or 7) was cloned into pCDNA3.1 containing a leader sequence (amino acids MGGS) for targeted secretion into the media of tissue cultured CHO cells. (i) Activity was measured on left panel after dilution of the supernatants (1:40 or 1:80) to optimize activity against His-tagged CD20 protein; (ii) right panel the optimized supernatants of scFv-3 and scFv-7 were assayed against biotinylated CD20 peptide as indicated in the materials and methods. Antibody scFv binding to antigen was detected using peroxidase conjugated protein A and resolved with TMB-based ELISA at an OD of 450nm. Controls included media only or PBS.*

Alongside bacterial expression was carried out into pTRCHisB, the antibody expression was followed by purification using a Ni-NTA column. The antibody was used at a dilution of 1:40, 1:80, 1:160 and 1:320 onto CD20 extracellular protein (figure 3.22).

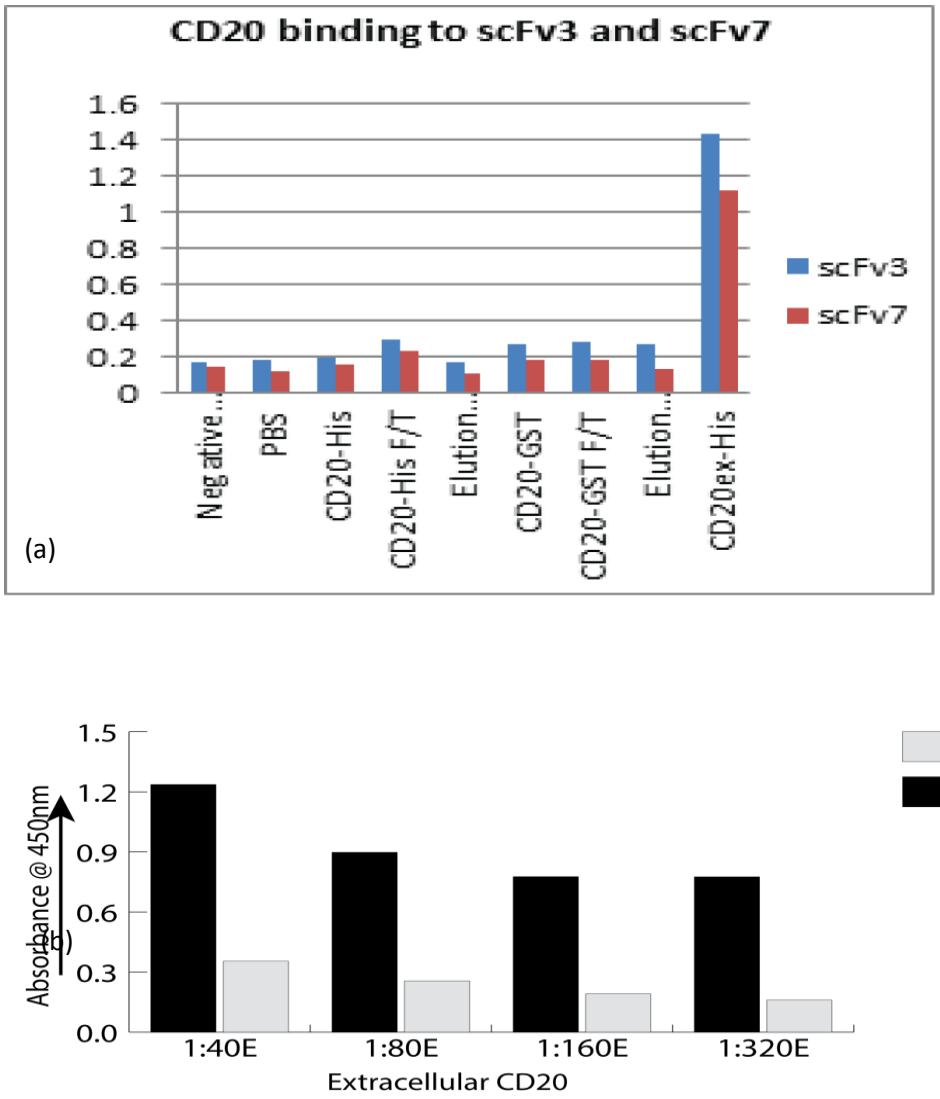

Figure 3.22: Bacterial expression of scFv (ELISA): *(a) Binding efficiency of purified scFv 3, 7 onto GST-CD20 and extracellular CD20-His tagged with all controls. (b) Titration of extracellular CD20 was added to fixed amount of scFv (500 ng/well) and absorbance read at 450nm after addition of TMB.*

3.2.11 Sequence analysis of scFv 3, 7

Both scFv were sequenced and the amino acid of each has been shown below in the figure 3.23 upper panel. All three CDRs and four FRs have been shown, with variation only in light chain in CDR1 and CDR2 region between the scFvs. In theory both scFv should have same sequence throughout as both scFvs are isolated from a single hybridoma cell. Interestingly we notice here that both scFvs have been obtained from a single hybridoma cell and the variability was only seen in the light chain CDRs whereas the heavy chains were totally identical. To further prove this, we designed primers using the initial sequence of each light chain. The PCR was performed with three different cycles (20, 25 and 30 cycles) and as it can be seen in the figure 3.23 lower panel both light chains were amplified using the designed primers from different scFv.

CD20 ScFv antibody sequence

Light chain

	FR1	CDR1	FR2	CDR2	FR3	CDR3	FR4
scFv3:	PPAIMSASPGEKVTMT	CSASSSVSYMH	WYQQKSGTSPKRWIY	DTSKLAS	GVPDRFSSSGSGTDFTLRISRVEAEDVGVYYC	AQNLELPFT	FGGGTKLEIK
scFv7:	AAAFSNPVTLGTSVSIS	CRSSKSLLHRGFTYLY	WYLQRPGQSPQLLIY	QMSNLAS	GVPDRFSSSGSGTDFTLRISRVEAEDVGVYYC	AQNLELPFT	FGGGTKLELK

Heavy chain

	FR1	CDR1	FR2	CDR2	FR3	CDR3	FR4
scFv3:	VESGGGLVQPGDSLRLSCATSGFTFT	DYFMS	VRQPPGKSLEWLG	LIRNKVNGYTAEYSASVKG	RFTISRDNSRGILYLQMYTLRAEDSATYYCVR	ASTG	TSFVYWGQGTLVTVSA
scFv7:	VESGGGLVQPGDSLRLSCATSGFTFT	DYFMS	VRQPPGKSLEWLG	LIRNKVNGYTAEYSASVKG	RFTISRDNSRGILYLQMYTLRAEDSATYYCVR	ASTG	TSFVYWGQGTLVTVSA

Clone3:GTDIVMTQPPAIMSASPGEKVTMTCSASSSVSYMHWYQQKSGTSPKRWIYDTSKLASGVPDRFSSSGSGTDFTLRISRVEAEDVGVYYCAQNL
ELPFTFGGGTKLEIKSSGGGGSGGGGGGGSSRSSLEVNVVESGGGLVQPGDSLRLSCATSGFTFTDYFMSWVRQPPGKSLEWLGLIRNKVNGYTAEYSAS
VKGRFTISRDNSRGILYLQMYTLRAEDSATYYCVRASTGTSFVYWGQGTLVTVSA

Clone7:GTDIVMTAAAFSNPVTLGTSVSISCRSSKSLLHRGFTYLYWYLQRPGQSPQLLIYQMSNLASGVPDRFSSSGSGTDFTLRISRVEAEDVGVYYCAQNL
ELPFTFGGGTKLELKSSGGGGSGGGGGGSSRSSLEVQGVESGGGLVQPGDSLRLSCATSGFTFTDYFMSWVRQPPGKSLEWLGLIRNKVNGYTAEYSAS
VKGRFTISRDNSRGILYLQMYTLRAEDSATYYCVRASTGTSFVYWGQGTLVTVSA

(a)

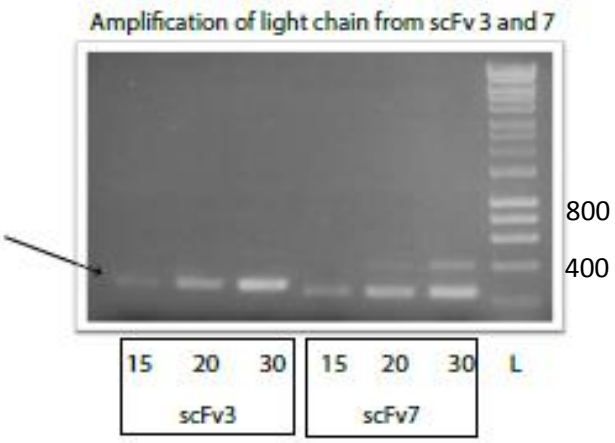

(b)

Figure 3.23: Sequence analysis of scFv 3 and scFv 7: *(a)The amino acid sequences of the light chain and heavy chain framework and CDR regions are as indicated. The CDRs of the light chain are highlighted in red, since the sequences diverge in CDR1 and CDR2 of the two light chains, but are identical in the CDR3 of the light chain. The full amino acid sequence of scFv-3 and scFv-7 including the linker is highlighted. (b) RT-PCR using primers directed to the divergent light chains (from CDR1 to Framework 4) of cDNA scFv-3 and scFv-7 from NCD1.2 hybridoma cell line to establish that the light chain mRNA for scFv-3 and scFv-7 are both expressed to similar levels indicating that the hybridoma produces two light chains with an identical CDR3. The size of the CDR1-FR4 PCR product is approximately 300 bp and the ladder is Hyperladder (Bioline).*

3.2.12 scFv-CpG2 Bioconjugate

Bacterial production was evaluated after creating a CPG2-bioconjugate with an aim to determine whether the scFv scaffolds would be suitable for ADEPT (antibody directed enhanced pro-drug therapy) type immunotherapeutics. CPG2 is Carboxypeptidase G2, originally derived from *Pseudomonas* that has been used to convert Nitrogen mustards into potent DNA cross-linking agents. CPG2 was cloned into pHISTEV at *NcoI* and *NotI* sites to create pJGS101. The scFv-3 and scFv-7 were cloned into pcDNA3.1-his/ lacZ with CPG2 cloned into the KpnI - EcoRI sites of the vector. The anti-CD20 scFv - CPG2 bioconjugates were relatively insoluble in bacteria (Figure 3.24 C, left panel). However, we optimized the production of soluble scFv-CPG2 fusion proteins that permitted affinity purification of the protein (Figure 3.24 C, right panel). The purified scFv-3:CPG2 and scFv-7: CPG2 fusion proteins were tested for activity on the CD20 derived peptides. We notice that both scFv actively binds with a proposed epitope defined by the overlapping binding towards peptide 32 and peptide 38 derived from CD20 protein (Figure 3.24 D). These latter data suggest that although the CPG2 - scFv fusions have the potential to be used as a bioconjugate, bacterial expression systems might not be the optimized source of protein for future trials in canine cancers. CHO cells might remain the standard source for production of recombinant bio-conjugates such as scFv3 and scFv7 in the near future.

A. Bioactivity of scFV-3 and scFv-7 from mammalian CHO cells

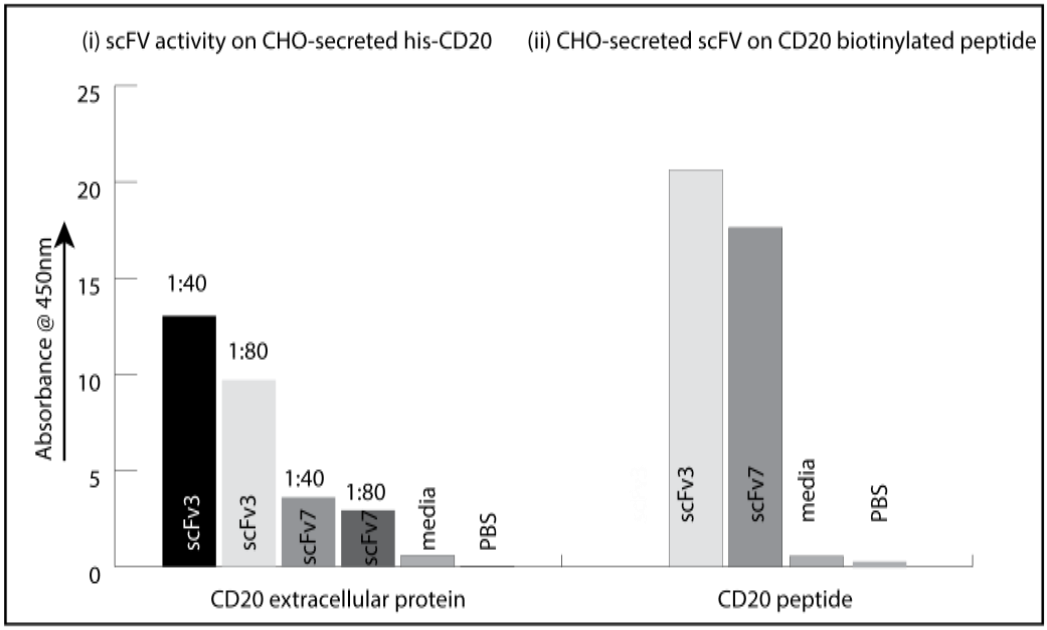

B. Bioactivity of CPG2-biocnjugated scFV-3 and scFv-7 from bacterial cells

Light Chain-Linker-Heavy Chain-CPG2-6xHIS-STOP

C. Purificaiton of scFv-CPG2 from bacterial expression systems

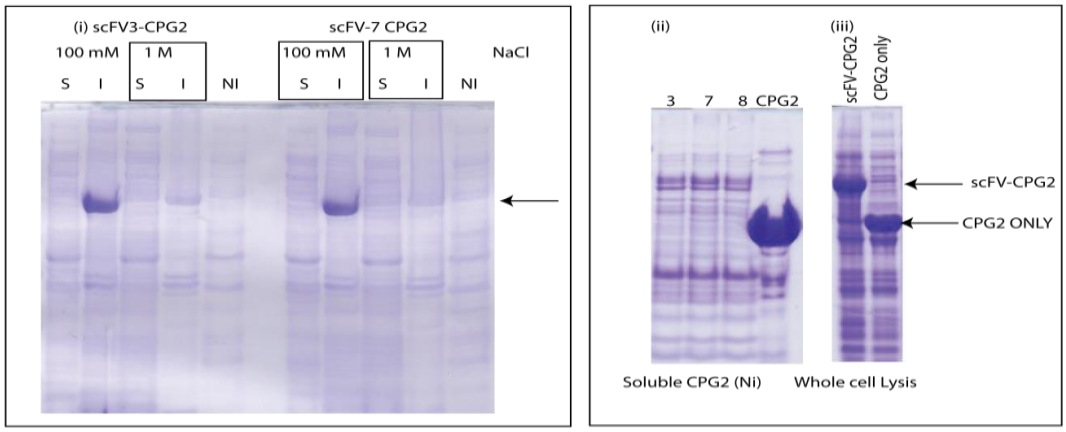

D. Bioactivity of scFv-CPG2 bioconjugate

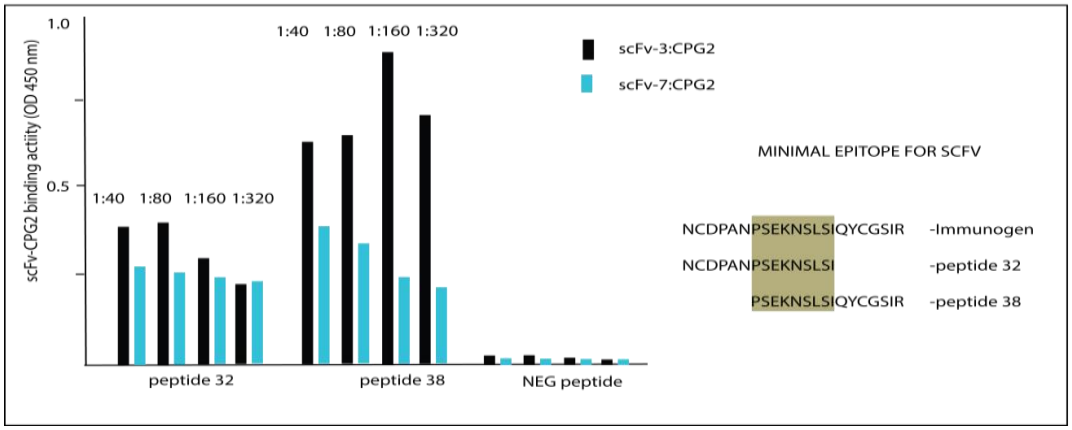

Figure 3.24: Bioactivity of recombinant scFv-3 and scFv-7 secreted from CHO cells and produced in bacteria as a CpG2-bioconjugate: *(A) The indicated scFv (3 or 7) was cloned into pCDNA3.1 containing a leader sequence (amino acids MGGS) for targeted secretion into the media of tissue cultured CHO cells. (i) Activity was measured on left panel after dilution of the supernatants (1:40 or 1:80) to optimize activity against His-tagged CD20 protein; (ii) right panel the optimized supernatants of scFv-3 and scFv-7 were assayed against biotinylated CD20 peptide 32 as indicated in the materials and methods. Antibody scFv binding to antigen was detected using peroxidase conjugated protein A and resolved with TMB-based ELISA at an OD of 450nm. Controls included media only or PBS. (B). A schematic of the scFv-3 and scFv-7 CPG2 fusion protein. (C). Bacteria were grown and scFv-3 or scFv-7 CPG2 bioconjugates were induced with IPTG. Following lysis with 100 mM or 1 M NaCl lysis buffer, the samples were separated into soluble and insoluble fractions. These fractions were mixed with SDS loading buffer, were separated on an SDS gel, and stained with Coomassie blue. The Left panel (i) displays the solubility (S) or insolubility (I) of scFv-3 and scFv-7 from bacterial expression systems in lysis buffer containing the indicated NaCl concentrations. The arrow highlights the position of the scFv-CPG2 fusion protein. The NI lane represents the amount of soluble scFv- 3 recovered from the S fraction after nickel chromatography, which was negligible. The right panel (ii) shows the relative purify of the scFv-3 and scFv-7 (and scFv-8 as a control antibody) after lysis using stabilizing lysis buffer (as in Methods) and followed by nickel affinity chromatography. The relative expression and purity of CPG2 alone is shown by comparison to highlight its enhanced yield relative to the scFv-CPG2 fusion. The insolubility remains a problem from bacterial expression systems, as the total synthesis of scFv-CPG2 and CPG2 alone is relatively similar using whole cell lysis buffer (right panel (iii). (D). Bioactivity of affinity purified scFv-3 and scFv-7 from bacteria. The normalized affinity-purified scFv fractions (from Figure 3.23 C) were assayed for binding to the indicated canine CD20 peptides (peptide 32 and peptide 38) where the core epitope resides (in gold shade). scFv-3 : CPG2 was more active than scFv-7:CPG2 on both peptide 32 and peptide 38. The enhanced activity of scFv-3:CPG2 as a bioconjugate is consistent with its enhanced activity when secreted as a single chain from CHO cells (Figure 3.23 A) and when fused to M13 gIII protein (Figure 3.23 C).*

3.2.13 Yeast expression and purification of scFv3-CpG2

To further increase the affinity of the scFv.CpG2 conjugate, we cloned conjugate into yeast expression vector with an aim of improved antibody secretion. Yeasts are eukaryotic micro-organisms provide an advantage of additional protein folding pathways and can be rapidly grown on yeast growth media [236]. In this case only scFv3 was considered and was carried out in collaboration with Eva, Brno, Czech Republic.

Expression

scFv was expressed on a small scale (20 ml) as well as large scale (1 litre) in the yeast strain *Pichia pastoris*. Single colony was inoculated in 25 ml of BMGY in a 250 ml baffled flask. The colony was grown overnight (approximately 16-18 hours) at 28-30^0 C in a shaking incubator (250 rpm) and the cells reach an OD_{600} of 2-6 which indicates the cells will be in the log phase. The cells were centrifuged at 1500-3000 x g for 5 minutes at RT. The supernatant was discarded and cell pellet was resuspended to an OD_{600} of 1.0 in BMMY medium to induce expression (approximately 100 ml). The culture was placed in a 1 litre flask and the flask was covered with 2 layers of sterile cloth and returned to incubator to continue growth. 100% methanol was added to a final concentration of 0.5% methanol every 24 hours to maintain induction. At each of the time point i.e. 0, 6, 12 , day 1, day 2 , day 3 and day 4; 1ml of the expressed culture was transferred to a 1.5 ml microcentrifuge tube. These samples were then used to analyse the expression levels and determine the optimal time post induction to harvest. These were then spun down at maximum speed in a table top microcentrifuge for 2-3 minutes at room temperature. For secreted expression, the supernatants were analysed via Coomassie staining as well as functional assay such as ELISA (figure 3.25 A, B).

Purification

Cell pellet was resuspended in sucrose buffer (30 mM Tris/HCl, 20% sucrose, adjust pH to 8.0). The cells were kept on ice with a dropwise addition of 500 mM EDTA to 1 mM and incubated on ice for 5-10 minutes with gentle agitation. The cell suspension was spun down at 8000 x g for 20 minutes at 4^{0}C. The cell pellet was

resuspended in buffer B (100 mM NaH_2PO_4, 10 mM Tris/HCl, 8 M urea, adjust pH 8.0). The cells were sonicated at an amplitude of 10 (3x 15seconds) on ice. The cells were centrifuged at 10,000 x g for 20-30 minutes at room temperature to pellet the cellular debris. 1 ml of 50% Ni- NTA to 4 ml lysate and mixed gently by shaking at 4^0C for 60 minutes. This lysate –Ni-NTA mixture was loaded onto a column with capped bottom outlet, bottom cap was removed and flow through was collected. The column was washed with 100 mM NaH_2PO_4, 10 mM Tris/HCl, 8 M urea, adjust the pH to 6.3. The protein was then eluted in 100 mM NaH_2PO_4, 10 mM Tris/HCl, 8 M urea, adjust the pH to 4.5. The samples were then analysed by Coomassie staining and ELISA (figure 3.25 A, B). Thus in conclusion, the results indicate that yeast expression of scFv3-CpG2 does not yield a great amount in comparison to bacterial and mammalian expression as shown in 3.2.10.

(A)

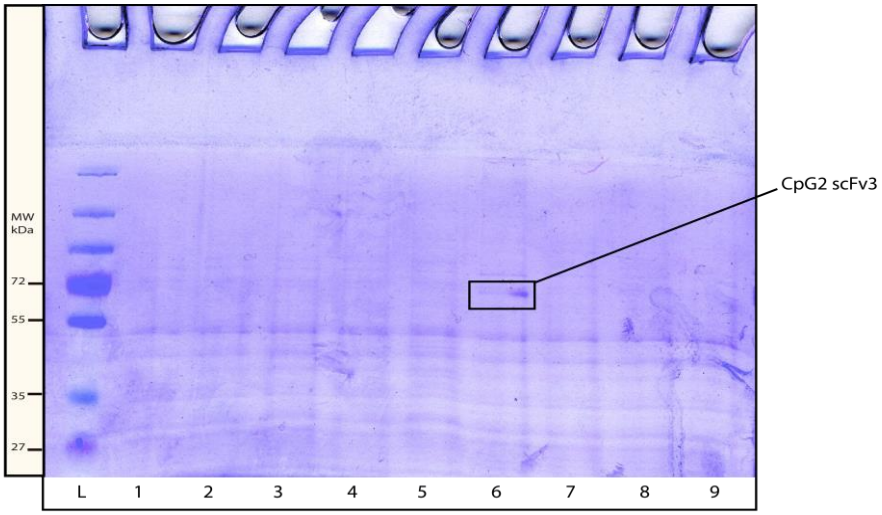

L: Ladder
Lane 1: uninduced scFv
Lane 2: inducecd scFv (day 3)
Lane 3: inducecd scFv (day 2)
Lane 4: inducecd scFv (day 1)
Lane 5: wash
Lane 6: purified fraction 3 CpG2-scFv3
Lane 7: purified fraction 2 CpG2-scFv3
Lane 8: purifiifed fraction 1 CpG2-scFv3
Lane 9: purifiifed fraction ifitm1 scFv

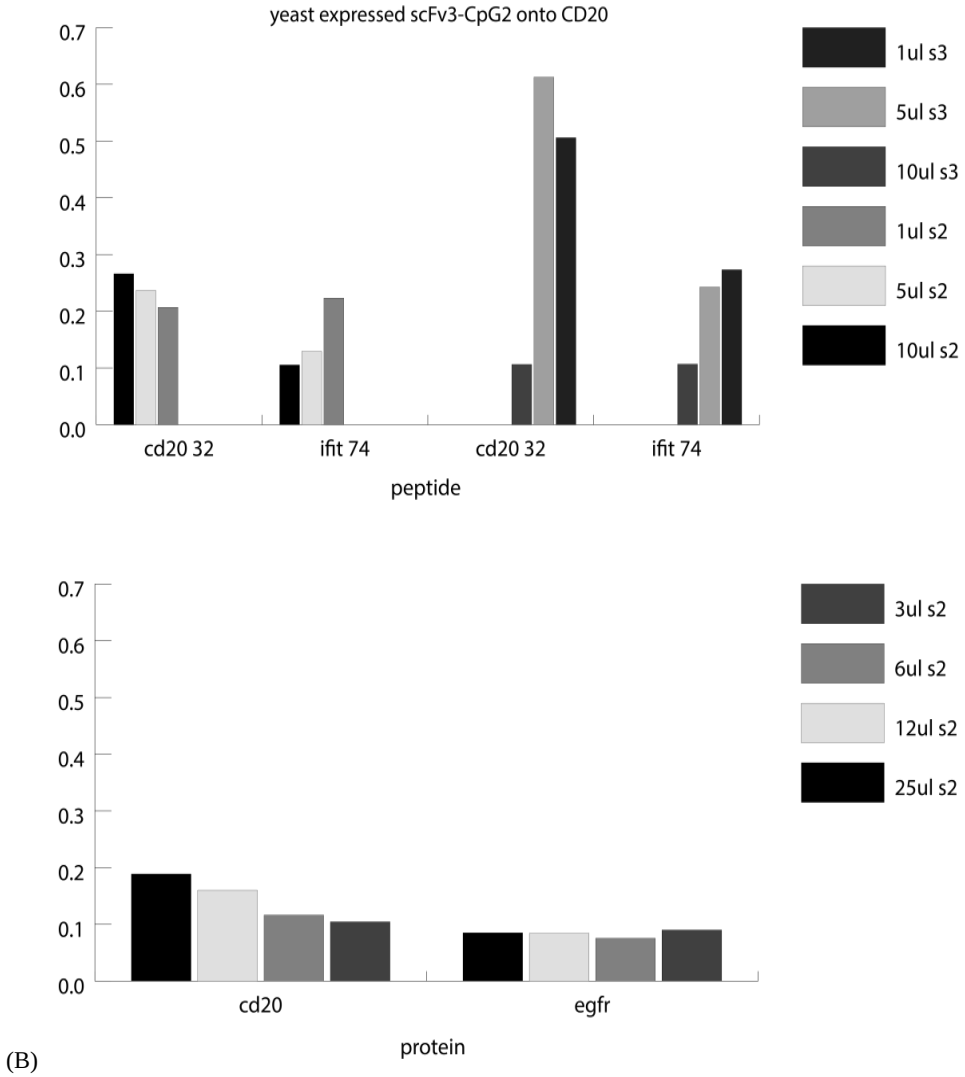

(B)

Figure 3.25: scFv3-CpG2 expression, purification in *Pichia pastoris* *(A) Coomassie staining 10µl of expressed, purified scFv3-CpG2 along with IFITM scFv-CpG2. Lane I: uninduced scFv, Lane 2,3,4 : induction day3, 2 and 1 respectively; lane 5: wash, lane 6, 7 and 8: purified fractions 3, 2 and 1 respectively and lane 9: IFITM scFv. (B) Binding activity of purified scFv3-CpG2 onto CD20 peptide (immunization peptide) as well as CD20 protein with IFITM peptide and EGFR as negative controls respectively. The overall data suggests that the scFv3- CpG2 construct was purified and ran at ~70 kDa and with activity higher onto the peptide as compared to the protein which correlates with our earlier data.*

3.3 Discussion

Experimental animals have long been a part of clinical research as a model for studying drug effects, signalling pathways etc. but choosing the right one turns out to be an important factor.. The emergence of companion therapeutics has also led to the development of the first approved anti- CD20 mAb for use in canine lymphoma [237] and additional mouse monoclonal antibodies are being generated to CD20 thus creating a competitive landscape [238]. Canine non-Hodgkin's lymphoma is the most common type of malignancies in dogs, accounting for 24% of all reported neoplasm and dogs are affected during their middle and later stages in life [188, 239]. CD20 was an interesting target choice due to the fact that it is expressed in premature and growing B cells whereas not present in terminally differentiated B cells (i.e. plasma cells) [240]. Here we develop an antibody against canine CD20 that is indeed capable of binding to its human counterpart. Having established that NCD1.2 can bind to both human CD20 and its canine counterpart we set out to investigate whether or not we could increase its affinity towards using different antibody scaffolds.

Using FACS, Jubala et al demonstrated that CD20 is present in abundance in most canine B cell lymphomas [198]. However it was also demonstrated that the predominant forms of CD20 were present in both normal and malignant B cells, whereas hypophosphorylated forms of CD20 were seen only in normal canine B cells [198]. Against this membranous target, Rituximab was the first monoclonal antibody approved, followed by few more with either modifications in CDR or binding to a different epitope. Not all the antibodies have gained clinical significance due to high toxicity or re-occurrence of tumor. Another reason as to why this target becomes an interesting choice is that although these cells are normal B cells, the stem cells that give rise to new B cells do not express CD20 [241]. This means that when the cells are targeted by any therapy, B cells that die after therapy can be replaced with CD20 negative cells (figure 3.26). Replacement of B cells is necessary as B cell lymphoma is clonal in nature and thus many of cells are present in such populations.

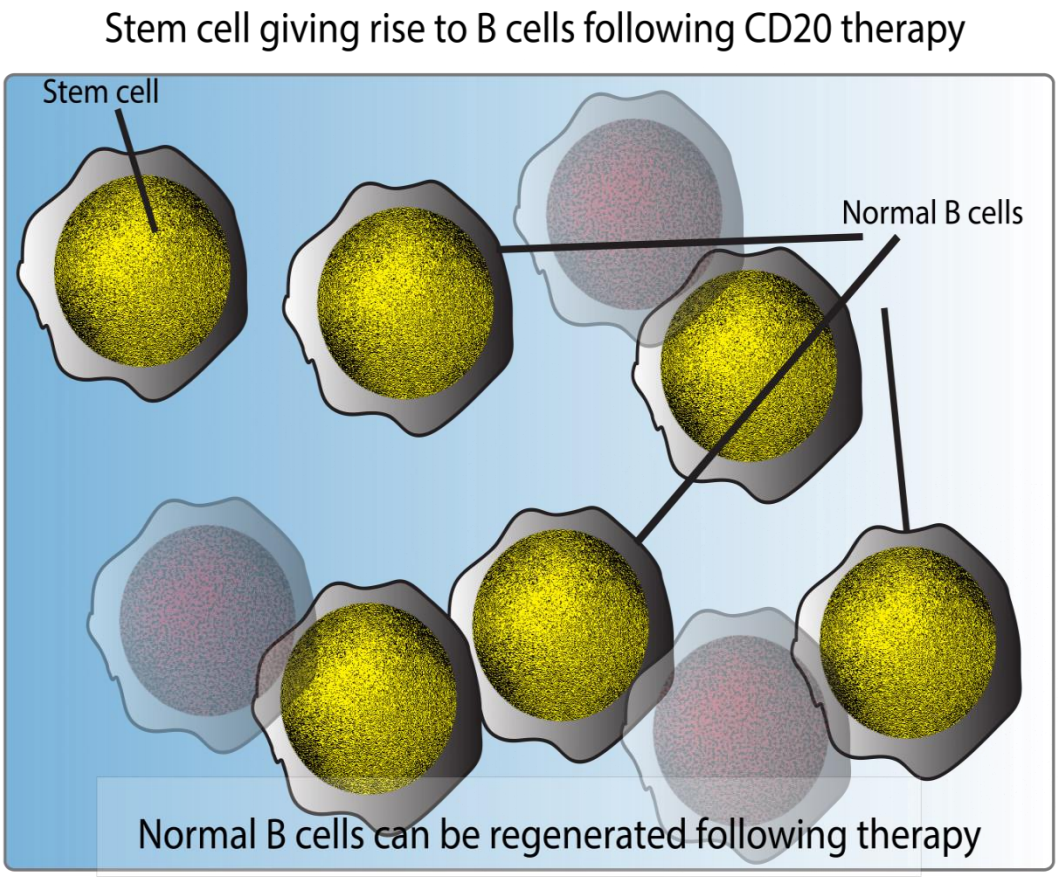

Figure 3.26: Regeneration of B cells: *Normal B cells are targeted by different B cell therapies but these B cells are replaced by stem cells following therapy and these B cells do not express CD20.*

Due to the fact that Rituximab does not bind to its canine counterpart, the need for antibodies that can bind to canine CD20 still remains from the veterinary oncology point of view. A mouse was immunized with canine CD20 peptide (NCDPANPSEKNSLSIQYCGS) and on testing the monoclonals, NCD1.2 was found to bind CD20 protein as well as CD20 in canine B cell lymphoma cells. Although full length monoclonal antibody can induce anti-tumor effects via several mechanisms, accessibility to the tumor still remains an issue in some cases due to the size of an antibody. For all such purposes, the aim of this project was to screen hybridomas obtained after mice immunizations with canine extracellular portion of CD20 onto canine CD20 as well as its human counterpart (figure 3.10) for future inter-species application, measuring the kD of the antibody NCD1.2; to show the

binding efficiency of the NCD1.2 onto CD20 protein in canine lymphoma cells, lymphoma tissues in different types of B cell lymphomas. Results from immunohistochemistry (figure 3.12) show that the antibody stains positive for B cell lymphoma whereas results obtained were negative when tested for T cell lymphoma ($CD20^-$). It is important to mention that T cell lymphomas are devoid of CD20 [242] and thus for this T cell lymphomas became an ideal model to demonstrate the specific binding efficiency of NCD1.2. The data obtained from FACS using NCD1.2 onto canine lymphoma cells correlates with our IH results and prove that NCD1.2 binds to only B cell lymphoma which express CD20. Interestingly, we noticed that NCD1.2 does not bind to CD20 positive cell line (Raji cells) via IF whereas the data from FACS and IH showed significant binding to the target tissue. The data suggests that performing IF on living cells using NCD1.2 might result in a better outcome which in turn can be useful for in-vivo immunotherapy. The only drawback we consider with this NCD1.2 is the dog anti-mouse response upon administration to dogs, for this reason we thought making a recombinant antibody or dogizing the antibody might be of great advantage. Ongoing work in this project is being carried out to caninize NCD1.2 antibody for administration in dog patients.

Further the aim of developing a scFv library to build single chain antibody scaffold by amplification of variable heavy and light chains and cloning into a phagemid vector was met. We used phagemid vector for cloning the scFv into due to the fact that they possess better transformation efficiencies and well assembled after the addition of helper phage M13KO7. Once the library was made from the dog spleen as well as from hybridoma cells, only 40% of the clones had the scFv in frame (i.e. light chain- linker- heavy chain). In order to overcome these frame shift mutations which have been on occasions shown to occur due to PCR error or purity level of the primers, another library was made from hybridoma cells using HPLC purified primers and the obtained library had 60% clones in frame. 5 positives were obtained after selection using the process of biopanning (figure 3.20) but the stability was always an issue with the secreted scFv as they did not even retain activity for 24 hours. In order to overcome the stability issues, more rounds of panning were carried out; different blocking buffers were used onto the immunotube, expressed in a different strain of *E.coli*. Finally, following a number of troubleshooting steps, the

ultimate solution came from the colonies from output sets which were grown in 20 mls, PEG precipitated and used as antibodies (phage linked scFv) onto ELISA. These resuspended phage scFv retained activity even after a month at 4^0C when they were tested on ELISA.

The outcome of this experiment resulted in two scFvs with one binding better than the other (named as scFv3 and 7, figure 3.22). The sequencing data of both scFv revealed that there was a difference in the CDR3 region of the light chain whereas the heavy chain sequence was exactly the same. It was surprising due to the fact that both scFv come from a single hybridoma so they should code for the same sequence. Also to prove this we performed RT-PCR to amplify the light chain using the primers designed from the sequence of the light chain of both scFv (figure 3.23 lower panel). Previously only on one occasion it has been shown where an anti-DNA hybridoma codes for two different kappa light chains [243]. On the basis of ELISA results, it was shown that scFv 3 exhibited greater binding capacity to CD20 peptide as well as CD20 protein. Not much has been published in the literature as to what percentage of variation in the light or heavy chain could be expected from a single hybridoma cell. Cloning the core scFv into an ADEPT bioconjugate system or can be secreted into active form from CHO cells was another of our research for increasing the affinity of antibody and to build a scaffold suitable to deliver in humans. As it is well known that scFvs are highly unstable and some manipulations, mutagenesis being one of them have proved to be effective in improving the stability of the antibody [244]. From future immunotherapeutic point of view, we thought it was better to clone the scFv into an ADEPT system as it can be delivered as an antibody enzyme conjugate followed by prodrug administration. We used CpG2 as an enzyme to be linked to scFv and expressed in bacteria to look for antibody secretion. As shown in figure 3.24D, not much antibody was secreted after lysis but following optimizations we managed to pull out scFv – CpG2.

Furthermore, scFv-CpG2 conjugate was cloned into *pICZalpha* and its expression was carried out in yeast. The expression was determined at various time points and 1ml of media was taken out each day until proceeded with purification. scFv- CpG2 conjugate was clearly visible on the gel and its activity was determined onto CD20

peptide via ELISA using IFITM1 as a control peptide. With such results obtained with antibody scaffolds we are currently in the process of developing full length recombinant antibody using scFv sequence. Thus we show the efficacy of monoclonal antibody NCD1.2 and using this hybridoma we also developed several antibody scaffolds for optimizing the binding affinity. Based on our results we conclude that NCD1.2 binds to canine CD20 as well as to its human counterpart and in future could be useful from both veterinary once it has been dogized and human therapeutics following humanization against B cell lymphoma.

..

CHAPTER 4: Developing monoclonal antibodies and assays to biophysically characterized α-synuclein

4.1. Introduction

4.1.1. Immunotherapy as tool for treatment of neurodegenerative diseases

The concept of immunotherapy in neurodegenerative disease evolved from Dale Schenk's work on Aβ vaccine targeting Alzheimer's disease (AD) [245] which further encouraged development of immunotherapy based approaches towards Parkinson's disease (PD). The self-assembly of proteins and peptides into amyloid fibrils is the characteristic of more than 20 human diseases, including Parkinson's disease (PD) and Alzheimer's disease (AD) [246]. In case of PD, insoluble amyloid fibrils are the final detrimental product formed from monomeric species, whereas oligomeric assemblies are transitory phase species. The best example of such a transitory protein from monomeric to amyloid fibrillar structure is α-synuclein that becomes aberrantly folded in Parkinson's disease, a disease which still does not have medical cure. From a therapeutic point of view, the need for antibody/drug conjugates still remains that can target α-synuclein at different stages before the amyloid fibrils are formed. It has been reported on few occasions now that although fibrillar structures are the main characteristics of α-synuclein related neurodegenerative disease the oligomeric form of α-synuclein remains the main toxic form [247-249]. Intriguingly, antibodies have been developed that selectively bind to the conformational epitope exposed in the target i.e. oligomeric species. Also recently it has been shown that the oligomerization of α-synuclein is not a pre-requisite for aggregation and the aggregates rather develop through sequential assembly of assembly of monomers [250]. One study has highlighted the fact that N-terminal acetylated form of α-synuclein does not form dimers, trimers, etc or higher

molecular weight proteins but can alter the conformational state of the monomeric form [251]. It is surprising that the antibodies have been developed against either oligomeric form of the protein or fibrillar species but it still remains a massive challenge to develop such biological tools that can target both species.

Both active and passive immunizations have proved to be effective in degrading accumulated α-synuclein and toxic aggregates via autophagy or macrophage activation [252]. In the recent past, antibodies targeting oligomeric species of protein have been isolated but their mechanisms of action are still not very well understood. However, on one occasion it has been demonstrated that anti-α-synuclein antibodies reduce α-synuclein pre formed fibrils which are known to induce inclusion bodies i.e. lewy bodies (LBs) and rescue synaptic or neuronal loss in primary neuronal cultures [253]. On another occasion it has been shown that multivalent IgM with 10 independent sites selectively bound to oligomers due to exposure of multiple epitopes in the oligomeric assemblies [254]. It is also important to identify the precise region on the protein which is embedded in fibrils and exposed in the case of oligomers. Consequently, following intense research in this field only one antibody has managed to enter clinical phase I trial (AFFITOPE) by Affiris. Although antibodies have been shown to bind oligomeric species, their ability to target proteins in other fibrillar structural forms still remains a concern. Here we isolated anti-α-synuclein antibodies with an aim to target α-synuclein at different stages of transitions from monomeric form to fibrillar form in PD and also develop peptide aptamers via peptide phage display screening to identify interacting proteins using next generation deep sequencing (Chapter 5).

4.1.2. Current available treatment

Although the etiology of PD is still not very well understood, indicators such as the formation of aggregates, fibrils and loss of dopaminergic neurons have become an ultimate target for PD therapies. All the therapies used in the case of PD treatment have a similar goal which is to induce dopamine with minimum side effects. The treatment for PD patients is divided into several categories. Multiple clinical trials have demonstrated that Levodopa provides the best symptomatic benefit for Parkinson's disease by increasing dopamine concentration in the brain and shows

less risk of developing hallucinations, impulse control disorders as compared to dopamine agonists [255]. Levodopa induces dopamine by aromatic amino acid decarboxylase and are usually administered with peripheral aromatic amino acid decarboxylase (AADC) inhibitor such as carbidopa or bensarazidenin order to reduce the side effects [256]. However, dopamine based treatment therapies have been effective in PD patients below 60 years of age and are known to cause less dopaminergic motor complications. From experimental therapeutic treatment, vaccine developed by Affiris has been under clinical trials and has shown promising results against α-synuclein. In most available clinical I and II trials, entacapone and tolcapone significantly reduced off time (mechanisms based on improved medication) and several adjuvants have been shown to reduce off time and avoid severe side effects [257]. There still remains a concern over the effect of Levodopa with or without agonists based on its mechanism of action on neurons. However, for advanced PD patients, Levodopa and different agonists may fail to provide satisfactory control, thus for such patients surgical therapies become an alternative option. Another drug that has shown promising results over the years is Phenserine; a derivative of physotigmine which has shown to improve cognition in various experimental paradigms in rodents as well as dog models.

4.1.3. Parkinson's disease

Parkinson's disease is the second most common disorder affecting all ethnic groups and both genders which is characterized by loss of pigmented neurons in substantia nigra of the midbrain [258]. The characteristic features of progressive neurological disorder were first described by James Parkinson in 1817. The epidemiological studies have indicated there are a number of factors which might increase the risk of developing Parkinson's disease which might be environmental factors, industrial chemicals, pesticides, herbicides, toxins [259]. Parkinson's disease occurs in both familial and sporadic forms; however sporadic form of PD is more common. Parkinson's disease is often described either as a movement disorder or as an idiopathic disorder, thus it is known to cause issues with movement, autonomic dysfunction and neuropsychiatric problems. Under normal circumstances, the proteins that are not folded properly are directed to the waste disposal mechanisms

such as ubiquitin-proteosomal degradation. However in cases where such proteins are not degraded tend to form thread like structures which further lead to formation large proteinaceous masses that might disrupt the normal functioning of the surrounding tissues [260-263].

Although extensive research has been carried out for years now, the definitive markers are still not very well described and thus the hallmark of the disease is marked by formation of inclusion eosinophilic lewy bodies in PD patients. However it is important to note that lewy bodies are not specific to PD but also found in AD as well as dementia with lewy body disease. Parkinson's disease is characterized by presence of abnormal intracytoplasmic aggregates of lewy bodies and lewy neurites in axons and neurons respectively. These inclusion bodies are present in specific regions of the brain and vary in shape, frequency and size [264]. The reported components of lewy bodies include synphilin-1, ubiquitin and various ubiquitin related enzymes [265, 266]. However the major component of LBs is an aggregated form of presynaptic protein i.e. α-synuclein and is relatively well characterized marker available for PD related patients. The classical brainstem lewy bodies are spherical, a dense core surrounded by a halo of 10 nm wide radiating fibrils. Moreover, abnormal accumulation of α-synuclein is not only observed in PD but also in dementia with lewy bodies, multiple system dystrophy and lewy body variant of AD [267, 268]. For this reason, such diseases are described as α-synucleinopathies [269, 270]. It has been shown that 3-4% neurons in the substantia nigra show presence of lewy bodies in PD patients, irrespective of disease severity [271].

4.1.4. Genes involved in PD

Some of the identified genes that underlie familial form of PD include two autosomal dominant genes: leucine rich repeat kinase, α-synuclein and three autosomal recessive genes: parkin, DJ1 (PARK 7) and PTEN induced putative kinase-1(PINK1) [272]. Also, there have been ubiquitin related and other genes reported in a few cases of PD but the importance of such genes is still not very well understood. With an ultimate aim of understanding the whole mechanism responsible for cause of Parkinson's disease, it is important to link environmental factors and disease associated genes which could result in the modification of associated molecular

pathways. Although the role of above mentioned genes has been identified in PD traits but it is still unknown whether genes apart from α-synuclein have any role in formation of lewy bodies. Parkin mutations have been found mainly in PD patients below the age of 30 and such mutations have led to the dysfunctioning and loss of dopaminergic neurons [273]. Parkin is a 465 amino acid protein and is known to be an E3 ubiquitin ligase which is well known for proteosomal degradation. In fact it has been shown that mutation in Parkin gene affects its ability to perform ubiquitination and also its ability to degrade the protein in proteasome [273]. DJ1 mutations have been associated with autosomal recessive PD [274] and it has been implicated in oxidative stress.

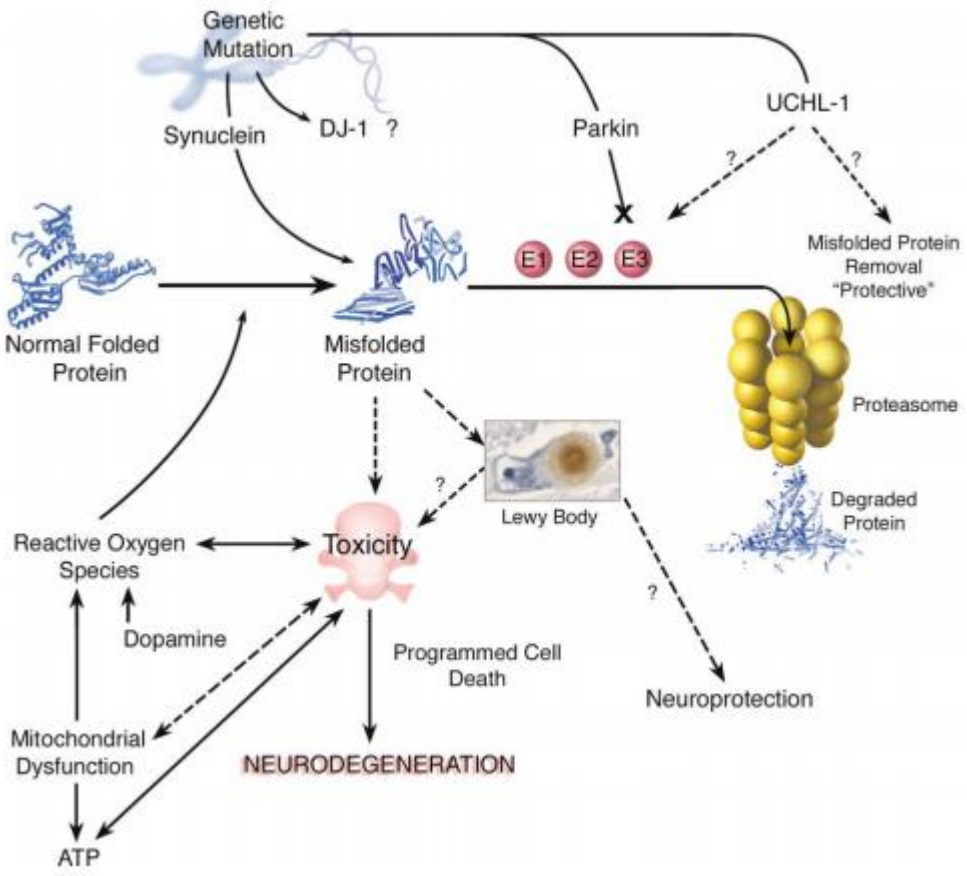

Figure 4.1: Mechanism of neurodegeneration: *Misfolding of the protein could be a result of either genetic mutation in either α-synuclein, DJ1, Parkin and UCHL-1 or due to toxins. Normally misfolded protein is degraded by mechanisms such as Ubiquitin proteosomal pathway. In PD patients, this misfolded protein leads to the formation of lewy bodies which avoids cell death due to mitochondrial dysfunction and ultimately the ability to produce dopamine is lost resulting in neurodegeneration [7].*

As explained by Dauer and Przedborski in 2003, accumulation of misfolded protein is the key event in PD neurodegeneration. Mutations can either lead to change in the confirmation of protein causing it to misfold or damage the ability of cellular machinery to destroy misfolded and degraded protein. In fact mutations in different parkin genes have been reported on various occasions but it is still not known whether these mutations are the ultimate cause of lewy body formation [275, 276].

4.1.5. Synuclein family

Synucleins are 15-20 kDa proteins which make up synuclein family consisting of three different types: α - synuclein, β - synuclein and γ - synuclein. All three types are well known to be expressed in the brain [267, 277] and share 55-60 % similarity among themselves. A-synuclein was first identified as a precursor protein for non-amyloid beta component of Alzheimer's disease [278]. Synucleins are characterized by a N-terminal amphipathic domain consisting of a consensus motif of KTKEGV which facilitates their lipid binding properties [279]. The highly conserved N terminal domain is a common feature among all synuclein members and is known to be characterized by two helical domains separated by KTKEGV [280]. Out of all the three members of synuclein family, only α-synuclein is known to be present in lewy bodies which means both β and γ-synuclein have not been found in formation of inclusion bodies [281, 282]. The most common missense mutation reported until recently has been A53T which was first reported in an Italian American family, another one being A30P first identified in a German family in α-synuclein gene and a third mutation at residue 46 has been reported recently (G46L) in Spanish kindred [283]. After years of vast genetic research on α-synuclein gene (SNCA), another breakthrough was made in analysing SNCA in PD patients where triplication of the gene was identified in a family called the Iowa kindred [284]. As it can be seen in the figure 4.2, α-synuclein is the longest gene among synuclein family (14 kDa in length) and it has been shown that all three types of synuclein are expressed in brain [277].

Figure 4.2: Sequence analysis of synuclein family: *The sequence comparison of α, β and γ synuclein. α-synuclein is 140 amino acids in length and is the largest among the synuclein family, whereas β and γ synuclein are 143 and 127 in length respectively. The difference in the amino acid sequence is marked by white colour and the sites for mutation have been indicated i.e. A30P and A53T.*

Following the sequence analysis of different types of synucleins, distribution of all three types has been well studied and characterized. As seen in figure 4.3, the relative expression of synucleins in several tissues as well as their distribution throughout brain parts has been shown by northern blot analysis [1-3]. No or little expression of β synuclein in brain tissues might be an indicative of relative amino acid sequence variation among the synuclein family [285].

Tissue expression of human synuclein genes

	Pancreas	Kidney	Skeletal muscle	Liver	Lung	Placenta	Brain	Heart
α syn	+	+	++	-	+	+	++++	++
β syn	-	-	+	-	-	-	++++	-
γ syn	+	+	++	+	-	-	++++	++

Expression of synucleins in brain

	Thalamus	Subthalamic nucleus	Substantia nigra	Hippocampus	Corpus collasum	Caudate nucleus	Amydgala
α syn	++	+	+++	+++	++	+++	+++
β syn	++	-	++	++	-	+	++
γ syn	+++	+++	+++	++	+	++	+++

Figure 4.3: Expression of synucleins among different tissues: *The relative expression of all three types of synuclein genes in pancreatic, kidney, skeletal muscle, liver, lung, placenta, brain and heart tissues (top panel). Expression of synucleins in thalamus, subthalamic nucleus, substantia nigra, hippocampus, corpus collasum, caudate nucleus and amydgala parts of brain. This expression pattern is based northern blot analysis [1-3].*

4.1.6. α-synuclein

A-synuclein is a 140 amino acid protein accounting for 1% of the total amount of cytoplasmic protein. It is comprised of a amphipathic N-terminal domain, a hydrophobic non-amyloid component (NAC) domain and an acidic C terminal domain [286]. The protein is thought to lack a proper secondary structure and exist as an unfolded coil in aqueous solution. It has been shown that α-synuclein is expressed in two different forms i.e. free and membrane bound (plasma membrane or vesicle bound) [287]. It is mainly expressed in neurons of neocortex, hippocampus, substantia nigra, cerebellum and is also expressed to a certain degree in red blood cells, kidney, liver, etc [288]. On the basis of membrane association, it is known to

have a role in synaptic neurotransmission and dopamine release [289]. The precise function of α-synuclein is still unknown but it is known to interact with other proteins for regulation of neurotransmission and also known to act as a chaperone involved in the process of folding of synaptic proteins [290, 291]. It has been shown previously that α-synuclein binds to a 90 kDa cytoplasmic protein synphilin-1 which might play an anchoring role for transporting α-synuclein to interact with intracellular proteins that are involved in vesicle transport and cytoskeletal function [292].

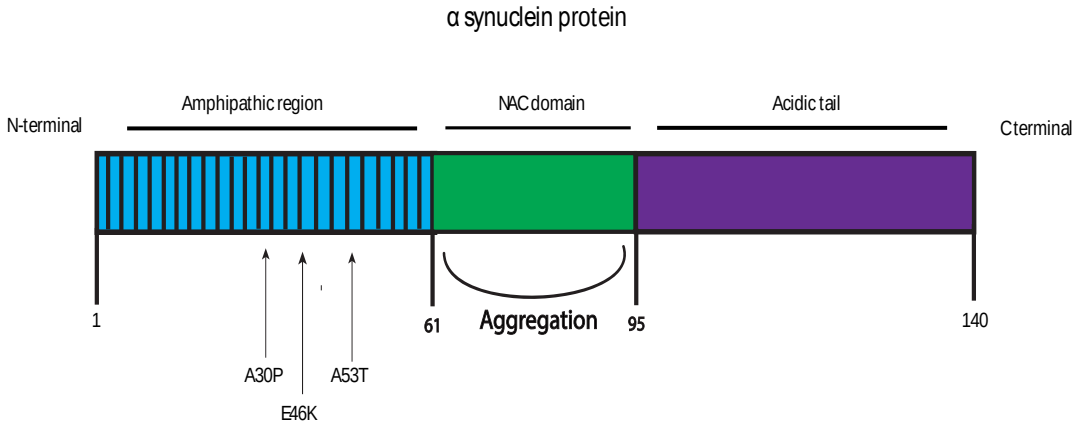

Figure 4.4: Detailed structure of α-synuclein: *α-synuclein contains N-terminus which is the amphipathic domain (sites for mutations), non-amyloid β component (NAC) domain and acidic tail towards the C-terminus.*

4.1.7. α-synuclein in Parkinson's disease

α-synuclein pathology in the brain stem in PD patients is thought to be responsible for motor symptoms limbic and neocortical areas of brain [293]. Detection of α-synuclein in enteric nervous system as a biomarker of PD in gastrointestinal (GI) tract has been suggested. Interestingly, detection of α-synuclein aggregates in colon biopsies have been seen much before PD diagnosis using other symptoms [294]. For the removal of misfolded and abnormal proteins, ubiquitination and autophagy lysosome are the most common pathways. In the ubiquitin-proteasome misfolded proteins are polyubiquitinated and guided through a series of enzymes to proteasome for degradation. Lysosomes maintain the activity of various enzymes, both of these pathways are known to be affected in PD as the immunoreactivity of both proteosomal and lysosomal degradation markers were found to be reduced compared

to age matched controls [295]. α-synuclein oligomers have been reported in PD patients possessing SNCA triplication [296], A30P [297] as well as in recently identified E57K [298] mutations. It has been established that recombinant α-synuclein under defined conditions can lead the formation of insoluble aggregates and possess similar morphological behaviour to the disease affected forms of α-synuclein [299-301].

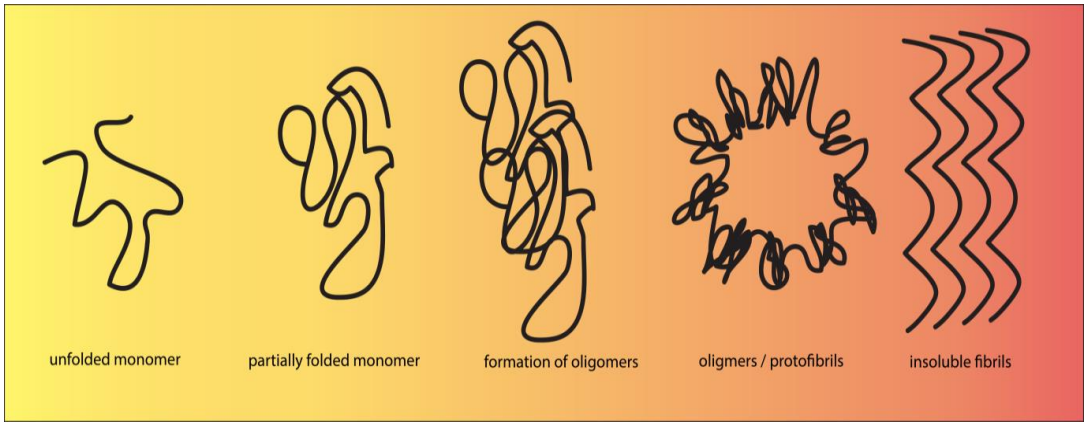

Figure 4.5: Structural changes in α-synuclein in PD: *Misfolding of α-synuclein which is natively unfolded in nature causes it to be partially folded initially. This intermediate form further leads to the formation of oligomers which comprise of both soluble and insoluble. Some oligomers lead form large clusters i.e. protofibrils and lastly these protofibrils form insoluble fibrillar structures.*

4.1.8. Controversial state of native α-synuclein

Several spectroscopic and structural studies such as NMR have been carried to determine the structural status of native α-synuclein. It has been shown that this unfolded protein is structurally disordered under physiological conditions [302, 303]. To support this fact, work carried out by Davidson et al proved that α-synuclein is highly disordered in solution; however striking conformational change was seen from disordered structure to α helical upon lipid binding. A number of proteins have been identified in lewy bodies and lewy neurites using light microscopy such as ubiquitin and neurofilaments [304-307]. On contrary to α-helical state, another study has shown that conformational state of α-synuclein changes from random coiled to β-pleated sheet [308, 309]. The structural changes occurring in α-synuclein leading to PD is shown in figure 4.5.

The role of α-synuclein in cell membrane dynamics suggests that when α-synuclein binds to the lipid membranes, it changes its conformation from disordered structure to α-helical secondary structure [280, 310]. This highlights the importance and role of lipid binding to α-synuclein in synaptic terminals which might be useful to study the dynamics of the protein in more details. It has been shown that the conformation of α-synuclein can be affected by various factors such as low pH, storage conditions and high temperature which can cause α-synuclein to be aggregated and fibrillated [311]. Several models have been created to show α-synuclein under certain defined conditions can lead to change in the structure of the protein [312] but fundamental question still remains as to what forces drive this mechanism of structural change. With extensive research on the morphology of α-synuclein, it has been well demonstrated that conformational change in the modulation of α-synuclein could be due to a variety of factors such as pH and temperature conditions in vitro, α-synuclein interacting with other proteins in brain models, etc. On previous occasions, there have been models that show protein aggregation in-vitro under certain conditions suggesting that the protein is amyloidogenic [313-315]. Few properties assigned to α-synuclein in native state are: (i) unfolded, disordered structure (demonstrated by CD), (ii) stable to heat denaturation, and (iii) aberrant SDS binding ability leading to unusual mobility onto SDS PAGE [302]. It still remains to be determined whether the unfolded disordered orientation of protein contributes directly or indirectly in the formation of lewy bodies.

4.1.9. AIM

Our experimental aim was to determine the precise native state and secondary structure of α-synuclein in different conditions by native gels and Circular dichroism respectively. Also, due to its aberrant nature we planned to develop monoclonal antibodies to look at the expression pattern of α-synuclein in neuroblastoma cells as well as in parts of brain and kidney. The final aim of this project was to measure co-localization of α-synuclein using co-transfection of α-synuclein constructs and PLA in α-synuclein expressing cells.

4.2. RESULTS

4.2.1. Expression and purification of WT α-synuclein

To begin with, α-synuclein was cloned in pT7-7 vector (by Vikram Narayan, Ball lab) and results were confirmed by restriction digestion and sequencing. Subsequently, the expression of recombinant α-synuclein was carried out in one litre culture volume. The filtered lysate was passed through the His trap column and each of the fractions following IMAC purification was collected, snap frozen in liquid nitrogen and stored at -80^{0}C. Each of the fractions obtained after elusion was stored and alternative fractions were run onto a SDS gel and Coomassie stained. As it can be seen in the figure 4.6 below, highly purified fractions could be seen from fraction 17 to fraction 38 with no contaminating bands and thus was pure enough to carry out further experiments for studying protein in detail and also to immunize mice for antibody development.

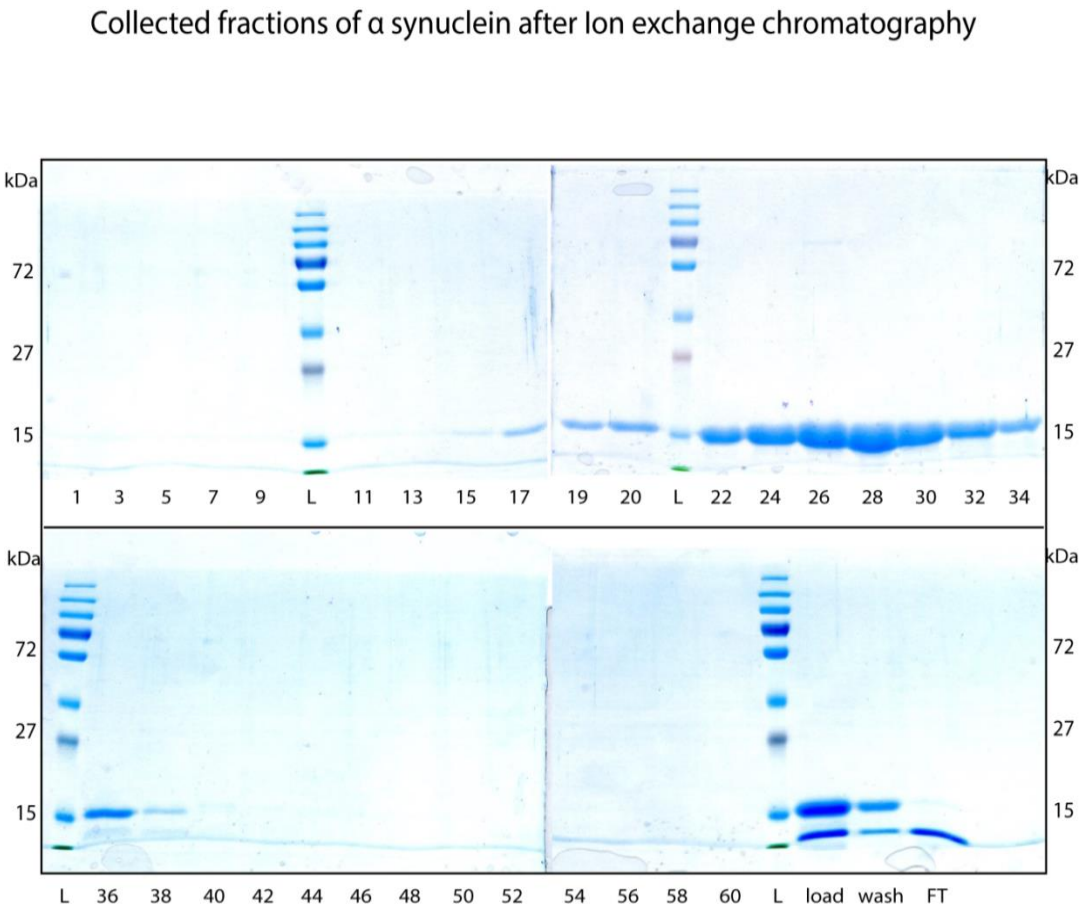

Figure 4.6: Purification of recombinant α-synuclein: *10 µl of each alternative purified fractions following IMAC purification of recombinant α-synuclein after expression in pT7-7 vector were ran on a 12% SDS gel. The top section of the figure show the purified fractions from 1-34 and the bottom half shows the fractions from 36- 60. The bottom right panel shows load before purification, wash and flowthrough. Purified recombinant α-synuclein runs around 15 kDa on a SDS gel.*

As seen above that the purified recombinant α-synuclein was found to run at a size of 14 kDa on a 12% SDS gel. Due to its controversial and still unknown precise native form, we decided to run the purified protein on 8% native gel which involved different buffer recipes including sample preparation (described in section 2.11). The prepared samples contained no SDS, were not boiled and also no DTT was added to the sample buffer as described in section 2.11. These conditions made sure that the protein was run in its absolute native state. The gel was pre-run at 4^0C for 1 hour at 50V; the samples along with BSA as a control were loaded onto the gel and ran at 50V, followed by 100V for 3-4 hours. The gel was then either stained using instant blue (Expedeon) or Coomassie stained for 1 hour followed by destaining.

To determine firstly the optimal running temperature of native gels we first ran native gels at 4^0C and RT. As seen in the figure 4.7 (top left panel), native gel needs to be run at 4^0C for bands to be clearly visible. Also we notice here that the protein runs at a size of 140 kDa clearly higher than its monomeric form. For this reason we thought of looking at the effect of different temperature conditions and thus we incubated purified protein overnight at different temperature conditions. The protein was incubated at 4^0C, RT and 37^0C for 24 hours and the samples were then run at 4^0C on a native gel. The gel image shows the protein still ran at 140 kDa so it is not temperature dependent (4.7 top right panel). Subsequently, we incubated protein overnight with different concentrations of SDS (0.05%, 0.1%, 0.5% and 1%) at 4^0C. The results show that the protein collapses down to different oligomeric forms of protein after addition of SDS (4.7 lower right panel). This mechanism indeed correlates with known interactions of α-synuclein with lipids [316].

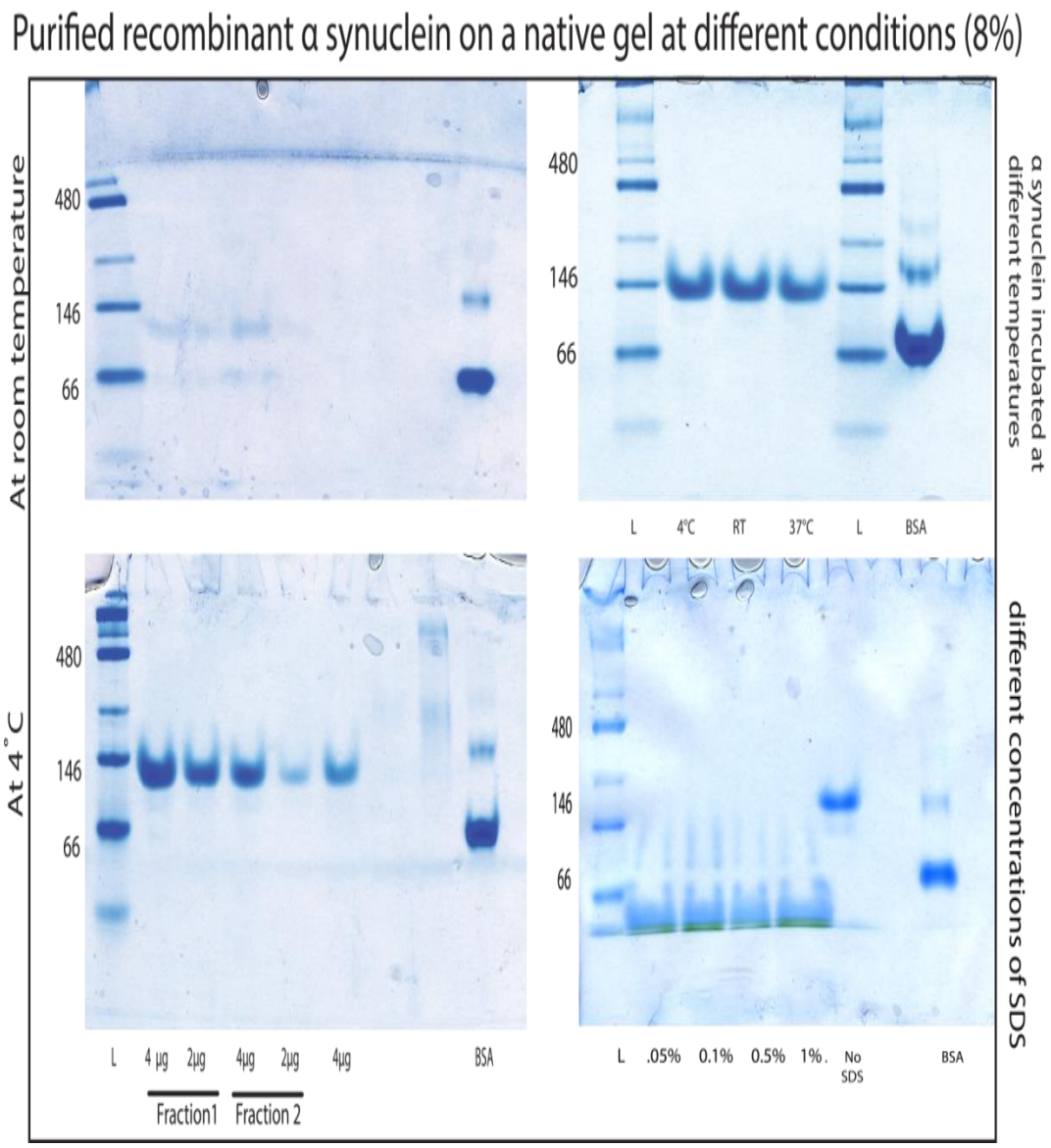

Figure 4.7: α-synuclein on a native gel: *The left panel of the figure shows running of different fractions of purified WT α-synuclein on a native gel at different temperatures i.e. RT (upper left panel) and 4^0C (lower left panel). As seen the protein does not run properly when ran at RT, whereas when the gel was run at 4^0C purified WT α-synuclein runs at ~140 kDa which suggests it might be an oligomer. The BSA was used as a control in all the experiments which runs at 66kDa. The top right panel shows α-synuclein where it was incubated overnight at different temperatures and the gel was ran at 4^0C where no disruption of oligomer was seen. The lower right panel shows collapsing of the purified WT α-synuclein oligomer after an overnight incubation with (0.05%, 0.1%, 1% SDS).*

Due to such intriguing results obtained with SDS, we thought of looking at the effect of different detergents such as Triton-X100, Tween 20 on the purified WT protein. Figure 4.7 lower right panel shows the effect of SDS when incubated with the purified WT α-synuclein overnight causes the collapse to a size of monomer. However when incubated for specific number of hours (0.5 - 6 hours) SDS did not fully collapse it down to a monomer (figure 4.8a). Similarly the right panel of figure 4.8a shows the extent to which α-synuclein collapses down from its oligomeric state after addition of different concentrations of SDS. Moreover, while analysing the effect of different detergents such Triton, Tween-20 and DMSO no change in the oligomeric state of this protein was seen (figure 4.8b). In the bottom right panel (figure 4.8b), we ran different amounts of purified α-synuclein with and without SDS as well as boiled sample with no SDS. One of the prepared samples was boiled in order to see the effect of high temperature on this protein. The overall results from native gels indicate that temperature does not affect α-synuclein in any case whereas SDS plays a role in degrading the oligomeric state of α-synuclein to a monomeric 14 kDa size protein. Moreover to rule out the possibility that freezing and thawing of recombinant α-synuclein could cause α-synuclein to aggregate on a native gel, we ran fractions after IMAC purification before and after freezing. Here we notice that freeze thaw does not affect the oligomeric state of the protein at all due to which the state of protein remains oligomeric.

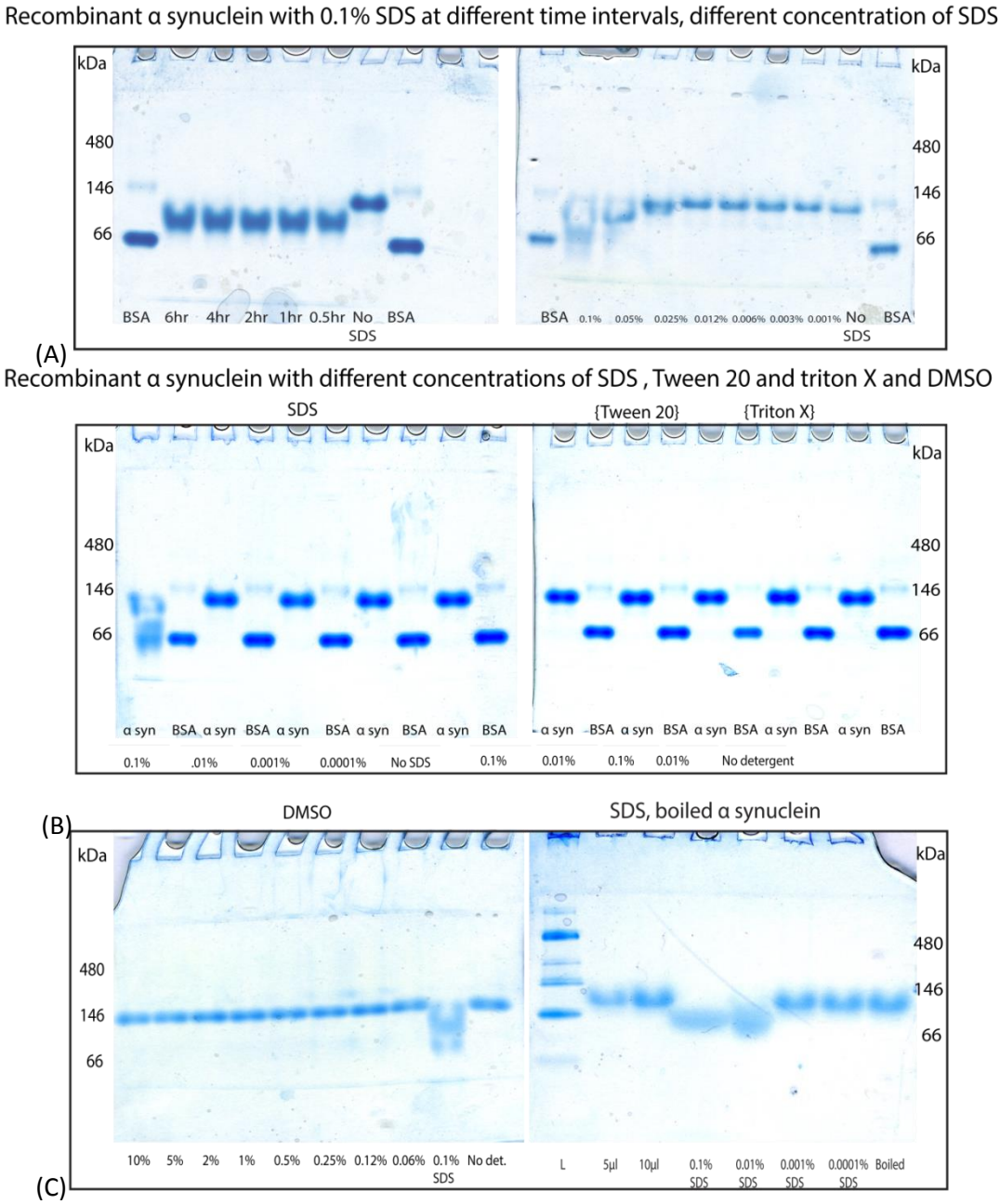

Figure 4.8: Recombinant purified α-synuclein in different conditions on native gel: (*A) Left panel shows the time scale for which purified α-synuclein incubated with 0.1% SDS (0.5, 1, 2, 4 and 6 hours) along with BSA as a control. The right panel shows purified α-synuclein after incubation with different concentrations of SDS (0.1%, 0.05%, 0.025%, 0.012%, 0.006%, 0.003% and 0.001%). (B) Effect of different amounts of SDS (left panel); Tween and Triton-X100 (right panel) with an incubation period of 30 minutes on recombinant α-synuclein with BSA as a control (C) Effect of different amounts of DMSO onto α-synuclein(left panel). The right panel shows 5, 10µl of purified protein, protein with 0.1%, 0.001%, 0.0001% SDS; alongside boiled purified protein was run on the native gel.*

4.2.2. Biophysical studies of α-synuclein

After determining the native state of α-synuclein using native gels, we performed some biophysical studies with purified α-synuclein. Biophysical studies with α-synuclein have indicated dynamic flexibility with respect to its dynamic structure [317]. Gel filtration studies from our group earlier have indicated that α-synuclein acts as an oligomer (tetramer). In order to look at the native state of the protein in more detail, we used a differential absorption technique called as Circular dichroism (CD) onto this controversial protein. We also measured CD onto a critical micelle concentration of SDS onto α-synuclein in solution.

Circular dichroism works on the basis of factors such as purity level of the protein should be quite high, presence of Tris-HCL as chloride ions in the buffer can give false signals. As seen in the above figure 4.6, although the purity of purified protein was quite high with no contaminating bands, the storage buffer for protein used was Tris that contains high amount of salts. As this condition is not suitable for carrying out CD, we performed a buffer exchange of the purified α-synuclein into phosphate buffer with no chloride ions. To start with, we performed buffer exchange into phosphate buffer at different pH to see which desalting/ buffer exchange is best suited for the protein. Using fraction 28 of the purified protein (figure 3.8), we performed buffer exchange using Zeba desalting columns (Thermo scientific) into 4 different pH (6.2, 6.8, 7.2 and 7.8) of phosphate buffer. The buffer recipe and different amount of ingredients needed for maintaining pH have been shown and described below:

Components of phosphate buffer for buffer exchange

Phosphate buffer: 1 M K_2HPO_4, 1 M KH_2PO_4

pH	1 M K_2HPO_4 vol.	1 M KH_2PO_4 vol.
6.2	19.2	80.8
6.8	49.7	50.3
7.2	71.7	28.3
7.8	90.8	9.2

100 ml of each pH solution was prepared and 1 ml of fraction was divided into 25 ml each halves to perform buffer exchange at four different pH. Desalting protocol was followed according to the manufacturer's protocol (Thermo scientific). 50 µl of phosphate buffer was added as stacking buffer at the final elusion step from the beads. After final elusion for each pH, 10 µl of the protein following buffer exchange with BSA as a control to measure protein concentration was run onto a 12% SDS gel (figure 4.9A). Subsequently, two of the buffer exchanged samples (pH 6.8 and pH 7.8) were run in three different amounts (5, 2 and 1 µl) along with titrations of BSA (4, 2 and 1 µg) onto a SDS gel in order to compare the amount of protein lost after buffer exchange (figure 4.9B).

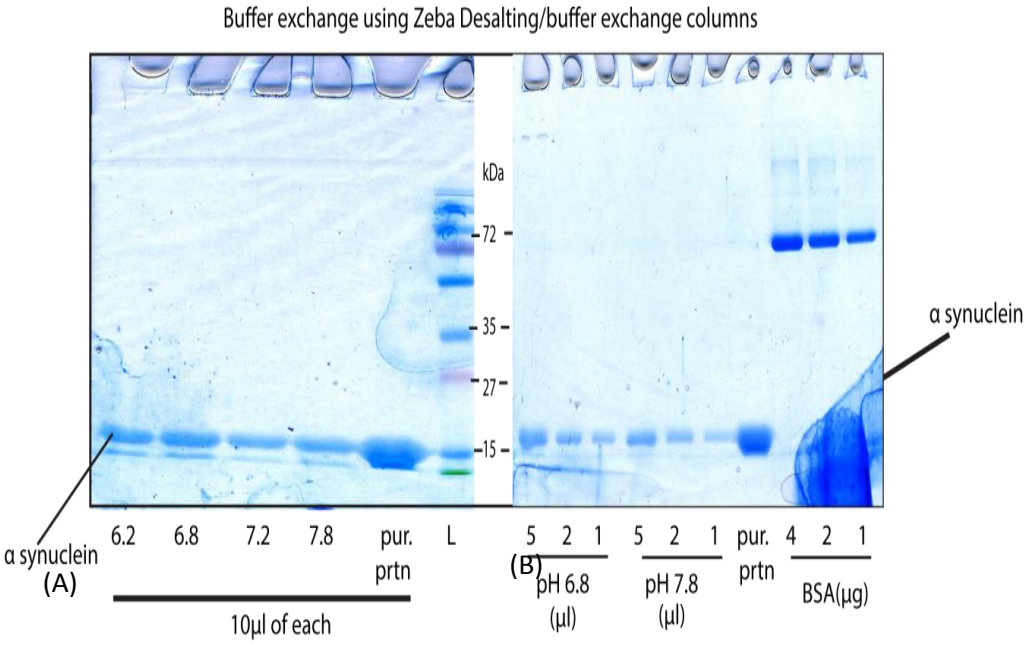

100µl was buffer exchanged for each pH Buffer exchange into phosphate buffer (0.5L of 1M K2HPO4 + 0.5L of 1M KH2PO4)
1. pH6.8
2. pH6.8
3. pH7.2
4. pH7.8
The pH was obtained by adding different amounts of above mentioned ingrediants (so no salts in the buffer).

Figure 4.9: Purified recombinant α-synuclein after buffer exchange: *(A) 10 µl of each sample obtained after buffer exchange into different pH phosphate buffer solutions (6.2, 6.8, 7.2 and 7.8) along with same amount of non-desalted purified protein. (B) 5, 2 and 1 µl of buffer exchanged pH 6.8 and pH 7.8 samples with 5 µl of non-desalted purified α-synuclein onto 12% SDS gel. 4, 2 and 1 µg of BSA run alongside as a control. A-synuclein runs at 14 kDa on a SDS gel.*

Further we decided to run these samples on a native gel to see the effect of different pH of phosphate buffer on the state of purified recombinant buffer exchanged α-synuclein. We notice here that this protein in phosphate buffer runs at the same size (~ 140 kDa) as it does when it was in Tris buffer even at different pH. Figure 4.10 shows 5 µl, 2 µl and 1 µl of buffer exchanged α-synuclein at pH 6.8 and pH 7.8 runs at ~140 kDa with BSA as a control onto a native gel. Buffer exchange using Zeba desalting columns offers rapid desalting and maximum protein recovery.

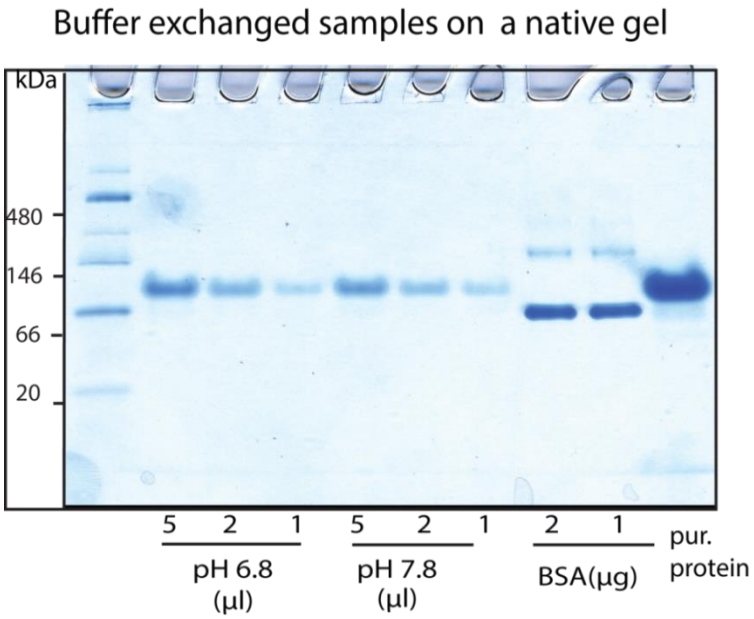

Figure 4.10: Buffer exchange of recombinant α-synuclein: *Buffer exchange of α-synuclein into 10 mM phosphate buffer, pH 6.8 and 7.8. 5, 2 and 1 µl of buffer exchanges sample along with 1 and 2 µg of BSA was run onto a 12% native gel.*

Determination of concentration of buffer exchanged α-synuclein

The precise concentration of the protein was determined by reading absorbance at 280 nm and using the molar extension coefficient of the protein. Phosphate buffer was used as a blank; the absorbance was read at 280 nm and was found to be 0.0006. Subsequently, absorbance of α-synuclein at 280 nm was found to be 0.6052. These values along with the molar extension coefficient were used to calculate the concentration of the protein on the basis of Beer-lambert law.

Absorbance = ε c l

ε = Epsilon, c= concentration of the protein in aqueous solution (mol dm^{-3}), and

l = length of solution the light passes through (cm)

$$0.6 = 5960 \times c \times 1$$

$$\downarrow$$

Concentration of α-synuclein = 1.006 mg/ml

4.2.3. Circular Dichroism

After determining the concentration of the protein, samples were then prepared for Circular Dichroism (CD). Three parameters were taken into consideration while using JASCO CD spectropolarimeter which are: path length, band width and data pitch. We performed CD onto three different samples: (i) recombinant purified α-synuclein in phosphate buffer (no SDS), (ii) α-synuclein incubated overnight with SDS (0.1%) and (iii) α-synuclein incubated with SDS for 10 minutes (0.1%). The samples were subjected to dilutions based on the CD spectral behaviour which is explained below:

The selected wavelength range for CD was chosen from 185 to 285 nm, path length of 1 nm, data pitch of 0.1 nm and band width changed depending upon quick or a slow scan. The instrument settings were adjusted by following the instructions from the manual (Jasco) and the instrument was turned on 30 minutes before use. CD cuvette was cleaned with ethanol before use; air dried and holds a capacity of not more than 400 µl of sample. Phosphate buffer (400 µl) was added to the clean cuvette and CD was measured using a quick scan with a band width of 100 nm/ minute. Following this, another three scans were performed on the same sample with a band width of 20 nm/minute. On running the phosphate buffer on its own on a CD spectrum machine, it was no change noted in the far UV CD spectrum in the whole range from 185-285 nm. This indicated that there was no chiral structure induced by phosphate buffer which in turn could lead to the formation of structures. This followed by CD spectral analysis of recombinant α-synuclein in phosphate buffer.

This protein (1.006 mg/ml) when passed through the CD gave a high signal to noise ratio and thus the protein was passed through CD analysis with several lower concentrations. The final diluted concentration of the protein was 0.027 mg/ml and three different scans were performed in the same wavelength range from 185-285 nm. As reported in literature, the UV spectrum shows a typical unfolded disordered structure at neutral pH at 25^0C. The spectrum has an intense minimum in the vicinity of 195 nm, with absence of any characteristic bands in the wavelength range of 220 to 260 nm (figure 4.11). This demonstrates the negative spectrum which in turn indicates the right circularly polarized component of plane polarized light absorbing more than the left component showing a negative CD spectrum. The data was interpreted using several algorithm based programs on spectrum software Dichroweb after calculating the mean residue weight using the formula shown below:

$$\text{Mean reside weight (Daltons)} = \frac{\text{Molecular weight of the protein}}{\text{(Number of amino acid residues} - 1)}$$

$$\text{MRW} = 104.02$$

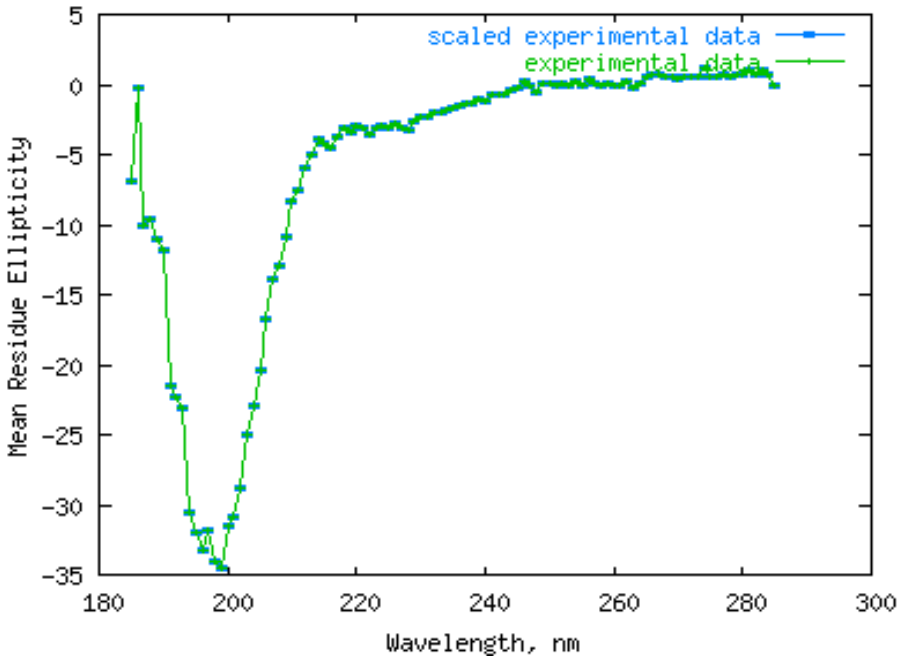

Figure 4.11: Circular Dichroism spectra of recombinant α-synuclein: *Sample was prepared in 10 mM phosphate buffer with a pH of 6.8 at a final concentration of 0.02 mg/ml. The molar ellipticity was measured at 25^0C in a 0.1 cm path length in a wavelength range from 185-285 nm.*

Subsequently, for performing CD onto SDS α-synuclein the cuvette was cleaned with SDS made in phosphate buffer and air-dried after cleaning with ethanol. The cuvette was then filled with phosphate buffer containing SDS (0.000125%) and passed through the CD spectrum to see if SDS was sticking to the cuvette and giving any false signals which could lead to formation of chiral structures. A quick scan followed by three timely scans was performed for the spectral analysis in a wavelength range from 185-285 nm. The curve from the SDS phosphate buffer indicates that the circular polarized radiation gives a similar spectrum as obtained using phosphate buffer with no SDS. This spectral analysis made sure that SDS by itself neither had any effect on phosphate buffer nor induced any chiral structure.

Following this, CD spectrum analysis of the second sample i.e. α-synuclein incubated overnight with SDS was carried after dilution to a final concentration of 0.06 mg/ml with a final SDS concentration of 0.00006%. A quick scan was performed at 100 nm/ min in vicinity absorption wavelength range of 185-285 nm, followed by three timely scans at a band width of 20 nm/min. As it can be seen in figure 4.12B, interestingly the protein in presence of SDS gives an unexpected spectrum with a negative peak at 205 nm and a strong positive peak at 190 nm. This suggests a transition of conformation of the protein from unfolded disordered structure to some folded form due to addition of SDS. This structural transition might provide an insight into association of α-synuclein with lipids in the synaptic area for future research. Due to such compelling results, we performed CD on α-synuclein – SDS (0.00006%) in phosphate buffer with an incubation period of 10 minutes. Here we notice that both negative and positive peaks are similar but stronger as compared to the samples with overnight SDS (figure 4.12b). From this data we can conclude that SDS has potential ability to change conformation to a significant amount of ordered secondary structure of the protein.

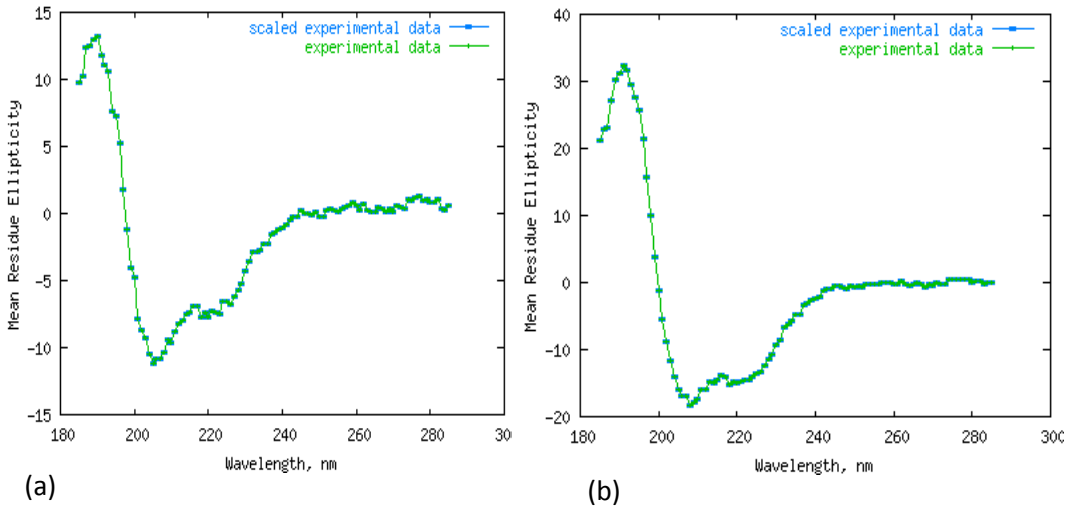

Figure 4.12: Circular Dichroism of recombinant α-*synuclein incubated with SDS:* *Samples were prepared in 10 mM phosphate buffer, pH 6.8 at a final concentration of 0.06mg/ml and SDS (0.00006%) was added overnight (a) and freshly added SDS (b) SDS incubated overnight. The ellipticity of the samples was measured at 25^{0}C in a 0.1 cm path length in a wavelength range of 185-285 nm.*

On the basis of data obtained from CD spectral experiment, we thought of determining the type of secondary structure that the protein attains after addition of SDS. In order to do this, we used DICHROWEB which provides a user friendly interface and platform for a range of popular secondary structures with use of several algorithms and reference database. Out of all the 5 available algorithm programs, we used CDSSTR and CONTIN which are known to produce most reliable data in comparison to other available database [318]. The files from the CD spectral software are uploaded onto the DICHROWEB website, input units selected as millidegrees and the wavelength range from 185-285 nm. The analysis program as mentioned was selected as CDSSTR with a reference set optimized for 190-240 nm and an output unit of mean residue ellipticity. For additional information, MRW (104), protein concentration (0.06 mg/ml) and path length (0.1 cm) was mentioned as well. Following submission of the data onto the software, it was found that 78% of the total structure was α-helical which was divided into two types based on the modified helical structures. From secondary structure analysis, helix structures per 100 residues were 5.426 with an average helix length per segment of 14.280. Infact CD studies have indicated earlier that α-synuclein natively occurs as a tetramer under

non denaturing conditions [319]. Thus on the basis of CD spectral analysis we show that α-synuclein from a natively unfolded disordered structure attains a highly α-helical secondary structural conformation with an addition of SDS. This data prompted us to develop different tools and assays that in turn could be useful to target as well as study this protein in more detail.

4.2.4. Development of antibodies binding to WT α-synuclein

With such intriguing data obtained from the native gels and biophysical studies of WT α-synuclein, targeting this aberrant protein by various biological tools could be indeed useful from PD treatment point of view. Thus developing tools that can target this protein in different states could turn out to be more than useful from various aspects such as understanding the behaviour of α-synuclein in its native state as well as its controversial monomeric or oligomeric expression in cells. To begin with, we developed monoclonal antibodies using standard hybridoma technology against this target (described in section 1.3). Two immunization cycles were carried out in Balb/c mice with α-synuclein to isolate antibody producing cycles (in Morbvian Biotech, Brno, Czech Republic). Following hybridoma technology, the monoclonals after growing were tested for activity onto recombinant protein. All the positive clones were grown and were tested for IgG via Dot blot using IgG specific secondary antibody. The supernatants from the clones that were found to bind WT protein in ELISA were tested for the IgG isotype via dot blot (figure 4.13). From the first batch of immunization, clone 2E12 was found to be positive for IgG (1.1) and similarly in case of 2nd batch; 2E4 was found to be positive for IgG (3.1). These antibodies have been referred to as 1.1 and 3.1 from here on for further experiments.

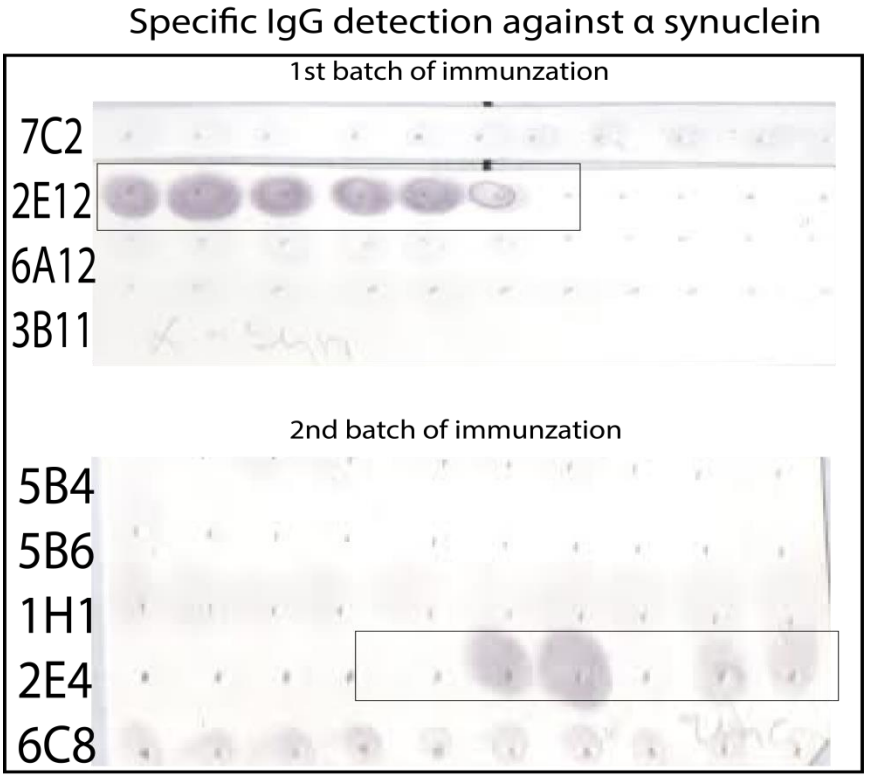

Figure 4.13: Dot blot of individual clones to test for IgG isotype. *2 batches of immunizations carried out, from the 1st batch of α-synuclein binding clones, clone 2E12 was found to be a positive clone for α-synuclein as well as IgG isotype. In the 2nd batch clone 2E4 was found to bind recombinant α-synuclein as well as positive for IgG isotype.*

4.2.5. Binding efficacy of monoclonal antibodies to α-synuclein

Following dot blot analysis, we tested all the monoclonal antibodies (18 mAbs including IgM and IgG) onto WT α-synuclein as well as a set of overlapping peptides designed from the WT protein. The ELISA plates were coated with 200 ng of protein overnight and antibody serum from positive clones was added in 5 different titrations (neat, 1:2, 1:5, 1:10 and 1:50) to the coated ELISA plates. As shown below, 4 out of 18 mAbs showed binding to the WT protein (figure 4.14a). Out of these positive ones, 2 of the antibodies were found to be IgM and other two were identified as IgG. After analysing the binding potential of these antibodies on the WT protein, we performed another ELISA where we titered α-synuclein against fixed amount (1:20) of these 4 positive antibody supernatants in duplicates (figure 4.14b). This was done in order to determine the precise amount of WT protein needed for different

antibodies to bind, commercial anti-α-synuclein antibody (BD Biosciences) was used as a positive control in all experiments.

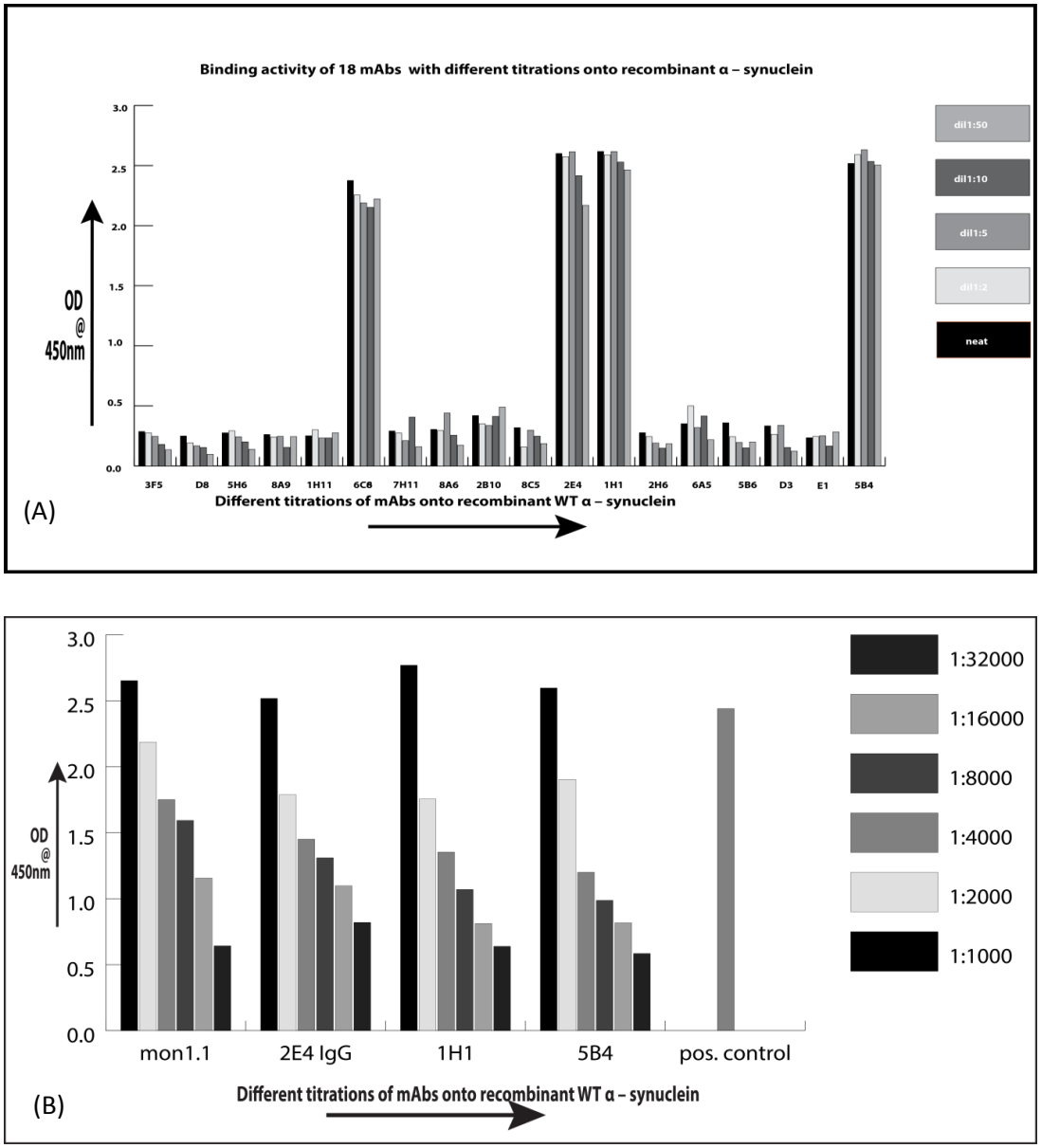

Figure 4.14: ELISA onto WT α-synuclein *(a) Activity of 18 monoclonal antibodies (including all IgGs and IgMs) obtained after mice immunizations with WT α-synuclein onto purified WT α-synuclein. 4 out of 18 bound to α-synuclein (mon.1.1, 2E4, 1H1 and 5B4). The titrations were performed for the monoclonals onto 500ng of the WT protein coated onto each well of the ELISA plate. (B) ELISA showing binding of the positive monoclonal antibodies onto titered WT α-synuclein. The protein was diluted from 500 ng to 25 ng and as it can be seen in the figure monoclonal antibodies bind to α-synuclein via ELISA developed using TMB.*

Following this, in collaboration with Borek Vojtesek's lab we purified the antibodies that showed significant binding activity, stored in sodium azide and also HRP conjugated the antibodies. Further on, we performed an ELISA onto α-synuclein to see if the HRP conjugated antibodies still retained the activity. A titration of the purified monoclonal antibodies was performed onto 200 ng of the WT protein coated onto each well of the ELISA plate. Monoclonal antibody 2.1 was added as a negative control onto the ELISA, whereas mAb 1.1 (IgG) and 3.1 (IgG) bound to protein along with IgM (4.1). The results indicate that all positive clones even after HRP conjugation retained the antibody binding capacity (figure 4.15).

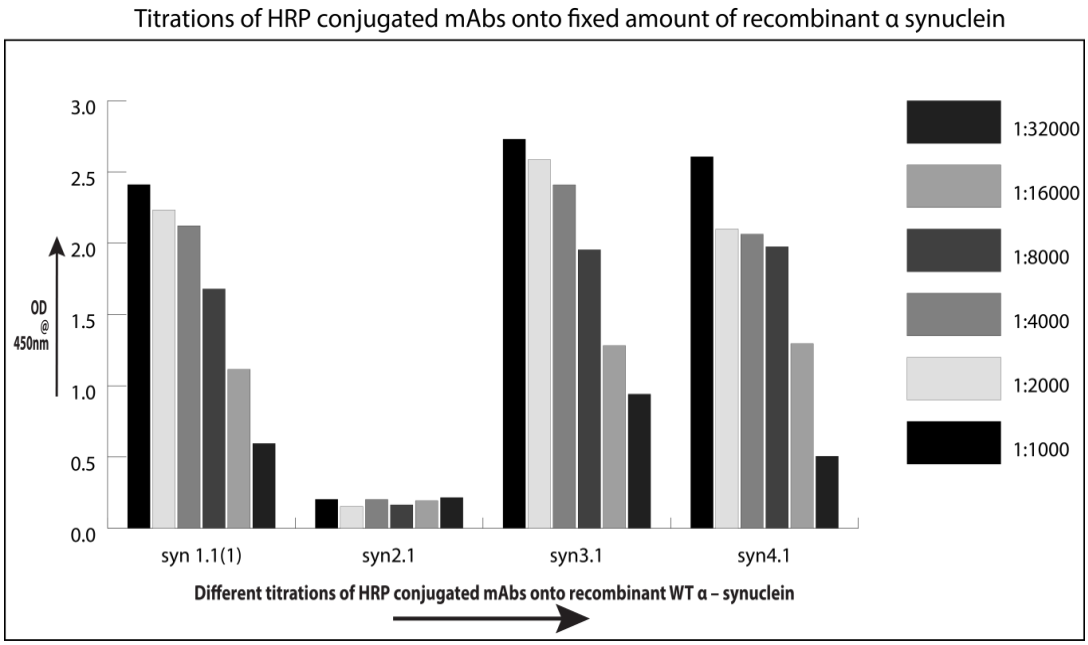

Figure 4.15: Activity of HRP conjugated antibodies onto purified WT α-synuclein: *ELISA demonstrating activity of 4 different monoclonal antibodies (1 mg/ml) after conjugation to HRP onto recombinant α-synuclein in several titrations (1:1000, 1:2000, 1:4000, 1:8000, 1:16000 and 1:32000).*

4.2.6. Epitope mapping of the anti-α-synuclein antibodies

After determining the activity of all the monoclonal antibodies onto WT α-synuclein, we performed epitope mapping in duplicates on the set of overlapping peptides derived from WT α-synuclein to determine the precise epitope of each antibody. Epitope mapping was performed for all 4 mAbs that bound to the wild type α-

synuclein. The 140 amino acid sequence was divided into 9 short overlapping peptides to determine specific residues that could be critical in antibody binding. The sequence of the designed overlapping peptides is mentioned below:

Peptides sequences	5 SGSGEQVTNVGGAVVTGVTAVAQK
1 SGSGMDVFMKGLSKAKEGVVAAAE	6 SGSGAVAQKTVEGAGSIAAAATGFV
2 SGSGVAAAEKTKQGVAEAAGKTKE	7 SGSGATGFVKKDQLGKNEEGAPQE
3 SGSGGKTKEGVLYVGSKTKEGVVH	8 SGSGGAPQEGILEDMPVDPDNEAY
4 SGSGEGVVHGVATVAEKTKECVTN	9 SGSGDNEAYEMPSEEGYQDYEPEA

The epitope mapping for all antibody clones was performed onto the set of peptides and all IgGs binding efficeincy to the peptides has been shown below (figure 4.16). The results indicate that out of 18 monoclonal antibodies only 2 bound to peptide. Out of the above 4 positive clones (shown in above ELISA results figure 4.14), only two show binding to the peptide i.e. 2E4 (3.1) which has been identified as an IgG and the other one being 6C8 which is identified as IgM. It is also important to mention that mAb 1.1 obtained from first batch of immunization binds to same epitope as IgM. Although IgM provides an advantage of targeting different epitopes exposed because of its multimeric nature, but it is not possible to recombinantly express which hampers its potential abilty to be a therapeutic tool. Interestingly, one of the commercial antibody (BD Biosciences) was also subjected to epitope analysis and has been found to bind to the same epitope as the 2E4 Ab (IgG). Also, another interesting fact to be noticed was that IgM (6C8) binds to a different epitope in comparison to 2E4 mAb and does not bind to endogenous α-synuclein in cells.

This differential binding of these mAbs might be due to the fact that epitope is either being masked in someway or presented differently to the antibody. The epitope of positive clones lie in region between residues 100 – 125 of the WT α-synuclein and

our finding indicate that peptides involved in binding are ^{92}ATGFVKKDQLGKNEEGAPQE^{112} and ^{106}GAPQEGILEDMPVDPDNEAY^{125}. The common residues present in both peptide sequences are 'GAPQE' which could be critical for both antibody binding to α-synuclein. These residues form the end of non-amyloid component (NAC) domain which is known to be important in protein aggregation along with acidic tail of α-synuclein.

Epitope mapping of positive clones (9 peptides)

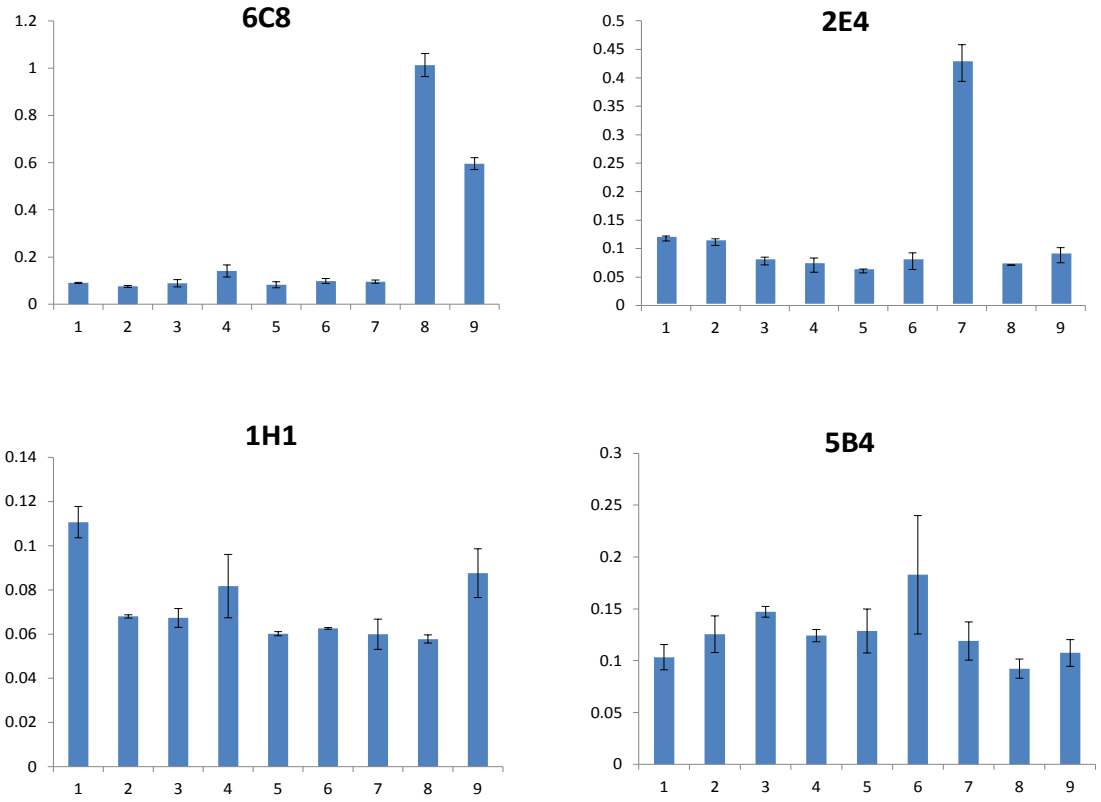

1. MDVFMGLSKAKEGVVAAAE
2. VAAAEKTKQGVAEAAGKTKE
3. GTKEGVLYVGSKTKEGVVH
4. EGVVHGVATVAEKTKECVTN
5. EQVTNVGGAVVTGVTAVAQK
6. AVAQKTVEGASIAAAATGFV
7. ATGFVKKDQLGKNEEGAPQE
8. GAPQEGILEDMPVDPDNEAY
9. DNEAYEMPSEEGYQDYEPEA

Figure 4.16: Epitope mapping of all the positive clones that bound to WT α-synuclein *Top half of the figure shows the epitope mapping of all the monoclonal antibodies that bound to recombinant α-synuclein. Epitope mapping was performed onto a panel of overlapping peptides designed from the protein sequence onto WT protein. The region that the epitope for all antibodies lie is outlined i.e. peptide 7, 8 and 9.*

4.2.7. Cell model to study α-synuclein oligomeric state

After determining the binding efficiency of the above mentioned monoclonal antibodies using ELISAs, we thought of looking at their efficacy for binding onto purified recombinant protein using western blot. A titration of recombinant WT α-synuclein was carried out and detected using IgGs at a dilution of 1:20 that were found to bind WT protein using ELISA (figure 4.17A). Also, alongside we decided to look at the expression of α-synuclein in dox repressible SHSY5Y cells (neuroblastoma cell line) to look at the precise size of α-synuclein within cells. As it can be seen in figure 4.17A, all three IgG antibodies could detect purified recombinant α-synuclein (14 kDa). Out of three antibodies, it is important to mention here that 5B4 did not bind to any of the derived α-synuclein peptides; however it binds to the protein using ELISA as well as immunoblotting.

The other part of the figure shows the detection of α-synuclein in SHSY5Y cells, where addition of doxycycline (dox) relatively supresses α-synuclein within these cells (figure 4.17B). Another interesting aspect of this figure is the band formation around 57 kDa which indicates formation of aggregates within the cells, whether it forms lewy bodies within these cells or not is still controversial. Also doxorubicin did not affect the oligomeric state of α-synuclein, however monomeric state was seen to be reduced. Infact it is these types of oligomers that are the more toxic form causing neurological disorder rather than aggregates (lewy bodies) [320].

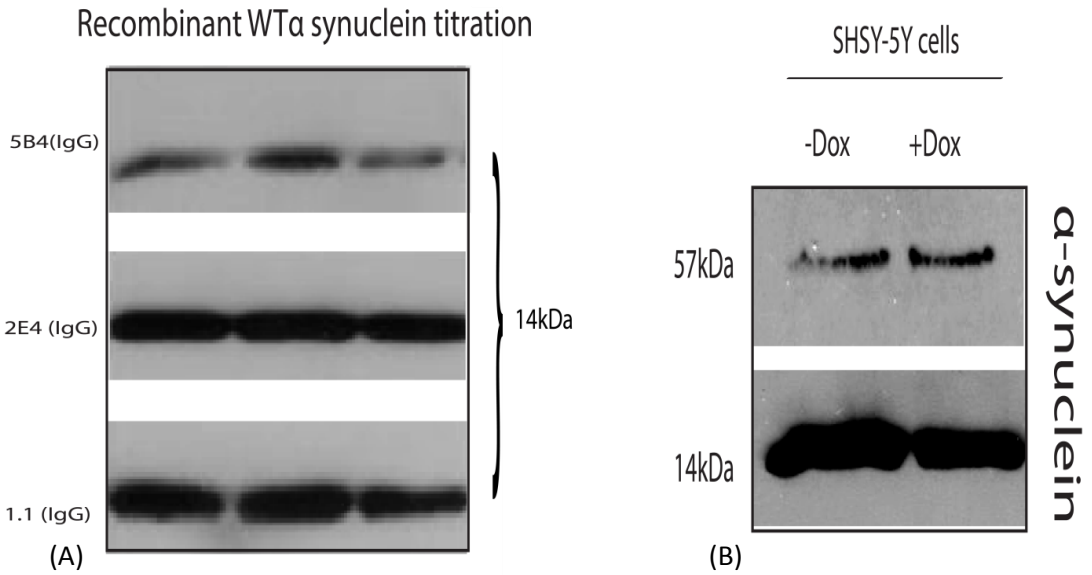

Figure 4.17: Binding efficiency of IgGs onto α-synuclein: *(a) Binding of all IgG (5B4, 2E4 and 1.1) at a dilution of 1:1000 onto a series of titrations of recombinant WT α-synuclein (50, 25 and 10 ng of protein) via immunoblot. (b) Expression level of α-synuclein in neuroblastoma cell line SHSY5Y (probed with commercial anti-α-synuclein antibody), effect of dox in repressing α-synuclein monomer.*

4.2.8. Different Lysis methods, Fixing of immunoblot

Further on, we used another neuroblastoma derived SHSY5Y cell line that expresses lower amount of α-synuclein. Following harvesting of cells from 10 cm petri dishes, we performed lysis in different lysis buffers (RIPA, Urea, Hypotonic and triton) to find out the most efficient way of extracting α-synuclein from SHSY5Y cells. Subsequently, Bradford assay was used to measure the total protein concentration and 50 µg of total protein was run onto a 12% SDS gel. All four differently lysed samples were loaded in duplicates onto a SDS gel and following the transfer of bands onto nitrocellulose membrane, membrane was divided into two halves.

Generally while visualizing immunoblot the monomeric band of α-synuclein is usually lost or retained in very low amount due to washes. For this reason we looked at the effect of paraformaldehyde (PFA) on SHSY5Y cells to see if monomeric band could be retained after fixing the blot. First half of the membrane was fixed with 0.4% paraformaldehyde to see if the monomeric form could be retained via a fixing

solution and other half was not fixed with PFA. As seen below in the figure 4.18, the oligomer as well as the monomer was retained after lysis except when hypotonic buffer was used where only monomer was retained. The figure indicates that hypotonic lysis is not efficient to extract the oligomeric α-synuclein from SHSY5Y cells. Also it can be seen that the intensity of the monomer band (~14 kDa) obtained after fixing with 0.4% PFA was quite high as compared to the one not fixed at all (figure 4.18). Fixing blots with PFA has previously been shown on various cell lines to fix the bands and intensify them [321]. This can indeed be useful for studies such as post-translational modifications, etc where the critical changes in monomeric state are to be visualized via immunoblot.

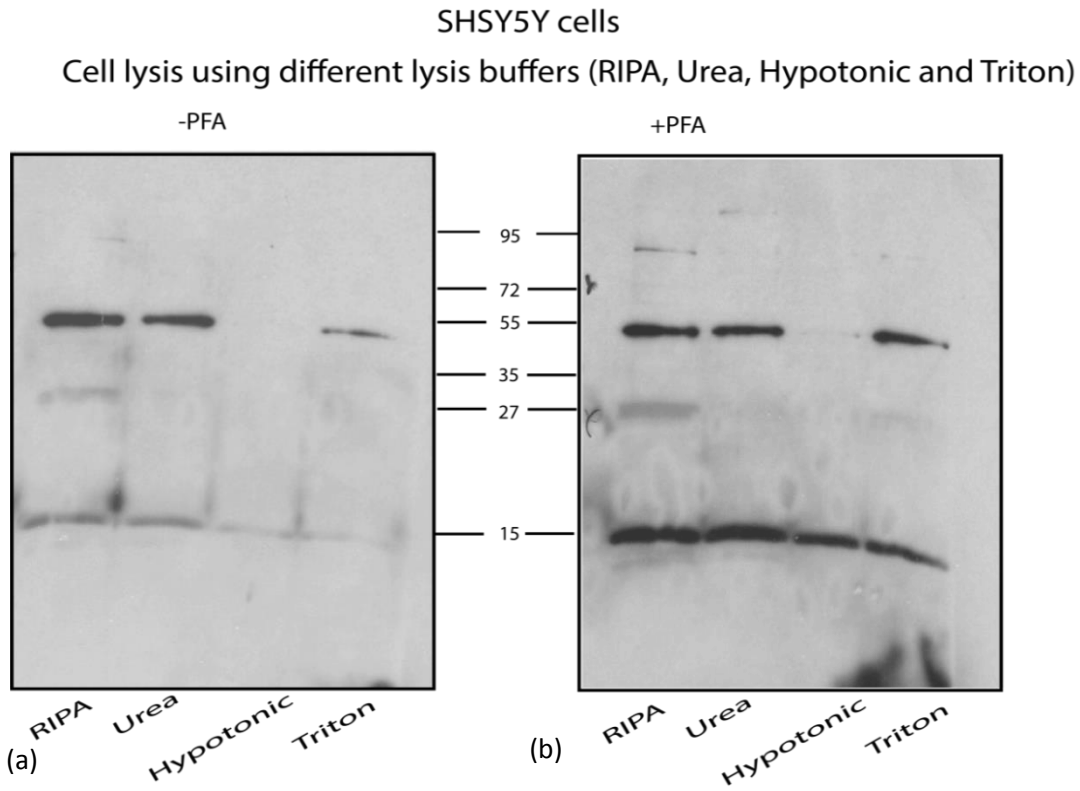

Figure 4.18: Different types of lysis of SHSY5Y cells: *Lysis of SHSY5Ycells was carried out in 3 different types of lysis buffers – RIPA (radioimmunoprecipitation assay lysis buffer), Urea, Hypotonic and Triton buffer. The cells were lysed for 30 minutes and then centrifuged at 13,000 rpm for 5 minutes. (a) Lysis of SHSY5Y cells and blots were straight away blocked without fixing, (b) Blots were fixed with PFA for 30 minutes before blocking with milk.*

4.2.9. Immunofluorescence

For further characterization and in-vitro application of anti-α-synuclein antibody, we performed immunofluorescence (IF) onto α-synuclein expressing SHSY5Y cells. The protocol followed for IF is described in section 2.2. Here we demonstrated binding potential of antibody 3.1 as well as 4.1 to α-synuclein using commercial antibody as the positive control and secondary antibody (AF488) only to demonstrate background staining. The antibodies were used at 1:500 and we notice here that antibody 3.1 binds in a similar way as commercial antibody (1:1000). Moreover, no staining pattern was seen with antibody 4.1 which gave background similar to the secondary antibody control. Based on our earlier finding, mAb 4.1 binds to recombinant α-synuclein but does not bind to α-synuclein within cells, this result correlates with our IF result as we do not see any staining pattern with 4.1. Antibody 1.1 did not detect α-synuclein within cells via IF (data not shown). However mAb1.1 bound to α-synuclein within cells when observed via immunoblotting which in turn might be useful along with 3.1 to study α-synuclein in brain tissue models. The staining pattern of monoclonal antibodies binding to α-synuclein in SHSY5Y cells is shown in figure 4.19. The figure distinctly shows DAPI cellular staining, green in form of antibody binding and merged images.

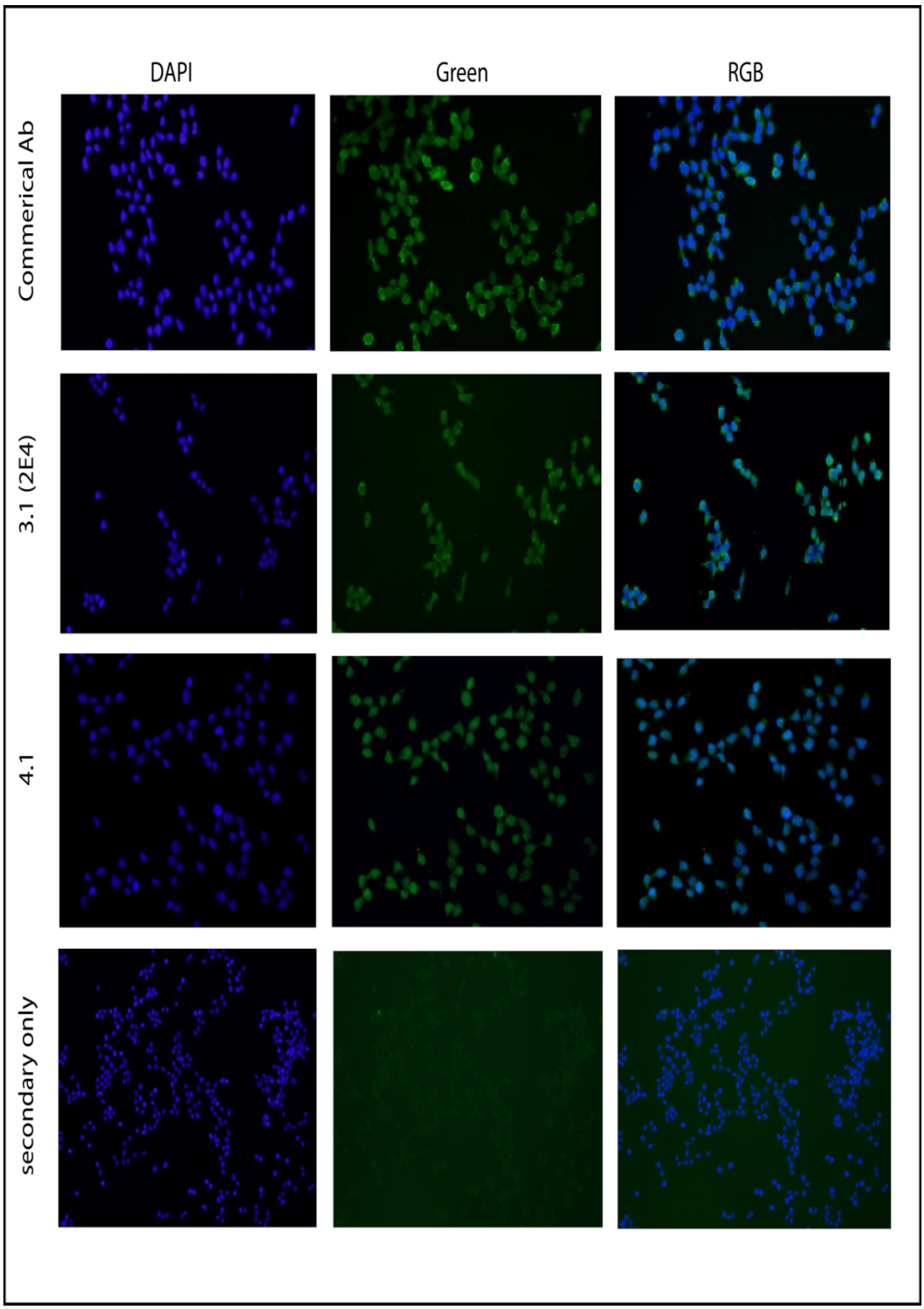

Figure 4.19: Characterization of mAb 3.1, 4.1 onto SHSY5Y cells via immunofluorescence: *Commercial anti-α-synuclein antibody (BD biosciences) and secondary antibody were used as positive and negative control respectively. The antibodies were used at a concentration of 1:500 commercial antibody used at a final concentration of 1:1000.*

4.2.10. Immunohistochemistry

With intriguing and contrasting results obtained with mAb 1.1 and for its further characterization along with antibody 3.1, we also looked at the presence of α-synuclein in different tissues by IHC on brain as well as kidney tissues. This was performed in collaboration with Rudolf Nenutil, Brno, Czech Republic onto deparaffinised tissues. We also performed tissue staining studies with antibody 2.1 but it was found to be negative in all the cases which correlates with our ELISA and immunoblotting results obtained above. It has been shown on previous occasions that α-synuclein is present in most of tissues including kidney, colon, lymph node and parts of brain. Immunohistochemistry was performed on formalin fixed tissues of normal brain and kidney samples. We stained a range of tissues such as Henle's loop, skin mast cells, brain gray matter and kidney glomerulus and proximal tubules. The purified antibodies were used at a concentration of 1:1000 in both cases.

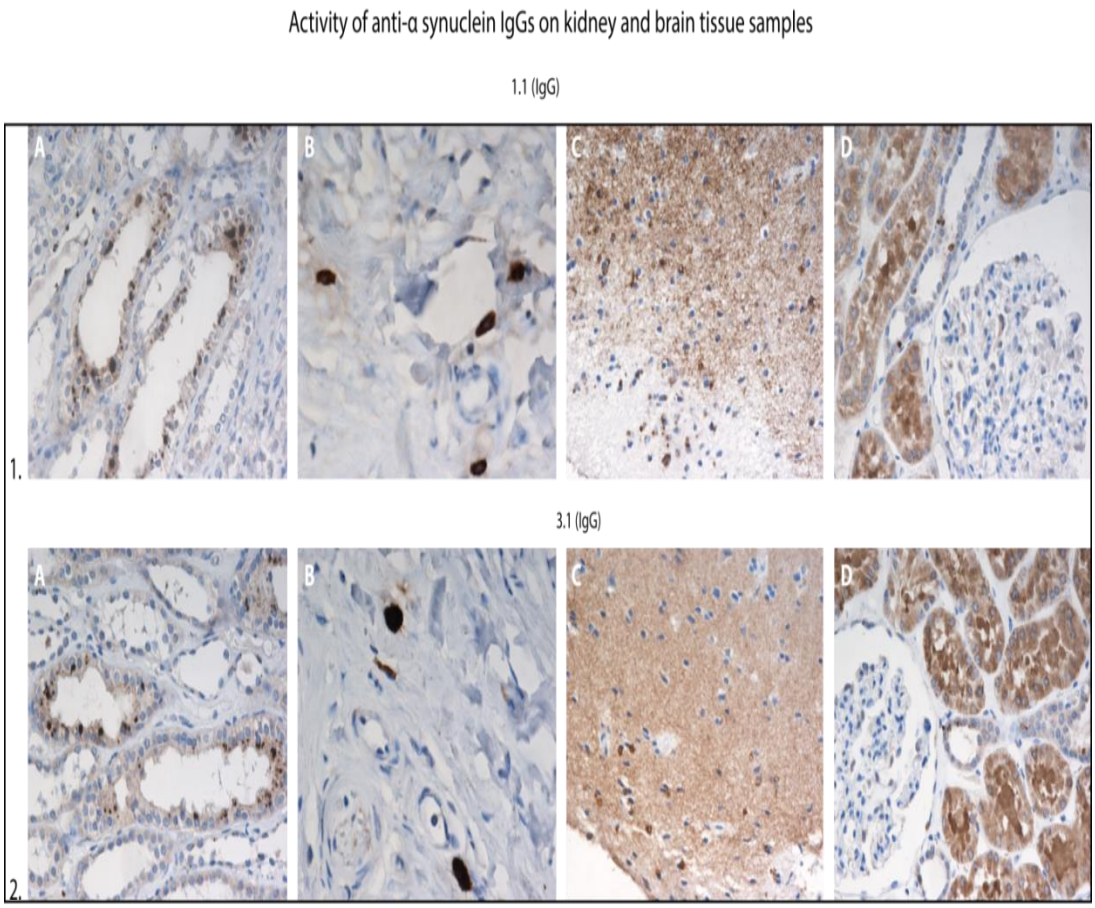

Figure 4.20: Immunohistochemistry on brain and kidney tissues: *Staining of parts of brain and kidney to look for presence of α-synuclein as well as to determine the binding potential of monoclonal antibodies. A. Henle's loop, B. skin mast cells, C. brain matter and D. kidney glomerulus and proximal tubules. The fixed tissues were stained with 3.1 and 1.1 and the presence of α-synuclein was demonstrated in all mentioned tissues.*

Figure 4.20 depicts that both antibodies 1.1 and 3.1 stain in a similar manner, we see no or very less staining in the kidney glomerulus, as well as skin melanocytes. However we notice that there is positive staining observed in the case of neurites and dendrites of brain gray matter in both cases, moreover there is a strong granular staining obtained in skin mast cells as well as in epithelium of Henle's loop. In some tissue samples we see a very weak binding which might fade away with higher antibody dilution and no staining was noticed while characterising Ab 4.1 onto tissue

samples. In the recent past intensive research has been carried out mainly in the brain region, reason being that the significant role that this protein plays in Parkinson's disease where its accumulation leads to the formation of lewy bodies. However within different tissues expression pattern of α-synuclein varies, for example it is expressed in cytosol of brain cells as well as in nucleus of mammalian neurons [288, 322]. These results prompted us to look at the expression pattern of α-synuclein in cells using several assays described below.

4.2.11. Co-localization of α-synuclein

4.2.11.1. Development of distinct constructs of α-synuclein

Even after tremendous amount of research on α-synuclein, the protein's state is still controversial as it is considered as a monomer by some research groups whereas it is thought to be aggregated by other research groups. Thus extensive research still needs to be performed to determine the precise state of this protein in neural cells. For such studies, we thought of cloning WT α-synuclein in two different mammalian expression vectors containing distinct tags and to look at their effects against each other as well as onto endogenous α-synuclein in SHSY5Y cells and HCT116+ cells. Primers were designed for PCR cloning of α-synuclein into pMCherry C1 (cherry tagged), pEGFP-C1 (GFP tagged) and confirmed via restriction digestion of colonies after transformation. The plasmids were then sequenced in order to make sure the plasmids contained α-synuclein with no mutation. Subsequently, after maxiprep of α-synuclein containing plasmids we transfected both constructs in different amounts in both above mentioned cell lines. After determining the concentration of total protein following lysis we ran 50 µg onto 12% SDS gel. From all the data obtained within these experiments, we show that the amount of Cherry tagged α-synuclein needed is more than three times to show the same expression level as GFP tagged α-synuclein. Moreover we detected transfected as well as endogenous α-synuclein in cells via commercial antibody (BD Biosciences) as well as antibody 3.1 (figure 4.21a, b).

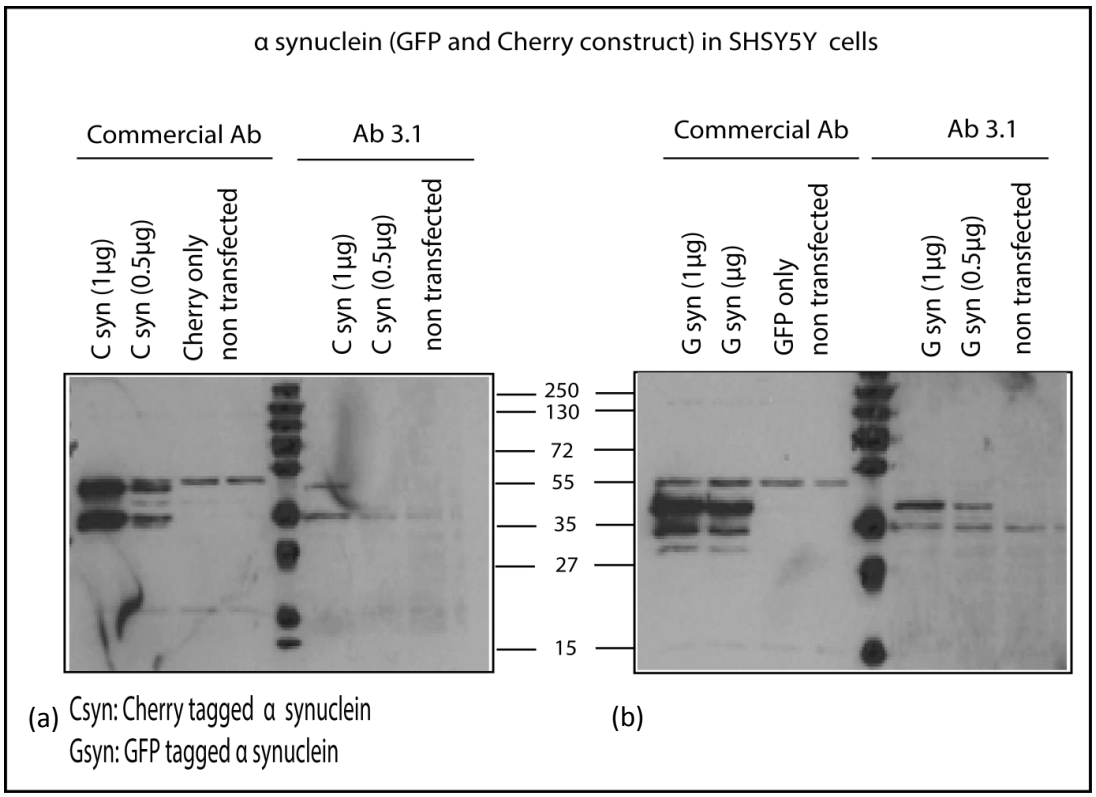

Figure 4.21: Transfection of α-synuclein constructs in SHSY5Y cells: *(a) Transfection of Cherry tagged α-synuclein (C syn) in two different amounts (1 and 0.5 µg), Cherry empty vector control and no transfection control. (b) Transfection of GFP tagged α-synuclein in two different amounts (1 and 0.5 µg), GFP empty vector control and no transfection control. Both blots were probed separately with commercial as well as mAb 3.1.*

As seen in figure 4.21, Cherry tagged α-synuclein was transfected in different amounts (0.5 and 1 µg) with empty cherry vector as a control and immunoblotted with anti-α-synuclein commercial (BD Biosciences) as well as 2E4 (IgG 3.1). The results indicate that when transfected constructs were immunoblotted using commercial antibody, a band around ~ 42 kDa was seen indicating the presence of cherry tagged α-synuclein along with a lower molecular weight product around ~ 35 kDa which might be indicative of cleaved cherry tag with α-synuclein within the cells. Similarly when this blot was probed using mAb 3.1, 1 µg of DNA was found sufficient for antibody to detect but 0.5 µg was found to be very low for detection. However, another observation in the figure 4.21a is the detection of endogenous α-synuclein in SHSY5Y cells by commercial antibody which always detects a band around 55 kDa. This is still not acknowledged by some research groups believing it could be due to sequence homology with another protein.

Although 3.1 has the same epitope as commercial antibody, it does not give a characteristic band around 55 kDa but it showed a band around 35 kDa which could be a different form of α-synuclein occurring within cells. Similarly immunoblotting with commercial antibody for GFP tagged α-synuclein transfection showed a band at 40 kDa and cleaved GFP tagged α-synuclein around 35 kDa and 30 kDa (figure 4.22b). Antibody 3.1 detects GFP tagged α-synuclein as well but not in any of the cases mAb 3.1 was able to detect cleaved products.

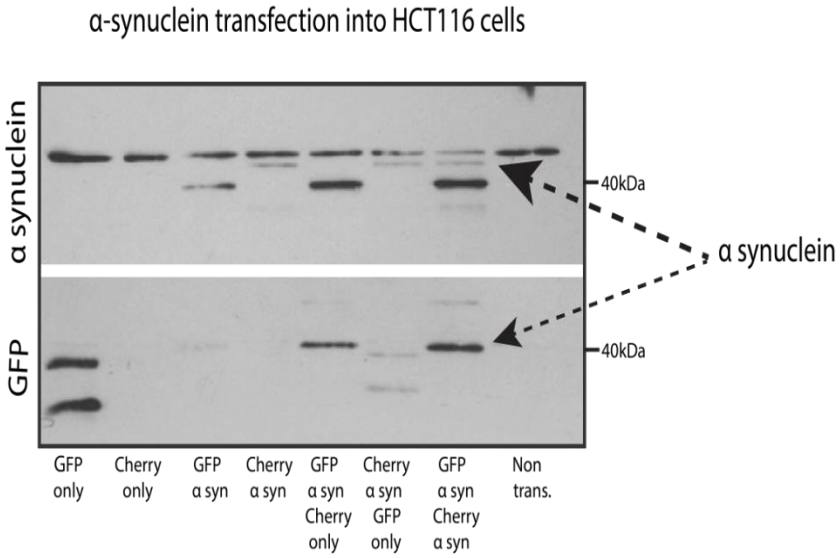

Figure 4.22: Transfection of α-synuclein constructs in HCT116+ cells: *Transfection of GFP and Cherry tagged α-synuclein into HCT116+ cells: GFP empty vector, Cherry empty vector, GFP tagged α-synuclein, Cherry tagged α-synuclein, GFP tagged α-synuclein with cherry empty vector, Cherry tagged α-synuclein with empty GFP vector, GFP tagged α-synuclein with Cherry tagged α-synuclein and non-transfected as a control. These samples were immunoblotted using commercial antibody and anti-GFP antibody.*

Further on, transfection of both constructs was performed in HCT116+ cells. The transfected samples included empty vectors, each construct along with empty vectors and both Cherry as well as GFP tagged α-synuclein. The transfected samples were immunoblotted for α-synuclein (commercial Ab) as well as for GFP. Based on this result, it appears as if either GFP tagged α-synuclein is being stabilized by cherry tag or more cleaved products are formed due to transfection of both α-synuclein constructs. For deeper understanding of α-synuclein interaction, we also used these constructs for Fluorescence resonance energy transfer –fluorescence lifetime imaging

microscopy (FRET-FLIM). However we did not see a significant difference in the radioactive decay half-life of Cherry α-synuclein with respect to GFP tagged α-synuclein. Based on our results we think that this might again be due to lower intensity of Cherry tagged α-synuclein. This model with significant optimizations in transfectable amount could be further useful to demonstrate oligomerization of α-synuclein in cells.

4.2.11.2. Proximity Ligation Assay (PLA)

Another well characterized technique for visualization and quantification of protein – protein interaction that has gained significant importance in the recent years is proximity ligation assay (PLA). To further prove co-localization of α-synuclein we used PLA technique to visualize its interaction pattern. This Duolink assay uses two primary antibodies selected from two different species such as a mouse and a rabbit antibody. The secondary antibodies contain a unique oligonucleotide sequence attached to them. When the proteins are in close proximity to each other, oligonucleotides are ligated together by a ligase to form a circular loop template. This template is then subsequently amplified by polymerase and the detection signal is obtained through complementary labelled probes. This amplification reaction is visible in the form of distinct spots using a fluorescent microscope. Due to the robustness of this technique and controversial state of α-synuclein, we thought of studying interaction of α-synuclein with itself i.e. to see if it forms oligomers within SHSY5Y cells. We employ PLA technique to study oligomerization in two different sets of SHSY5Y cells i.e. lower and higher expression of α-synuclein. Here we modify the standard protocol (Veronika Brychtova from Borek Vojtesek laboratory, Brno, Czech Republic) and prepare anti-α-synuclein Ab (3.1) directly linked to a (-) probe and similarly anti-α-synuclein Ab linked to a (+) probe. Due to direct linkage of probes to primary antibody, secondary antibodies were not required in the experiment.

Firstly mAb 3.1 was buffer exchanged using Zeba column into PBS to remove sodium azide that might interfere in conjugation process. The antibody was concentrated down and the concentration was measured on Nanodrop. Succinimidyl

6-hydrazinonicotinate acetone hydrazone (SANH) solution was prepared and stored in the dark just before use. SANH is a heterobifunctional protective linker used to introduce hydrazinonicotinimide functional groups into proteins including antibody and has been used extensively for labelling of biomolecules [323]. The antibody was conjugated to SANH (1:25) with gentle shaking in dark for 2 hours at room temperature. Following antibody conjugation, mixture was buffer exchanged once again into 1X conjugation buffer on a ZEBA column to remove any unconjugated product. To prepare oligo linked antibody, aldehyde modified DNA (oligonucleotide) was mixed with SANH activated antibody in 1X conjugation buffer in a ratio of 3:1 (oligo: SANH linked antibody). To assist the conjugation reaction, 10 mM aniline was added as a catalyst and finally incubated for 2 hours 30 minutes at RT in dark. Using Zeba columns oligo-SANH linked antibody was buffer exchanged into PBS to remove any unconjugated products. The final concentration of the both probes linked to antibody was determined using Nanodrop.

Further on, using these antibody linked to probes we performed PLA onto SHSY5Y cells along with controls. After fixing and permeabilising the cells, the coverslips were blocked using 3 % BSA for 45 minutes. For setting up the controls for this experiment, mAb 3.1 linked to – probe, mAb 3.1 linked to + probe and no antibody i.e. only BSA. Subsequently, mAb linked to – probe was added along with mAb linked to + probe onto the coverslip. The dilutions maintained throughout for antibody linked probe was 1:250 in each case. Figure 4.23 shows PLA onto SHSY5Y cells that express higher amount of α-synuclein (Dox repressible). Here upon visualizing PLA results under fluorescent microscope we notice that in controls containing either – probe or + probe only few spots were seen which corresponded to background staining count. However upon addition of both probes i.e. antibody linked to – probe as well as + probe, we see that the amount of spots obtained in this case were significantly higher as compared to the individual probe controls as well BSA control (figure 4.23).

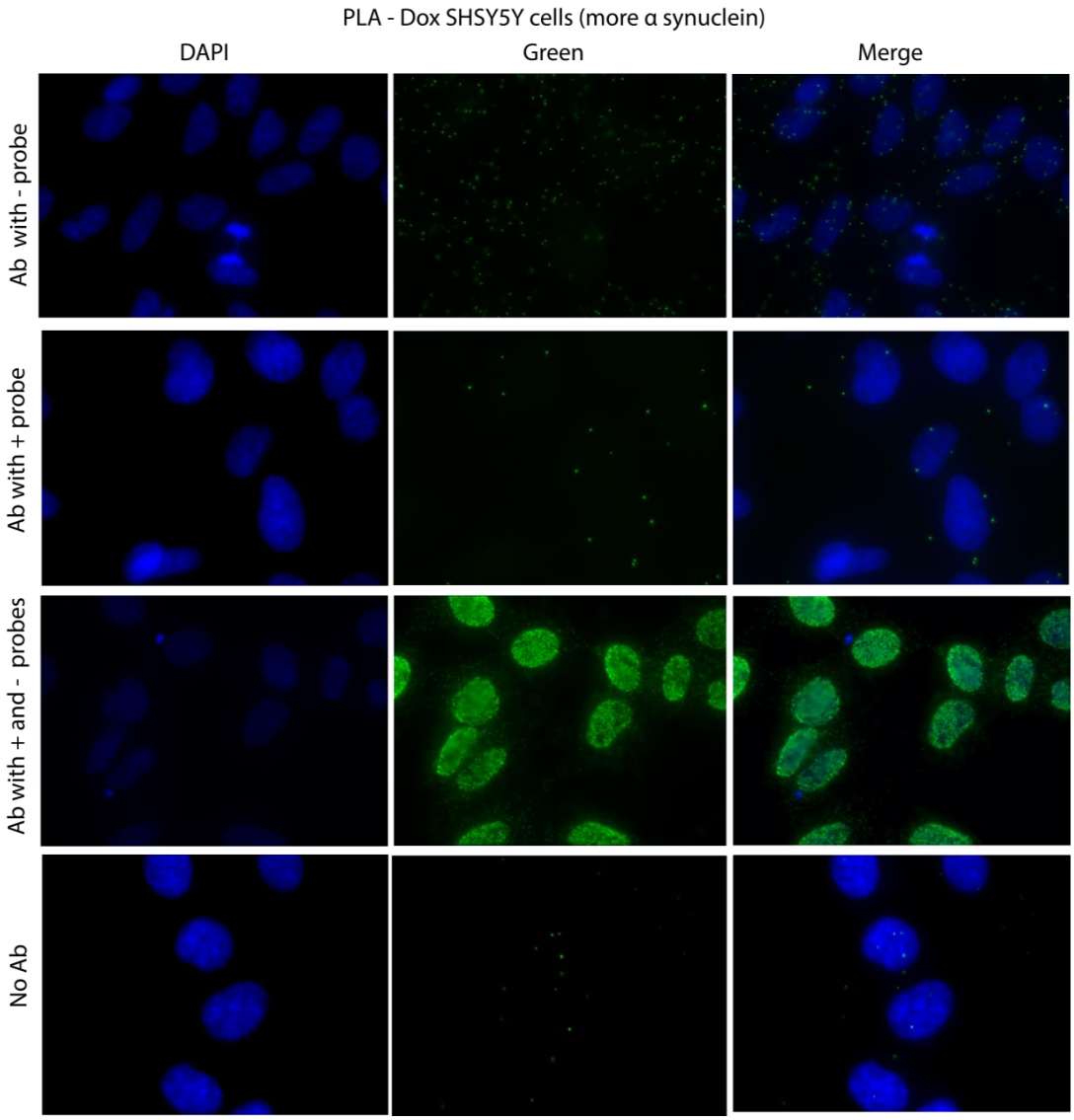

Figure 4.23: Proximity ligation assay (PLA) on higher α-synuclein expressing cell line (SHSY5Y): *PLA using antibody 3.1 showing DAPI only, green and merged (left to right) containing – Row 1 shows PLA using antibody lined to – probe only, row 2 shows PLA using antibody linked to + probe only, row 3 shows PLA using antibody containing both probes and row 4 shows PLA with no probe attached as a control.*

Similarly while visualizing the data from PLA on SHSY5Y cells (low α-synuclein) we once again notice that spot formation in case of PLA with both probes is quite high as compared to controls (figure 4.24). This data correlates with above mentioned PLA results obtained on higher α-synuclein expressing cell line. These

results indicate that α-synuclein might be self-interacting and forming oligomers within cells.

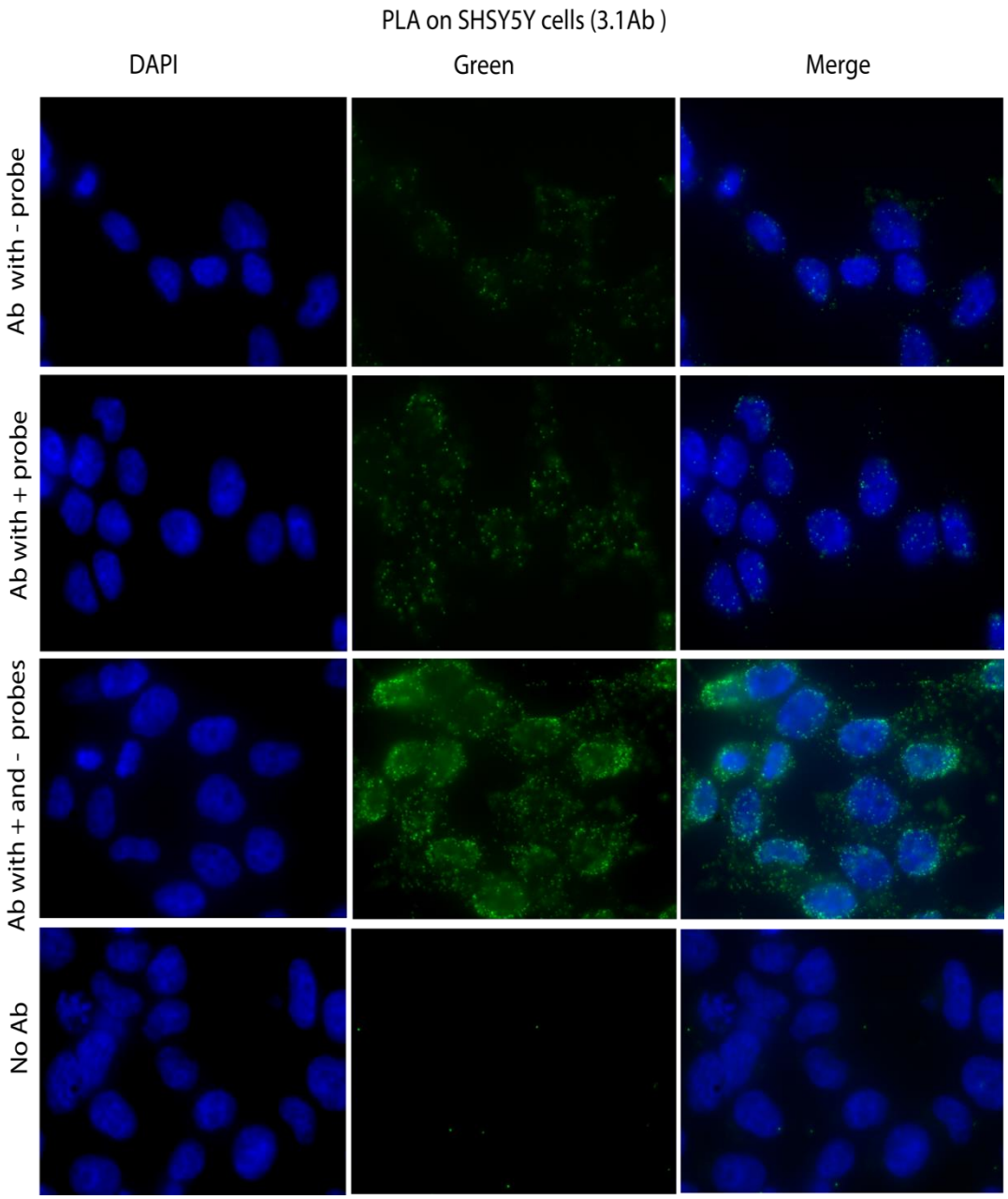

Figure 4.24: Proximity ligation assay (PLA) on lower α-synuclein expressing cell line (SHSY5Y): *PLA using antibody 3.1 showing DAPI only, green and merged (left to right) containing – Row 1 shows PLA using antibody lined to – probe only, row 2 shows PLA using antibody linked to + probe only, row 3 shows PLA using antibody containing both probes and row 4 shows PLA with no probe attached as a control.*

Thus here we show using PLA that it is likely that α-synuclein is interacting with itself in SHSY5Y cells. Interestingly, the staining pattern of antibody seen was not similar as in the case of IF. In the case of IF staining pattern indicated that the antibody binds to the membrane of the cell whereas in case of PLA the staining indicated binding pattern all over the cell which might be due to exposure of epitope via interaction.

4.3. Discussion

In this study we demonstrated the secondary structure of native α-synuclein and also potential efficacy of anti-α-synuclein antibodies against aberrantly folded protein (α-synuclein) in PD via in-vitro assays. Parkinson's disease is a highly prevalent neurodegenerative disorder which is characterized by accumulation of protein inclusion including α-synuclein and ubiquitin like proteins [324]. This disease is characterized by loss of dopaminergic neurons and is marked by the presence of lewy bodies similar to few other diseases such as LBD [325]. Protein aggregation in various neurodegenerative disorders is due to aberrant folding of the proteins which can lead to formation of oligomers and ultimately insoluble fibrillar structures. This phenomenon of protein accumulation which leads to formation of lewy bodies and its toxicity effects could be due to various reasons such as (i) impairment of ubiquitin-proteosomal pathway, (ii) chronic endoplasmic stress and (iii) glutamate receptor dysfunction [326]. A study carried out using transgenic mice expressing WT α-synuclein indicated loss of dopaminergic neurons characterized by formation of lewy bodies. α-synuclein can act as a pathogenic agent spreading from one cell to another throughout the course of PD by various mechanisms. Possible mechanisms involved in intercellular transfer of α-synuclein include secretion, exocytosis and recently found extensions called nanotubes (tunnel like structures between two cells) [327]. Exocytosis is the most common mechanism for α-synuclein to leave the cells which is supported by its intraluminal vesicular localization [328], whereas the precise role of tunnelling nanotubes (TNTs) is still being investigated. Inhibition of such mechanisms through antibodies or peptides can indeed play a major role in treating PD. Potential treatment strategies developed and ones under process with different mechanism of action target oligomers by either making these oligomers in soluble form or disrupting the already formed oligomers. Although the function of α-synuclein is still unknown, it is known to be enriched at presynaptic terminals where it promotes the assembly of SNARE machinery (Soluble N-ethylmaleimide sensitive factor attachment protein receptor). A-synuclein has been widely accepted as a structurally unfolded intrinsically disordered protein in its native state [329, 330],

however a few studies have suggested α-synuclein occurs as a α-helically tetramer in its native state [319, 331].

Interestingly, the results with native state of synuclein have always been conflicting and not always replicated and thus its physiological form is still questioned. Thus in order to study the physiological state of this protein in detail, we expressed and purified the recombinant construct for α-synuclein. In order to avoid any potential breakdown of any physiological assemblies by detergent, we initially ran the recombinant purified WT α-synuclein on a native gel under different conditions. Here we notice that α-synuclein runs at a higher molecular weight i.e. ~140 kDa whereas no monomeric form (14 kDa) was identified. However, when WT α-synuclein was run on a SDS gel we noticed that all the oligomeric protein was degraded down to a monomeric protein which compelled us to look at the effects of different detergents. Among all detergents (SDS, Triton X-100, tween-20 and DMSO), only SDS was seen to collapse the protein to a monomer with as low as 0.01% final concentration causing the collapse. It has been shown on various occasions that secondary structure of α-synuclein can be affected by boiling of sample, pH changes, etc. A study carried out using Gel filtration on native α-synuclein in brain cytosol as well as recombinant α-synuclein without any boiling or detergents showed this protein occurs as a folded tetramer which correlates to the earlier results [319, 332].

In fact CD spectral studies have indicated that protein possesses α helical secondary structure i.e. containing 65% α - helical, 17% turns and 8% unfolded calculated using DICHROWEB [309, 333]. The conformation of native form α-synuclein has always been a topic of debate and so is its secondary structure in lewy bodies (inclusion bodies). Another study on secondary structural analysis via CD spectrum has indicated that unfolded disordered conformational state of α-synuclein could be transformed into partially folded intermediates subjective to changes in pH and temperature [312]. It has also been shown by CD experiments; α-helicity is increased from 3 to 80% upon binding of α-synuclein to phospholipid bilayers [280]. Our CD data indicates that α-synuclein is structurally unfolded and disordered in its native state in the spectra range of 185 nm to 285 nm. Interestingly we see that after

addition of SDS (0.00006%) to WT α-synuclein α-helicity was attained from an unfolded disordered secondary structure based on the algorithms from DICHROWEB. Among all the algorithms used, α helical structures were best estimated by CONTIN method using SP175 as the reference set. In addition to this, using CONTIN we looked at the percentage increase in the α-helicity from a native unfolded protein after addition of SDS overnight as well as fresh. The reason behind adding SDS overnight as well as fresh was to look at the stability of the structure and also to analyse the percentage change in other types of secondary structures. Figure 4.25 depicts a pie chart that shows percentage of occurrence of different types of structure in native α-synuclein with and without SDS. Based on analysis using CONTIN algorithm, native α- synuclein is 63% disordered, 7% helical, 4% stranded and 26% other structures. However, overnight and freshly added SDS induces structural changes which increase α helicity of the protein from 7% to 38% and 67% respectively. This structural variability induced due to addition of SDS is an indicative of interactive ability of α-synuclein with lipids.

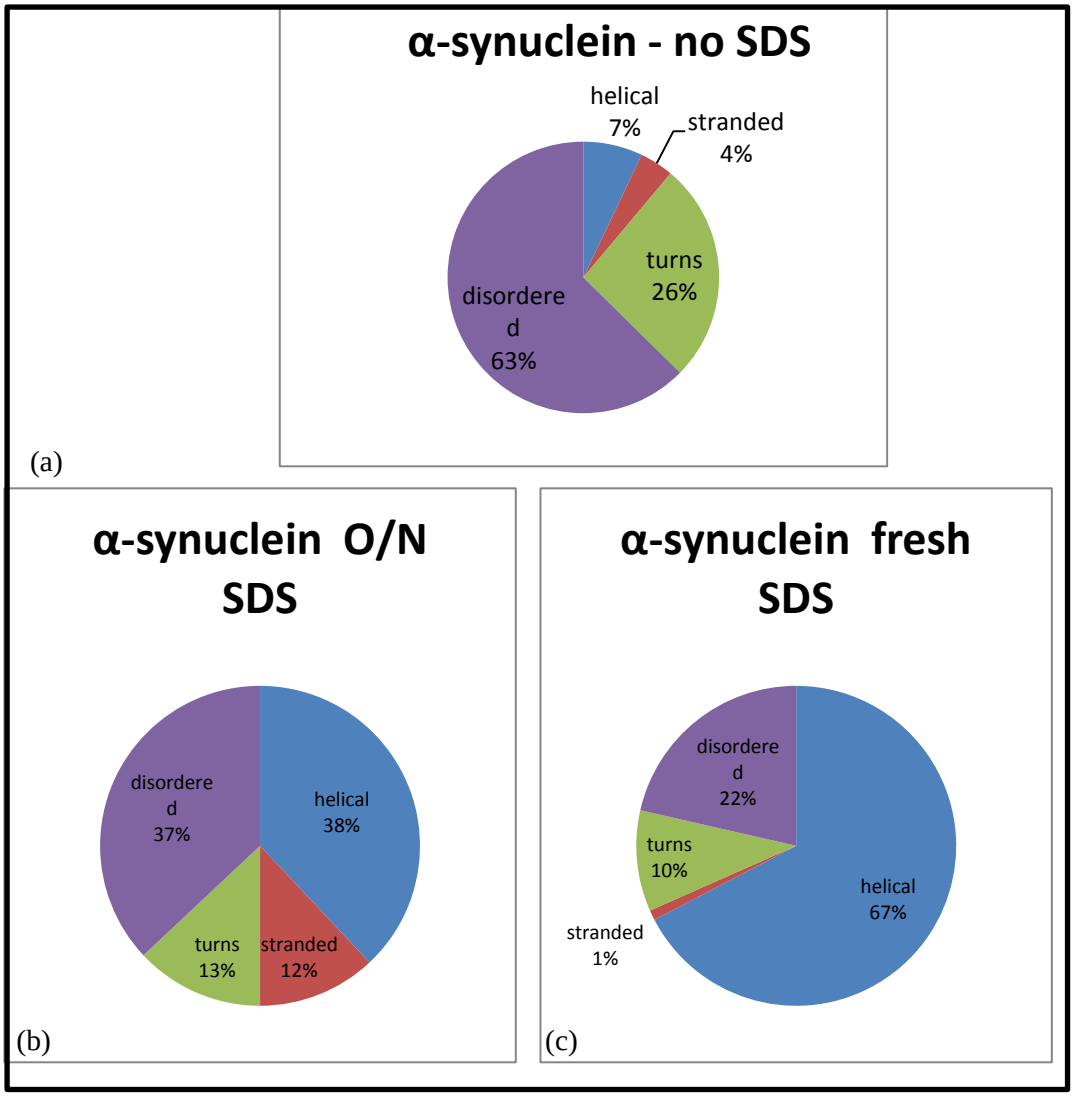

Figure 4.25: Structural analysis of recombinant α-synuclein after CD spectral analysis: *Using CONTIN as algorithm in DICHROWEB website, percentage of different types of structures was determined for each data set. (a) Native α-synuclein with no detergent showing 63% to be structurally disordered, 7% helical, 4% stranded and 26% turns. (b) α-synuclein with overnight SDS appears 37% to be structurally disordered, 38% helical, 12% stranded and 13% turns and (c) α-synuclein with fresh SDS incubation appears to be 22% structurally disordered, 67% helical, 1% stranded and 10% turns by software analysis.*

From PD studies point of view, this protein becomes misfolded and leads to formation of insoluble oligomers which have become the ultimate hallmark of PD patients and a suitable target for therapies. With multiple approaches aimed at targeting different steps along aggregation pathway and different toxicity levels are being examined in basic laboratory research and pre-clinical studies [326]. For this reason, we immunized mice with recombinant α-synuclein to obtain monoclonal antibodies and tested against a panel of antigens as well as on recombinant protein. Interestingly one of the antibodies (2E4- 3.1) has the same epitope as the commercial antibody from BD Biosciences and two of mAbs (1H1 and 5B4) bind to the recombinant protein but not to any of the derived peptides. We also determined the activity of all these mAbs onto recombinant α-synuclein by immunoblotting as well as onto α-synuclein expressing neuroblastoma cell line (SHSY5Y). Also, fixing of the blotting membranes after Immunoblot transfer with PFA intensified the monomeric band which correlates with the published results [321]. Following testing and epitope mapping of antibodies on recombinant α-synuclein and a panel of peptides respectively, we immunohistochemically detected the presence of α-synuclein in several brain tissues as well as kidney organs. α-synuclein is principally known to be expressed in brain but also expressed in low concentrations in all other tissues except in liver. Moreover, we demonstrated the binding potential of mAb 3.1 (2E4) via immunofluorescence and it was found that antibody stains in a similar pattern to that of commercial antibody in α-synuclein expressing cells.

Previously, there have been attempts to understand the mechanism involved in the formation of oligomerization of α-synuclein in neuronal cells. For studying the behaviour of α-synuclein in cells we developed two constructs of α-synuclein with different tags onto each (GFP and Cherry) via cloning. The aim was to investigate the effect of both constructs onto each other as well as their effect on endogenous α-synuclein via transfection into SHSY5Y cells. We demonstrated that GFP α-synuclein was stabilized by cherry tagged α-synuclein (figure 4.21), however we did not see any signs of oligomerization of tagged α-synuclein occurring within the cells. Also, increasing the transfection amount of Cherry tagged α-synuclein DNA might be useful for studying α-synuclein interaction in cells.

To further study α-synuclein's self-interaction we used PLA to illustrate that α-synuclein indeed interacts with itself; however it remains to be determined what stable state this protein attains in cells and if it contributes to lewy body formation. PLA is a useful technique to microscopically visualize protein-protein interaction occurring within cells [334]. While analysing PLA onto SHSY5Y cells, we see spots (indicator of PLA signal) throughout the surface of cells indicating self-interaction of α-synuclein in SHSY5Y cells (high and low α-synuclein expressing cells). Thus these assays in future could be more than useful tools to demonstrate self -interaction of a protein occurring within cells or possibly even in tissues using well characterized antibodies. Moreover, our results with monoclonal antibodies developed against α-synuclein indicate that these antibodies could be a useful tool following further characterization from future therapeutic point of view for PD patients. Finally, antibody development combined with novel assays demonstrated in this research in turn could provide a major breakthrough in studying proteins involved in neurological diseases.

CHAPTER 5: Peptide phage display screening against α-synuclein

5.1. Introduction

5.1.1. Phage display

With continuous success and efficacy of immunotherapy over the years against intracellular proteins such as tau [335, 336], Huntingtin [337] and α-synuclein [338] in neurological diseases, new era immunotherapeutic challenges are highly demanding in order to be implemented in humans. One such approach towards clinical success is developing new tools not only distinct from available ones but also possess higher efficacy towards the target. Phage display is one such promising selection approach that uses a combinatorial library containing random peptide sequences displayed on surface of bacteriophage. The advent of phage display has allowed a physical linkage between phenotype and genotype.

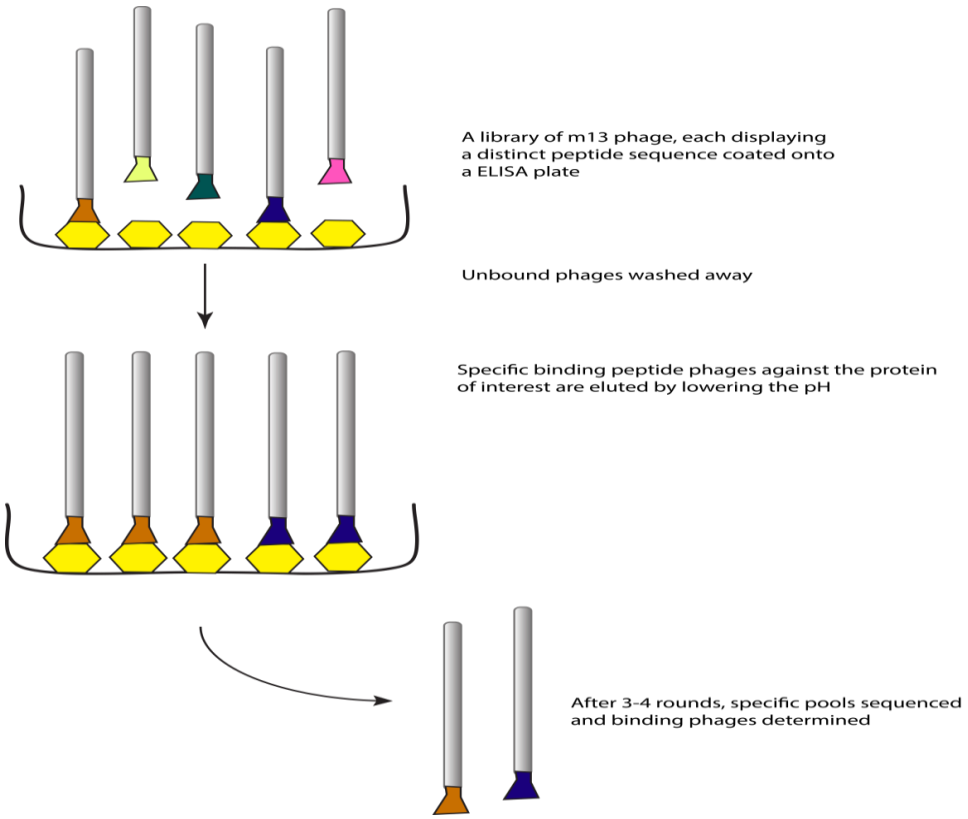

Figure 5.1: Peptide phage display: *Each phage displaying a distinct peptide sequence (peptide library) added to target of interest onto 96 well plate. Unbound phages washed away during biopanning and specific bound phages eluted and re-amplified for next round. The specific peptides are then sequenced and tested via different assays onto target protein.*

Several groups have demonstrated the display of random peptides on the surface of phage and binding peptides using phage display have been identified to various biomolecules [339-341] . The most common display systems used for peptide phage display include filamentous phage in which peptides are fused to either minor coat protein (p3) or major coat protein (p8); this in turn ultimately determines the valency of the library. However, pharmacokinetics studies with peptides have always shown an area of concern and often contributes to its disadvantages, to overcome some issues such as low immunogenicity the ability of peptides is improved by making them oligomeric [342]. Oligomerization of the peptides could in turn act by increasing the selective binding to the target protein, for example dimeric peptide against EpoR and TpoR [343]. The trouble with current available immunotherapeutic tools for synucleinopathies is the extent to which biologics can induce any significant reduction in α-synuclein oligomers. Since α-synuclein is only 140 amino acids and intrinsically disordered i.e. lacking a stable 3D structure, peptide specifically binding to a pocket in the protein could be a useful tool for molecular imaging.

5.1.2. Need for peptides binding to α-synuclein

Selection process of peptides binding to a target is performed by a process called biopanning which involves incubation of combinatorial library with the target of interest in an immunotube or ELISA 96 well plate. Such screening can be easily performed due to the availability of commercially available peptide libraries such as 7 mer and 12 mer Ph.D. libraries from New England Biolabs (NEB). A cyclic peptide library has shown its importance in reducing the toxicity of α-synuclein and resulted in prevention of dopaminergic neurons in the PD model [344]. α-synuclein is prone to misfolding, aggregation and can ultimately lead to ER stress, accumulation of lipid, mitochondrial dysfunction and finally cell death [345, 346].

There is evidence supporting the importance of non-amyloid component (NAC) domain in aggregation and cytotoxicity of α-synuclein [347]. Infact the GAV motif (residues from hydrophobic region 66 to 74) which is comprised of hydrophobic residues is known to be critical for α-synuclein fibrillation [348]. Several mouse models have been developed to study synucleinopathies for determination of high levels or mutant forms of α-synuclein. These models focused more on investigating whether or not α-synuclein results in loss of dopaminergic neurons and also demonstrate that its aggregation is necessary for formation of lewy bodies in animal models. Due to such pathological properties of α-synuclein, it might be useful to develop peptide aptamers to target this protein that occurs in various forms. These tools are developed with an aim of targeting fibrils at early stages rather than mature fibrils as the former is mainly involved in neuronal cell death whereas the later might play a protective role in some cases [349].

An advantage of combinatorial peptide phage display screening is that it can provide novel peptide sequences that can bind to many proteins expressed within cells because of its diversity. The issue with other available technologies is their inability to identify millions of sequences straight from the phage pools, also restricted to number of sequences that can be identified and their difficulty to interpret data. Phage display is no longer limited by sequencing constraints as it is now possible to sequence millions of peptide sequences by technologies such as -next generation deep sequencing, etc. These binding peptides might have capability of inducing conformational change in the protein and ultimately result in disruption of aggregates and fibrillar forms. Agents that can interact with aggregate forms of α-synuclein could be very useful not only in studying the mechanism of α-synuclein aggregation, lewy body formation but also from a diagnostic as well as a therapeutic development for PD patients. Since experimental studies have indicated that α-synuclein's amino terminal repeats play a role in its binding ability to lipids [292], developing peptides to this region could in turn have a significant potential for understanding its biophysical properties. These peptides could be delivered to the target site by linking it to a macromolecule that does not induce any major side effects and also does not affect peptide binding ability.

5.1.3. AIM

The aim of this study was to screen and identify peptides using peptide phage display technology that bind specifically to α-synuclein. Here we used Ph.D. 12 mer library from NEB for screening against α-synuclein using the selection process of biopanning. Binding peptides derived from the amplified pools of phage bound to peptide were sequenced and identified via next generation deep sequencing (NGS) and ultimately test for their ability to dissociate monomers and preventing aggregation. The identified peptides were then analysed for binding onto recombinant WT α-synuclein as well as neuroblastoma cell line (SHSY5Y) expressing α-synuclein.

5.2. Results:

5.2.1. Peptide phage display againstα-synuclein

Peptide phage display technology which involves displaying of randomized peptide sequences onto phage is widely employed for selection of specific binding peptides to a target immobilized onto an ELISA plate. This technique provides an advantage of presence of millions of peptide sequences on the surface of phage particles; this demonstrates the diversity of library. The Ph.D. 12 mer commercial phage library stock from NEB was sequenced in order to identify the repetitive sequences as well as to determine the diversity of library before subjecting the library to biopanning. Based on our earlier studies carried out on MDM2 (by Anne Sophie Huart, Hupp lab), it has been demonstrated that Ph.D. 12 mer library has different level of diversity with high number of repetitive sequences (Anne Sophie Huart, personal communication, 2013). For this reason before proceeding with our screening experiments onto α-synuclein we determined the diversity of peptides by determining cumulative copy number in the peptide phage library. As it can be seen in the figure 5.2 a, uniqueness of the peptide sequences in peptide phage library before screening for mdm2 protein is quite low with cumulative number of copies exceeding over 100,000. However, diversity of another stock of new Ph.D. 12 mer library used for screening against α-synuclein in comparison to the above mentioned library was quite high as not more than 100 repetitive numbers of copies were noted following sequencing (figure 5.2b).

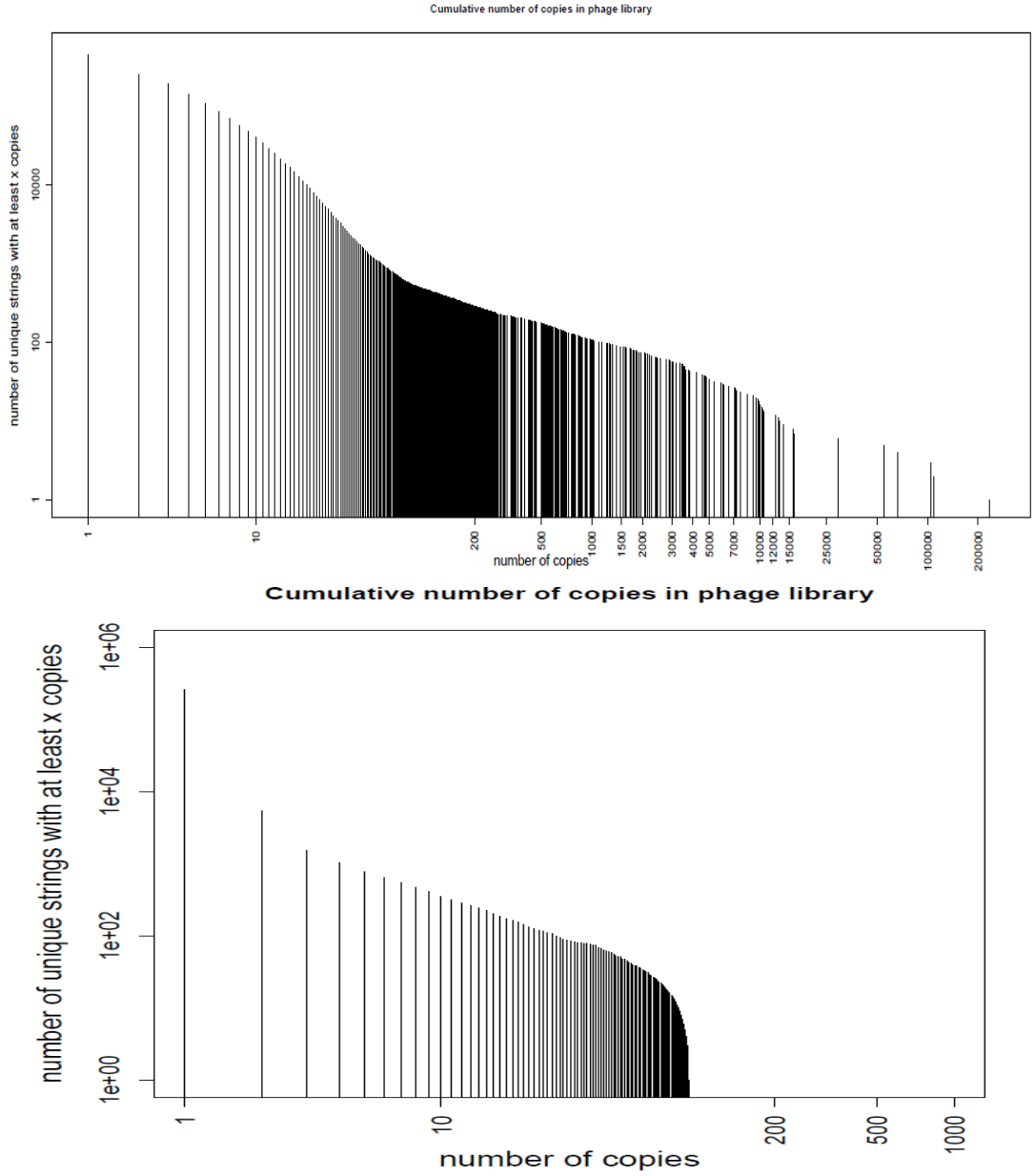

Figure 5.2: Comparison of Cumulative number of copies in phage library prior to use for biopanning: *(a) Diversity of P.h.D 12 mer library used for screening onto mdm2 protein (b) Diversity of P.h.D 12 mer library used for α-synuclein screening. Each based on identification of unique sequences within the library*

Due to the ease of availability of commercially made peptide phage display libraries, screening of peptides onto a target can be performed quickly by the process of biopanning which is demonstrated below in figure 5.3. Two rounds of biopanning were performed onto recombinant α-synuclein in an ELISA well. The non-specific phages bound to the well were washed away by performing stringent washes and the

specific ones were eluted in appropriate elusion buffer. A fraction of all phage pools after elusion were stored for the subsequent round of panning as well as for PCR amplification to have enough DNA to further proceed for sequencing. Several controls such as incubation of library with blank wells and incubation with different proteins were used in the following experiments to remove any non-specific, repetitive peptide sequences.

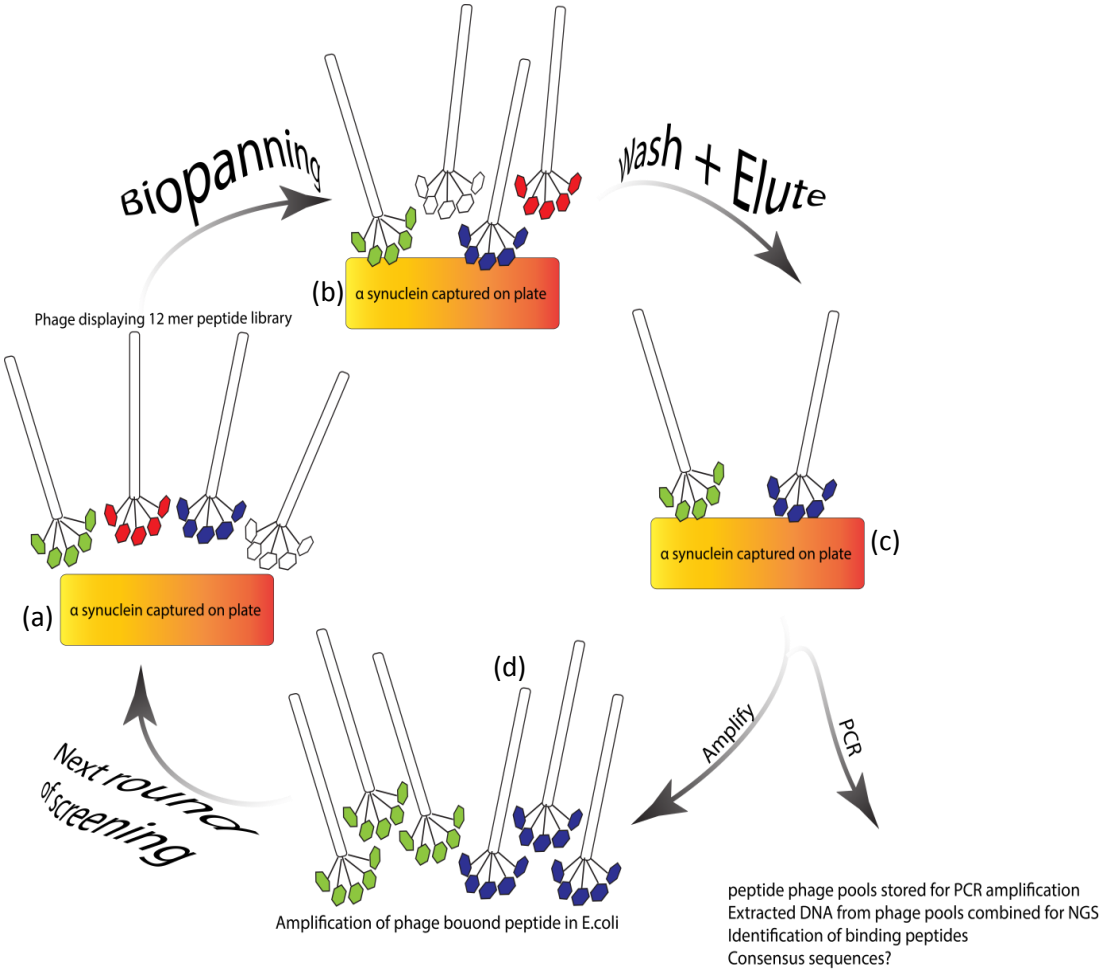

Figure 5.3: Biopanning protocol for peptide library screening onto target of interest: *(a) PhD 12 mer peptide phage library containing different peptide sequences pentavalent in nature onto the phage. (b) Biopanning i.e. addition of library onto α-synuclein coated plate, (c) washes to get rid of non-specific phages followed by elusion of specific phages and (d) amplification in E.coli for subsequent round of panning and PCR for amplification of phage pool DNA for NGS.*

Amplification of phage by infection into *E.coli* ER2378 was necessary from each round in order to amplify the specific binding clones by multiplying the copy number

of specific clones. Few sequences might be over-expressed within the commercial library itself which could in turn cause their amplification in all the rounds of panning after re-infection into E.coli cells. For this reason, the phage DNA was amplified using PCR from the eluates obtained from each round of panning to minimize chances of amplified based bias obtained in sequencing data. A recent review described a few peptide sequences that have been known to amplify independent of target, thus these sequences are suspected as a non-specific binder [350]. Thus all the binding peptide sequences were selected if they were minimally expressed in the parental library in comparison to α-synuclein. In recent years, a number of web tools including databases and programs have been developed in the field of peptide phage display to analyse sequencing data. Based on the published data, it has been shown that 12 mer library binds better to the targets which require a chain of few amino acids that can fold into structural elements [351]. It is therefore not surprising to get high variability in the amount of peptide sequences as in theory peptide might bind to different hotspot residues distributed all over the surface of a protein. Using Next generation deep sequencing as a sequencing tool, we identified numerous peptides against αsynuclein following phage display.

5.2.2. Identification of peptides binding to α-synuclein

5.2.2.1. Abundance Method

The number of repetitions of each peptide against α-synuclein is referred to as iteration number. Iteration of each peptide sequence was determined as a percentage within each sample set to be able to compare it to the other proteins (controls) via sequencing numbers. The advent of MEME software enabled us to identify several motifs containing identical sites within the selected peptide sequences. These selected peptides were passed through MEME software in order to identify different motifs containing identical amino acids. From all the peptides identified, 20 different motifs were identified on the basis of occurrence of several repetitive amino acids in all the selected peptides. As shown in the table 5.1 below, ‘GDGDNSVLKPGNW’ peptide was identified in 41 sites, another motif ‘EITHPGWSTVTH’ in 35 sites and thus these consensus peptides were further categorized.

Using this commercially available 12 mer Ph.D. peptide phage display library, peptides binding to recombinant α-synuclein were selected following DNA amplification. DNA was amplified from each phage pool that was stored following every round of panning, gel extracted and concentration of each DNA was measured as mentioned in section 2.17. The purified amplicons were pooled together in equal concentrations in order to obtain a total of 5 µg for Next generation sequencing (NGS) to obtain the list containing all possible peptide sequences. These combined phage pool DNA containing a combination of phage linked peptide DNA was sequenced and data from NGS was obtained in FASTA format. Along with α-synuclein, screening was also carried out on a panel of proteins such as ZNF, npm and reptin. The data was converted from FASTA into xlsx format and further sorted out in an excel sheet. A total of approximately 1 million distinct peptide sequences present in the 12 mer library based on various combinations were derived from next generation deep sequencing data.

5.2.2.1.1. Iteration number of each peptide

Firstly, the identified peptides were arranged in decreasing order based on the iteration number of each peptide binding to a specific protein. For selection of peptide binding to α-synuclein, only peptides that showed at least two fold higher occurrence as compared to other proteins, controls as well as parental library were further characterized. As mentioned earlier in section 2.17 screening was performed in the form of fast washes and slow washes to obtain highly specific α-synuclein binding peptides. A control was used in each case to determine the background score and it was noticed that count obtained for the binding peptides obtained was significantly higher in slow wash as compared to fast wash. During different rounds of biopanning, the count obtained in case of slow washes was significantly higher as compared to fast washes which indicate better amplification of specific ones. Also, the total number of peptide sequences obtained in slow washes was less as compared to fast washes which might give an indication of amplification of non-specific peptide sequences in subsequent rounds in fast washes. Moreover in order to remove any false positives, the peptide library was first added to the well containing blocking buffer only (3% BSA) and then added to the well containing the protein of interest.

This could also in turn indicate that most of the plastic binders would remain bound to the plastic and remaining library could be subsequently added to the well coated with the target protein. A comparison of α-synuclein binding peptides based on different consensus sites obtained from slow washes along with different controls and parental library, a few examples have been shown below:

peptide from motif	Parental library	α-synuclein (SW)	npm	ZNF350	control (SW)
GDGNSVLKPGNW	197	27515	186	202	373
EITHPGWSTVTH	356	16146	521	374	759
SSWWHHLVADRV	32	2474	35	26	66
SALKGLFPADHH	124	3268	916	708	219
MADVRHPGGFFF	0	6	0	0	0

Table 5.1: Iteration number of peptides: *Peptides with higher iteration number against α-synuclein compared with iteration number against parental library, nmp, ZNF350 and control. For example, GDGNSVLKPGNW has an iteration number of 27515 against α-synuclein which is more than 8 fold compared to parental library and other proteins.*

5.2.2.1.2. Comparison of selected peptides (Fast wash vs Slow wash)

As it can be seen in table 5.1, the iteration number of binding peptides to α-synuclein was at least more than two fold higher as compared to the parental library, other proteins and control. Each peptide sequence was associated with its sample identity and iteration number. Following the comparison of binding peptides between different proteins, we further defined the behaviour of peptides based on their percentage occurrence in different rounds including unamplified round. As seen in table 5.2, iteration number of peptides is expressed in terms of percentage in round one before amplification (unamplified), round one amplified and round two amplified. One common feature noted among all peptides was the higher counts observed in round one amplified of slow washes as compared to fast washes. For

peptide GDGNSVLKPGNW, the total iteration number for this peptide was 47270. Using this total number, percentage of occurrence of this peptide in different rounds was determined in fast and slow washes. Similarly for other peptides amplification pattern was determined in different rounds of panning.

peptide from motif	FR1ua	FR1 a	FR2	SR1ua	SR1a	SR2
GDGNSVLKPGNW	3.5	0.19	1.45	1.08	59.2	12.5
EITHPGWSTVTH	2.85	0.85	2.24	5.57	17.1	4.5
SSWWHHLVADRV	2.47	0.1	1.97	1.7	30.5	27.9
SALKGLFPADHH	1.8	10.6	6.5	1.33	11.6	4
MADVRHPGGFFF	9.1	0	9.1	0	54.5	9.1

Table 5.2: Selected peptides iteration number in percentage: *Each peptide with higher iteration number was expressed in percentage in both rounds of panning in slow as well as fast washes.*

We also determined iteration number of peptide GDGNSVLKPGNW selected against α-synuclein in comparison to several other proteins, parental library and control. It is important to mention here that against all proteins and control the same library was used and the same protocol was followed. Figure 5.4 shows this peptide had a total occurrence of 77 % when tested against α-synuclein. The numbers obtained were comparatively low against other proteins i.e. 8%, 5%, 1%, 2% and 7% in npm, control, parental library, ZNF and reptin respectively.

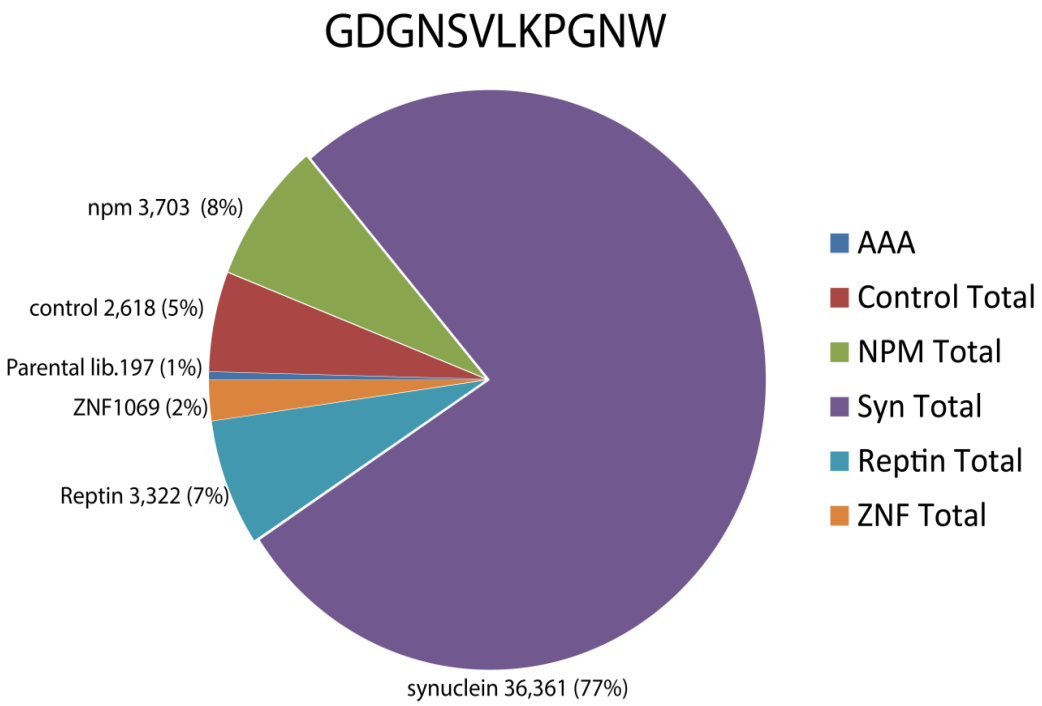

Figure 5.4: Percentage distribution of peptide GDGNSVLKPGNW: *Percentage distribution of GDGNSVLKPGNW against α-synuclein along with other proteins, blocking buffer as controls. This peptide has an occurrence of peptide against α-synuclein is 77% whereas it is lower than 10% against all other proteins and control.*

Following the selection of peptides on the basis of their iteration number, we performed MEME analysis to identify different consensus sites present in the selected panel of peptides. All selected peptides on the basis of abundance were scanned through this software and a list of motifs was obtained containing extent of variability observed between sequences. A total of 20 sets of motifs (shown below in figure 5.5) showing abundance of each amino acid were identified and ones with maximum identical sites were further categorized.

5.2.2.1.3. MEME analysis and identification of interacting proteins:

Motif 1	• 2.2e-352 • 41 sites	
Motif 2	• 8.4e-309 • 35 sites	
Motif 3	• 3.0e-161 • 21 sites	
Motif 4	• 2.7e-061 • 10 sites	
Motif 5	• 4.9e-019 • 4 sites	
Motif 6	• 6.6e-019 • 5 sites	
Motif 7	• 5.4e-018 • 5 sites	
Motif 8	• 7.8e-010 • 3 sites	
Motif 9	• 8.0e-007 • 4 sites	
Motif 10	• 1.2e-006 • 3 sites	

Motif 11	• 8.3e-006 • 3 sites	
Motif 12	• 1.0e-003 • 2 sites	
Motif 13	• 1.2e-002 • 2 sites	
Motif 14	• 1.6e-002 • 2 sites	
Motif 15	• 4.8e-001 • 5 sites	
Motif 16	• 7.3e-001 • 2 sites	
Motif 17	• 1.7e+000 • 2 sites	
Motif 18	• 1.9e+000 • 3 sites	
Motif 19	• 2.0e+000 • 2 sites	
Motif 20	• 4.8e+000 • 2 sites	

Figure 5.5: MEME analysis: *All selected peptides were passed through MEME software to identify identical amino acid residues present within the peptide sequences. All peptides with high iteration number against α-synuclein were considered in this case*

The most statistically significantly identified motifs against α-synuclein using MEME analysis are mentioned below in table 5.3. E value is the statistical significance of the motif and gives an estimate of number of motifs with given approximate ratio.

Discovered motif	E-value	Number of sites
GDGNSVLKPGNW	2.2e-352	41
EITHPGWSTVTH	8.4e-309	35
SSWWHHLVADRW	3.0e-161	21
SALKGLFPADHH	2.7e-061	10
MADVRHPG$^{G/}_{D}$F$^{L}_{/F}$F	4.9e-019	4
HI$^{G/}_{V}$$^{T/}_{K}$VTSWL$^{R/}_{L}$$^{P/}_{H}$D	6.6e-019	5

Table 5.3: Discovered motifs containing maximum sites: *Selected top 6 motifs showing e-value and number of sites that it contains among all sequences identified against α-synuclein*

Table 5.3 shows number of identical sites present in each motif identified by passing filtered sequences through MEME analysis. This indicates that even after filtering 5 fold, few peptide sequences are highly dominating when visualized by MEME for example GDGNSVLKPGNW was identified in 41 sites after MEME. For further characterization of 12 mer GDGDNSVLKPGNW peptide, we directed and scanned this peptide to protein blast (pBlast- NCBI) in order to identify different proteins containing similar motifs which might interact directly or indirectly with α-synuclein. The proteins were selected only if they were associated with α-synuclein (Parkinson's disease), synucleinopathies or any other neurological disorder. Using blast analysis a total of 15 proteins were identified based on sequence alignment and the list containing all fifteen proteins is mentioned below:

GDGDNSVLKPGNW blast analysis:

1.	protein FAN isoform 2- 0.9kb
2.	Protein O mannosyl transferase 2- 2.2kb
3.	Thrombopoietin receptor precursor- 1.9kb
4.	Hydroxyl-coenyme A dehydrogenase, mitochondrial isoform 1 precursor- 0.8kb
5.	Aminopterin induced protein 1 precursor- 1.47kb
6.	Gap junction beta 4 protein- 0.67kb
7.	Ornithine carbamoyltransferase, mitochondrial precursor- 1kb
8.	Progestin and adipoQ receptor family member 9- 1.1kb
9.	Protein Smaug homolog 1 isoform 2- 1.8kb
10.	ADAMTS-like protein 5 precursor- 1.4kb
11.	Killer cell lectin like receptor subfamily member 1-0.8kb
12.	Rho GTPase activating protein 25 isoform d -1.8kb
13.	Alpha-1B-glycoprotein precursor-500bp
14.	Indolethylamine N methyl transferase isoform 2-786bp
15.	ATP binding cassette sub family D member 2- 2.2kb

All the identified genes that were associated with their expression in brain are described briefly below. Factor associated with neutral sphingomyelinase activation (FAN) is an adaptor protein belonging to the BEACH family and is found in a variety of tissues [352]. Thrombopoietin (THPO) is a protein encoded by THPO gene playing a central role in normal megakaryocytopoiesis and thrombopoiesis [353]. This protein becomes highly relevant as its expression in brain is releaved and can be highly useful in exploring its association with α-synuclein. Hydroxyl-coenyme A dehydrogenase is a mitochondrial enzyme belonging to dehydrogenase family and its protective role in PD has been shown before [354]. It functions in mitochondrial fatty acid oxidation by catalysing oxidation of 3-hydroxyl CoAs [355]. Gap junctions have always been present in a higher amount in brain and various organs for cell to cell communication. Ornithine carbomoyltransferase is an enzyme that cataylses the reaction between carabomoyl phosphate and ornithine to form citrulline and

phosphate. Its role and importance in brain has been determined to some extent in sparse fur mouse [356]. ADAMTS (a disintegrin and metalloprotease with thrombospondin motifs) was identified as another protein via phage display and are predicted by structural domains to be extracellular matrix proteins [357].

Primers were designed for cloning these above mentioned genes into mammalian expression vectors i.e. pMCherry (N, C terminus) as well as pEGFP (N, C terminus) vectors and ordered from Sigma Aldrich. Neuroblastoma cell line derived cDNA was used as template to amplify these genes. A gradient PCR was performed for all genes with a temperature range from 62 to 85^0 C. The PCR amplification of some of these above mentioned genes is shown below in figure 5.6. The cloning results were confirmed via restriction digestion of miniprep purified DNA obtained after transformation. Once the genes were confirmed via digestion, they were sequenced (Sanger Sequencing, Source Bioscience, Cambridge) and maxiprep purified (Qiagen). The successfully cloned genes from the whole panel were hydroxyl acyl co-enzyme A (HADH), thrombopoietin and GAP junction β-4.

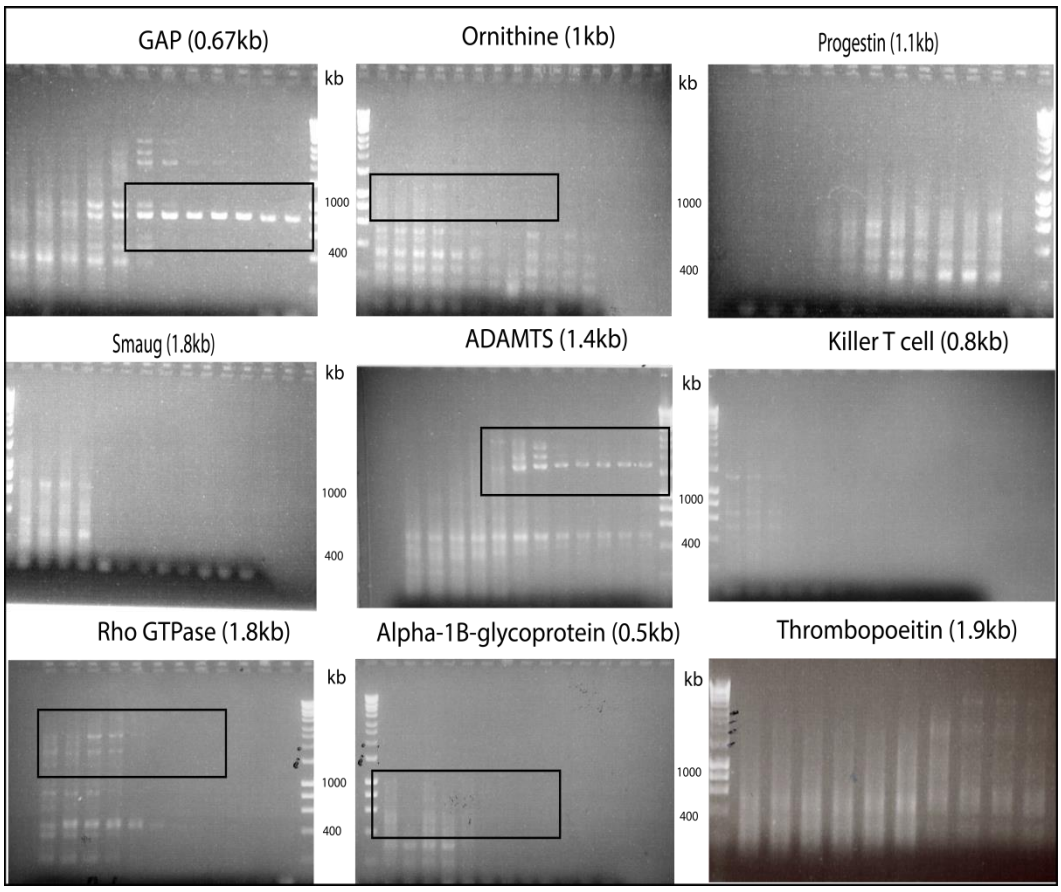

Figure 5.6: PCR amplification of identified genes: *Gradient PCR of genes within a temperature range of 62-85^{0}C. The genes included GAP, Ornithine, Progestin, Smaug, ADAM-TS, Killer T cell, Rho GTPase, Alpha-1β glycoprotein and thrombopoietin. 5 genes out of 9 amplified, gel extracted and restriction digested to clone into vector.*

5.2.2.1.4. Transfection of cloned genes identified by phage display

To investigate the interaction level of these identified proteins with α-synuclein we planned transfection of these constructs into SHSY5Y cells and to look at their effect on endogenous α-synuclein. Out of the whole panel of identified genes we managed to successfully clone three genes, namely, GAP, thrombopoietin and HADH and thus we proceeded further with these genes. These three cloned genes were further characterized by transfection into SHSY5Y cells which contain endogenous α-synuclein. The following day the cells were lysed in 10% triton lysis buffer for 30 minutes and concentration was measured via Bradford assay. As shown in figure 5.7a below, 5 μg of hydroxyl acyl co-enzyme A dehydrogenase (HADH) resulted in the collapse of synuclein oligomeric protein into monomer i.e. 15 kDa. However no difference in α-synuclein state was noticed as an effect of GAP as well as thrombopoietin transfection in different amounts when immunoblotted with anti-α-synuclein antibody. The transfected lysed samples were once again ran on 10 % SDS gel and probed with anti-GFP antibody at a dilution of 1: 2000 in 5 % skimmed milk to determine the efficiency of transfection with empty GFP vector as a control. 50 μg of these lysates was run on 10 % native gel to confirm HADH effect onto endogenous α-synuclein that was obtained on SDS gel. The blots were again immunoblotted with commercial anti-α-synuclein antibody (BD Bioscience) and a distinct effect of HADH was seen on a native gel as a smear appeared (2nd lane figure 5.7c). This indicated that screening for peptides using peptide phage display might assist in identifying interacting proteins. This new finding could indeed be useful in studying HADH role in PD as well as its interaction with α-synuclein in brain models.

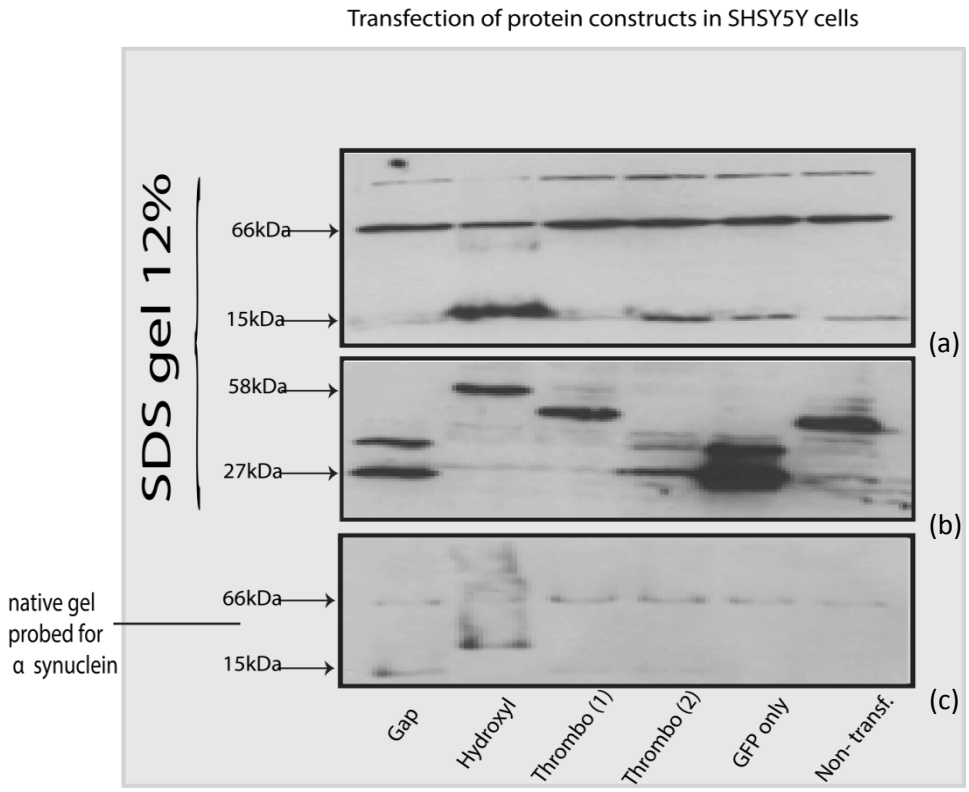

Figure 5.7: Transfection of GAP, Hydroxyl coenzyme A (HADH), thrombopoietin and empty vector control into SHSY5Y cells (50 µg): *(a) Immunoblotted for α-synuclein, (b) Immunoblotted for GFP and (c) all samples on native gel and probed for α-synuclein. α-synuclein oligomer formation around 55 kDa and monomer at 14 kDa.*

Following such encouraging results, we performed similar experiments to reproduce HADH effect but on every occasion the results varied which gave an impression that the effect of this protein might be cell density dependent. Following on, we transfected different amounts of GFP - HADH with an empty vector control in SHSY5Y and $HCT116^{+}$ cells. Also, cells were grown at different densities to see the effect of cell density in induction of GFP - HADH change onto endogenous α-synuclein. The transfection was then performed in SHSY5Y, $HCT116^{+}$ cells and immunoblotted for α-synuclein as well as GFP. Interestingly on this occasion a faint band appeared in all different densities ~ 40 kDa in SHSY5Y cells (figure 5.8). Similarly the samples were immunoblotted using anti-GFP antibody (1: 2000) to determine the transfection efficiency. In all experiments performed it was noticed that HADH effect was seen only if concentration was atleast 5 µg. Even though results obtained with HADH were not reproducible, these experiments indicated that

HADH has an effect on endogenous α-synuclein directly or indirectly. Also a few genes while selecting from BLAST analysis were not considered due to their large size, thus only genes less than 2.5 kb in length and are known to be in relation with α-synuclein or ND were selected.

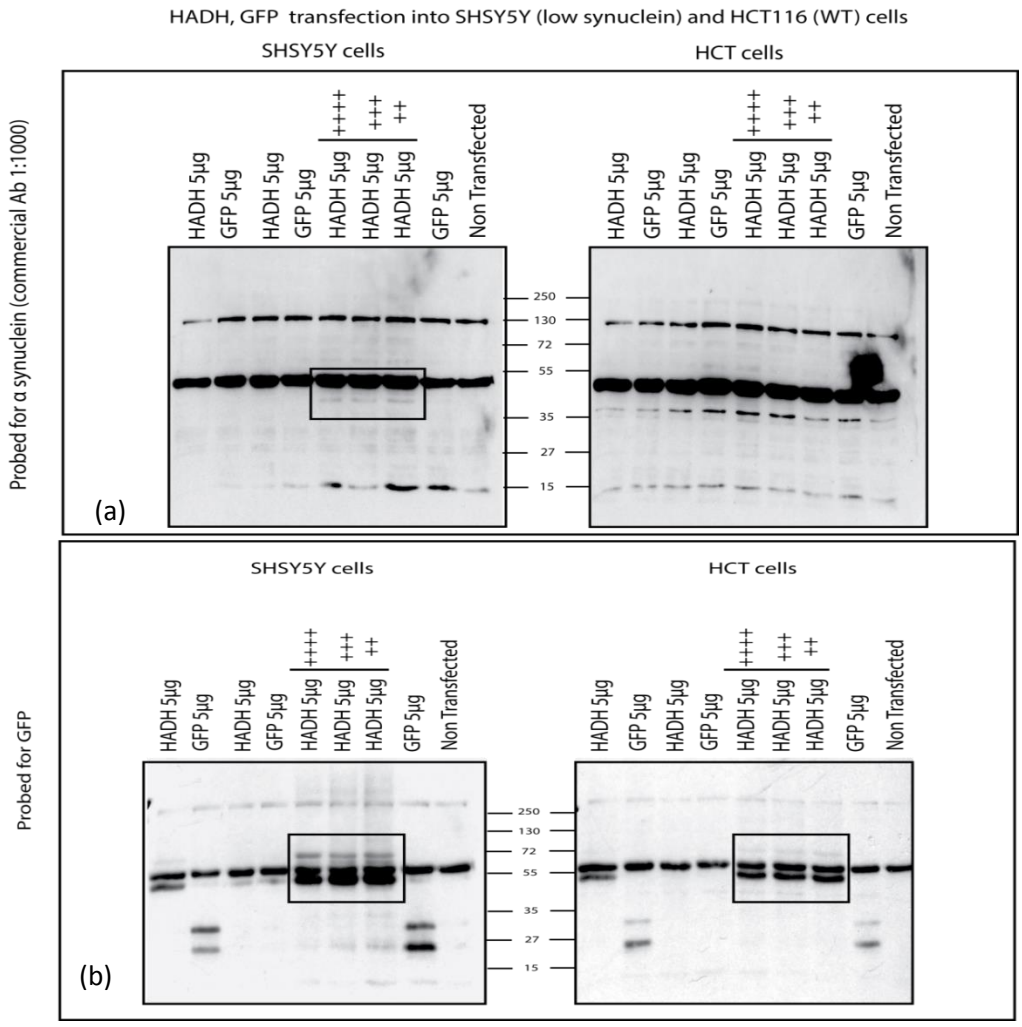

Figure 5.8: GFP-HADH transfection in SHSY5Y and HCT116^{+} cells: *(a) HADH transfection in cells maintained at different densities, left panel shows transfected samples in SHSY5Y cells (rectangular box shows HADH effect on α-synuclein) whereas right panel shows transfected samples in HCT116+ cells. Both blots were immunoblotted for α-synuclein. (b) Same samples (left panel- SHSY5Y and right panel- HCT116^{+} cells) but immunoblotted with GFP antibody to visualize the transfection efficiency.*

5.2.2.2. Percentage based method for identification of binding peptides

Following this abundance method used for the selection of peptides binding to α-synuclein, another method was employed in order to identify peptides based on total count of each peptide against a panel of proteins. The sum total of the each peptide was carried out i.e. total peptide count in parental library, controls, npm, reptin, ZNF350 and α-synuclein. After determining the total peptide count, percentage of each peptide was calculated in the relevant protein i.e. α-synuclein. For example, peptide GDGNSVLKPGNW gave a total of 47,270 (total of this peptide count in parental library, npm, ZNF350, α-synuclein, reptin and control). This total for each peptide was inclusive of all rounds i.e. round one unamplified, round one amplified and round two amplified. Subsequently, total of GDGNSVLKPGNW peptide in all rounds of α-synuclein screening was calculated and was found to be 36,361. Thus using these total counts, percentage of this peptide against α-synuclein was calculated i.e. 77%. Similarly, percentage of iteration number for all the peptides following screening procedure was calculated against α-synuclein. For selection of α-synuclein binding peptides, percentage of peptide exceeding 70% were filtered out and further characterized. The top 32 peptides were selected based on the percentage occurrence against α-synuclein and are shown below in table 5.4. Interestingly some peptides showed iteration number only against α-synuclein and not in other proteins and control.

sequence	sum	AAA	control	α synuclein	α synuclein (%)
GDGNSVLKPGNW	47270	197	2618	36361	77%
DGAYWVSSLGLR	9740	36	705	6803	70%
LSVHLPVVDSPN	8139	40	628	5786	71%
HVIQSIREFRFT	4400	19	279	3143	71%
LSGHDRNNWHNM	3065	6	175	2178	71%
SQLKPILAWANS	2834	20	235	2048	72%
DGTASIPVSQTS	2834	16	136	2006	71%
SSLLTFYPIGVS	1856	8	80	1373	74%
FEPSAPSNVPGS	1860	15	83	1351	73%

GNSAWQINSLTD	1581	11	82	1237	78%
FEDPRTWWVTHL	1688	5	132	1231	73%
ELVGGLHFWGST	1623	2	105	1205	74%
KVSSTGGLSPYT	1403	7	61	1090	78%
MRSATLGDWSVT	1405	6	93	1079	77%
YSLGLRVDTQGY	1497	4	83	1072	72%
WPSSGVNPAQGS	1258	7	58	990	79%
KCCWPAVLPDSI	1090	4	70	853	78%
KCCFSTTVMEPK	1084	5	75	830	77%
INFTPDRSTRDM	1062	0	46	793	75%
GNCKSYSPTFTL	946	6	58	711	75%
DSYYIATSAMAG	820	0	39	677	83%
KLWDLGLGPIET	829	3	52	671	81%
YSLGPDVKLERY	771	4	36	621	81%
NGEKIAWRTLSL	622	3	208	478	77%
GGDGADRRSSFA	11	0	0	11	100%
LPYKIPQTFFNI	11	0	0	11	100%
MISISGTDYAHP	11	0	0	11	100%
SHACWWDECTGS	11	0	0	11	100%
VLGLPVTFSIRA	11	0	0	11	100%
GDGNSVLKPGNQ	10	0	0	10	100%
IGVPRVIAVEVS	10	0	0	10	100%
LDFSRGQGLPRK	10	0	0	10	100%
NHAYIGLAFDRP	10	0	0	10	100%
NTFPLTGHPYTT	10	0	0	10	100%
NTRTQAYIPVIP	10	0	0	10	100%
RNESPGMVFPAS	10	0	0	10	100%
ICFFAHSGSPRC	**26**	**0**	**0**	**25**	**96%**
GSPDLDFTYAKT	**25**	**0**	**1**	**24**	**96%**
FEVQSLHPKRLY	**21**	**0**	**1**	**20**	**95%**
GDGNSVLQPGNW	**21**	**0**	**0**	**20**	**95%**
NTRWFDHRAPSD	**19**	**0**	**0**	**18**	**95%**
LTGLMAAVGLKS	**18**	**0**	**0**	**17**	**94%**
DPAVGITDATLP	**18**	**0**	**0**	**17**	**94%**
HVSRSLHQTSPV	**18**	**0**	**0**	**17**	**94%**
TSNWSLSGPTLN	**18**	**0**	**0**	**17**	**94%**

SSGDWDYARGAT	17	0	0	16	94%
SSGLVHGYRAWN	17	0	0	16	94%
LKVSFDALPMPS	16	0	0	15	94%

Table 5.4: Peptide occurrence in percentage against α-synuclein: *Percentage calculation of each peptide against α-synuclein based on total count of peptide against all proteins, parental library and control (including slow and fast washes).*

These above mentioned 32 peptides identified through peptide phage display were designed containing N-terminal biotin tag were ordered from Mimotopes, Victoria, Australia. The N terminal biotinylated tagged peptides were resuspended in 200 µl DMSO to a final concentration of 5 mg/ml. Subsequently, these peptides were tested for their binding efficiency against purified recombinant α-synuclein. ELISA was performed in two different formats. Firstly, one 96 well ELISA plate was incubated with streptavidin overnight whereas the other plate was incubated for just one hour with streptavidin as the designed peptides were biotinylated. The following day peptides were added onto the washed wells for one hour and subsequently the wells were blocked with 3% BSA. Further on, α-synuclein was added to the wells for 1 hour, washed 3 times with PBS-T and incubated with secondary antibody (1:1000 rabbit anti-mouse Ab) for another 45 minutes. On reading the plates it was found out that none of the peptide showed binding to WT α-synuclein.

Secondly, activity of all the peptides was determined onto α-synuclein coated plates. Once again one of the plates was incubated overnight whereas the other one was incubated for just 60 minutes with WT α-synuclein at room temperature to see if the incubation time and temperature affect the peptide protein interaction. There was a significant difference noticed in the interaction level of the peptides with WT α-synuclein when the plates were coated with α-synuclein for 1 hour and overnight for the same. It was seen that the peptides did not show any interaction with α-synuclein when the plate was coated overnight with WT α-synuclein. However, when α-synuclein was coated for 1 hour, peptide 20 (SHACWWDECTGS) showed significant binding in comparison to other peptides when the plate was read at 450 nm (figure 5.9a). This binding difference could be due to various factors such as change in the conformation of the protein due to overnight incubation, temperature

dependency, buffer solubilized, etc. To further validate this peptide, we performed another ELISA to measure the effect of DTT (+/-) along with random selected peptides out of the panel onto α-synuclein. As seen in figure 5.9b, peptide 20 binds to WT α-synuclein in absence of DTT whereas there was no interaction observed after addition of 1 mM DTT to the peptides.

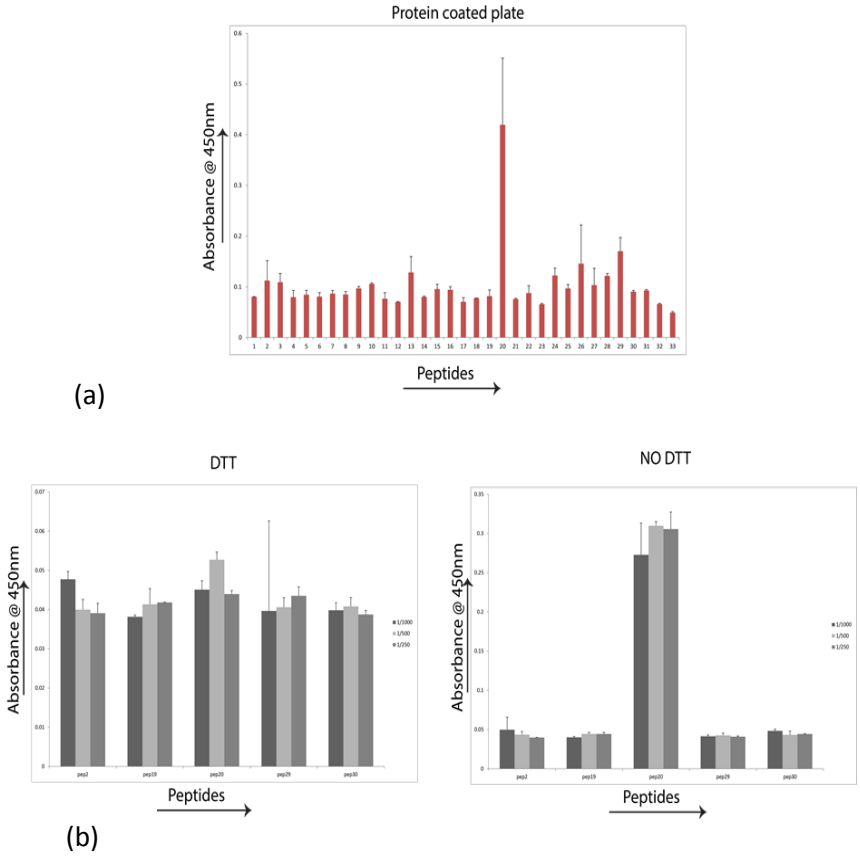

Figure 5.9: Peptide- protein interaction ELISA: *(a) Activity of all 32 peptides onto ELISA plate coated with recombinant α-synuclein for 60 minutes. (b) Activity of selected panel of peptides (2, 19, 20, 29 and 30) in presence and absence of 1mM DTT. Left panel of 5.9a shows binding in absence of DTT whereas the right panel shows binding in presence of DTT.*

While understanding the structure of binding peptide SHACWWDECTGS, we notice that interestingly this peptide contains two cysteine residues which could explain the reason of DTT effect on its interaction with the protein. The disulphide bond between the cysteine residues present at position 4 and 10 in the peptide was reduced with the action of DTT which is expected based on the chemistry of the molecule.

This peptide was cloned in a GFP and Cherry tagged (N and C terminal) vectors for mammalian expression. The primers were designed in such a way that they amplified GFP or Cherry sequence containing the peptide sequences and re-cloned into the digested purified vectors. The primers designed for cloning of these peptides into plasmids have been mentioned below:

Primers for cloning of the peptides into cherry and gfp tagged vectors (N and C terminal)

1.	GDGNSVLKPGNW CHERRY C FORWARD AGEI	5' GC ACC GGTC ATG GTG AGC AAG GGC GAG 3'
2.	GDGNSVLKPGNW CHERRY C REVERSE KPNI	5' GGT ACC TCA CCA GTT GCC GGG TTT CAA AAC GGA GTT GCC GTC GCC GCC GGA GCC GGA CTT GTA CAG CTC GTC CAT GCC 3'
3.	SHACWWDECTGS CHERRY C REVERSE KPNI	5' GGT ACC TCA AGA CCA TGT ACA CTC ATC CCA CCA ACA GGC GTG AGA GCC GGA GCC GGA CTT GTA CAG CTC GTC CAT GCC 3'
4.	SHACWWDECTGS GFP C REVERSE KPNI	5' GGT ACC TCA AGA CCA TGT ACA CTC ATC CCA CCA ACA GGC GTG AGA GCC GGA GCC GGA GTA CAG CTG GTC CAT GCC 3'
5.	GDGNSVLKPGNW GFP C REVERSE KPNI	5' GGT ACC TCA CCA GTT GCC GGG TTT CAA AAC GGA GTT GCC GTC GCC GCC GGA GCC GGA CTT GTA CAG CTC GTC CAT 3'
6.	GDGNSVLKPGNW CHERRY N FORWARD HINDIII	5' GC AAG CTT ATG GGC GAC GGC AAC TCC GTT TTG AAA CCC GGC AAC TGG TGA GGT ACC TCC GGC TCC GGC GTG AGC AAG GGC GAG 3'
7.	SHACWWDECTGS CHERRY N FORWARD HINDIII	5' AAG CTT ATG TCT CAC GCC TGT TGG TGG GAT GAG TGT ACA TGG TCT TCC GGC TCC GGC GTG AGC AAG GGC GAG 3'
8.	CHERRY N REVERSE NOTI	5' GC GGC CGC A CAG CTC GTC CAT GCC 3'
9.	GFP N REVERSE NOTI	5' GC GGC CGC T GTA CAG CTC GTC CAT 3'

Table 5.5: Primers to clone identified peptides: *Primers containing restriction sites for cloning of peptides binding to α-synuclein identified by NSG into cherry and gfp tagged vectors (N and C terminal).*

These primers were used to amplify gene (cherry/ GFP sequence) from the empty vectors pMCherry C, N and pEGFP N, C terminal vectors. The amplified genes were double digested and cloned into digested above mentioned vectors. The sequencing data from cloning indicated point mutations in the peptide sequences which might be due to cloning of small fragments i.e. small peptide (12 amino acid chains) into plasmids. Since the cloning of the peptides was not successful on this occasion we went on to perform peptide pull down assay as means of another way to identify the activity of identified peptides.

In order to see the effect of all the peptides onto α-synuclein in SHSY5Ycells we performed peptide pull down assays to see if the binding peptides could pull down α-synuclein from α-synuclein expressing SHSY5Y cell line. The pull down was carried out in three different ways based on pre-clearing described here. Before proceeding with peptide pull down 10 mg of total fresh lysates was prepared from SHSY5Y cells grown in 10 cm petri dishes. We performed avidin treatment for 30 minutes to pre clear the SHSY5Y cell lysate. Firstly no pre-clearing was carried out using avidin and the lysate was immediately added to streptavidin beads incubated with peptides. Here we do not see any binding with some of the peptides i.e. peptide 1, 2, 9, 12, 13, 18, 19, 25, 26, 29, 30 and 31. As seen in figure 5.10a, remaining peptides (peptide 3, 4, 5, 6, 7, 8, 10, 11, 14, 15, 16, 17, 20, 21, 22, 23, 24, 27 and 28) pulled down oligomeric α-synuclein. Secondly, peptide pull down was performed after lysing the cells for 30 minutes followed by pre-clearing the lysate using sepharose beads for 30 minutes. Interestingly here we see only peptide number 17, 22, 24, 26, 29, 30, 31 and 32 manage to pull down endogenous α-synuclein from the cell lysate. Lastly, 20 μg/ml avidin was added along with lysis buffer before lysing the cells for 30 minutes and only peptide 2, 5, 24, 28, 29, 30, 31 and 32 did not pull down α-synuclein (figure 5.10c). The difference noticed in all three different cases could be due to the manner in which the peptide is exposed during the incubation of α-synuclein expressing lysate. Also, further validation of these peptides is necessary to prove their binding ability to α-synuclein.

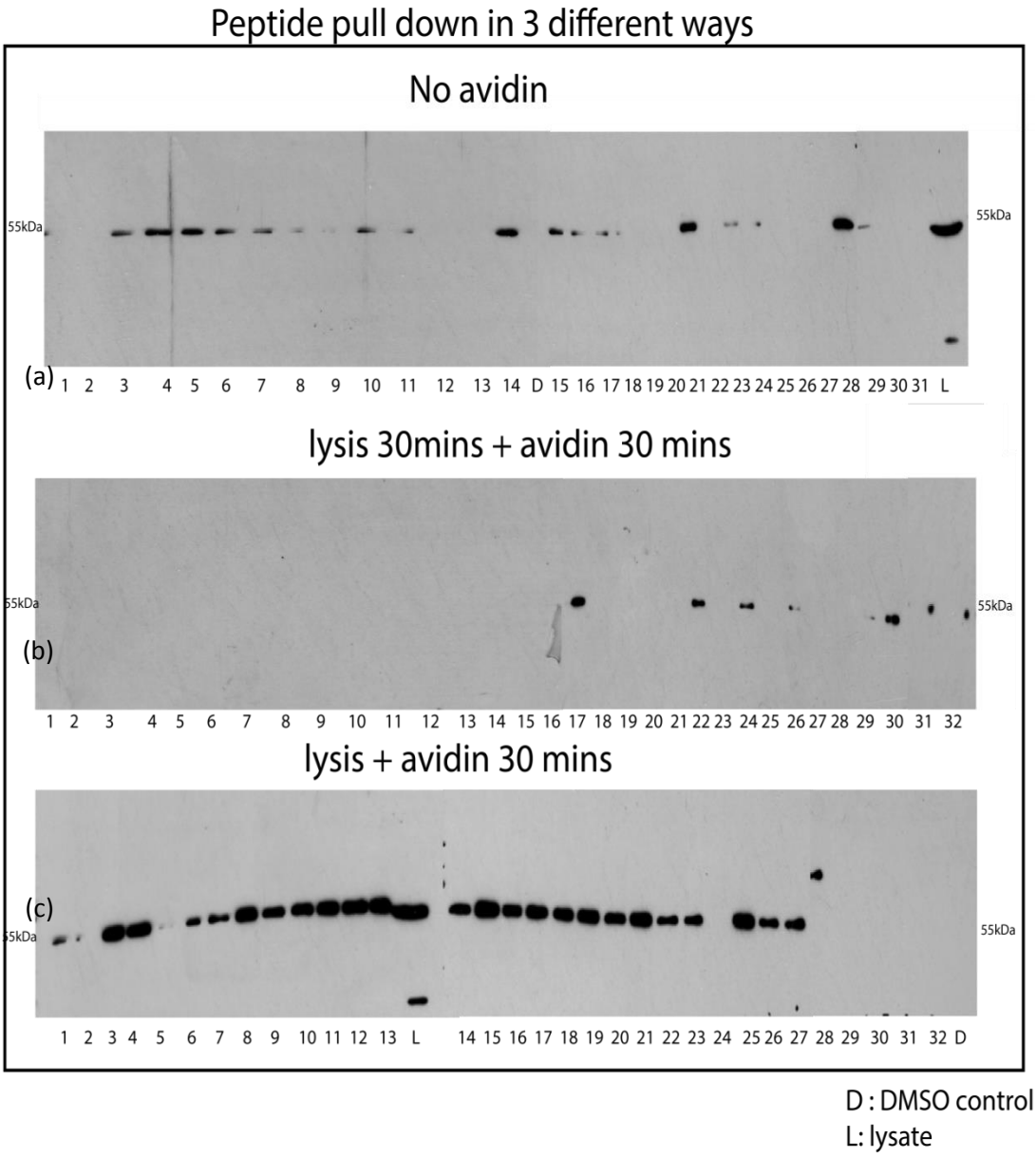

Figure 5.10: Peptide pull down assay: *(a) No pre clearing step involved in peptide pull down i.e. lysate straight away added to beads containing peptides. (b) Lysis for 30 minutes followed by pre-clearing using avidin for 30 minutes before adding to peptides, and (c) lysis together with pre-clearing for 30 minutes, followed by addition to peptides onto beads for pull down. All the samples were run on 10% SDS gel and immunoblotted for α-synuclein*

5.3. Discussion

Phage display provides a useful technique for display of numerous distinct peptides onto its surface and the process of biopanning has enabled selection of peptides binding specifically to a protein. Peptides have an advantage of greater stability as compared to antibodies and via phage display they have routinely been found with high specificity to bind to different proteins with kD values from 3 nm to 5 μM [358]. In our experiments we subjected Ph.D. 12 mer library to the process of biopanning and carried out two rounds in order to select for highly binding peptides to α-synuclein. With the availability of NGS, two rounds of panning are usually enough to identify specific binding peptides as NGS has capability of generating data using extracted DNA out of the phage pool and can also be easily interpreted. Thus we carried out two rounds for identification of all binding peptides from the library. For increasing the amount of controls in our experiment and to obtain highly specific peptides binding to α-synuclein, we performed screening in a 96 well plate that contain α-synuclein, npm, ZNF350 and reptin. The phage pools stored from each round before and after amplification of peptide sequences. The DNA from the phage pools was gel extracted, purified and total of 5 μg was sent for next generation deep sequencing. NGS is capable of analysing millions of sequences reducing the number of selection rounds required and eliminates artifacts that arise during PCR or selection process [359, 360]. Following NGS we used two different methods with help of Adam Krejci (RECAMO, Brno, Czech Republic) to isolate all binding peptides identified from screening. With advancement in NGS it is not necessary anymore to carry out more selection rounds and binding peptides can be easily found out based on its iteration number.

As shown in our experiments NGS can also be useful in identifying proteins interacting with α-synuclein and ultimately their role in PD. Using NGS we determined the iteration number for each peptide against α-synuclein and associated controls. It is important to mention here that deep sequencing of DNA from phage pools after single round of biopanning gives sufficiently positive phages. Furthermore, increasing the number of rounds on occasions possess a risk of losing some promising clones that propagate slowly [361]. Since other types of available

deep sequencing techniques have an error rate of >1%, NGS is capable of sequencing millions of peptide sequences from a single pool with minimum error. The peptides based on their iteration number were then arranged in decreasing order from top to bottom and were compared against parental library, other proteins and control. On looking at the binding ability of these peptides to α-synuclein, only one peptide SHACWWDECTGS showed binding to WT α-synuclein with no detectable activity among other peptides. Due to the presence of two cysteine residues in this peptide, we looked at the effect of strong reducing agent i.e. DTT and as expected the binding was diminished after its addition. Figure 5.11 illustrates secondary structure of SHACWWDECTGS with marked cysteine residues responsible for diminishing the activity of peptide after addition of DTT. DTT reduces the disulphide bonds and thus for this reason peptide is unable to bind to the protein.

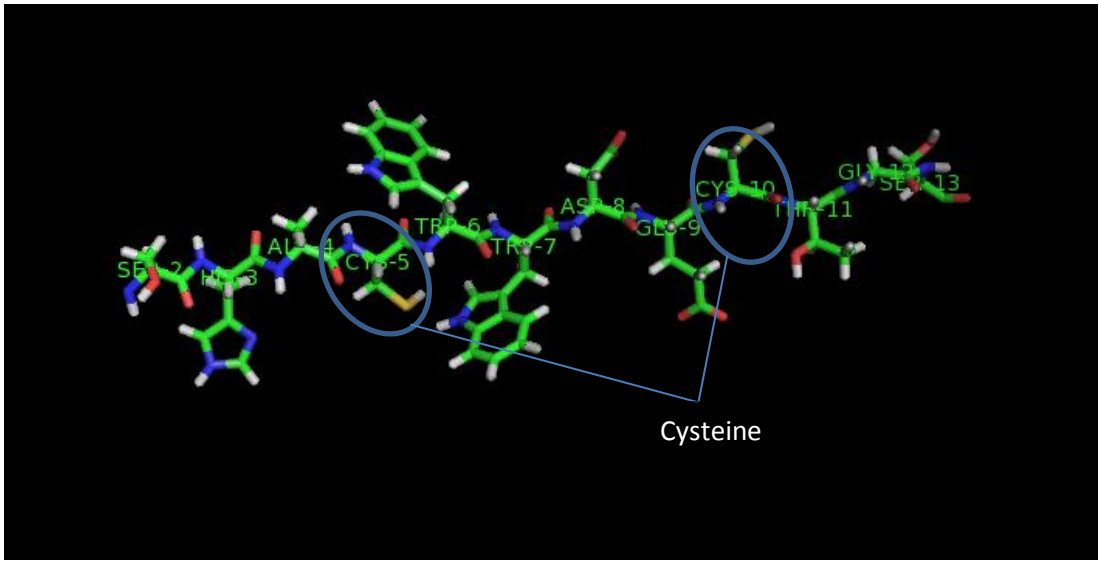

Figure 5.11: Secondary structure of SHACWWDECTGS: *Illustration of SHACWWDECTGS peptide secondary structure built using pymol.* Cysteine residues within the peptide which affect the activity of this peptide binding to α-synuclein after addition of DTT have been indicated.

Consensus sites were found after subjecting all peptides to MEME analysis and each motif containing identical sites has been shown in figure 5.5. Moreover the most common peptide obtained via both methods was 'GDGDNSVLKPGNW', however unfortunately this peptide did not bind to α-synuclein via ELISA. This phenomenon

could be due to variety of reasons such as exposure of α-synuclein in a different manner; however this peptide turned out to be a useful tool in order to identify interacting proteins. Interestingly upon scanning this peptide to BLAST analysis, this motif identified a panel of proteins that appear to be either interacting with α-synuclein or involved in ND. The list of interacting proteins is shown in table 5.5 and the sequence analysis of cloned genes along with designed primers is shown in appendix IV.

In conclusion to this chapter, we have successfully demonstrated that different stocks of same peptide library from NEB can cause substantial loss in the diversity of library. The peptide phage display screening against α-synuclein could indeed serve a dual advantage, firstly to identify peptides binding to various domains of proteins and secondly to identify interacting proteins that can assist in studying protein's role in relevant disease. As it has been shown that α-synuclein self-associates into oligomeric state and plays a key role in driving PD, it becomes a promising target for such peptide based therapies. As noticed in this chapter 15 interacting proteins were found out using a scan of a single peptide identified through screening, out of which we validated three of the interacting proteins. Thus future work of this project will focus more on identifying interacting proteins by means of identified motifs and validating them against endogenous α-synuclein. Following sufficient validation of the peptides, these tools could in turn be a useful tool in blocking several signalling pathways in PD models.

CHAPTER 6: Summary and future work

6.1. CD20 as an intriguing target in canine B cell Lymphoma

Developing biologics especially monoclonal antibodies seems to be the likely way forward to combat various diseases including cancer. The acquisition of monoclonal antibody technology by various pharmaceutical companies is an indication of continuously growing interest in the field of antibody therapeutics. Here we developed several types of tools against two totally distinct targets that behave aberrantly in two different diseases. The reason for choosing CD20 and α-synuclein as targets for therapy is their high level of expression in B cell lymphoma and Parkinson's disease respectively. CD20 is a non-glycosylated transmembrane phosphoprotein expected to display a loop of 40 amino acids between third and fourth transmembrane helical loop. Due to the well-known fact that this protein is only expressed on growing B cells and not expressed on terminally differentiating plasma cells [240], we developed antibody tools to have a net effect on CD20 expressing lymphoma cells. CD20 is mainly expressed in B cell lymphomas and not in T cell lymphoma which correlates with our finding.

It is now very well known that dogs develop cancer spontaneously in a similar manner to that of humans, for example B cell lymphoma. Rituximab is the first generation antibody approved against B cell lymphoma in humans, however it does not bind to its canine counterpart. Following Rituximab, even second generation antibodies against human CD20 have failed to bind to canine CD20. Here we develop a monoclonal antibody (NCD1.2) against canine CD20 that binds to larger loop of extracellular region and determine its binding efficiency in canine lymphoma cells, tissues via FACS, IF and IHC. Also we demonstrate NCD1.2 binds to its human counterpart by Fluorescent polarization assay, immunofluorescence, etc. Following on we also developed scFv (variable heavy and light chains) via antibody phage display in different scaffolds to increase affinity of the antibody. We also show two different kappa light chains were produced from a single hybridoma cell, this has only been reported on a single occasion previously against an anti-DNA

hybridoma. We also demonstrate the technique to obtain stable clones from the process of biopanning i.e. phage linked to scFv is stable as compared to scFv alone. We also performed bacterial as well as mammalian expression of two scFvs (3 and 7) to test the affinity of the antibody. Finally we cloned scFv into CpG2 for ADEPT cloning, carried out yeast expression and purification. As another approach we also developed recombinant IgG using scFv 3 sequences with canine Fc region to avoid any anti-canine responses and determine its binding efficacy on recombinant CD20 using IFITM1 as a negative control. One of the promising ELISA results using recombinant canine IgG onto canine extracellular CD20 using HRP conjugated anti-dog IgG as a secondary antibody is shown below (figure 6.1).

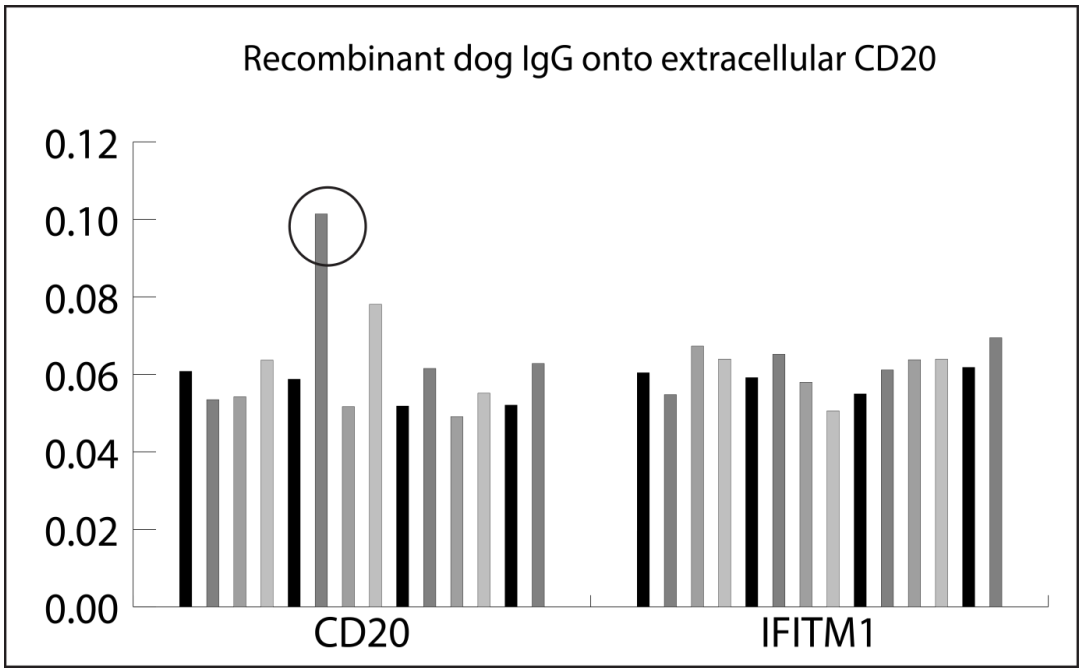

Figure 6.1: Recombinant dog IgG binding efficacy: *Recombinant IgG following expression in CHO cells onto extracellular CD20 and IFITM1 as a negative control protein. As seen above one of the clone binds better to CD20 in comparison to IFITM1.*

Thus we develop a monoclonal antibody that has promising potential for therapeutic approach for canine B cell lymphoma and hopefully could be translated into humans. Along with full length, several scaffolds of scFvs were constructed that could be useful in future for deep penetration into tissues. With such promising results we hope to take this antibody forward by caninizing followed by imaging in canine B

cell lymphoma models and determine its dosing effects from veterinary therapeutics point of view.

6.2. Biophysical studies and developing aptamers to α-synuclein

Secondly, another intriguing target chosen was α-synuclein which is known to be aberrantly expressed in PD against which antibodies have not managed to pass through the clinical trials stage due to non-availability of animal models. Infact recently α-synuclein aggregates have been found in colon biopsies of PD patients, it is proposed that protein aggregation begins before other factors become visible which in turn can serve as a diagnostic marker [362]. Since aggregation of this protein is responsible for formation of insoluble protein aggregates i.e. lewy bodies, the need for antibody targeting this protein still remains. Passive immunotherapy might indeed be the way forward for treatment of PD patients if α-synuclein is targeted at early onset of disease. To start with we cloned, expressed, purified α-synuclein and ran fractions onto native gels to determine its native state. After looking at the effect of various detergents we show that α-synuclein is collapsed after addition of SDS and runs around 140 kDa on a native gel and at 14 kDa on a 10% SDS gel. Moreover to confirm its oligomeric nature as well as secondary structure we used CD and on this basis we can conclude that this protein is structurally disordered. However, in presence of SDS α-synuclein attains helical structure. Here we developed monoclonal antibodies against α-synuclein and tested via ELISA, IHC on recombinant protein and tissues respectively (chapter 4). Such antibodies in future will be tested on PD brain tissues to visualize the binding pattern and distribution of α-synuclein throughout brain in PD patients.

For gaining deeper understanding into controversial state of α-synuclein, we developed two constructs of α-synuclein and studied them via transfection, FRET-FLIM and IF in cells. Subsequently using PLA we show that α-synuclein oligomerizes within cells, however it remains to be demonstrated if this contributes to lewy body formation within cells. We also developed peptide aptamers against α-synuclein by subjecting 12 mer Ph.D. library to the process of biopanning. Using NGS we interestingly identified peptides binding to α-synuclein via sequence sorting

in comparison to controls. Identified peptides were tested via ELISA as well as peptide binding assay onto recombinant α-synuclein and SHSY5Y cells respectively. One of the identified peptide was found to bind α-synuclein via ELISA, however no binding was reported in presence of 1 mM DTT. These above mentioned findings indicate that peptide aptamers could be useful tools with high potential that can be further translated into conjugation or cell model study.

6.3. Conclusion

In conclusion, biologics, especially antibodies and peptides have revolutionized the available treatment regimens for many diseases including cancer. For oligomerization studies, techniques such as PLA, FRET-FLIM and also developing two different constructs of target protein might prove to be efficient with significant optimizations. Similarly with advancement in screening techniques along with next generation sequencing, specific peptides binding to a protein can be identified and validated further as shown in chapter 5.

CHAPTER 7: APPENDICES

Appendix I: scFv construction

Clustalw analysis of human and canine CD20

Clustalw analysis of human and canine CD20

```
human           MTTPRNSVNGTFPAEPMKGPIAMQSGPKPLFRRMSSLVGPTQSFFMRESKTLGAVQIMNG 60
canine          MTTPRNSMSGTLPVDPMKSPTAMYPVQKIIPKRMPSVVGPTQNFFMRESKTLGAVQIMNG 60
                *******:.**:*.:***.* ** .  * : :**.*:*****.*****************

human           LFHIALGGLLMIPAGIYAPICVTVWYPLWGGIMYIISGSLLAATEKNSRKCLVKGKMIMN 120
canine          LFHIALGSLLMIHTDVCAPICITMWYPLWGGIMFIISGSLLAAADKNPRKSLVKGKMIMN 120
                *******.**** :.: ****:*:*********:*********::**.**.*********

human           SLSLFAAISGMILSIMDILNIKISHFLKMESLNFIRAHTPYINIYNCEPANPSEKNSPST 180
canine          SLSLFAAISGIIFLIMDIFNITISHFFKMENLNLIKAPMPYVDIHNCDPANPSEKNSLSI 180
                **********:*: ****:**.****:***.**:*:*  **::*:**:********* *

human           QYCYSIQSLFLGILSVMLIFAFFQELVIAGIVENEWKRTCSRPKSN-IVLLSAEEKKEQT 239
canine          QYCGSIRSVFLGVFAVMLIFAFFQKLVTAGIVENEWKKLCSKPKSDVVVLLAAEEKKEQP 240
                *** **:*:***:::*********:** *********: **:***: :***:*******.

human           IEIKEEVVGLTETSSQPKNEEDIEIIPIQEEEEEETETNFPEPPQDQESSPIENDSSP 297
canine          IETTEEMVELTEIASQPKKEEDIEIIPVQEEEGE-LEINFAEPPQEQESSPIENDSIP 297
                ** .**:* *** :****:********:**** *  * **.****:********** *
```

Biopanning (4 rounds)

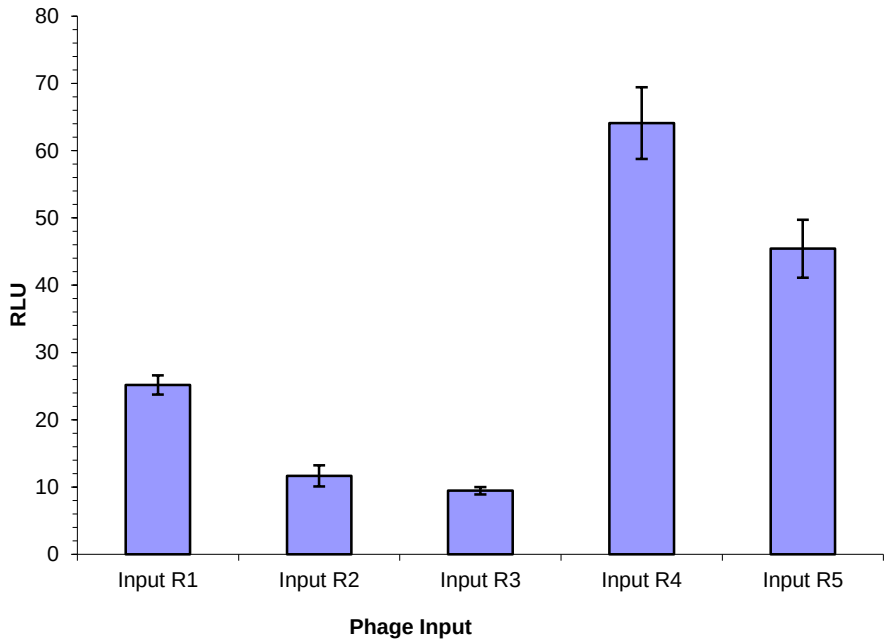

Figure 7.1: ELISA (4 rounds of biopanning): *ELISA of input phage pools obtained during 4 different rounds of biopanning onto CD20 peptide 32 coated plate*

Sequencing data obtained from antibody library from spleen

As shown in figure 3.25, two different kappa chains were isolated from anti-CD20 antibody library made using single hybridoma cell. However while sequencing clones from a library made using mouse spleen, significantly higher amount of diversity was noticed among sequences (shown below).

ELDIVMTQAAFSNPVTLGTSVSISCRSSKSLLHRNGFTYLYWYLQRPGQ
SPQLLIYQMSNLASGVPDRFSSSGSGTDFTLRISRVEAEDVGVYYCAQN
LELPFTFGGGTKLELKSSGGGGSGGGGGGSSRSSLEVNVVESGGGLVQ
PGDSLRLSCATSGFTFTDYFMSWVRQPPGKSLEWLGLIRNKVNGYTAE
YSASVKGRFTISRDNSRGILYLQMYTLRAEDSATYYCVRASTGTSFXLL
GPRDSGHCLCSXNDTPIXSLVARPASTITITMAHTRTTFPDYXS

KRQLSRXAVALAGFATVAQAAELDIVMTQAAFSNPVTLGTSVSISCRS
SKSLLHRNGFTYLYWYLQRPGQSPQLLIYQMSNLASGVPDRFSSSGSG
TDFTLRISRVEAEDVGVYYCAQNLELPFTFGGGTKLELK**SSGGGGSGG
GGGGSSRSS**LEVNVVESGGGLVQPGDSLRLSCATSGFTFTDYFMSWV
RQPPGKSLEWLGLIRNKVNGYTAEYSASVKGRFTISRDNSRGILYLQM
YTLRAEDSATYYCVRASTGTSFVYWGQGTLVTVSAAKTTPPSVTSGQ
AGQHHH

VALAGFATVAQAAELDIVMTQAAFSNPVTLGTSVSISCRSSKSLLHRNG
FTYLYWYLQRPGQSPQLLIYQMSNLASGVPDRFSSSGSGTDFTLRISRV
EAEDVGVYYCAQNLELPFTFGGGTKLELK**SSGGGGSGGGGGGSSRSS**
LEVQVVESGGGLVQPGDSLRLSCATSGFTFTDYFMSWVRQPPGKSLE
WLGLIRNKVNGYTAEYSASVKGRFTISRDNSRGILYLQMYTLRAEDSA
TYYCVRASTGTSFVYWGQGTLVTVSAAKTTPPSVTSGQAGQHHHHH

ALAGFATVAQAAELDIVMTQAAFSNPVTLGTSVSISCRSSKSLLHRNGF
TYLYWYLQRPGQSPQLLIYQMSNLASGVPDRFSSSGSGTDFTLRISRVE
AEDVGVYYCAQNLELPFTFGGGTKLEIK**SSGGGGSGGGGGGSSRSS**L
EVKLMESGGGLVQPGDSLRLSCATSGFTFTDYFMSWVRQPPGKSLEW
LGLIRNKVNGYTAEYSASVKGRFTISRDNSRGILYLQMYTLRAEDSAT
YYCVRASTGTSFVYWGQGTLVTVSAAKTTPPSVTSGQAGQHHHHH

RPSSNIVMTQAAFSNPVTLGTSVSISCRSSKSLLHRNGFTYLYWYLQRP
GQSPQLLIYQMSNLASGVPDRFSSSGSGTDFTLRISRVEAEDVGVYYCA
QNLELPFTFGGGTKLEIK**SSGGGGSGGGGGGSSRSS**LEVKLMESGGGL
VQPGDSLRLSCATSGFTFTDYFMSWVRQPPGKSLEWLGLIRNKVXGYT
AEYSASVKGRFTISRDNSRGILYLQMYTLRAEDSATYYCVRASTGTSFV
YWGQGTLVTSAATTPPSVTSGQAGHHHH

RDCSGTGWFRYRGPGGRXXHCDDAXCILQSSHSWNISFHXPAGLVRV
SYIGMASLICIXYLQRPGQSPQLXIYQMSNLASGVPDRFSSSGSGTDFTL
RISRVEAEDVGVYYCAQNLELPFTFGGGTKLEIK**SSGGGGSGGGGGG**
SSRSSLEVKLMESGGGLVQPGDSLRLSCATSGFTFTDYFMSWVRQPPG
KSLEWLGLIRNKVNGYTAEYSASVKGRFTISRDNSRGILYLQMYTLRA
EDSATYYCVRASTGTSFVYWGQGTLVTVSAAKTTAPSVTSGQAGQHH
HHH

Appendix II: Recombinant dog IgG activity

Cloning of scFv into CpG2 construct for ADEPT

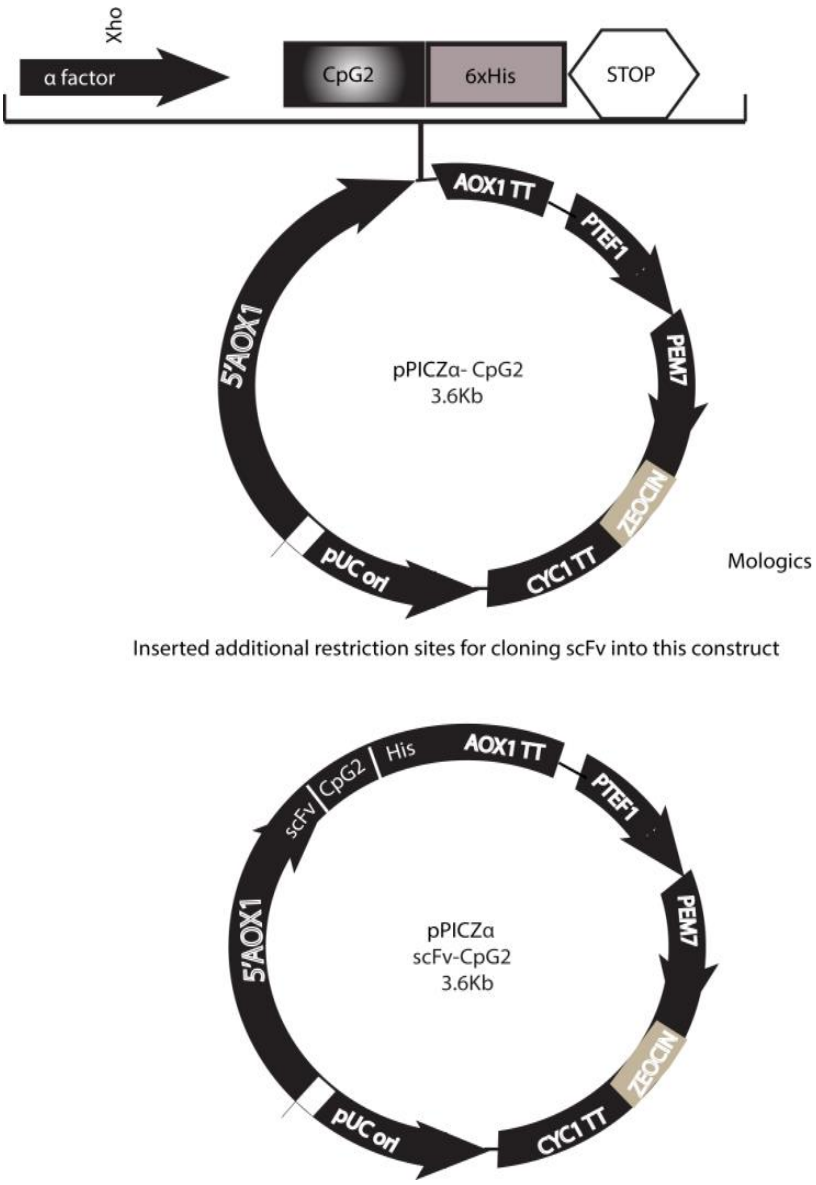

Figure 7.2: Vector construction (Mologics): *pICZα vector (3.6kb) construction for cloning of scFv.CpG2 by addition of XhoI site in collaboration with Mologics.*

Recombinant IgG (dog Fc) onto CD20 peptide (32 and 38)

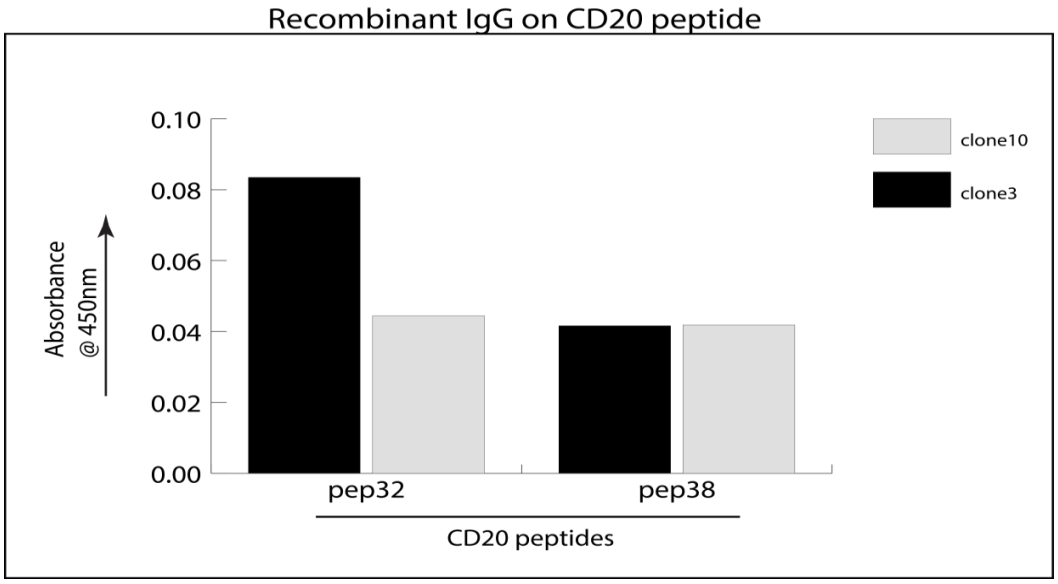

Figure 7.3: Dog IgG ELISA: *Binding efficiency of two isolated clones of recombinant dog IgG was estimated via ELISA using TMB as a substrate solution onto ELISA plate coated with CD20 peptide (32 and 38).*

Appendix III: Transfection of protein constructs identified through phage display

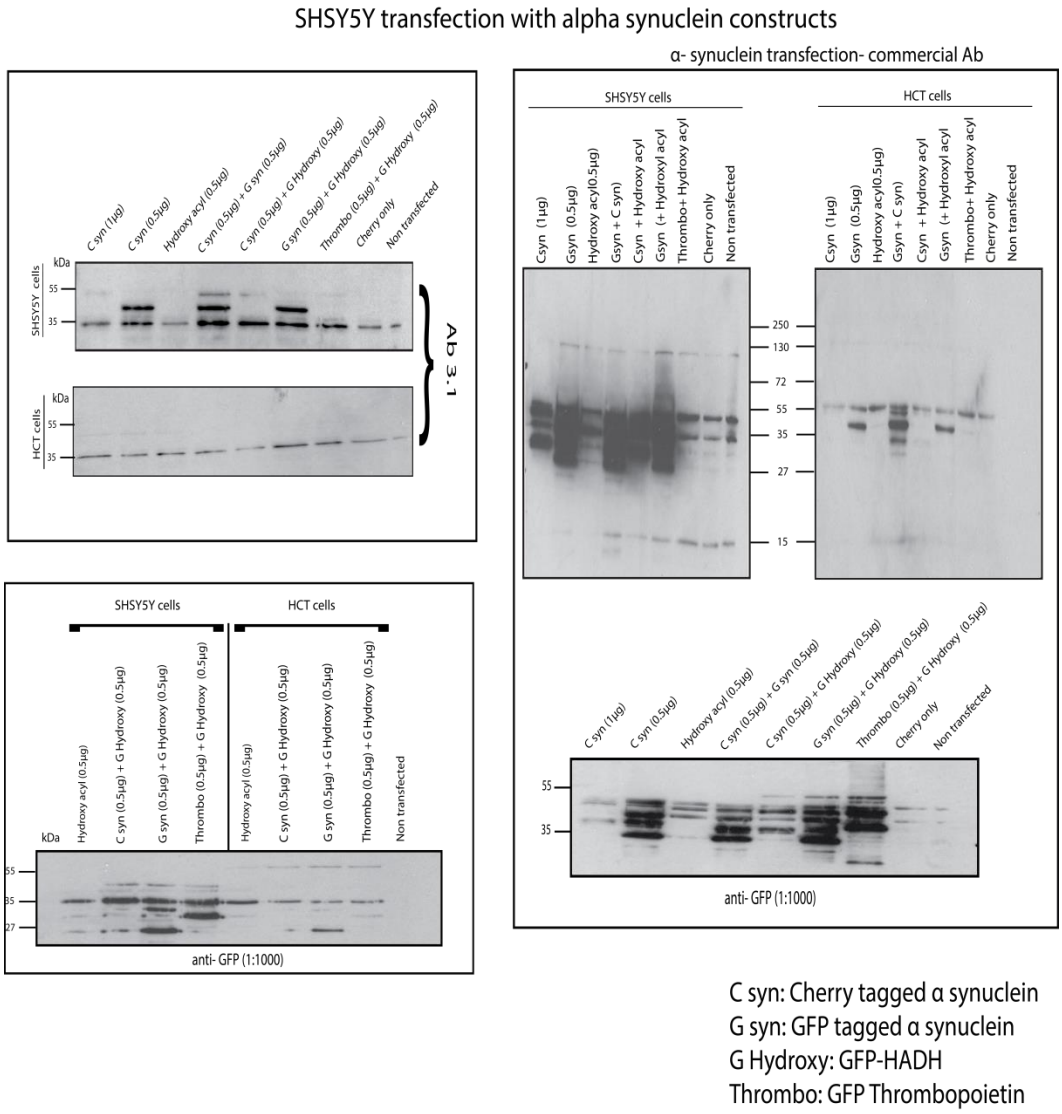

Figure 7.4: Identified protein constructs transfection: *Transfection of proteins (thrombopoietin, GAP, HADH and α-synuclein) identified via BLAST scanning of peptide sequence into SHSY5Y and HCT116^{+} cells.*

Appendix IV: Peptide phage display screening identified peptides

Identified peptides following MEME (whole)

identified motifs	Phage Library	Control FR1a	Control FR2	Control SR1a	Control SR2	Syn FR1a	Syn FR2	Syn SR1a	Syn SR2
GDGNSVLKPGNW	197	131	537	373	530	86	684	27515	5913
GDGNSVLKQGNW	0	1	1	0	0	0	1	19	9
GDGNSVMKPGNW	0	0	1	1	0	0	1	21	9
GDGNQVLKPGNW	0	0	2	1	1	0	0	20	7
GDGNWVLKPGNW	0	0	2	1	1	0	0	20	7
GDGNSMLKPGNW	0	0	0	0	0	0	0	5	1
GDGNSALKPGNW	0	0	1	1	1	0	0	24	6
GDGNSVLKPGNC	0	0	0	0	0	0	0	28	1
GDGNSELKPGNW	0	0	0	0	0	0	0	9	3
GDGNSVLKAGNW	0	0	1	0	0	0	1	16	1
GDDNSVLKPGNW	0	0	0	0	0	0	0	2	1
GDGNSVLKTGNW	0	0	0	0	0	0	5	32	12
GDGNSVLKPGDW	1	0	3	0	1	0	1	65	12
WDGNSVLKPGNW	0	1	1	0	0	0	0	12	3
GDGNSVLKPWNW	0	0	0	0	0	0	0	11	1
GDGNSLLKPGNW	0	0	3	0	0	0	2	19	7
GDGNSGLKPGNW	0	0	0	0	1	0	0	38	7
GDGNSVLKLGNW	0	0	0	0	0	0	0	11	1
GDGNSVLKPGIW	0	0	0	0	0	0	0	5	1
GDGNSVLKSGNW	0	0	0	0	1	0	0	25	1
GDVNSVLKPGNW	0	0	0	0	0	1	1	18	5
GDGNSVLKPGHW	0	1	2	0	3	0	3	85	21
GDGNSVLKPVNW	0	0	0	0	0	0	1	11	4
VDGNSVLKPGNW	0	1	0	1	1	0	1	4	3
GYGNSVLKPGNW	1	0	2	1	0	0	2	27	8
GDGNSVLKPGYW	0	0	1	0	1	0	2	66	11
GDSNSVLKPGNW	0	0	0	1	0	0	0	4	1
GDGNSVLKPGNQ	0	0	0	0	0	0	0	7	2
GDGNSVLKPGSW	0	0	2	0	0	0	1	5	1
GDGNSVLKPGTW	0	0	0	0	0	0	1	8	3
GDGTSVLKPGNW	0	0	0	0	0	0	0	3	2
GAGNSVLKPGNW	0	1	1	0	0	0	0	23	8
GDGNSVLKPGNL	1	0	0	1	0	0	0	21	3
GVGNSVLKPGNW	0	0	1	0	0	0	1	22	5
GGGNSVLKPGNW	0	0	0	0	0	0	0	12	1
GDGNSVLQPGNW	0	0	0	0	0	0	0	18	2

GDGNSVLNPGNW	0	0	2	1	0	0	0	19	8
GDGNSVLTPGNW	0	0	0	0	0	0	0	5	1
GDGNSGLKPGDW	0	0	0	0	0	0	0	4	1
EITHPGWSTVTH	356	295	1500	759	1067	799	2115	16146	4264
EITHPCWSTVTH	0	0	2	0	1	1	0	17	7
EITHPGWQTVTH	0	0	1	1	1	2	3	14	5
EITHPGWSTVMH	0	1	1	0	1	0	5	7	7
EITHPGWSTVKH	1	0	2	3	0	1	4	26	2
EITHPGWSTVTQ	0	0	0	1	0	0	1	4	1
EITHPGWATVTH	0	0	1	0	0	0	0	16	3
EITYPGWSTVTH	0	0	0	0	0	0	0	1	1
EIIHPGWSTVTH	0	0	0	1	0	0	0	5	1
EITHPGWSTVTY	0	0	0	0	1	1	0	3	2
EITHPGWSNVTH	0	0	3	0	2	6	1	20	5
EITHPGWSTVRH	0	0	0	0	0	0	1	2	1
EITHPGWSTATH	0	0	0	1	0	1	1	3	3
EITHPGWPTVTH	0	0	1	0	0	0	0	5	1
EINHPGWSTVTH	1	0	2	0	1	0	2	16	10
EITHPGWSTVSH	0	0	1	1	0	0	2	13	1
EITNPGWSTVTH	0	1	1	2	1	0	2	12	4
EFTHPGWSTVTH	0	0	0	1	0	0	1	5	1
EITHPGWSSVTH	0	0	0	0	0	0	1	6	2
EITHHGWSTVTH	1	1	0	0	0	0	1	11	5
EITHTGWSTVTH	0	0	8	0	1	1	4	12	7
EITHPGWSTVPH	0	0	0	0	1	0	1	4	3
EITHLGWSTVTH	1	0	0	1	2	0	1	9	2
EITHPGWSTLTH	0	0	1	1	1	2	5	11	5
EITHSGWSTVTH	0	0	0	0	0	1	2	4	1
EITHPVWSTVTH	0	0	2	0	0	0	4	14	8
EITHPGWSTGTH	0	0	1	0	1	0	2	5	4
EITHPGWSTVTL	0	0	0	0	0	0	1	10	1
EITHPGWSTVTP	0	0	1	4	0	0	3	14	4
EITHPGLSTVTH	1	0	1	1	1	1	1	16	6
DITHPGWSTVTH	0	0	1	1	2	1	3	16	7
QITHPGWSTVTH	1	0	0	1	0	1	6	14	2
AITHPGWSTVTH	0	0	0	0	0	0	1	5	2
SSWWHHLVADRV	32	16	202	66	185	9	159	2474	2263
SIWWHHLVADRV	0	0	0	0	0	0	0	3	2
SSWWHHLAADRV	1	0	0	0	0	0	1	3	6
SSWWHHLVADRA	1	0	0	0	1	0	0	11	4
SSWWHHLEADRV	0	0	0	0	0	0	0	2	4
SSWWHHLVADRF	0	0	0	0	0	0	0	6	5
SSWWHNLVADRV	0	0	0	0	0	0	0	5	1

SSWCHHLVADRV	0	0	0	0	2	0	0	4	6
SSWWNHLVADRV	0	1	0	0	1	0	0	4	5
SSWWHHLVSDRV	1	0	0	0	0	0	0	1	1
SSWWHHLVADMV	0	0	0	0	0	0	0	2	4
SSWWHHLVAYRV	0	0	0	0	0	0	0	4	1
SSWWHHLGADRV	0	0	0	0	0	0	1	5	6
SSWWHHLVADRG	2	0	0	2	2	2	1	37	31
SSWWHLLVADRV	0	0	0	0	0	0	1	2	3
SSWWHHLVAARV	0	0	0	1	0	0	0	9	7
SSWWHHLVAVRV	0	0	3	0	0	0	0	6	9
SSWWHHLVAGRV	0	0	1	0	1	0	1	11	6
SSWRHHLVADRV	0	0	0	0	0	0	0	5	3
SSWLHHLVADRV	0	0	0	1	0	0	0	2	6
SSWGHHLVADRV	0	0	0	0	1	0	0	3	1
SALKGLFPADHH	124	104	733	219	493	2974	1826	3268	1127
SALKGLFPADYH	0	0	0	1	0	5	3	6	2
SALKGLFLADHH	0	0	1	0	0	2	0	4	1
SALKVLFPADHH	0	0	1	1	0	8	7	4	2
SALNGLFPADHH	0	0	0	1	1	0	5	4	2
MADVRHPGGFFF	0	0	0	0	0	0	1	6	1
MADVRHPGDFFF	0	0	0	0	1	0	0	21	4
MADVRHPGGFLF	2	0	1	0	2	0	2	73	29
MADVRHPGDFLF	3	2	13	3	11	0	5	315	99
HIGTVTSWLRPD	6	10	43	30	35	5	41	1163	412
HIGKVTSWLRPD	0	0	0	0	0	0	0	3	1
HIGTVTSWLRHD	0	0	0	0	0	0	0	2	2
HIVTVTSWLRPD	0	0	0	0	0	0	0	4	2
HIGTVTSWLLPD	0	0	0	0	0	0	0	5	2
SMGPNTSYSLAH	38	21	69	53	61	8	125	1808	380
SMGPNTSYILAH	0	0	0	0	0	0	0	5	2
SMWPNTSYSLAH	0	0	0	0	0	0	0	3	1
SMGPNTSYSLAP	0	0	0	0	0	0	0	3	1
EDLRKEFSRLVD	0	0	0	0	0	0	0	1	2
EDLRKEASRLVD	0	0	0	0	0	0	1	5	1
EDLRKESSRLVD	24	12	41	43	42	7	33	477	110
SQLKPILAWAN	20	9	42	34	44	7	42	1403	456
SQLKPILAWEN	0	0	0	0	0	0	3	5	1
SECKATCQAIN	2	1	0	3	1	1	1	57	4
GGQIPYLKLGA	0	0	0	0	0	0	0	1	3

Table 7.1: Comparison of identified peptides: *Specific peptides identified by phage display screening against α-synuclein in slow (SR) as well as fast washes (FR). Next generation deep sequencing was used to obtain the iteration number of each peptide in the parental library and against the protein.*

Gene sequences with designed primers (peptide phage display)

Thrombopoietin receptor precursor- 635a.a

MPSWALFMVTSCLLLAPQNLAQVSSQDVSLLASDSEPLKCFSRTFEDLTCFW
DEEEAAPSGTYQLLYAYPREKPRACPLSSQSMPHFGTRYVCQFPDQEEVRLF
FPLHLWVKNVFLNQTRTQRVLFVDSVGLPAPPSIIKAMGGSQPGELQISWEEP
APEISDFLRYELRYGPRDPKNSTGPTVIQLIATETCCPALQRPHSASALDQSPC
AQPTMPWQDGPKQTSPSREASALTAEGGSCLISGLQPGNSYWLQLRSEPDGI
SLGGSWGSWSLPVTVDLPGDAVALGLQCFTLDLKNVTCQWQQQDHASSQG
FFYHSRARCCPRDRYPIWENCEEEEKTNPGLQTPQFSRCHFKSRNDSIIHILVE
VTTAPGTVHSYLGSPFWIHQAVRLPTPNLHWREISSGHLELEWQHPSSWAAQ
ETCYQLRYTGEGHQDWKVLEPPLGARGGTLELRPRSRYRLQLRARLNGPTY
QGPWSSWSDPTRVETATETAWISLVTALHLVLGLSAVLGLLLLRWQFPAHY
RRLRHALWPSLPDLHRVLGQYLRDTAALSPPKATVSDTCEEVEPSLLEILPKS
SERTPLPLCSSQAQMDYRRLQPSCLGTMPLSVCPPMAESGSCCTTHIANHSY
LPLSYWQQP

Forward primer (XhoI)

5’ ATGCCCTCCTGGGCCCTC 3’

Reverse primer (SacII)

5’ CCGCGGTATTGGCAGCAG 3’

Hydroxyl-coenzyme A dehydrogenase, mitochondrial isoform 1 precursor- 331a.a

MAFVTRQFMRSVSSSSTASASAKKIIVKHVTVIGGGLMGAGIAQVAAATGHT
VVLVDQTEDILAKSKKGIEESLRKVAKKKFAENLKAGDEFVEKTLSTIATST
DAASVVHSTDLVVEAIVENLKVKNELFKRLDKFAAEHTIFASNTSSLQITSIA
NATTRQDRFAGLHFFNPVPVMKLVEVIKTPMTSQKTFESLVDFSKALGKHPV
SCKDTPGFIVNRLLVPYLMEAIRLYERDFQTCGDSNSGLGFSLKGDASKEDID
TAMKLGAGYPMGPFELLDYVGLDTTKFIVDGWHEMDAENPLHQPSPSLNKL
VAENKFGKKTGEGFYKYK

Forward primer: Xho1

CTCGAGATGGCCTTCGTCACCAGG

Reverse primer: SacII

5’ CCGCGGCTTGTATTTGTAAAATCC 3’

Gap junction beta 4 protein-266a.a

MNWAFLQGLLSGVNKYSTVLSRIWLSVVFIFRVLVYVVAAEEVWDDEQKD
FVCNTKQPGCPNVCYDEFFPVSHVRLWALQLILVTCPSLLVVMHVAYREER
ERKHHLKHGPNAPSLYDNLSKKRGGLWWTYLLSLIFKAAVDAGFLYIFHRL
YKDYDMPRVVACSVEPCPHTVDCYISRPTEKKVFTYFMVTTAAICILLNLSE
VFYLVGKRCMEIFGPRHRRPRCRECLPDTCPPYVLSQGGHPEDGNSVLMKA
GSAPVDAGGYP

Forward primer: XhoI

CTCGAGATGAACTGGGCATTTCTG

Reverse primer: SacII

5’ CCGCGGTGGATACCCACCTGCATC 3’

CHAPTER 8: Bibliography

1. Ueda, K., T. Saitoh, and H. Mori, *Tissue-dependent alternative splicing of mRNA for NACP, the precursor of non-A beta component of Alzheimer's disease amyloid.* Biochem Biophys Res Commun, 1994. **205**(2): p. 1366-72.
2. Jakes, R., M.G. Spillantini, and M. Goedert, *Identification of two distinct synucleins from human brain.* FEBS Lett, 1994. **345**(1): p. 27-32.
3. Lavedan, C., et al., *Identification, localization and characterization of the human gamma-synuclein gene.* Hum Genet, 1998. **103**(1): p. 106-12.
4. Adams, G.P. and L.M. Weiner, *Monoclonal antibody therapy of cancer.* Nat Biotechnol, 2005. **23**(9): p. 1147-57.
5. Baumann, A., *Early development of therapeutic biologics--pharmacokinetics.* Curr Drug Metab, 2006. **7**(1): p. 15-21.
6. Ruigrok, V.J., et al., *Alternative affinity tools: more attractive than antibodies?* Biochem J, 2011. **436**(1): p. 1-13.
7. Dauer, W. and S. Przedborski, *Parkinson's disease: mechanisms and models.* Neuron, 2003. **39**(6): p. 889-909.
8. Johnson, I.S., *Human insulin from recombinant DNA technology.* Science, 1983. **219**(4585): p. 632-7.
9. Tang, L., et al., *Pharmacokinetic aspects of biotechnology products.* J Pharm Sci, 2004. **93**(9): p. 2184-204.
10. Crommelin, D.J., et al., *Shifting paradigms: biopharmaceuticals versus low molecular weight drugs.* Int J Pharm, 2003. **266**(1-2): p. 3-16.
11. Malik, N.N., *Controlling the cost of innovative cancer therapeutics.* Nat Rev Clin Oncol, 2009. **6**(9): p. 550-2.
12. Till, S.J., et al., *Mechanisms of immunotherapy.* J Allergy Clin Immunol, 2004. **113**(6): p. 1025-34.
13. Waldmann, T.A., *Immunotherapy: past, present and future.* Nat Med, 2003. **9**(3): p. 269-77.
14. Chambers, C.A., et al., *CTLA-4-mediated inhibition in regulation of T cell responses: mechanisms and manipulation in tumor immunotherapy.* Annu Rev Immunol, 2001. **19**: p. 565-94.
15. Kreitman, R.J., et al., *Phase I trial of recombinant immunotoxin anti-Tac(Fv)-PE38 (LMB-2) in patients with hematologic malignancies.* J Clin Oncol, 2000. **18**(8): p. 1622-36.
16. Kim, P.S., et al., *Antibody association with HER-2/neu-targeted vaccine enhances CD8 T cell responses in mice through Fc-mediated activation of DCs.* J Clin Invest, 2008. **118**(5): p. 1700-11.
17. Beck, A., et al., *Strategies and challenges for the next generation of therapeutic antibodies.* Nat Rev Immunol, 2010. **10**(5): p. 345-52.
18. Storey, S., *Respiratory syncytial virus market*: Nat Rev Drug Discov. 2010 Jan;9(1):15-6. doi: 10.1038/nrd3075.
19. Strohl, W.R., *Optimization of Fc-mediated effector functions of monoclonal antibodies.* Curr Opin Biotechnol, 2009. **20**(6): p. 685-91.
20. Oflazoglu, E. and L.P. Audoly, *Evolution of anti-CD20 monoclonal antibody therapeutics in oncology.* MAbs, 2010. **2**(1): p. 14-9.

21. Kohler, G. and C. Milstein, *Continuous cultures of fused cells secreting antibody of predefined specificity.* Nature, 1975. **256**(5517): p. 495-7.
22. Salvana, E.M. and R.A. Salata, *Infectious complications associated with monoclonal antibodies and related small molecules.* Clin Microbiol Rev, 2009. **22**(2): p. 274-90.
23. Scott, A.M., et al., *A phase I clinical trial with monoclonal antibody ch806 targeting transitional state and mutant epidermal growth factor receptors.* Proc Natl Acad Sci U S A, 2007. **104**(10): p. 4071-6.
24. Hughes, B., *Antibody-drug conjugates for cancer: poised to deliver?*: Nat Rev Drug Discov. 2010 Sep;9(9):665-7. doi: 10.1038/nrd3270.
25. Weiner, L.M., R. Surana, and S. Wang, *Monoclonal antibodies: versatile platforms for cancer immunotherapy.* Nat Rev Immunol, 2010. **10**(5): p. 317-27.
26. Cohen, S., *Structure of antibody molecules.* Nature, 1967. **214**: p. 449-541.
27. Angal, S., et al., *A single amino acid substitution abolishes the heterogeneity of chimeric mouse/human (IgG4) antibody.* Mol Immunol, 1993. **30**(1): p. 105-8.
28. Press, M.F., C. Cordon-Cardo, and D.J. Slamon, *Expression of the HER-2/neu proto-oncogene in normal human adult and fetal tissues.* Oncogene, 1990. **5**(7): p. 953-62.
29. Slamon, D.J., et al., *Human breast cancer: correlation of relapse and survival with amplification of the HER-2/neu oncogene.* Science, 1987. **235**(4785): p. 177-82.
30. Courtenay-Luck, N.S., et al., *Development of primary and secondary immune responses to mouse monoclonal antibodies used in the diagnosis and therapy of malignant neoplasms.* Cancer Res, 1986. **46**(12 Pt 1): p. 6489-93.
31. Schroff, R.W., et al., *Human anti-murine immunoglobulin responses in patients receiving monoclonal antibody therapy.* Cancer Res, 1985. **45**(2): p. 879-85.
32. Shawler, D.L., et al., *Human immune response to multiple injections of murine monoclonal IgG.* J Immunol, 1985. **135**(2): p. 1530-5.
33. Ober, R.J., et al., *Differences in promiscuity for antibody-FcRn interactions across species: implications for therapeutic antibodies.* Int Immunol, 2001. **13**(12): p. 1551-9.
34. Morrison, S.L., et al., *Chimeric human antibody molecules: mouse antigen-binding domains with human constant region domains.* Proc Natl Acad Sci U S A, 1984. **81**(21): p. 6851-5.
35. Riechmann, L., et al., *Reshaping human antibodies for therapy.* Nature, 1988. **332**(6162): p. 323-7.
36. Jones, P.T., et al., *Replacing the complementarity-determining regions in a human antibody with those from a mouse.* Nature, 1986. **321**(6069): p. 522-5.
37. Boulianne, G.L., N. Hozumi, and M.J. Shulman, *Production of functional chimaeric mouse/human antibody.* Nature, 1984. **312**(5995): p. 643-6.
38. Hoogenboom, H.R., et al., *Multi-subunit proteins on the surface of filamentous phage: methodologies for displaying antibody (Fab) heavy and light chains.* Nucleic Acids Res, 1991. **19**(15): p. 4133-7.
39. Chao, G., et al., *Isolating and engineering human antibodies using yeast surface display.* Nat Protoc, 2006. **1**(2): p. 755-68.

40. Yau, K.Y., et al., *Selection of hapten-specific single-domain antibodies from a non-immunized llama ribosome display library.* J Immunol Methods, 2003. **281**(1-2): p. 161-75.
41. Boss, M.A., et al., *Assembly of functional antibodies from immunoglobulin heavy and light chains synthesised in E. coli.* Nucleic Acids Res, 1984. **12**(9): p. 3791-806.
42. Holliger, P. and P.J. Hudson, *Engineered antibody fragments and the rise of single domains.* Nat Biotechnol, 2005. **23**(9): p. 1126-36.
43. Chapman, A.P., et al., *Therapeutic antibody fragments with prolonged in vivo half-lives.* Nat Biotechnol, 1999. **17**(8): p. 780-3.
44. Stork, R., et al., *N-glycosylation as novel strategy to improve pharmacokinetic properties of bispecific single-chain diabodies.* J Biol Chem, 2008. **283**(12): p. 7804-12.
45. Constantinou, A., et al., *Modulation of antibody pharmacokinetics by chemical polysialylation.* Bioconjug Chem, 2008. **19**(3): p. 643-50.
46. Simmons, L.C., et al., *Expression of full-length immunoglobulins in Escherichia coli: rapid and efficient production of aglycosylated antibodies.* J Immunol Methods, 2002. **263**(1-2): p. 133-47.
47. Cabilly, S., et al., *Generation of antibody activity from immunoglobulin polypeptide chains produced in Escherichia coli.* Proc Natl Acad Sci U S A, 1984. **81**(11): p. 3273-7.
48. Skerra, A. and A. Pluckthun, *Assembly of a functional immunoglobulin Fv fragment in Escherichia coli.* Science, 1988. **240**(4855): p. 1038-41.
49. Better, M., et al., *Escherichia coli secretion of an active chimeric antibody fragment.* Science, 1988. **240**(4855): p. 1041-3.
50. de Marco, A., *Strategies for successful recombinant expression of disulfide bond-dependent proteins in Escherichia coli.* Microb Cell Fact, 2009. **8**(26): p. 1475-2859.
51. Wieland, W.H., et al., *Display and selection of chicken IgA Fab fragments.* Vet Immunol Immunopathol, 2006. **110**(1-2): p. 129-40.
52. Sheikholvaezin, A., et al., *Optimizing the generation of recombinant single-chain antibodies against placental alkaline phosphatase.* Hybridoma, 2006. **25**(4): p. 181-92.
53. Takemura, S., et al., *Construction of a diabody (small recombinant bispecific antibody) using a refolding system.* Protein Eng, 2000. **13**(8): p. 583-8.
54. Nelson, A.L., *Antibody fragments: hope and hype.* MAbs, 2010. **2**(1): p. 77-83.
55. Jostock, T., et al., *Rapid generation of functional human IgG antibodies derived from Fab-on-phage display libraries.* J Immunol Methods, 2004. **289**(1-2): p. 65-80.
56. Flanagan, R.J. and A.L. Jones, *Fab antibody fragments: some applications in clinical toxicology.* Drug Saf, 2004. **27**(14): p. 1115-33.
57. Whitlow, M., et al., *An improved linker for single-chain Fv with reduced aggregation and enhanced proteolytic stability.* Protein Eng, 1993. **6**(8): p. 989-95.
58. Horton, R.M., et al., *Engineering hybrid genes without the use of restriction enzymes: gene splicing by overlap extension.* Gene, 1989. **77**(1): p. 61-8.

59. Lilley, G.G., et al., *Recombinant single-chain antibody peptide conjugates expressed in Escherichia coli for the rapid diagnosis of HIV.* J Immunol Methods, 1994. **171**(2): p. 211-26.
60. Jain, M., N. Kamal, and S.K. Batra, *Engineering antibodies for clinical applications.* Trends Biotechnol, 2007. **25**(7): p. 307-16.
61. Kortt, A.A., et al., *Single-chain Fv fragments of anti-neuraminidase antibody NC10 containing five- and ten-residue linkers form dimers and with zero-residue linker a trimer.* Protein Eng, 1997. **10**(4): p. 423-33.
62. Atwell, J.L., et al., *scFv multimers of the anti-neuraminidase antibody NC10: length of the linker between VH and VL domains dictates precisely the transition between diabodies and triabodies.* Protein Eng, 1999. **12**(7): p. 597-604.
63. Dolezal, O., et al., *ScFv multimers of the anti-neuraminidase antibody NC10: shortening of the linker in single-chain Fv fragment assembled in V(L) to V(H) orientation drives the formation of dimers, trimers, tetramers and higher molecular mass multimers.* Protein Eng, 2000. **13**(8): p. 565-74.
64. Ahmad, Z.A., et al., *scFv antibody: principles and clinical application.* Clin Dev Immunol, 2012. **980250**(10): p. 15.
65. Smith, G.P., *Filamentous fusion phage: novel expression vectors that display cloned antigens on the virion surface.* Science, 1985. **228**(4705): p. 1315-7.
66. McCafferty, J., et al., *Phage antibodies: filamentous phage displaying antibody variable domains.* Nature, 1990. **348**(6301): p. 552-4.
67. Rader, C. and C.F. Barbas, 3rd, *Phage display of combinatorial antibody libraries.* Curr Opin Biotechnol, 1997. **8**(4): p. 503-8.
68. Clackson, T., et al., *Making antibody fragments using phage display libraries.* Nature, 1991. **352**(6336): p. 624-8.
69. Marks, J.D., et al., *By-passing immunization: building high affinity human antibodies by chain shuffling.* Biotechnology, 1992. **10**(7): p. 779-83.
70. Davies, E.L., et al., *Selection of specific phage-display antibodies using libraries derived from chicken immunoglobulin genes.* J Immunol Methods, 1995. **186**(1): p. 125-35.
71. Yamanaka, H.I., T. Inoue, and O. Ikeda-Tanaka, *Chicken monoclonal antibody isolated by a phage display system.* J Immunol, 1996. **157**(3): p. 1156-62.
72. Barbas, C.F., 3rd, et al., *Molecular profile of an antibody response to HIV-1 as probed by combinatorial libraries.* J Mol Biol, 1993. **230**(3): p. 812-23.
73. Cai, X. and A. Garen, *Anti-melanoma antibodies from melanoma patients immunized with genetically modified autologous tumor cells: selection of specific antibodies from single-chain Fv fusion phage libraries.* Proc Natl Acad Sci U S A, 1995. **92**(14): p. 6537-41.
74. Kettleborough, C.A., et al., *Isolation of tumor cell-specific single-chain Fv from immunized mice using phage-antibody libraries and the re-construction of whole antibodies from these antibody fragments.* Eur J Immunol, 1994. **24**(4): p. 952-8.
75. Chester, K.A., et al., *Phage libraries for generation of clinically useful antibodies.* Lancet, 1994. **343**(8895): p. 455-6.

76. Arbabi Ghahroudi, M., et al., *Selection and identification of single domain antibody fragments from camel heavy-chain antibodies.* FEBS Lett, 1997. **414**(3): p. 521-6.
77. Hoogenboom, H.R., *Overview of antibody phage-display technology and its applications.* Methods Mol Biol, 2002. **178**: p. 1-37.
78. Marks, J.D., et al., *By-passing immunization. Human antibodies from V-gene libraries displayed on phage.* J Mol Biol, 1991. **222**(3): p. 581-97.
79. Nelson, B. and S.S. Sidhu, *Synthetic antibody libraries.* Methods Mol Biol, 2012. **899**: p. 27-41.
80. Chothia, C., et al., *Conformations of immunoglobulin hypervariable regions.* Nature, 1989. **342**(6252): p. 877-83.
81. Hawkins, R.E., S.J. Russell, and G. Winter, *Selection of phage antibodies by binding affinity. Mimicking affinity maturation.* J Mol Biol, 1992. **226**(3): p. 889-96.
82. Crameri, A., S. Cwirla, and W.P. Stemmer, *Construction and evolution of antibody-phage libraries by DNA shuffling.* Nat Med, 1996. **2**(1): p. 100-2.
83. Virnekas, B., et al., *Trinucleotide phosphoramidites: ideal reagents for the synthesis of mixed oligonucleotides for random mutagenesis.* Nucleic Acids Res, 1994. **22**(25): p. 5600-7.
84. Wu, A.M., et al., *Tumor localization of anti-CEA single-chain Fvs: improved targeting by non-covalent dimers.* Immunotechnology, 1996. **2**(1): p. 21-36.
85. Wu, A.M., et al., *High-resolution microPET imaging of carcinoembryonic antigen-positive xenografts by using a copper-64-labeled engineered antibody fragment.* Proc Natl Acad Sci U S A, 2000. **97**(15): p. 8495-500.
86. Adams, G.P., et al., *Delivery of the alpha-emitting radioisotope bismuth-213 to solid tumors via single-chain Fv and diabody molecules.* Nucl Med Biol, 2000. **27**(4): p. 339-46.
87. Napier, M.P., et al., *Antibody-directed enzyme prodrug therapy: efficacy and mechanism of action in colorectal carcinoma.* Clin Cancer Res, 2000. **6**(3): p. 765-72.
88. Kreitman, R.J., *Immunotoxins in cancer therapy.* Curr Opin Immunol, 1999. **11**(5): p. 570-8.
89. Graff, C.P. and K.D. Wittrup, *Theoretical analysis of antibody targeting of tumor spheroids: importance of dosage for penetration, and affinity for retention.* Cancer Res, 2003. **63**(6): p. 1288-96.
90. Kobayashi, N., et al., *Generation of a single-chain Fv fragment for the monitoring of deoxycholic acid residues anchored on endogenous proteins.* Steroids, 2005. **70**(4): p. 285-94.
91. Galeffi, P., et al., *Functional expression of a single-chain antibody to ErbB-2 in plants and cell-free systems.* J Transl Med, 2006. **4**: p. 39.
92. Shadidi, M. and M. Sioud, *An anti-leukemic single chain Fv antibody selected from a synthetic human phage antibody library.* Biochem Biophys Res Commun, 2001. **280**(2): p. 548-52.
93. He, J., et al., *Construction and preliminary screening of a human phage single-chain antibody library associated with gastric cancer.* J Surg Res, 2002. **102**(2): p. 150-5.

94. Ravn, P., et al., *Multivalent scFv display of phagemid repertoires for the selection of carbohydrate-specific antibodies and its application to the Thomsen-Friedenreich antigen.* J Mol Biol, 2004. **343**(4): p. 985-96.
95. Dai, K., H. Zhu, and C. Ruan, *Generation and characterization of recombinant single chain Fv antibody that recognizes platelet glycoprotein Ibalpha.* Thromb Res, 2003. **109**(2-3): p. 137-44.
96. Men, R., et al., *Identification of chimpanzee Fab fragments by repertoire cloning and production of a full-length humanized immunoglobulin G1 antibody that is highly efficient for neutralization of dengue type 4 virus.* J Virol, 2004. **78**(9): p. 4665-74.
97. King, M.C. and A.C. Wilson, *Evolution at two levels in humans and chimpanzees.* Science, 1975. **188**(4184): p. 107-16.
98. Bettauer, R.H., *Systematic review of chimpanzee use in monoclonal antibody research and drug development: 1981-2010.* Altex, 2011. **28**(2): p. 103-16.
99. Hamers-Casterman, C., et al., *Naturally occurring antibodies devoid of light chains.* Nature, 1993. **363**(6428): p. 446-8.
100. Sabir, J.S., et al., *Construction of naive camelids VHH repertoire in phage display-based library.* C R Biol, 2014. **337**(4): p. 244-9.
101. Nguyen, V.K., A. Desmyter, and S. Muyldermans, *Functional heavy-chain antibodies in Camelidae.* Adv Immunol, 2001. **79**: p. 261-96.
102. Mage, R.G., D. Lanning, and K.L. Knight, *B cell and antibody repertoire development in rabbits: the requirement of gut-associated lymphoid tissues.* Dev Comp Immunol, 2006. **30**(1-2): p. 137-53.
103. McWhirter, J.R., et al., *Antibodies selected from combinatorial libraries block a tumor antigen that plays a key role in immunomodulation.* Proc Natl Acad Sci U S A, 2006. **103**(4): p. 1041-6.
104. Rader, C., et al., *The rabbit antibody repertoire as a novel source for the generation of therapeutic human antibodies.* J Biol Chem, 2000. **275**(18): p. 13668-76.
105. Akimenko, M.A., O. Heidmann, and F. Rougeon, *Complex allotypes of the rabbit immunoglobulin kappa light chains are encoded by structural alleles.* Nucleic Acids Res, 1984. **12**(11): p. 4691-701.
106. Greenberg, A.S., et al., *A new antigen receptor gene family that undergoes rearrangement and extensive somatic diversification in sharks.* Nature, 1995. **374**(6518): p. 168-73.
107. Dooley, H., M.F. Flajnik, and A.J. Porter, *Selection and characterization of naturally occurring single-domain (IgNAR) antibody fragments from immunized sharks by phage display.* Mol Immunol, 2003. **40**(1): p. 25-33.
108. Hatta, H., et al., *Productivity and some properties of egg yolk antibody (IgY) against human rotavirus compared with rabbit IgG.* Biosci Biotechnol Biochem, 1993. **57**(3): p. 450-4.
109. McCormack, W.T., L.W. Tjoelker, and C.B. Thompson, *Avian B-cell development: generation of an immunoglobulin repertoire by gene conversion.* Annu Rev Immunol, 1991. **9**: p. 219-41.
110. Andris-Widhopf, J., et al., *Methods for the generation of chicken monoclonal antibody fragments by phage display.* J Immunol Methods, 2000. **242**(1-2): p. 159-81.

111. Braganza, A., et al., *Generation and validation of canine single chain variable fragment phage display libraries.* Vet Immunol Immunopathol, 2011. **139**(1): p. 27-40.
112. Guglielmi, L. and P. Martineau, *Expression of single-chain Fv fragments in E. coli cytoplasm.* Methods Mol Biol, 2009. **562**: p. 215-24.
113. Ho, M., S. Nagata, and I. Pastan, *Isolation of anti-CD22 Fv with high affinity by Fv display on human cells.* Proc Natl Acad Sci U S A, 2006. **103**(25): p. 9637-42.
114. Choo, A.B., et al., *Soluble expression of a functional recombinant cytolytic immunotoxin in insect cells.* Protein Expr Purif, 2002. **24**(3): p. 338-47.
115. Pluckthun, A., *Antibody engineering.* Curr Opin Biotechnol, 1991. **2**(2): p. 238-46.
116. Lameris, R., et al., *Bispecific antibody platforms for cancer immunotherapy*: Crit Rev Oncol Hematol. 2014 Aug 20. pii: S1040-8428(14)00135-8. doi: 10.1016/j.critrevonc.2014.08.003.
117. Haas, C., et al., *Mode of cytotoxic action of T cell-engaging BiTE antibody MT110.* Immunobiology, 2009. **214**(6): p. 441-53.
118. Feldmann, A., et al., *Novel humanized and highly efficient bispecific antibodies mediate killing of prostate stem cell antigen-expressing tumor cells by CD8+ and CD4+ T cells.* J Immunol, 2012. **189**(6): p. 3249-59.
119. Kontermann, R.E., *Strategies for extended serum half-life of protein therapeutics.* Curr Opin Biotechnol, 2011. **22**(6): p. 868-76.
120. Sievers, E.L. and P.D. Senter, *Antibody-drug conjugates in cancer therapy.* Annu Rev Med, 2013. **64**: p. 15-29.
121. Tsukazaki, K., E.G. Hayman, and E. Ruoslahti, *Effects of ricin A chain conjugates of monoclonal antibodies to human alpha-fetoprotein and placental alkaline phosphatase on antigen-producing tumor cells in culture.* Cancer Res, 1985. **45**(4): p. 1834-8.
122. Pirker, R., et al., *Anti-transferrin receptor antibody linked to Pseudomonas exotoxin as a model immunotoxin in human ovarian carcinoma cell lines.* Cancer Res, 1985. **45**(2): p. 751-7.
123. Coombes, R.C., et al., *In vitro and in vivo effects of a monoclonal antibody-toxin conjugate for use in autologous bone marrow transplantation for patients with breast cancer.* Cancer Res, 1986. **46**(8): p. 4217-20.
124. Teicher, B.A. and R.V. Chari, *Antibody conjugate therapeutics: challenges and potential.* Clin Cancer Res, 2011. **17**(20): p. 6389-97.
125. Maloney, D., et al., *Diversity in antibody-based approaches to non-Hodgkin lymphoma.* Leuk Lymphoma, 2010. **1**: p. 20-7.
126. Verma, S., et al., *Trastuzumab emtansine for HER2-positive advanced breast cancer.* N Engl J Med, 2012. **367**(19): p. 1783-91.
127. Katz, J., J.E. Janik, and A. Younes, *Brentuximab Vedotin (SGN-35).* Clin Cancer Res, 2011. **17**(20): p. 6428-36.
128. Zhao, R.Y., et al., *Synthesis and evaluation of hydrophilic linkers for antibody-maytansinoid conjugates.* J Med Chem, 2011. **54**(10): p. 3606-23.
129. Kovtun, Y.V., et al., *Antibody-maytansinoid conjugates designed to bypass multidrug resistance.* Cancer Res, 2010. **70**(6): p. 2528-37.
130. Bagshawe, K.D., et al., *A cytotoxic agent can be generated selectively at cancer sites.* Br J Cancer, 1988. **58**(6): p. 700-3.

131. Bagshawe, K.D., *Antibody directed enzymes revive anti-cancer prodrugs concept.* Br J Cancer, 1987. **56**(5): p. 531-2.
132. Osipovitch, D.C., et al., *Design and analysis of immune-evading enzymes for ADEPT therapy.* Protein Eng Des Sel, 2012. **25**(10): p. 613-23.
133. Zawilska, J.B., J. Wojcieszak, and A.B. Olejniczak, *Prodrugs: a challenge for the drug development.* Pharmacol Rep, 2013. **65**(1): p. 1-14.
134. Albert, A., *Chemical aspects of selective toxicity.* Nature, 1958. **182**(4633): p. 421-2.
135. Bagshawe, K.D., *Targeting: the ADEPT story so far.* Curr Drug Targets, 2009. **10**(2): p. 152-7.
136. Searle, F., et al., *The potential of carboxypeptidase G2-antibody conjugates as anti-tumour agents. I. Preparation of antihuman chorionic gonadotrophin-carboxypeptidase G2 and cytotoxicity of the conjugate against JAR choriocarcinoma cells in vitro.* Br J Cancer, 1986. **53**(3): p. 377-84.
137. Lutterotti, A. and R. Martin, *Getting specific: monoclonal antibodies in multiple sclerosis.* Lancet Neurol, 2008. **7**(6): p. 538-47.
138. Steplewski, Z., M.D. Lubeck, and H. Koprowski, *Human macrophages armed with murine immunoglobulin G2a antibodies to tumors destroy human cancer cells.* Science, 1983. **221**(4613): p. 865-7.
139. Clynes, R.A., et al., *Inhibitory Fc receptors modulate in vivo cytotoxicity against tumor targets.* Nat Med, 2000. **6**(4): p. 443-6.
140. Golay, J., et al., *Rituximab-mediated antibody-dependent cellular cytotoxicity against neoplastic B cells is stimulated strongly by interleukin-2.* Haematologica, 2003. **88**(9): p. 1002-12.
141. Presta, L.G., *Molecular engineering and design of therapeutic antibodies.* Curr Opin Immunol, 2008. **20**(4): p. 460-70.
142. Rogers, L.M., S. Veeramani, and G.J. Weiner, *Complement in monoclonal antibody therapy of cancer.* Immunol Res, 2014. **59**(1-3): p. 203-10.
143. Uchida, J., et al., *The innate mononuclear phagocyte network depletes B lymphocytes through Fc receptor-dependent mechanisms during anti-CD20 antibody immunotherapy.* J Exp Med, 2004. **199**(12): p. 1659-69.
144. Nimmerjahn, F., et al., *FcgammaRIV deletion reveals its central role for IgG2a and IgG2b activity in vivo.* Proc Natl Acad Sci U S A, 2010. **107**(45): p. 19396-401.
145. Carmi, C., et al., *Clinical perspectives for irreversible tyrosine kinase inhibitors in cancer.* Biochem Pharmacol, 2012. **84**(11): p. 1388-99.
146. Mendelsohn, J. and J. Baselga, *Epidermal growth factor receptor targeting in cancer.* Semin Oncol, 2006. **33**(4): p. 369-85.
147. Miller, M.J., K.C. Foy, and P.T. Kaumaya, *Cancer immunotherapy: present status, future perspective, and a new paradigm of peptide immunotherapeutics.* Discov Med, 2013. **15**(82): p. 166-76.
148. Colas, P., et al., *Genetic selection of peptide aptamers that recognize and inhibit cyclin-dependent kinase 2.* Nature, 1996. **380**(6574): p. 548-50.
149. Borghouts, C., C. Kunz, and B. Groner, *Peptide aptamers: recent developments for cancer therapy.* Expert Opin Biol Ther, 2005. **5**(6): p. 783-97.
150. Seigneuric, R., et al., *From nanotechnology to nanomedicine: applications to cancer research.* Curr Mol Med, 2010. **10**(7): p. 640-52.

151. Borghouts, C., C. Kunz, and B. Groner, *Current strategies for the development of peptide-based anti-cancer therapeutics.* J Pept Sci, 2005. **11**(11): p. 713-26.
152. Mendoza, F.J., et al., *Anti-tumor chemotherapy utilizing peptide-based approaches--apoptotic pathways, kinases, and proteasome as targets.* Arch Immunol Ther Exp, 2005. **53**(1): p. 47-60.
153. Zhang, J., H. Spring, and M. Schwab, *Neuroblastoma tumor cell-binding peptides identified through random peptide phage display.* Cancer Lett, 2001. **171**(2): p. 153-64.
154. Thundimadathil, J., *Cancer treatment using peptides: current therapies and future prospects.* J Amino Acids, 2012. **967347**(10): p. 20.
155. Bjorklund, M., P. Heikkila, and E. Koivunen, *Peptide inhibition of catalytic and noncatalytic activities of matrix metalloproteinase-9 blocks tumor cell migration and invasion.* J Biol Chem, 2004. **279**(28): p. 29589-97.
156. Fairbrother, W.J., et al., *Novel peptides selected to bind vascular endothelial growth factor target the receptor-binding site.* Biochemistry, 1998. **37**(51): p. 17754-64.
157. Marks, C. and J.D. Marks, *Phage libraries--a new route to clinically useful antibodies.* N Engl J Med, 1996. **335**(10): p. 730-3.
158. Luengo-Fernandez, R., et al., *Economic burden of cancer across the European Union: a population-based cost analysis.* Lancet Oncol, 2013. **14**(12): p. 1165-74.
159. Tiwari, A.K. and H.K. Roy, *Progress against cancer (1971-2011): how far have we come?* J Intern Med, 2012. **271**(4): p. 392-9.
160. Vogelstein, B. and K.W. Kinzler, *Cancer genes and the pathways they control.* Nat Med, 2004. **10**(8): p. 789-99.
161. Hanahan, D. and R.A. Weinberg, *Hallmarks of cancer: the next generation.* Cell, 2011. **144**(5): p. 646-74.
162. Mittra, J. and J. Tait, *Analysing stratified medicine business models and value systems: innovation-regulation interactions.* N Biotechnol, 2012. **29**(6): p. 709-19.
163. Ballestar, E. and M. Esteller, *Epigenetic gene regulation in cancer.* Adv Genet, 2008. **61**: p. 247-67.
164. Zhang, K., *Endoplasmic reticulum stress response and transcriptional reprogramming.* Front Genet, 2015. **5**(460).
165. Hansen, K. and C. Khanna, *Spontaneous and genetically engineered animal models; use in preclinical cancer drug development.* European journal of cancer, 2004. **40**(6): p. 858-80.
166. Osburn, B., C. Scott, and P. Gibbs, *One world--one medicine--one health: emerging veterinary challenges and opportunities.* Rev Sci Tech, 2009. **28**(2): p. 481-6.
167. Porrello, A., P. Cardelli, and E.P. Spugnini, *Oncology of companion animals as a model for humans. an overview of tumor histotypes.* J Exp Clin Cancer Res, 2006. **25**(1): p. 97-105.
168. Henry, C.J. and J.N. Bryan, *Not lost in translation: how study of diseases in our pets can benefit them and us.* Mo Med, 2013. **110**(3): p. 216-9.
169. Withrow, S.J., et al., *Comparative aspects of osteosarcoma. Dog versus man.* Clin Orthop Relat Res, 1991. **270**: p. 159-68.

170. Mueller, F., B. Fuchs, and B. Kaser-Hotz, *Comparative biology of human and canine osteosarcoma.* Anticancer Res, 2007. **27**(1A): p. 155-64.
171. Vail, D.M. and E.G. MacEwen, *Spontaneously occurring tumors of companion animals as models for human cancer.* Cancer Invest, 2000. **18**(8): p. 781-92.
172. Gordon, I., et al., *The Comparative Oncology Trials Consortium: using spontaneously occurring cancers in dogs to inform the cancer drug development pathway.* PLoS Med, 2009. **6**(10): p. 13.
173. Weiden, P.L., et al., *Treatment of canine malignancies by 1200 R total body irradiation and autologous marrow grafts.* Exp Hematol, 1975. **3**(2): p. 124-34.
174. Tsoi, M.S., P.L. Weiden, and R. Storb, *Lymphocyte reactivity to autochthonous tumor cells in dogs with spontaneous malignancies.* Cell Immunol, 1974. **13**(3): p. 431-9.
175. Storb, R., et al., *Marrow engraftment by allogeneic leukocytes in lethally irradiated dogs.* Blood, 1967. **30**(6): p. 805-11.
176. Benjamini, E., et al., *Tumor vaccines for immunotherapy of canine lymphosarcoma.* Ann N Y Acad Sci, 1976. **277**(00): p. 305-12.
177. Lander, E.S., et al., *Initial sequencing and analysis of the human genome.* Nature, 2001. **409**(6822): p. 860-921.
178. Kirkness, E.F., et al., *The dog genome: survey sequencing and comparative analysis.* Science, 2003. **301**(5641): p. 1898-903.
179. Paoloni, M. and C. Khanna, *Translation of new cancer treatments from pet dogs to humans.* Nat Rev Cancer, 2008. **8**(2): p. 147-56.
180. Rowell, J.L., D.O. McCarthy, and C.E. Alvarez, *Dog models of naturally occurring cancer.* Trends Mol Med, 2011. **17**(7): p. 380-8.
181. Lindblad-Toh, K., et al., *Genome sequence, comparative analysis and haplotype structure of the domestic dog.* Nature, 2005. **438**(7069): p. 803-19.
182. Sargan, D.R., *IDID: inherited diseases in dogs: web-based information for canine inherited disease genetics.* Mamm Genome, 2004. **15**(6): p. 503-6.
183. Parker, H.G., A.L. Shearin, and E.A. Ostrander, *Man's best friend becomes biology's best in show: genome analyses in the domestic dog.* Annu Rev Genet, 2010. **44**: p. 309-36.
184. Shearin, A.L. and E.A. Ostrander, *Leading the way: canine models of genomics and disease.* Dis Model Mech, 2010. **3**(1-2): p. 27-34.
185. Bronson, R.T., *Variation in age at death of dogs of different sexes and breeds.* Am J Vet Res, 1982. **43**(11): p. 2057-9.
186. Parker, H.G., et al., *Genetic structure of the purebred domestic dog.* Science, 2004. **304**(5674): p. 1160-4.
187. de Jong, D. and O. Balague Ponz, *The molecular background of aggressive B cell lymphomas as a basis for targeted therapy.* J Pathol, 2011. **223**(2): p. 274-82.
188. Marconato, L., M.E. Gelain, and S. Comazzi, *The dog as a possible animal model for human non-Hodgkin lymphoma: a review.* Hematol Oncol, 2013. **31**(1): p. 1-9.
189. Pleiman, C.M., D. D'Ambrosio, and J.C. Cambier, *The B-cell antigen receptor complex: structure and signal transduction.* Immunol Today, 1994. **15**(9): p. 393-9.

190. Song, H., et al., *Antibody feedback and somatic mutation in B cells: regulation of mutation by immune complexes with IgG antibody.* Immunol Rev, 1998. **162**: p. 211-8.
191. Tarlinton, D., *Germinal centers: form and function.* Curr Opin Immunol, 1998. **10**(3): p. 245-51.
192. Hollander, N., *Immunotherapy for B-cell lymphoma: current status and prospective advances.* Front Immunol, 2012. **3**(3).
193. Salter, D.M., A.S. Krajewski, and S. Cunningham, *Activation and differentiation antigen expression in B-cell non-Hodgkin's lymphoma.* J Pathol, 1988. **154**(3): p. 209-22.
194. Prevodnik, V.K., et al., *The predictive significance of CD20 expression in B-cell lymphomas.* Diagn Pathol, 2011. **6**(33): p. 1746-1596.
195. Stashenko, P., et al., *Characterization of a human B lymphocyte-specific antigen.* J Immunol, 1980. **125**(4): p. 1678-85.
196. Oksvold, M.P., et al., *Expression of B-cell surface antigens in subpopulations of exosomes released from B-cell lymphoma cells.* Clin Ther, 2014. **36**(6): p. 847-862.
197. Denzer, K., et al., *Exosome: from internal vesicle of the multivesicular body to intercellular signaling device.* J Cell Sci, 2000. **19**: p. 3365-74.
198. Jubala, C.M., et al., *CD20 expression in normal canine B cells and in canine non-Hodgkin lymphoma.* Vet Pathol, 2005. **42**(4): p. 468-76.
199. Clark, E.A. and J.A. Ledbetter, *Structure, function, and genetics of human B cell-associated surface molecules.* Adv Cancer Res, 1989. **52**: p. 81-149.
200. Maloney, D.G., *Anti-CD20 antibody therapy for B-cell lymphomas.* N Engl J Med, 2012. **366**(21): p. 2008-16.
201. Tedder, T.F., G. McIntyre, and S.F. Schlossman, *Heterogeneity in the B1 (CD20) cell surface molecule expressed by human B-lymphocytes.* Mol Immunol, 1988. **25**(12): p. 1321-30.
202. Plosker, G.L. and D.P. Figgitt, *Rituximab: a review of its use in non-Hodgkin's lymphoma and chronic lymphocytic leukaemia.* Drugs, 2003. **63**(8): p. 803-43.
203. Solal-Celigny, P., *Rituximab as first-line monotherapy in low-grade follicular lymphoma with a low tumor burden.* Anticancer Drugs, 2001. **12**(2): p. S11-4.
204. von Schilling, C., *Immunotherapy with anti-CD20 compounds.* Semin Cancer Biol, 2003. **13**(3): p. 211-22.
205. Griffin, M.M. and N. Morley, *Rituximab in the treatment of non-Hodgkin's lymphoma--a critical evaluation of randomized controlled trials.* Expert Opin Biol Ther, 2013. **13**(5): p. 803-11.
206. Maloney, D.G., et al., *IDEC-C2B8 (Rituximab) anti-CD20 monoclonal antibody therapy in patients with relapsed low-grade non-Hodgkin's lymphoma.* Blood, 1997. **90**(6): p. 2188-95.
207. Impellizeri, J.A., et al., *The role of rituximab in the treatment of canine lymphoma: an ex vivo evaluation.* Vet J, 2006. **171**(3): p. 556-8.
208. Chambers, S.A. and D. Isenberg, *Anti-B cell therapy (rituximab) in the treatment of autoimmune diseases.* Lupus, 2005. **14**(3): p. 210-4.
209. Sinha, A. and A. Bagga, *Rituximab therapy in nephrotic syndrome: implications for patients' management.* Nat Rev Nephrol, 2013. **9**(3): p. 154-69.

210. Lee, S. and M. Ballow, *Monoclonal antibodies and fusion proteins and their complications: targeting B cells in autoimmune diseases.* J Allergy Clin Immunol, 2010. **125**(4): p. 814-20.
211. Castillo-Trivino, T., et al., *Rituximab in relapsing and progressive forms of multiple sclerosis: a systematic review.* PLoS One, 2013. **8**(7).
212. Vo, A.A., et al., *Benefits of Rituximab Combined With Intravenous Immunoglobulin for Desensitization in Kidney Transplant Recipients.* Transplantation, 2014. **2**: p. 2.
213. Pouget, J.P., et al., *Clinical radioimmunotherapy--the role of radiobiology.* Nat Rev Clin Oncol, 2011. **8**(12): p. 720-34.
214. Grillo-Lopez, A.J., *Zevalin: the first radioimmunotherapy approved for the treatment of lymphoma.* Expert Rev Anticancer Ther, 2002. **2**(5): p. 485-93.
215. Michallet, A.S., L. Lebras, and B. Coiffier, *Maintenance therapy in diffuse large B-cell lymphoma.* Curr Opin Oncol, 2012. **24**(5): p. 461-5.
216. Coiffier, B., et al., *Rituximab (anti-CD20 monoclonal antibody) for the treatment of patients with relapsing or refractory aggressive lymphoma: a multicenter phase II study.* Blood, 1998. **92**(6): p. 1927-32.
217. Dotan, E., C. Aggarwal, and M.R. Smith, *Impact of Rituximab (Rituxan) on the Treatment of B-Cell Non-Hodgkin's Lymphoma.* P T, 2010. **35**(3): p. 148-57.
218. McLaughlin, P., et al., *Rituximab chimeric anti-CD20 monoclonal antibody therapy for relapsed indolent lymphoma: half of patients respond to a four-dose treatment program.* J Clin Oncol, 1998. **16**(8): p. 2825-33.
219. Rao, A., et al., *Safety, efficacy, and immune reconstitution after rituximab therapy in pediatric patients with chronic or refractory hematologic autoimmune cytopenias.* Pediatr Blood Cancer, 2008. **50**(4): p. 822-5.
220. Polyak, M.J. and J.P. Deans, *Alanine-170 and proline-172 are critical determinants for extracellular CD20 epitopes; heterogeneity in the fine specificity of CD20 monoclonal antibodies is defined by additional requirements imposed by both amino acid sequence and quaternary structure.* Blood, 2002. **99**(9): p. 3256-62.
221. Binder, M., et al., *The epitope recognized by rituximab.* Blood, 2006. **108**(6): p. 1975-8.
222. Takei, K., et al., *Analysis of changes in CD20, CD55, and CD59 expression on established rituximab-resistant B-lymphoma cell lines.* Leuk Res, 2006. **30**(5): p. 625-31.
223. Wang, S.Y., et al., *NK-cell activation and antibody-dependent cellular cytotoxicity induced by rituximab-coated target cells is inhibited by the C3b component of complement.* Blood, 2008. **111**(3): p. 1456-63.
224. Olejniczak, S.H., et al., *Acquired resistance to rituximab is associated with chemotherapy resistance resulting from decreased Bax and Bak expression.* Clin Cancer Res, 2008. **14**(5): p. 1550-60.
225. Beers, S.A., et al., *Antigenic modulation limits the efficacy of anti-CD20 antibodies: implications for antibody selection.* Blood, 2010. **115**(25): p. 5191-201.
226. Teeling, J.L., et al., *Characterization of new human CD20 monoclonal antibodies with potent cytolytic activity against non-Hodgkin lymphomas.* Blood, 2004. **104**(6): p. 1793-800.

227. Czuczman, M.S., et al., *Ofatumumab monotherapy in rituximab-refractory follicular lymphoma: results from a multicenter study.* Blood, 2012. **119**(16): p. 3698-704.
228. van Meerten, T. and A. Hagenbeek, *Novel antibodies against follicular non-Hodgkin's lymphoma.* Best Pract Res Clin Haematol, 2011. **24**(2): p. 231-56.
229. Maloney, D.G., *Follicular NHL: from antibodies and vaccines to graft-versus-lymphoma effects.* Hematology Am Soc Hematol Educ Program, 2007: p. 226-32.
230. Morschhauser, F., et al., *Humanized anti-CD20 antibody, veltuzumab, in refractory/recurrent non-Hodgkin's lymphoma: phase I/II results.* J Clin Oncol, 2009. **27**(20): p. 3346-53.
231. Bowles, J.A., et al., *Anti-CD20 monoclonal antibody with enhanced affinity for CD16 activates NK cells at lower concentrations and more effectively than rituximab.* Blood, 2006. **108**(8): p. 2648-54.
232. Salles, G.A., et al., *Obinutuzumab (GA101) in patients with relapsed/refractory indolent non-Hodgkin lymphoma: results from the phase II GAUGUIN study.* J Clin Oncol, 2013. **31**(23): p. 2920-6.
233. Ahmadzadeh, V., et al., *Design, expression and characterization of a single chain anti-CD20 antibody; a germline humanized antibody derived from Rituximab.* Protein Expr Purif, 2014. **102**: p. 45-51.
234. Chu, T.W., J. Yang, and J. Kopecek, *Anti-CD20 multivalent HPMA copolymer-Fab' conjugates for the direct induction of apoptosis.* Biomaterials, 2012. **33**(29): p. 7174-81.
235. Wang, W., et al., *Antibody structure, instability, and formulation.* J Pharm Sci, 2007. **96**(1): p. 1-26.
236. Verma, R., E. Boleti, and A.J. George, *Antibody engineering: comparison of bacterial, yeast, insect and mammalian expression systems.* J Immunol Methods, 1998. **216**(1-2): p. 165-81.
237. Caneva, M., et al., *Connective tissue grafts in conjunction with implants installed immediately into extraction sockets. An experimental study in dogs.* Clin Oral Implants Res, 2013. **24**(1): p. 50-6.
238. Cabrera, R., et al., *The anti-viral effect of sorafenib in hepatitis C-related hepatocellular carcinoma.* Aliment Pharmacol Ther, 2013. **37**(1): p. 91-7.
239. Johnson, R.E., T.P. Cameron, and R. Kinard, *Canine lymphoma as a potential model for experimental therapeutics.* Cancer Res, 1968. **28**(12): p. 2562-4.
240. Lehmann-Horn, K., H.C. Kronsbein, and M.S. Weber, *Targeting B cells in the treatment of multiple sclerosis: recent advances and remaining challenges.* Ther Adv Neurol Disord, 2013. **6**(3): p. 161-73.
241. Vale, A.M. and H.W. Schroeder, Jr., *Clinical consequences of defects in B-cell development.* J Allergy Clin Immunol, 2010. **125**(4): p. 778-87.
242. Matnani, R.G., et al., *Peripheral T-Cell Lymphoma with Aberrant Expression of CD19, CD20, and CD79a: Case Report and Literature Review.* Case Rep Hematol, 2013. **183134**(10): p. 28.
243. Zack, D.J., et al., *Two kappa immunoglobulin light chains are secreted by an anti-DNA hybridoma: implications for isotypic exclusion.* Mol Immunol, 1995. **32**(17-18): p. 1345-53.

244. Brockmann, E.-C., et al., *Selecting for antibody scFv fragments with improved stability using phage display with denaturation under reducing conditions.* Journal of Immunological Methods, 2005. **296**(1–2): p. 159-170.
245. Schenk, D., et al., *Immunization with amyloid-beta attenuates Alzheimer-disease-like pathology in the PDAPP mouse.* Nature, 1999. **400**(6740): p. 173-7.
246. Sipe, J.D., et al., *Amyloid fibril protein nomenclature: 2012 recommendations from the Nomenclature Committee of the International Society of Amyloidosis.* Amyloid, 2012. **19**(4): p. 167-70.
247. Lashuel, H.A., et al., *Neurodegenerative disease: amyloid pores from pathogenic mutations.* Nature, 2002. **418**(6895): p. 291.
248. Danzer, K.M., et al., *Different species of alpha-synuclein oligomers induce calcium influx and seeding.* J Neurosci, 2007. **27**(34): p. 9220-32.
249. Winner, B., et al., *In vivo demonstration that alpha-synuclein oligomers are toxic.* Proc Natl Acad Sci U S A, 2011. **108**(10): p. 4194-9.
250. Kumar, S., et al., *Stages and conformations of the Tau repeat domain during aggregation and its effect on neuronal toxicity.* J Biol Chem, 2014. **289**(29): p. 20318-32.
251. Kang, L., et al., *N-terminal acetylation of alpha-synuclein induces increased transient helical propensity and decreased aggregation rates in the intrinsically disordered monomer.* Protein Sci, 2012. **21**(7): p. 911-7.
252. Valera, E. and E. Masliah, *Immunotherapy for neurodegenerative diseases: focus on alpha-synucleinopathies.* Pharmacol Ther, 2013. **138**(3): p. 311-22.
253. Tran, H.T., et al., *Alpha-synuclein immunotherapy blocks uptake and templated propagation of misfolded alpha-synuclein and neurodegeneration.* Cell Rep, 2014. **7**(6): p. 2054-65.
254. Brannstrom, K., et al., *A generic method for design of oligomer-specific antibodies.* PLoS One, 2014. **9**(3).
255. Ferreira, J.J., et al., *Summary of the recommendations of the EFNS/MDS-ES review on therapeutic management of Parkinson's disease.* Eur J Neurol, 2013. **20**(1): p. 5-15.
256. Olanow, C.W., *The scientific basis for the current treatment of Parkinson's disease.* Annu Rev Med, 2004. **55**: p. 41-60.
257. Pahwa, R., et al., *Practice Parameter: treatment of Parkinson disease with motor fluctuations and dyskinesia (an evidence-based review): report of the Quality Standards Subcommittee of the American Academy of Neurology.* Neurology, 2006. **66**(7): p. 983-95.
258. Orr, C.F., D.B. Rowe, and G.M. Halliday, *An inflammatory review of Parkinson's disease.* Prog Neurobiol, 2002. **68**(5): p. 325-40.
259. Tanner, C.M. and J.W. Langston, *Do environmental toxins cause Parkinson's disease? A critical review.* Neurology, 1990. **40**(10 Suppl 3): p. 17-30.
260. Chiti, F. and C.M. Dobson, *Protein misfolding, functional amyloid, and human disease.* Annu Rev Biochem, 2006. **75**: p. 333-66.
261. Dobson, C.M., *Protein folding and misfolding.* Nature, 2003. **426**(6968): p. 884-90.
262. Soto, C., *Unfolding the role of protein misfolding in neurodegenerative diseases.* Nat Rev Neurosci, 2003. **4**(1): p. 49-60.

263. Forman, M.S., J.Q. Trojanowski, and V.M. Lee, *Neurodegenerative diseases: a decade of discoveries paves the way for therapeutic breakthroughs.* Nat Med, 2004. **10**(10): p. 1055-63.
264. Gibb, W.R., *Neuropathology of the substantia nigra.* Eur Neurol, 1991. **1**: p. 48-59.
265. Chung, K.K., V.L. Dawson, and T.M. Dawson, *The role of the ubiquitin-proteasomal pathway in Parkinson's disease and other neurodegenerative disorders.* Trends Neurosci, 2001. **24**(11 Suppl): p. S7-14.
266. Lotharius, J. and P. Brundin, *Pathogenesis of Parkinson's disease: dopamine, vesicles and alpha-synuclein.* Nat Rev Neurosci, 2002. **3**(12): p. 932-42.
267. Giasson, B.I., et al., *Oxidative damage linked to neurodegeneration by selective alpha-synuclein nitration in synucleinopathy lesions.* Science, 2000. **290**(5493): p. 985-9.
268. Jellinger, K.A., *Alpha-synuclein pathology in Parkinson's and Alzheimer's disease brain: incidence and topographic distribution--a pilot study.* Acta Neuropathol, 2003. **106**(3): p. 191-201.
269. Galvin, J.E., V.M. Lee, and J.Q. Trojanowski, *Synucleinopathies: clinical and pathological implications.* Arch Neurol, 2001. **58**(2): p. 186-90.
270. Marti, M.J., E. Tolosa, and J. Campdelacreu, *Clinical overview of the synucleinopathies.* Mov Disord, 2003. **18**(6): p. S21-7.
271. Greffard, S., et al., *A stable proportion of Lewy body bearing neurons in the substantia nigra suggests a model in which the Lewy body causes neuronal death.* Neurobiol Aging, 2010. **31**(1): p. 99-103.
272. Wood-Kaczmar, A., S. Gandhi, and N.W. Wood, *Understanding the molecular causes of Parkinson's disease.* Trends Mol Med, 2006. **12**(11): p. 521-8.
273. Hilker, R., et al., *Positron emission tomographic analysis of the nigrostriatal dopaminergic system in familial parkinsonism associated with mutations in the parkin gene.* Ann Neurol, 2001. **49**(3): p. 367-76.
274. Bonifati, V., et al., *Mutations in the DJ-1 gene associated with autosomal recessive early-onset parkinsonism.* Science, 2003. **299**(5604): p. 256-9.
275. Takahashi, H., et al., *Familial juvenile parkinsonism: clinical and pathologic study in a family.* Neurology, 1994. **44**(3 Pt 1): p. 437-41.
276. Mori, H., et al., *Pathologic and biochemical studies of juvenile parkinsonism linked to chromosome 6q.* Neurology, 1998. **51**(3): p. 890-2.
277. Galvin, J.E., et al., *Differential expression and distribution of alpha-, beta-, and gamma-synuclein in the developing human substantia nigra.* Exp Neurol, 2001. **168**(2): p. 347-55.
278. Ueda, K., et al., *Molecular cloning of cDNA encoding an unrecognized component of amyloid in Alzheimer disease.* Proc Natl Acad Sci U S A, 1993. **90**(23): p. 11282-6.
279. Jensen, P.H., et al., *Residues in the synuclein consensus motif of the alpha-synuclein fragment, NAC, participate in transglutaminase-catalysed cross-linking to Alzheimer-disease amyloid beta A4 peptide.* Biochem J, 1995. **310**(Pt 1): p. 91-4.
280. Davidson, W.S., et al., *Stabilization of alpha-synuclein secondary structure upon binding to synthetic membranes.* J Biol Chem, 1998. **273**(16): p. 9443-9.

281. Spillantini, M.G., et al., *Alpha-synuclein in Lewy bodies*: Nature. 1997 Aug 28;388(6645):839-40.
282. Spillantini, M.G., et al., *alpha-Synuclein in filamentous inclusions of Lewy bodies from Parkinson's disease and dementia with lewy bodies.* Proc Natl Acad Sci U S A, 1998. **95**(11): p. 6469-73.
283. Kruger, R., et al., *Ala30Pro mutation in the gene encoding alpha-synuclein in Parkinson's disease*: Nat Genet. 1998 Feb;18(2):106-8.
284. Singleton, A.B., et al., *alpha-Synuclein locus triplication causes Parkinson's disease.* Science, 2003. **302**(5646): p. 841.
285. Lavedan, C., *The synuclein family.* Genome Res, 1998. **8**(9): p. 871-80.
286. Lucking, C.B. and A. Brice, *Alpha-synuclein and Parkinson's disease.* Cell Mol Life Sci, 2000. **57**(13-14): p. 1894-908.
287. McLean, P.J., S. Ribich, and B.T. Hyman, *Subcellular localization of alpha-synuclein in primary neuronal cultures: effect of missense mutations.* J Neural Transm Suppl, 2000. **58**: p. 53-63.
288. Iwai, A., et al., *The precursor protein of non-A beta component of Alzheimer's disease amyloid is a presynaptic protein of the central nervous system.* Neuron, 1995. **14**(2): p. 467-75.
289. Abeliovich, A., et al., *Mice lacking alpha-synuclein display functional deficits in the nigrostriatal dopamine system.* Neuron, 2000. **25**(1): p. 239-52.
290. Perez, R.G., et al., *A role for alpha-synuclein in the regulation of dopamine biosynthesis.* J Neurosci, 2002. **22**(8): p. 3090-9.
291. Chandra, S., et al., *Alpha-synuclein cooperates with CSPalpha in preventing neurodegeneration.* Cell, 2005. **123**(3): p. 383-96.
292. Goedert, M., *Alpha-synuclein and neurodegenerative diseases.* Nat Rev Neurosci, 2001. **2**(7): p. 492-501.
293. Braak, H., et al., *Cognitive status correlates with neuropathologic stage in Parkinson disease.* Neurology, 2005. **64**(8): p. 1404-10.
294. Shannon, K.M., et al., *Is alpha-synuclein in the colon a biomarker for premotor Parkinson's disease? Evidence from 3 cases.* Mov Disord, 2012. **27**(6): p. 716-9.
295. Chu, Y., et al., *Alterations in lysosomal and proteasomal markers in Parkinson's disease: relationship to alpha-synuclein inclusions.* Neurobiol Dis, 2009. **35**(3): p. 385-98.
296. Miller, D.W., et al., *Alpha-synuclein in blood and brain from familial Parkinson disease with SNCA locus triplication.* Neurology, 2004. **62**(10): p. 1835-8.
297. Conway, K.A., et al., *Acceleration of oligomerization, not fibrillization, is a shared property of both alpha-synuclein mutations linked to early-onset Parkinson's disease: implications for pathogenesis and therapy.* Proc Natl Acad Sci U S A, 2000. **97**(2): p. 571-6.
298. Rockenstein, E., et al., *Accumulation of oligomer-prone alpha-synuclein exacerbates synaptic and neuronal degeneration in vivo.* Brain, 2014. **137**(Pt 5): p. 1496-513.
299. El-Agnaf, O.M., et al., *Effects of the mutations Ala30 to Pro and Ala53 to Thr on the physical and morphological properties of alpha-synuclein protein implicated in Parkinson's disease.* FEBS Lett, 1998. **440**(1-2): p. 67-70.

300. Uversky, V.N., J. Li, and A.L. Fink, *Metal-triggered structural transformations, aggregation, and fibrillation of human alpha-synuclein. A possible molecular NK between Parkinson's disease and heavy metal exposure.* J Biol Chem, 2001. **276**(47): p. 44284-96.
301. Fredenburg, R.A., et al., *The impact of the E46K mutation on the properties of alpha-synuclein in its monomeric and oligomeric states.* Biochemistry, 2007. **46**(24): p. 7107-18.
302. Weinreb, P.H., et al., *NACP, a protein implicated in Alzheimer's disease and learning, is natively unfolded.* Biochemistry, 1996. **35**(43): p. 13709-15.
303. Li, J., V.N. Uversky, and A.L. Fink, *Effect of familial Parkinson's disease point mutations A30P and A53T on the structural properties, aggregation, and fibrillation of human alpha-synuclein.* Biochemistry, 2001. **40**(38): p. 11604-13.
304. Goldman, J.E., et al., *Lewy bodies of Parkinson's disease contain neurofilament antigens.* Science, 1983. **221**(4615): p. 1082-4.
305. Schmidt, M.L., et al., *Epitope map of neurofilament protein domains in cortical and peripheral nervous system Lewy bodies.* Am J Pathol, 1991. **139**(1): p. 53-65.
306. Kuzuhara, S., et al., *Lewy bodies are ubiquitinated. A light and electron microscopic immunocytochemical study.* Acta Neuropathol, 1988. **75**(4): p. 345-53.
307. Manetto, V., et al., *Ubiquitin is associated with abnormal cytoplasmic filaments characteristic of neurodegenerative diseases.* Proc Natl Acad Sci U S A, 1988. **85**(12): p. 4501-5.
308. Arai, K., et al., *Pure autonomic failure in association with human alpha-synucleinopathy.* Neurosci Lett, 2000. **296**(2-3): p. 171-3.
309. Conway, K.A., J.D. Harper, and P.T. Lansbury, Jr., *Fibrils formed in vitro from alpha-synuclein and two mutant forms linked to Parkinson's disease are typical amyloid.* Biochemistry, 2000. **39**(10): p. 2552-63.
310. Eliezer, D., et al., *Conformational properties of alpha-synuclein in its free and lipid-associated states.* J Mol Biol, 2001. **307**(4): p. 1061-73.
311. Hashimoto, M., et al., *Human recombinant NACP/alpha-synuclein is aggregated and fibrillated in vitro: relevance for Lewy body disease.* Brain Res, 1998. **799**(2): p. 301-6.
312. Uversky, V.N., J. Li, and A.L. Fink, *Evidence for a partially folded intermediate in alpha-synuclein fibril formation.* J Biol Chem, 2001. **276**(14): p. 10737-44.
313. Barrow, C.J., et al., *Solution conformations and aggregational properties of synthetic amyloid beta-peptides of Alzheimer's disease. Analysis of circular dichroism spectra.* J Mol Biol, 1992. **225**(4): p. 1075-93.
314. Han, H., P.H. Weinreb, and P.T. Lansbury, Jr., *The core Alzheimer's peptide NAC forms amyloid fibrils which seed and are seeded by beta-amyloid: is NAC a common trigger or target in neurodegenerative disease?* Chem Biol, 1995. **2**(3): p. 163-9.
315. Iwai, A., et al., *Non-A beta component of Alzheimer's disease amyloid (NAC) is amyloidogenic.* Biochemistry, 1995. **34**(32): p. 10139-45.

316. Stockl, M.T., N. Zijlstra, and V. Subramaniam, *alpha-Synuclein oligomers: an amyloid pore? Insights into mechanisms of alpha-synuclein oligomer-lipid interactions.* Mol Neurobiol, 2013. **47**(2): p. 613-21.
317. Gould, N., et al., *Evidence of native alpha-synuclein conformers in the human brain.* J Biol Chem, 2014. **289**(11): p. 7929-34.
318. Greenfield, N.J., *Using circular dichroism spectra to estimate protein secondary structure.* Nat Protoc, 2006. **1**(6): p. 2876-90.
319. Bartels, T., J.G. Choi, and D.J. Selkoe, *alpha-Synuclein occurs physiologically as a helically folded tetramer that resists aggregation.* Nature, 2011. **477**(7362): p. 107-10.
320. Wan, O.W. and K.K. Chung, *The role of alpha-synuclein oligomerization and aggregation in cellular and animal models of Parkinson's disease.* PLoS One, 2012. **7**(6): p. 12.
321. Lee, B.R. and T. Kamitani, *Improved immunodetection of endogenous alpha-synuclein.* PLoS One, 2011. **6**(8): p. 19.
322. Yu, S., et al., *Extensive nuclear localization of alpha-synuclein in normal rat brain neurons revealed by a novel monoclonal antibody.* Neuroscience, 2007. **145**(2): p. 539-55.
323. He, J., et al., *Affinity enhancement pretargeting: synthesis and testing of a 99mTc-labeled bivalent MORF.* Mol Pharm, 2010. **7**(4): p. 1118-24.
324. Shimura, H., et al., *Ubiquitination of a new form of alpha-synuclein by parkin from human brain: implications for Parkinson's disease.* Science, 2001. **293**(5528): p. 263-9.
325. Donaghy, P.C., J.T. O'Brien, and A.J. Thomas, *Prodromal dementia with Lewy bodies.* Psychol Med, 2014. **3**: p. 1-10.
326. Kalia, L.V., et al., *alpha-Synuclein oligomers and clinical implications for Parkinson disease.* Ann Neurol, 2013. **73**(2): p. 155-69.
327. Recasens, A. and B. Dehay, *Alpha-synuclein spreading in Parkinson's disease.* Front Neuroanat, 2014. **8**(159).
328. Steiner, J.A., E. Angot, and P. Brundin, *A deadly spread: cellular mechanisms of alpha-synuclein transfer.* Cell Death Differ, 2011. **18**(9): p. 1425-33.
329. Volles, M.J. and P.T. Lansbury, Jr., *Vesicle permeabilization by protofibrillar alpha-synuclein is sensitive to Parkinson's disease-linked mutations and occurs by a pore-like mechanism.* Biochemistry, 2002. **41**(14): p. 4595-602.
330. Kim, H.Y., et al., *Structural properties of pore-forming oligomers of alpha-synuclein.* J Am Chem Soc, 2009. **131**(47): p. 17482-9.
331. Wang, W., et al., *A soluble alpha-synuclein construct forms a dynamic tetramer.* Proc Natl Acad Sci U S A, 2011. **108**(43): p. 17797-802.
332. Burre, J., et al., *Properties of native brain alpha-synuclein.* Nature, 2013. **498**(7453).
333. Sreerama, N. and R.W. Woody, *A self-consistent method for the analysis of protein secondary structure from circular dichroism.* Anal Biochem, 1993. **209**(1): p. 32-44.
334. Soderberg, O., et al., *Characterizing proteins and their interactions in cells and tissues using the in situ proximity ligation assay.* Methods, 2008. **45**(3): p. 227-32.

335. Boutajangout, A., et al., *Passive immunization targeting pathological phospho-tau protein in a mouse model reduces functional decline and clears tau aggregates from the brain.* J Neurochem, 2011. **118**(4): p. 658-67.
336. Yanamandra, K., et al., *Anti-tau antibodies that block tau aggregate seeding in vitro markedly decrease pathology and improve cognition in vivo.* Neuron, 2013. **80**(2): p. 402-14.
337. Wolfgang, W.J., et al., *Suppression of Huntington's disease pathology in Drosophila by human single-chain Fv antibodies.* Proc Natl Acad Sci U S A, 2005. **102**(32): p. 11563-8.
338. Bae, E.J., et al., *Antibody-aided clearance of extracellular alpha-synuclein prevents cell-to-cell aggregate transmission.* J Neurosci, 2012. **32**(39): p. 13454-69.
339. Scott, J.K. and G.P. Smith, *Searching for peptide ligands with an epitope library.* Science, 1990. **249**(4967): p. 386-90.
340. Devlin, J.J., L.C. Panganiban, and P.E. Devlin, *Random peptide libraries: a source of specific protein binding molecules.* Science, 1990. **249**(4967): p. 404-6.
341. Cwirla, S.E., et al., *Peptides on phage: a vast library of peptides for identifying ligands.* Proc Natl Acad Sci U S A, 1990. **87**(16): p. 6378-82.
342. Molek, P., B. Strukelj, and T. Bratkovic, *Peptide phage display as a tool for drug discovery: targeting membrane receptors.* Molecules, 2011. **16**(1): p. 857-87.
343. Cwirla, S.E., et al., *Peptide agonist of the thrombopoietin receptor as potent as the natural cytokine.* Science, 1997. **276**(5319): p. 1696-9.
344. Kritzer, J.A., et al., *Rapid selection of cyclic peptides that reduce alpha-synuclein toxicity in yeast and animal models.* Nat Chem Biol, 2009. **5**(9): p. 655-63.
345. Outeiro, T.F. and S. Lindquist, *Yeast cells provide insight into alpha-synuclein biology and pathobiology.* Science, 2003. **302**(5651): p. 1772-5.
346. Cooper, A.A., et al., *Alpha-synuclein blocks ER-Golgi traffic and Rab1 rescues neuron loss in Parkinson's models.* Science, 2006. **313**(5785): p. 324-8.
347. Periquet, M., et al., *Aggregated alpha-synuclein mediates dopaminergic neurotoxicity in vivo.* J Neurosci, 2007. **27**(12): p. 3338-46.
348. Du, H.N., et al., *A peptide motif consisting of glycine, alanine, and valine is required for the fibrillization and cytotoxicity of human alpha-synuclein.* Biochemistry, 2003. **42**(29): p. 8870-8.
349. Silveira, J.R., et al., *The most infectious prion protein particles.* Nature, 2005. **437**(7056): p. 257-61.
350. Matochko, W.L., et al., *Prospective identification of parasitic sequences in phage display screens.* Nucleic Acids Res, 2014. **42**(3): p. 1784-98.
351. Kiel, C. and L. Serrano, *The ubiquitin domain superfold: structure-based sequence alignments and characterization of binding epitopes.* J Mol Biol, 2006. **355**(4): p. 821-44.
352. Boecke, A., et al., *Factor associated with neutral sphingomyelinase activity mediates navigational capacity of leukocytes responding to wounds and infection: live imaging studies in zebrafish larvae.* J Immunol, 2012. **189**(4): p. 1559-66.

353. Iijima, K., et al., *Expression of thrombopoietin receptor and its functional role in human B-precursor leukemia cells with 11q23 translocation or Philadelphia chromosome.* Leukemia, 2000. **14**(9): p. 1598-605.
354. Tieu, K., et al., *L-3-hydroxyacyl-CoA dehydrogenase II protects in a model of Parkinson's disease.* Ann Neurol, 2004. **56**(1): p. 51-60.
355. Yang, S.Y., X.Y. He, and H. Schulz, *3-Hydroxyacyl-CoA dehydrogenase and short chain 3-hydroxyacyl-CoA dehydrogenase in human health and disease.* Febs J, 2005. **272**(19): p. 4874-83.
356. Robinson, M.B., et al., *Evidence of excitotoxicity in the brain of the ornithine carbamoyltransferase deficient sparse fur mouse.* Brain Res Dev Brain Res, 1995. **90**(1-2): p. 35-44.
357. Tang, B.L., *ADAMTS: a novel family of extracellular matrix proteases.* Int J Biochem Cell Biol, 2001. **33**(1): p. 33-44.
358. Huang, L., et al., *Novel peptide inhibitors of angiotensin-converting enzyme 2.* J Biol Chem, 2003. **278**(18): p. 15532-40.
359. Cho, M., et al., *Quantitative selection of DNA aptamers through microfluidic selection and high-throughput sequencing.* Proc Natl Acad Sci U S A, 2010. **107**(35): p. 15373-8.
360. Hoon, S., et al., *Aptamer selection by high-throughput sequencing and informatic analysis.* Biotechniques, 2011. **51**(6): p. 413-6.
361. t Hoen, P.A., et al., *Phage display screening without repetitious selection rounds.* Anal Biochem, 2012. **421**(2): p. 622-31.
362. Lebouvier, T., et al., *Colonic biopsies to assess the neuropathology of Parkinson's disease and its relationship with symptoms.* PLoS One, 2010. **5**(9): p. 0012728.